

Electronic Thesis and Dissertation Repository

4-20-2022 4:00 PM

The Impact of Excess Nutrients, Fatty Acids or Glucose, on BeWo Placental Trophoblast Metabolic Function

Zachary JW Easton, *The University of Western Ontario*

Supervisor: Regnault, Timothy RH., *The University of Western Ontario*

A thesis submitted in partial fulfillment of the requirements for the Doctor of Philosophy degree in Physiology and Pharmacology

© Zachary JW Easton 2022

Follow this and additional works at: <https://ir.lib.uwo.ca/etd>



Part of the [Cellular and Molecular Physiology Commons](#)

Recommended Citation

Easton, Zachary JW, "The Impact of Excess Nutrients, Fatty Acids or Glucose, on BeWo Placental Trophoblast Metabolic Function" (2022). *Electronic Thesis and Dissertation Repository*. 8507. <https://ir.lib.uwo.ca/etd/8507>

This Dissertation/Thesis is brought to you for free and open access by Scholarship@Western. It has been accepted for inclusion in Electronic Thesis and Dissertation Repository by an authorized administrator of Scholarship@Western. For more information, please contact wlsadmin@uwo.ca.

Abstract

An adverse intrauterine environment high in circulating nutrients in pregnancies complicated by maternal obesity and diabetes mellitus has been well linked with the development of metabolic health disorders in the exposed offspring. Impairments in placental development, mitochondrial respiration, and nutrient processing are thought to specifically underlie the *in-utero* programming of these metabolic diseases. In these “at-risk” pregnancies a maternal diet high in fat as well as poor glycemic control have been highlighted to be important regulators of placental metabolic functions (including the transport, storage, and oxidation of dietary nutrients), and consequently regulators of offspring metabolic health outcomes. However, the independent impacts of dietary saturated and monounsaturated fatty acid (FA) and glucose exposures on important placental metabolic functions, and their underlying regulation, remains poorly understood. Thus, the purpose of this thesis was to investigate placental metabolic function following independent exposure to increased levels of the dietary FA species palmitate and oleate, and hyperglycemia using an *in vitro* cell culture system. The impacts of nutrient overabundance on BeWo trophoblasts (an *in vitro* model of both progenitor cytotrophoblasts and differentiated syncytiotrophoblasts) were specifically examined using functional readouts of cellular metabolism and mitochondrial respiration, measurements of nutrient storage, in conjunction with multi-omic analyses integrating transcriptomics, metabolomics, and lipidomics. Through the work in this thesis, we demonstrated that saturated FA (palmitate) and glucose exposure was associated with alterations in placental metabolic function indicative of an early phenotype of mitochondrial dysfunction. Further, glucose and oleate exposures were demonstrated to increase nutrient stores in placental trophoblasts. Finally, BeWo trophoblast cells displayed differential transcriptomic, metabolomic, and lipidomic profiles following exposure to dietary FA species and hyperglycemia. These works further demonstrated that increased nutrient supply directly modulates important placental nutrient processing functions. More importantly, these investigations provided greater insight into the underlying mechanisms that regulate the responses of placental trophoblast cells following exposure to dietary nutrient overabundance. Overall, these data suggest that the clinical management of obese and diabetic pregnancies should continue to emphasize reducing placental exposures to excessive

saturated FA and glucose levels to preserve physiological placental nutrient handling, and ultimately limit risks to the developing fetus.

Summary for Lay Audience

The placenta is the central organ responsible for transferring nutrients and oxygen from mother to developing fetus over the 40-weeks of pregnancy. Normal placental functions ensure healthy fetal growth. In situations of excessive nutrient supply (pregnancies complicated by maternal obesity and diabetes) placental functions change leading to impacted fetal growth. This abnormal placental function has been shown to set the stage for later life metabolic diseases (obesity and type 1 diabetes) in the unborn baby. Recently, a poor maternal diet high in saturated fats in obese pregnancies and inadequate maternal control of blood glucose levels in diabetic pregnancies have been found to be important factors that promote changes in placental function. The objective of this thesis was to examine the independent impacts of different fat and glucose exposures on trophoblast (placental) cells and further characterize how these nutrients directly affect placental function. This thesis utilized a well characterized placental model (BeWo cells) to specifically determine how nutrient storage, and the breakdown of nutrients to produce cellular energy (ATP) are impacted in the placenta following exposure to excess dietary fats and glucose. Additionally transcriptomic profiles (examines the expression of all cellular genes), metabolomic profiles (quantifies all metabolites), and lipidomic profiles (quantifies the abundance of all fat types) were examined in nutrient-exposed placental cells to better understand how underlying placental cell functions are modified following these nutrient exposures. In this thesis, trophoblast cells exposed to elevated levels of saturated fats and glucose were found to have markers that suggested their mitochondria (important producers of ATP) were transitioning towards a state of failure. Additionally, placental cells exposed to excess levels of monounsaturated fats and glucose were found to have increased nutrient stores (triglycerides and glycogen). These nutrient-mediated alterations in placental cell functions may ultimately impact nutrient transfer from mother to baby and could be specifically involved in increasing the child's risk of developing metabolic diseases. Overall, this thesis further demonstrated that dietary fats and glucose are important regulators of

placental metabolism and suggests that reducing placental fat and glucose exposures could help protect the unborn baby from later life disease.

Keywords

Developmental Origins of Health and Disease; Placenta; Pregnancy; Pre-pregnancy obesity; Gestational diabetes; Intrauterine insults; Diet; Hyperglycemia; Mitochondrial respiration; Mitochondrial dysfunction; Metabolism; Transcriptomics; Metabolomics; Lipidomics; Seahorse XF Analyzer.

Co-Authorship Statement

Chapter 1 is adapted from “Easton ZJW, Regnault TRH. The Impact of Maternal Body Composition and Dietary Fat Consumption upon Placental Lipid Processing and Offspring Metabolic Health. *Nutrients*. 2020;12: 3031. doi:10.3390/nu12103031” and reproduced with permission from MDPI Publishers (Appendix A). The manuscript was written by ZJW Easton with critical feedback from TRH Regnault.

Chapter 2 is adapted from “Easton ZJW, Delhaes F, Mathers K, Zhao L, Vanderboor CMG, Regnault TRH. Syncytialization and prolonged exposure to palmitate impacts BeWo respiration. *Reproduction*. 2021;161: 73–88. doi:10.1530/REP-19-0433” and reproduced with permission from BioScientifica Ltd (Appendix B). ZJW Easton designed all experiments with critical feedback from TRH Regnault. F Delhaes, K Mathers, and CMG Vanderboor assisted with the optimization of the Seahorse XF activity assays and metabolic enzyme activity assays for use with BeWo trophoblast cells. L Zhao optimized the ZO1 immunofluorescent protocol for use with BeWo trophoblast cells. All data generated for figure preparation was collected by ZJW Easton. The manuscript was written by ZJW Easton with critical feedback from TRH Regnault.

Chapter 3 is adapted from a manuscript submitted for publication entitled “The impact of hyperglycemia upon BeWo trophoblast cell metabolic function: A multi-OMICS and functional metabolic analysis” co-authored with Luo X, Li L, and Regnault TRH. ZJW Easton designed all experiments critical feedback from TRH Regnault. All cell culture collections were performed by ZJW Easton. The extraction of cellular RNA and the subsequent mRNA microarray processing was performed at the Genome Québec Innovation Centre. Transcriptomic data analysis and figure preparation was performed by ZJW Easton. Metabolomic and lipidomic processing, data collection, and preliminary statistical analyses was performed at the Metabolomics Innovation Centre (Edmonton, Canada) by X Luo, and L Li. Biological interpretation of the transcriptomic and metabolomic data was performed by ZJW Easton with the assistance of TRH Regnault. The manuscript was written by ZJW Easton critical feedback from TRH Regnault.

Chapter 4 is adapted from a manuscript under preparation for submission entitled “Elevated Dietary Non-Esterified Fatty Acid Levels Impact BeWo Trophoblast Metabolism and Lipid Processing: A Multi-OMICS Outlook” co-authored with Luo X, Li L, Zhao L, Sarr O, and Regnault TRH. ZJW Easton designed all experiments with critical feedback from TRH Regnault. All cell culture collections were performed by ZJW Easton. The extraction of cellular RNA and the subsequent mRNA microarray processing was performed at the Genome Québec Innovation Centre. Transcriptomic data analysis and figure preparation was performed by ZJW Easton. Metabolomic and lipidomic processing, data collection, and preliminary statistical analyses was performed at the Metabolomics Innovation Centre (Edmonton, Canada) by X Luo, and L Li. Biological interpretation of the transcriptomic and metabolomic data was performed by ZJW Easton with the assistance of TRH Regnault. Extraction of cellular lipids for targeted gas-chromatography coupled flame ionization detection (GC-FID) and thin layer chromatography coupled flame ionization (TLC-FID) detected was performed by ZJW Easton and O Sarr. L Zhao collected the TLC-FID data. All GC-FID and TLC-FID data was analyzed by ZJW Easton, and all figures were prepared by ZJW Easton. The manuscript was written by ZJW Easton with critical feedback from TRH Regnault.

Acknowledgments

I first would like to thank the current, and former members of the Dean, Dan, and Tim (DDT) Lab for providing a safe, friendly, and welcoming work environment over past 5 years. I would especially like to thank Allyson Wood, Shelby Oke, and Alexandra Kozlov for your never-ending friendship and support, and for always wanting to go on coffee runs to the UCC when we needed to get out of the lab and get some fresh air. I would also like to thank Christie Vanderboor and Hailey Hunter for managing and organizing the day-to-day operations of the DDT lab and keeping the lab space running smoothly and efficiently. A thank you also goes out to Ousseynou Sarr and Lin Zhao for providing much needed technical support and advice, and for their assistance with the GC and TLC lipid analyses. A special thank you also goes to out Flavien Delhaes for not only being an excellent co-worker and lab-mate but for also being a great roommate.

A big thank you also goes out to all the members of the Department of Physiology and Pharmacology, and the Developmental Biology Specialization – all of you helped make my graduate studies a fun and enjoyable experience.

This thesis would not have been possible without the love and support of my family. To my parents, thank you for always encouraging me to pursue my education, and for re-assuring me on the days when grad school seemed impossible. To my wonderful partner Taylor, thank you for your ever-lasting patience and understanding, and for sticking by my side while I completed my PhD. I can't wait to see what awaits us when I am finally finished grad school.

I would also like to thank the members of my advisory committee – Dr. Stephen Renaud, Dr. Daniel Hardy, and Dr. Murray Huff – as well as Dr. Tom Drysdale for your guidance and helpful suggestions. Your advice has helped to improve both this thesis, and my research approach.

To my supervisor, Dr. Timothy Regnault, thank you for always encouraging me to do my best and for motivating me to improve both my research, writing, and communication skills. Your guidance and support over the past six years has helped make me a better and more well-rounded researcher and scholar.

Lastly, I would like to thank our funding sources, who allowed this project to be possible. I would like to thank the National Institutes of Health Human Placental Project (grant No. U01 HD087181-01) as well as the Department of Obstetrics and Gynaecology at Western for supporting me with an Obstetrics and Gynaecology Graduate Scholarship (OGGS).

Table of Contents

Abstract.....	ii
Summary for Lay Audience.....	iii
Co-Authorship Statement.....	v
Acknowledgments.....	vii
Table of Contents.....	ix
List of Tables.....	xv
List of Figures.....	xvii
List of Abbreviations.....	xxi
List of Appendices.....	xxiv
Chapter 1.....	1
1 Introduction.....	1
1.1 The Developmental Origins of Health and Disease.....	2
1.2 Impacts of maternal obesity and diet during pregnancy.....	2
1.2.1 Maternal obesity and offspring metabolic health.....	2
1.2.2 Is maternal BMI an accurate predictor of offspring metabolic health?.....	9
1.2.3 Maternal dietary fat consumption and offspring metabolic health.....	11
1.3 Maternal diabetes mellitus and pregnancy outcomes.....	13
1.3.1 Maternal diabetes mellitus and offspring metabolic health.....	13
1.4 The Developmental Origins of Health and Disease and the placenta.....	15
1.4.1 Placental metabolic impairments in adverse maternal environments.....	18
1.4.2 Mechanisms of fatty acid and glucose transport in the placenta.....	19
1.4.3 Placental nutrient storage.....	24
1.4.4 Placental mitochondrial function and nutrient oxidation.....	29
1.5 Omic analyses and the placenta.....	42

1.6 Thesis overview, rationale, and objectives	43
1.6.1 Chapter 2 – Objectives and hypothesis	44
1.6.2 Chapter 3 – Objectives and hypothesis	45
1.6.3 Chapter 4 – Objectives and hypothesis	45
1.7 References	47
Chapter 2	73
2 Syncytialization and prolonged exposure to palmitate impacts BeWo respiration.....	73
2.1 Introduction.....	74
2.2 Materials and Methods:.....	76
2.2.1 Materials	76
2.2.2 Cell culture conditions	76
2.2.3 Cell viability.....	78
2.2.4 Immunofluorescent analysis of BeWo syncytialization	78
2.2.5 Quantitative-PCR analysis of BeWo syncytialization	79
2.2.6 Quantification of apoptosis	80
2.2.7 Optimization of Seahorse XF assay protocols	80
2.2.8 BeWo cell oxidative function	80
2.2.9 BeWo cell glycolytic function	82
2.2.10 Immunoblot analysis	83
2.2.11 Metabolic enzyme activity assays.....	85
2.2.12 Statistical Analysis.....	87
2.2.13 Supplementary materials availability statement	87
2.3 Results.....	88
2.3.1 Characterization of BeWo CT and SCT cells treated with NEFAs	88
2.3.2 The impact of prolonged NEFA exposure upon respiratory activity of BeWo cells	92

2.3.3	Glycolytic function in BeWo cells is unaltered with NEFA treatments ...	95
2.3.4	NEFA impact upon electron transport chain complex protein abundance and activity	96
2.3.5	The impact of prolonged NEFA exposure on metabolic enzyme activity	99
2.3.6	Oxidative State in unaltered in NEFA-treated BeWo cells	101
2.3.7	The impact of prolonged NEFA exposure on metabolic enzyme expression	102
2.4	Discussion	105
2.4.1	Differentiation and BeWo Metabolic Function	105
2.4.2	NEFAs and BeWo Metabolic Function	106
2.4.3	Conclusion	108
2.5	References	109
Chapter 3		117
3	The impact of hyperglycemia upon BeWo trophoblast cell metabolic function: A multi-OMICS and functional metabolic analysis.....	117
3.1	Introduction.....	118
3.2	Materials and methods	120
3.2.1	Materials	120
3.2.2	Cell culture conditions	120
3.2.3	Cell viability.....	122
3.2.4	Immunofluorescent analysis of BeWo syncytialization	122
3.2.5	RT-qPCR analysis of BeWo syncytialization.....	122
3.2.6	Quantifying BeWo cell oxidative function	124
3.2.7	Quantifying BeWo cell glycolytic function.....	124
3.2.8	Immunoblot analysis.....	126
3.2.9	Enzyme activity assays	128
3.2.10	Analysis of nutrient storage	129

3.2.11	Transcriptomic analysis of gene expression changes	129
3.2.12	RT-qPCR validation of differentially expressed genes identified by mRNA microarray	130
3.2.13	Cell culture collections for metabolomic and lipidomic profiling of BeWo CT cells	131
3.2.14	Untargeted metabolomic profiling	131
3.2.15	Untargeted lipidomic profiling	132
3.2.16	Statistical analysis for non-omic experiments	134
3.2.17	Data and supplementary materials availability statement.....	134
3.3	Results.....	135
3.3.1	Characterization of BeWo viability and differentiation under high glucose culture conditions.....	135
3.3.2	BeWo mitochondrial respiratory and glycolytic activity	139
3.3.3	The impact of high glucose and syncytialization upon BeWo ETC complex protein abundance and activity.....	141
3.3.4	Metabolic enzyme activity and HG-cultured BeWo trophoblasts	141
3.3.5	HG-cultured BeWo trophoblast mitochondrial fission and fusion dynamics	145
3.3.6	HG culture conditions impact glycogen storage in BeWo trophoblasts .	147
3.3.7	HG culture conditions increases TG abundance in BeWo CT cells	150
3.3.8	Transcriptomic profiling of HG-cultured BeWo CT cells	152
3.3.9	Impacts of HG culture conditions on the metabolome of BeWo CT cells	157
3.3.10	Impacts of HG culture conditions of the lipidome profiles of BeWo CT cells.	161
3.4	Discussion.....	164
3.4.1	Hyperglycemia and nutrient stores in BeWo trophoblasts	164
3.4.2	Hyperglycemia and metabolic function in BeWo trophoblasts	166
3.4.3	Transcriptomic analysis of HG-cultured BeWo CT cells.....	167

3.4.4	Metabolomic and lipidomic analysis of HG-cultured BeWo CT cells ...	169
3.4.5	Conclusion	171
3.5	References	172
Chapter 4	180
4	Elevated Dietary Non-Esterified Fatty Acid Levels Impact BeWo Trophoblast Metabolism and Lipid Processing: A Multi-OMICS Outlook.....	180
4.1	Introduction.....	181
4.2	Materials and methods:	184
4.2.1	Materials	184
4.2.2	Cell culture protocol	184
4.2.3	Fatty acid and neutral lipid profile analysis	185
4.2.4	Transcriptomic analysis of gene expression changes	186
4.2.5	RT-qPCR validation of differentially expressed genes identified by mRNA microarray	187
4.2.6	Cell collections for untargeted metabolomic and lipidomic profiling of BeWo CT cells.....	188
4.2.7	Untargeted metabolomic profiling	188
4.2.8	Integration of BeWo cytotrophoblast transcriptomic and metabolomic profiles	189
4.2.9	Untargeted lipidomic profiling	189
4.2.10	Data and supplementary materials availability statement.....	190
4.3	Results.....	190
4.3.1	NEFA-treatments impact FA profiles of BeWo trophoblasts.....	190
4.3.2	The impact of NEFA treatments on desaturation and elongation indices in BeWo trophoblasts.....	193
4.3.3	OA-treatment alters neutral lipid profiles of BeWo trophoblasts.....	196
4.3.4	Transcriptomic profiles of BeWo cytotrophoblasts are impacted by NEFA treatment.	198
4.3.5	RT-qPCR Validation of Differentially Expressed Genes	202

4.3.6	Metabolomic profiles of BeWo Cytotrophoblast in response to NEFA treatment	206
4.3.7	BeWo Cytotrophoblast transcriptome and metabolome integration.....	212
4.3.8	The impact of NEFA-treatment of BeWo cytotrophoblast lipidome profiles	214
4.4	Discussion:	221
4.4.1	Impacts of dietary NEFA on BeWo FA and Neutral Lipid Profiles.....	222
4.4.2	A multi-omics analysis of NEFA-treated BeWo CT metabolic function	225
4.4.3	Conclusion	228
4.5	References.....	230
Chapter 5	239
5	General Discussion and Conclusions	239
5.1	Overview of thesis and major findings	240
5.2	Summary of Findings.....	241
5.2.1	Chapter 2: Syncytialization and prolonged exposure to palmitate impacts BeWo respiration	241
5.2.2	Chapter 3: The impact of hyperglycemia upon BeWo trophoblast cell metabolic function: A multi-omics and functional metabolic analysis ..	243
5.2.3	Chapter 4: Elevated Dietary Non-Esterified Fatty Acid Levels Impact BeWo Trophoblast Metabolism and Lipid Processing: A Multi-OMICS Outlook	251
5.3	Considerations for clinical diagnosis of placental dysfunction	258
5.4	Limitations and Future Considerations	260
5.5	Conclusion	264
5.6	References.....	265
Appendices	275
Curriculum Vitae	277

List of Tables

Table 1-1 Summary of diet fat or feeding treatments utilized in animal models of maternal diet-induced gestational obesity and gestational high-fat exposure with and without diet reversal	5
Table 2-1 Forward and reverse primer sequences used for quantitative Real-Time PCR measurement of BeWo cell syncytialization.....	79
Table 2-2 Specifications of antibodies utilized in immunoblotting experiments, and the protein mass loaded for each protein target	84
Table 2-3 Cell viability of NEFA-treated BeWo CT and SCT cells	88
Table 2-4 NEFA treatments did not affect the glycolytic activities of BeWo CT or SCT cells	95
Table 2-5 Maximal activity rates of mitochondrial enzymes in NEFA-treated BeWo CT and SCT cells.....	100
Table 3-1 Forward and reverse primer sequences used for quantitative Real-Time PCR analysis of BeWo cell syncytialization	123
Table 3-2 Specifications of antibodies utilized in immunoblotting experiments, and the protein mass loaded for each protein target	127
Table 3-3 Forward and reverse primer sequences used for quantitative Real-Time PCR mRNA microarray validation	130
Table 3-4 Syncytialization but not HG culture conditions impacts BeWo trophoblast mitochondrial respiratory activity.....	140
Table 3-5 HG culture conditions do not impact BeWo trophoblast glycolytic activity	140
Table 3-6 Syncytialization but not HG-culture media impacts BeWo metabolic enzyme activity and individual ETC complex activity	142

Table 4-1 Primer sequences used for quantitative Real-Time PCR validation of NEFA treatment microarrays, and their efficiencies.....	188
Table 4-2 FA profiles (% mol) of NEFA-treated BeWo trophoblast cells.....	192
Table 4-3 Neutral lipid profiles of NEFA-treated BeWo trophoblast cells.....	197

List of Figures

Figure 1-1 Structure of the human placenta.....	16
Figure 1-2 Schematic overview of mitochondrial nutrient oxidation.....	30
Figure 1-3 Summary illustration of the alterations to placental villous trophoblast nutrient processing and mitochondrial function under conditions of (A) maternal obesity and (B) maternal obesity with maternal dietary intervention.....	37
Figure 1-4 Summary illustration of the alterations to placental villous trophoblast nutrient processing and mitochondrial function under conditions of (A) maternal diabetes mellitus and (B) hyperglycemia in culture conditions.....	40
Figure 2-1 Cell culture timeline for BeWo cell NEFA-treatments.....	77
Figure 2-2 Representative Seahorse Mito Stress Test assay tracings.....	81
Figure 2-3 Representative Seahorse Glycolysis Stress Test assay tracings.....	82
Figure 2-4 100 μ M of PA, OA or P/O does not negatively impact BeWo cell syncytialization or upregulate pro-apoptotic pathways at 72H.....	91
Figure 2-5 Mitochondrial respiratory activity of BeWo cells following prolonged NEFA treatment.....	94
Figure 2-6 Prolonged NEFA treatment did not affect BeWo Electron Transport Chain complex protein abundance.....	98
Figure 2-7 Prolonged NEFA treatment does not alter oxidative state of BeWo cells.....	101
Figure 2-8 Prolonged NEFA treatments did not affect protein expression of enzymes involved in mitochondrial uptake of pyruvate or long-chain fatty acid species.....	104
Figure 3-1 Schematic of 72-hour hyperglycemic cell culture protocol.....	121
Figure 3-2 Representative tracings of the Seahorse XF Mito Stress Test and Glycolysis Stress Test in LG and HG-cultured BeWo trophoblasts.....	125

Figure 3-3 Viability of BeWo trophoblasts cultured under hyperglycemic (HG) conditions for 72h.....	136
Figure 3-4 Hyperglycemic (HG) culture conditions do not impact BeWo SCT cell fusion but are associated with increased CGB transcript abundance at 72h.....	138
Figure 3-5 Hyperglycemic (HG) culture conditions do not impact protein expression of Electron Transport Chain (ETC) complexes in BeWo trophoblasts.....	144
Figure 3-6 Syncytialization impacts mitochondrial dynamics in BeWo trophoblasts.....	146
Figure 3-7 Hyperglycemic (HG) culture conditions impact glycogen storage and regulation in BeWo trophoblasts.....	149
Figure 3-8 Hyperglycemic (HG) culture conditions impact triglyceride content in BeWo CT cells.	151
Figure 3-9 Principal Component Analysis (PCA) and volcano plot visualization of differentially expressed genes between low-glucose (LG) and hyperglycemic (HG) cultured BeWo CT cells.....	154
Figure 3-10 Heat map visualization of differentially expressed genes in hyperglycemic (HG) cultured BeWo CT cells.....	155
Figure 3-11 Pathway analysis of differentially expressed genes and RT-qPCR validation of microarray gene changes.....	156
Figure 3-12 Visualization of the degree of separation between metabolite profiles in HG and LG cultured BeWo CT cells.	158
Figure 3-13 Visualization of differentially abundant metabolites in HG-cultured BeWo CT cells.	159
Figure 3-14 Pathway analysis of metabolites identified in tiers 1 and 2.	160
Figure 3-15 Multivariate visualization of the degree of separation in lipidome profiles between LG and HG-cultured BeWo CT cells.	162

Figure 3-16 Volcano plot visualization of differentially abundant lipid species in HG-cultured BeWo CT cells.....	163
Figure 4-1 FA desaturase enzyme activity indices in NEFA-treated BeWo CT and SCT cells.	194
Figure 4-2 FA elongase enzyme activity Indices in NEFA-treated BeWo CT and SCT cells.	195
Figure 4-3 Principal Component Analysis (PCA) plot highlighting separation in transcriptome profiles between NEFA-treated BeWo CT cells.....	199
Figure 4-4 Volcano plot visualization of differentially expressed genes in BeWo CT cells cultured with 100 μ M NEFAs for 72 hours.....	200
Figure 4-5 Functional pathways enriched by NEFA-treatments in BeWo CT cells.....	201
Figure 4-6 Venn-diagram representation of differentially expressed genes between NEFA-treated BeWo CT cells and RT-qPCR validation of differentially expressed genes.	205
Figure 4-7 Multivariate visualization of the degree of separation between metabolite profiles in NEFA-treated BeWo CT cells.	208
Figure 4-8 Volcano plot visualization of the differentially abundant metabolites in NEFA-treated BeWo CT cultures.....	209
Figure 4-9 Venn Diagram highlighting the number of shared and unique differentially abundant metabolites in NEFA treated BeWo CT cells.	210
Figure 4-10 Pathway analysis of metabolite profiles of NEFA-treated BeWo CT cells.....	211
Figure 4-11 Joint Pathway Analysis of Transcriptome and Metabolome Profiles of NEFA-treated BeWo CT cells.....	213
Figure 4-12 Visualization of the degree of separation between lipidome profiles in NEFA-treated BeWo CT cells.....	216

Figure 4-13 Volcano Plot visualization of differentially abundant lipid species in NEFA-treated BeWo CT cells. 217

Figure 4-14 Differentially Abundant Lipid Classes in NEFA-treated BeWo CT cells. 219

Figure 4-15 Venn Diagram highlighting the number of shared and unique differentially abundant lipid classes in NEFA treated BeWo CT cells. 220

Figure 5-1 Summary illustration of the impacts of 8-Br-cAMP exposure on BeWo trophoblast cells. 247

Figure 5-2 Summary illustration of the impacts of hyperglycemia (25 mM) on BeWo trophoblast cells. 250

Figure 5-3 Summary illustration of the impact of OA-exposure (100 μ M) on BeWo trophoblast cells. 254

Figure 5-4 Summary illustration of the impacts of PA-exposure (100 μ M) on BeWo trophoblast cells. 256

Figure 5-5 Summary illustration of the impacts of P/O-exposure (50 μ M each PA and OA) on BeWo trophoblast cells. 257

List of Abbreviations

2WA	Two-Way ANOVA
4-HNE	4-Hydroxynonenol
AA	Arachidonic Acid (C20:4n6)
ACACB	Acetyl-CoA Carboxylase Beta
ACADVL	Very long-chain acyl-CoA dehydrogenase
ACSL1	Acyl-CoA Synthetase Long Chain Family Member 1
ACSL5	Acyl-CoA Synthetase Long Chain Family Member 5
ACTB	Beta Actin
AGA	Appropriate for Gestational Age birthweight
ATP	adenosine triphosphate
BCA	Bicinchoninic Acid
BHT	Butylated hydroxytoluene
BMI	Body-Mass-Index
BSA	Bovine Serum Albumin
CGB	Human chorionic gonadotropin subunit beta
CPT1	Carnitine Palmitoyltransferase 1
CPT2	Carnitine Palmitoyltransferase 2
CREB3L3	cAMP responsive element-binding protein 3-like 3
CS	Citrate Synthase
CT	Villous Cytotrophoblast
DEG	Differentially Expressed Gene
DHA	Docosahexaenoic Acid (C22:6n3)
DM	Diabetes Mellitus
DNP	Dinitrophenol
DOHaD	Developmental Origins of Health and Disease
DRP1	Dynamin-Related Protein 1
ECAR	Extracellular Acidification Rate
EL	Endothelial Lipase
ETC	Electron Transport Chain
EVT	Extravillous Trophoblast

FA	Fatty Acid
FABP	Fatty Acid Binding Protein
FADS1	Fatty Acid Desaturase 1
FADS2	Fatty Acid Desaturase 2
FASN	Fatty Acid Synthase
FAT/CD36	Fatty Acid Translocase
FATP	Fatty Acid Transport Protein
FC	Fold-Change
FDR	False Discovery Rate
GAPDH	Glyceraldehyde 3-phosphate dehydrogenase
GC-FID	gas chromatography coupled flame ionization detection
GDM	Gestational Diabetes Mellitus
GLUT	Glucose Transporter
GPAT3	Glycerol-3-Phosphate Acyltransferase 3
GSK3β	Glycogen Synthase Kinase 3 Beta
HbA1c	Glycated Hemoglobin
hCG	Human chorionic gonadotropin
HDL	High-Density Lipoprotein
HFD	High Fat Diet
HG	Hyperglycemic
HSD11B2	Hydroxysteroid 11-Beta Dehydrogenase 2
HSL	Hormone Sensitive Lipase
LC-MS	Liquid Chromatography Mass Spectrometry
LC-MS/MS	Liquid Chromatography with tandem Mass Spectrometry
LDH	Lactate Dehydrogenase
LDL	Low-Density Lipoprotein
LG	Low-Glucose
LGA	Large for Gestational Age birthweight
LPL	Lipoprotein Lipase
MUFA	Monounsaturated Fatty Acid
NAFLD	Non-Alcoholic Fatty Liver Disease
NHP	Non-Human Primate

OA	Oleic Acid (C18:1n9)
OCR	Oxygen Consumption Rate
OPA1	Optic Atrophy 1
OVOL1	Ovo Like Transcriptional Repressor 1
P/O	Palmitate and Oleate combination
PA	Palmitic Acid (C16:0)
PBS	Phosphate Buffered Saline
PCA	Principal Component Analysis
PDH	Pyruvate Dehydrogenase
PDHK1	Pyruvate Dehydrogenase Kinase 1
PHT	Primary Human Trophoblast
PLIN2	Perilipin 2
PLS-DA	Partial Least Squares Discriminant Analysis
PND	Post-Natal Day
PPP	Pentose Phosphate Pathway
PRPS1	phosphoribosyl pyrophosphate synthetase 1
PSMB6	Proteasome 20S subunit Beta 6
PUFA	Polyunsaturated Fatty Acid
QC	Quality Control
ROS	Reactive Oxygen Species
SCD1	Stearoyl-CoA Desaturase 1
SCT	Villous Syncytiotrophoblast
SGA	Small for Gestational Age birthweight
STZ	Streptozotocin
TCA Cycle	Tricarboxylic Acid Cycle
TG	Triglyceride
TLC-FID	Thin Liquid Chromatography coupled Flame Ionization Detection
VLDL	Very-Low Density Lipoprotein
WebGestalt	WEB-based Gene SeT AnaLysis Toolkit
WHO	World Health Organization
WHR	Waist-to-Hip Ratio
ZO-1	Zona occludens-1

List of Appendices

Appendix A Copyright permissions for Chapter 1	275
Appendix B Copyright permissions for Chapter 2	276

Chapter 1

1 Introduction

A version of this chapter has been published:

Easton ZJW, and Regnault TRH. The Impact of Maternal Body Composition and Dietary Fat Consumption upon Placental Lipid Processing and Offspring Metabolic Health. *Nutrients*. 2020;12: 3031. doi:10.3390/nu12103031

Reproduced with permission from MDPI (Appendix A)

1.1 The Developmental Origins of Health and Disease

Throughout the gestational period maternal nutrient handling must adapt to the increasing needs of the growing fetal-placental unit to ensure developmental processes continue in a healthy and physiological manner. For example, maternal insulin sensitivity diminishes, and fasting serum lipid levels rise late in gestation to preserve necessary macronutrients to support placental development, and fetal growth [1–3]. However, there is a fine balance within these physiological metabolic alterations that, when disrupted by environmental influences, can shift the course of in utero programming to promote the early life development of non-communicable metabolic disorders in the offspring.

The study of the impacts of maternal gestational environment on fetal growth and development is encompassed within the field of research known as The Developmental Origins of Health and Disease (DOHaD) [4,5]. This field of study evolved from the observations of Anders Forsdahl and David Barker in the 1970s and 80s. Forsdahl originally described an increased risk of death by coronary heart disease in those who were relatively impoverished during childhood, but later experienced prosperity [6]. Barker expanded these observations to include in utero gestational influences and reported that low birthweight babies were at a greater risk for developing metabolic complications such as obesity, type 2 diabetes (insulin resistance) and metabolic syndrome in adulthood [4,5]. This field of study has since expanded to include the observed increased risk of later life non-communicable diseases associated with metabolic syndrome in offspring exposed to adverse intrauterine environments such as those that occur with maternal nicotine use [7,8], perinatal hypoxia [9,10], and environmental and chemical toxicants [11]. Of particular interest in this thesis, are the adverse intrauterine environments caused by excessive nutrient abundance in pregnancies complicated by maternal gestational obesity, and diabetes mellitus (DM) [12–14].

1.2 Impacts of maternal obesity and diet during pregnancy

1.2.1 Maternal obesity and offspring metabolic health

The World Health Organization (WHO) categorizes healthy bodyweight in both adults and children via body-mass index (BMI, kg/m²), whereby a BMI > 25 is

overweight and a BMI>30 is obese [15]. The effects of an increased maternal body mass and associated adiposity during the gestational period on offspring later life health has been extensively documented in humans via population studies and meta-analyses [16–21]. In line with the DOHaD concept, obesity-exposed offspring have been found to be at a greater risk for later-life metabolic health issues due in part to an increased prevalence of having a birthweight that is not appropriate for their gestational age (AGA) [16,19]. While maternal gestational obesity has largely been associated with infants being born Large for their Gestational Age (LGA), there has also been a link between maternal obesity and greater risk of the offspring being born Small for their Gestational Age (SGA) [16,17,20]. Independent from maternal factors, LGA and SGA offspring are at an increased risk for developing non-communicable “adult-associated” metabolic disorders as early as four years of age [18,19]. However, there are concerning reports that children born to obese women are more likely to develop metabolic disorders regardless of their birthweight, suggesting that maternal body composition during pregnancy influences offspring metabolic health beyond simply altering birthweight [20]. Indeed, recent studies have suggested that maternal factors including pre-pregnancy BMI may better predict the development of offspring health complications than birthweight alone [20,21].

The negative influence that maternal adiposity has on offspring metabolic health has additionally been reported in numerous animal models that have attempted to elucidate the mechanisms that lead to early-life metabolic diseases in these offspring [22,23]. While maternal diet-induced obesity has been well associated with poor fetal metabolic outcomes in these models, it is important to note that variations are present in the dietary fat contents and periods of exposure used in these studies (**Table 1-1**). Rodent models in particular have been heavily utilized as pre-clinical models in studies examining the development of metabolic disorders. In these studies, pathological in utero programming has been suggested to facilitate the increased risk of metabolic disease in offspring born to high-fat diet (HFD) induced obese dams [24,25]. Specifically, high-fat exposed rodent offspring have been found to exhibit abnormal lipid profiles including hepatic steatosis that ultimately leads to Non-Alcoholic Fatty Liver Disease (NAFLD) and fibrosis at early life stages [26]. Altered glucose homeostasis is also prevalent in these obesity-exposed rodent offspring and is manifested as insulin resistance and an

eventual development of type 2 diabetes mellitus during adolescence [27,28]. Overall, the altered glucose and liver lipid metabolism observed in these offspring has been thought to be a precursor to the ultimate development of metabolic syndrome in gestational obesity-exposed adolescents [29,30].

Table 1-1 Summary of diet fat or feeding treatments utilized in animal models of maternal diet-induced gestational obesity and gestational high-fat exposure with and without diet reversal

Animal Model	Dietary Fat (% Caloric Intake)	Pre-gestational Obesity	Pre-conception Diet Exposure	Gestational Diet Exposure	Maternal Diet Reversal	Offspring Weaning	Reference
C57/B6 mice	60% High fat diet (HFD) 25% fat control diet	HFD-induced obesity	10–12-week HFD exposure before pregnancy	HFD maintained through pregnancy and lactation	Yes – 2-cell stage embryo transfer	Weaned onto control diet	Sasson [45]
C57/B6 mice	45% HFD 10% fat control diet	HFD-induced obesity	Diet commenced at 4 weeks; breeding at 10 weeks	HFD through pregnancy	No	Randomly assigned HFD or control diet	Elahi [26]
C57/BL6 mice	32% HFD 11% fat control diet	HFD-induced obesity	8-week pre-conception HFD-exposure	HFD through pregnancy	No	Fetal collections	Jones [23]
C57/B6 mice	16% HFD control diet 3% fat	Diet-induced obesity	6-week diet exposure pre-conception	HFD maintained through pregnancy and weaning	No	Pups weaned onto standard chow	Samuelsson [28]
C57/B6 mice	High trans-fat diet (6% partially hydrogenated vegetable oil + 1% soybean oil) 7% soybean oil control diet	No pre-pregnancy obesity	N/A	High trans-fat diet through pregnancy and weaning only	No	Weaned onto control diet	de Velasco [61]
Sprague-Dawley Rats	60% HFD 24% fat control diet	HFD-induced obesity	HFD commenced Postnatal day (PND) 24; breeding PND 120	HFD throughout pregnancy	No	Weaned onto control diet	Srinivasan [24]
Sprague-Dawley Rats	140% overfeeding model	Overfeeding-induced obesity	3-week overfeeding prior to conception	Overfeeding discontinued during pregnancy	Yes – dams switched to control feeding through pregnancy and lactation	Randomly weaned onto control (17% fat) or HFD (45% fat)	Borengasser [46]

Table 1-1 Summary of diet fat or feeding treatments utilized in animal models of maternal diet-induced gestational obesity and gestational high-fat exposure with and without diet reversal (continued)

Animal Model	Dietary Fat (% Caloric Intake)	Pre-gestational Obesity	Pre-conception Diet Exposure	Gestational Diet Exposure	Maternal Diet Reversal	Offspring Weaning	Reference
Sprague-Dawley Rats	140% overfeeding model	Overfeeding-induced obesity	3-week overfeeding prior to conception	Overfeeding discontinued during pregnancy	Yes – dams switched to control feeding through pregnancy and lactation	Randomly weaned onto control (17% fat) or HFD (45% fat)	Borengasser [47]
Wistar Rats	45% HFD 18% fat control diet	HFD-induced obesity with pre-gestational HFD exposure	Pre-conception HFD - commenced PND 22; breeding at PND 120 Pregnancy and lactation HFD - commenced at breeding and maintained through lactation)	HFD through pregnancy	No	Randomly assigned HFD or control diet	Howie [27]
Wistar Rats	38% HFD-diets 15% fat control diet	No pre-pregnancy obesity	N/A	HFD during pregnancy only; cross-fostered to lean dams during lactation	No	Weaned onto control diet; HFD exposure at 8 weeks	Dong [60]
Wistar Rats	20% lard supplement in HFD 5% fat control diet	HFD-induced obesity	HFD exposure from PND 21 to breeding at PND 120	HFD maintained through pregnancy and lactation	Yes – diet intervention back to control diet at PND 90	Not specified	Zambrano [44]
Sheep	155% overfeeding model	No pre-gestational obesity	Overfeeding commenced gestational day 115	Overfeeding from gestational day 115 to gestation (~day 150)	No	Control diet during lactation and weaning	Philip [32]
Sheep	150% overfeeding model	Overfeeding-induced obesity	60-day overfeeding exposure before mating	Overfeeding through gestation, control diet during lactation	No	control diet	Long [31]
Sheep	150% overfeeding model	Overfeeding-induced obesity	60-day overfeeding exposure before mating	Overfeeding until fetal collection	No	Fetal collection	Zhu [102]

Table 1-1 Summary of diet fat or feeding treatments utilized in animal models of maternal diet-induced gestational obesity and gestational high-fat exposure with and without diet reversal (continued)

Animal Model	Dietary Fat (% Caloric Intake)	Pre-gestational Obesity	Pre-conception Diet Exposure	Gestational Diet Exposure	Maternal Diet Reversal	Offspring Weaning	Reference
Sheep	150% overfeeding model	Overfeeding-induced obesity	60-day overfeeding exposure before mating	Overfeeding continued through pregnancy (with no intervention)	Yes - 150% overfeeding until gestational day 28 (with obesity intervention)	Fetal collection	Tuersunjiang [33]
Japanese Macaque	36% HFD 14% fat control diet	HFD-induced obesity	4–7-year HFD exposure pre-conception	HFD maintained through to fetal collections at gestational day 130	Yes – diet reversal 3 months prior to breeding	Fetal collection	Salati [105]
Japanese Macaque	32% HFD 14% fat control diet	HFD-induced obesity	2–4-year pre-gestational HFD induced obesity	HFD, or diet-reversal through pregnancy	Yes – pre-conception diet reversal on subsequent pregnancy	Weaned onto mothers gestational diet	McCurdy [34]
Japanese Macaque	32% HFD 14% fat control diet	HFD-induced obesity	4–7-year pre-gestational HFD exposure	HFD, or diet reversal through pregnancy	Yes – switched back to control diet in 5 th breeding season	Weaned onto <i>in utero</i> or reverse diet	Pound [35]
Japanese Macaque	32% HFD 14% fat control diet	HFD-induced obesity	2–9-year pre-conception HFD exposure	HFD, or diet reversal through pregnancy	Yes – switched back to control diet in 9 th breeding season	Fetal collections	Wesolowski [43]

Larger mammal species, including sheep, have also been used to study maternal overfeeding and obesity and its subsequent effects on offspring health and disease. As observed in human meta-analyses and experiments using rodent models, sheep offspring exhibit metabolic dysfunction both neonatally and into adulthood—including increased prevalence of obesity and aberrant lipid and glucose metabolism—in response to maternal obesity during gestation [31–33]. The non-human primate (NHP) model has also been well utilized to identify the underlying mechanisms that pre-dispose obesity-exposed offspring to later life metabolic disease. Specifically, these studies have demonstrated that third trimester fetal hepatic lipid and glucose metabolism is dysregulated in offspring exposed to maternal obesity during gestation [34,35].

Together, these human meta-analyses and animal models demonstrate that maternal obesity during the gestational period primes the exposed offspring for dysregulated lipid and glucose metabolism that ultimately results in metabolic disease development early in life. Furthermore, it is important to note that the negative impacts of maternal obesity on offspring in utero growth have been highlighted to occur in a sex-dependent manner, however different models have yielded conflicting data. For example, in humans maternal BMI has been demonstrated to correlate with bodyfat at birth in female infants, but not in males [36,37]. This increased risk of macrosomia at birth, may predispose females to greater risk of DOHaD related non-communicable diseases. Rodent models in contrast, have largely highlighted increased adiposity in adulthood is more prevalent in male offspring exposed to maternal obesity in utero than in female offspring. The increased risk of later life obesity in male offspring may be attributed to a greater rate of postnatal weight gain, increased food intake, increased circulating triglycerides levels, and increased susceptibility to visceral fat accumulation compared to their female counterparts [38–40]. These sex-dependent effects (and potential species-related differences in sex-dependent effects) need to be better elucidated to fully understand the impacts of in utero environment on later-life health.

1.2.2 Is maternal BMI an accurate predictor of offspring metabolic health?

The reports from these human and animal studies that link maternal obesity to offspring metabolic disease are of increasing importance to healthcare systems as the prevalence of obesity worldwide has reached unprecedented rates over the last several decades [41]. The WHO estimates that about 40% of men and women over the age of 18 were overweight or obese in 2016, and that proportion continues to rise [41]. More specific to pregnancy outcomes and in line with data from most industrialized nations, Health Canada reported in 2012-13 that 24% of Canadian women between 20-39 years of age (those of child-bearing age) were obese, and 44% had a waist circumference that was predictive of high risk for the development of health complications [42]. These reports suggest that the prevalence of early-onset metabolic syndrome in offspring will only continue to increase alongside the rising rates of maternal obesity.

Animal models utilizing dietary interventions in obese pregnancies, however, have highlighted that body composition metrics may not be the most accurate predictors of offspring future metabolic health and that maternal gestational diet is also an important influence on offspring health (**Table 1-1**). For example, in sheep models of gestational overfeeding-induced obesity, a maternal dietary intervention early in gestation resulted in lower circulating plasma triglyceride (TG) levels (improved lipid metabolic function) as well as decreased plasma insulin levels (improved glucose metabolism) in fetuses from obese pregnancies at both mid and late gestation [33]. Additionally, NHP data suggests that there are vast differences in the metabolic profiles of fetuses from obese mothers that consume different diets during gestation [34,35,43]. McCurdy et al. (2009) identified that a diet reversal to a control diet in obese pregnant Japanese macaques was sufficient to improve liver steatosis in third trimester fetuses, suggestive of a decreased risk of postnatal NAFLD. Subsequent studies described reductions in maternal and fetal dyslipidemia and oxidative stress in diet-reversed obese pregnancies leading to benefits in fetal liver development during the third trimester [43]. Additionally, improved third trimester pancreatic islet vascularization has been reported in response to diet reversal in NHP models, which suggests that these offspring would be less susceptible to later-life

development of type-2 diabetes mellitus [35]. These NHP studies highlight that maternal gestational obesity alone may not be the best predictor of offspring metabolic health and suggest that gestational diet is important in determining metabolic health risk in the obesity-exposed offspring.

Rodent models of obese pregnancy have also demonstrated the benefits of gestational diet reversals (**Table 1-1**). For example, male offspring of obese rats given a dietary intervention during the gestational period have improved metabolic outcomes including improved insulin sensitivity both neonatally and into adulthood [44]. However, additional rodent studies have suggested that a diet-reversal during pregnancy may not be sufficient to reverse the effects of maternal pre-pregnancy obesity, as has observed in sheep and NHP models. For example, mouse embryos transferred at the 2-cell stage from high-fat fed dams to control fed dams displayed poor *in utero* growth and neonatal catch-up growth, as well as an altered expression of imprinted genes that have been associated with obesity development [45]. These findings suggest that oocytes may be primed for adverse development as a direct result of poor maternal diet pre-conception [45]. Furthermore, other rodent models have reported poor liver and skeletal muscle mitochondrial health at post-natal day 35 in offspring exposed to maternal pre-pregnancy obesity [46,47]. Specifically, hepatic tissue of rat offspring born to obese dams displayed a marked decrease in the protein expression of markers of mitochondrial health and biogenesis despite both control and obese dams being fed a control diet during the gestational period [47].

The presence of the conflicting data between rodent and larger mammal (sheep and NHP) models may simply arise from physiological differences between these species. For example, the longer gestational period of sheep and NHP, and the fact that these species, like humans, have largely prenatal developmental processes potentially underlies the impacts of a gestational diet reversal intervention on fetal growth and development [48,49]. Further studies must be conducted to fully understand whether dietary changes during human pregnancy are sufficient to reverse insults from a poor maternal diet as in the NHP and sheep models and some rodent models or if human oocytes are ‘primed’ for metabolic disease with pre-gestational obesity exposure. Overall,

these diet reversal studies have suggested that maternal diet prior to conception and during pregnancy has a profound impact of the metabolic health of the offspring.

1.2.3 Maternal dietary fat consumption and offspring metabolic health

Human population data has demonstrated that circulating maternal free fatty acid (FA) levels are predictive of offspring metabolic health risks independent from measures of maternal body composition, highlighting the importance of dietary lipids during gestation [50]. Additionally, in animal-based studies, dietary fat components are altered in obese pregnancy dietary interventions further signifying dietary fats themselves are important in promoting the development of metabolic disorders in obesity-exposed offspring.

In general, different FA species have varying impacts on metabolic health based on the length of the FA chain (short, medium, long, or very-long chain FA) as well as on the degree of saturation of the FA [51,52]. For example, a diet rich in cis-monounsaturated FA species (MUFAs) and polyunsaturated fats (PUFAs)) has been associated with increased level of High-Density Lipoprotein (HDL), the “good cholesterol”, and thus a healthier lipid metabolic profile [52,53]. Consumption of omega-3 PUFA species is also associated with reduced hepatocyte production of TG-rich very-low density lipoprotein (VLDL) particles, resulting in decreased delivery of FA species to peripheral tissues [54–56]. Overall, omega-3 PUFAs have been linked to improvements in metabolic health and function and may be an important factor in preventing insulin resistance and type 2 diabetes in obese populations [57,58]. In contrast, a high consumption of trans-unsaturated FA species has been found to lower serum levels of HDL and promote a less healthy metabolic profile [53]. Additionally, a high consumption of saturated FA species has been associated with poor metabolic profiles including increased serum levels of TGs (stored in VLDL particles), free cholesterol, low-density lipoprotein (LDL; the “bad cholesterol”) and an increased risk of metabolic syndrome [52,59].

More importantly, consumption of certain FA species during pregnancy may promote the development of metabolic disorders in the offspring. For example, studies in rodent models have highlighted maternal diets comprised of different saturated FA chain lengths have varying impacts on offspring later-life metabolic health [60]. Specifically, gestational diets that were overabundant in medium chain length FA species from coconut oil (55% of FA species C14:0 or shorter) resulted in decreased offspring obesity development compared to offspring exposed to a maternal overconsumption of longer-chain FA species from soybean oil (all FA C16:0 or longer) [60]. Additional rodent models have demonstrated that maternal diets rich in trans-unsaturated FA species adversely affect offspring liver mitochondrial oxidative function, as well as increase circulating levels of TGs, highlighting an overall dysregulation of hepatic lipid handling [61]. These studies further highlight that maternal dietary fat consumption is important an independent factor in offspring risk for metabolic disease development.

To determine the impact of maternal dietary fat content upon fetal health outcomes in human populations, it is important to fully understand the diet consumption patterns of pregnant women. More importantly, it is necessary to understand how these maternal diets deviate from the recommendations of government health agencies and clinical guidelines to provide insight into possible dietary interventions that can reduce offspring metabolic health complications. Canada's food guide for example, recommends that pregnant women only consume a small amount (1-3 tbsp) of saturated fat each day. In addition to limiting saturated fat intake, it is also recommended that these less healthy FA species are replaced with more polyunsaturated omega-3 and omega-6 FAs (PUFAs). Specifically for pregnant women, Health Canada guidelines suggest consumption of at least 200 mg of Docosahexaenoic acid (DHA) (an omega-3 PUFA) as this FA is necessary for proper fetal brain development [62]. However, despite these guidelines, blood lipid analysis has suggested that a majority of pregnant women consume diets that greatly deviate from food guide recommendations [63]. It is estimated that on average one-third of total caloric intake in pregnant women is from lipid sources [63–65]. While this total fat intake falls within current Food Guide recommendations, many women do not consume healthy amounts of PUFAs and saturated fats [63–65]. Specifically, these women have been found to consume diets that are calorie-dense but low in nutrients,

overabundant in long-chain saturated FA, and lacking in important unsaturated FA species such as DHA [65–67].

Overall, an increased maternal consumption of long-chain saturated FAs and limited intake of omega-3 PUFAs during pregnancy may be an important in utero insult that predisposes the offspring to metabolic complications early in life and may specifically underlie poor outcomes in obese pregnancies.

1.3 Maternal diabetes mellitus and pregnancy outcomes

1.3.1 Maternal diabetes mellitus and offspring metabolic health.

Similar to maternal obesity and also in line with the DOHaD hypothesis, maternal DM during pregnancy has been associated with poor metabolic health outcomes in the exposed offspring. For example, offspring of mothers with gestationally-developed DM (GDM) have an increased risk of being born LGA, and developing non-communicable cardiometabolic diseases such as obesity, type 2 diabetes, and metabolic syndrome [68–71]. It is important to note that there is significant overlap between obese and GDM pregnancies, as obesity is an independent risk factor of GDM development [72,73]. Thus, offspring metabolic disease in GDM pregnancies may be partially mediated by maternal obesity. However, recent studies have highlighted that GDM, and obesity are independent regulators fetal growth and development despite the overlaps in these co-morbidities [74,75]. Interestingly, maternal dietary patterns have also been linked to the pathophysiology of GDM, and a maternal adherence to a healthy lifestyle diet lowers the risk of maternal GDM development [76–78]. These data further highlight that maternal diet during pregnancy is an important factor in not only determining fetal metabolic health outcomes, but maternal metabolic health outcomes as well.

In addition to GDM, maternal pre-pregnancy type 2 DM has been linked with poor pregnancy outcomes, and offspring metabolic disease [79]. However, as maternal GDM and type 2 DM are often concurrent with maternal obesity, the direct impacts of maternal DM on offspring outcomes may be confounded in these pregnancies. Thus, examining the impacts of pre-existing type 1 DM, may better highlight the independent negative impacts of DM during pregnancy on fetal development. For example, children

born to type 1 diabetic mothers have an increased risk of developing obesity, and metabolic syndrome compared to peers born to healthy mothers, and these diseases are manifested as early as 7 years of age [80–83]. Additionally, offspring of type 1 diabetic mothers are often born LGA which, as described previously, may directly underlie their increased risk of metabolic disease development [84,85]. Like in cases of maternal obesity, the negative impacts of pre-pregnancy DM on offspring health have been highlighted in studies utilizing animal models. For example, studies using rodent models exposed to streptozotocin (STZ, a pancreatic β -cell toxin) to induce pre-pregnancy diabetes have demonstrated increased adiposity, and impaired glucose metabolism in diabetic-exposed offspring both neonatally and into adulthood [86–88]. Additional readouts in STZ-induced diabetes in larger mammals such as sheep have likewise highlighted impaired glucose metabolism in the exposed offspring [89].

The impacts of maternal diabetes during pregnancy, much like those of maternal gestational obesity, have been highlighted to occur in a sex-dependent manner. In humans, maternal diabetes and gestational hyperglycemia has been associated with macrosomia, increased rates of congenital abnormalities, and increased rates of respiratory disorders in males but not females [36,90]. Follow-up cohort investigations have further revealed that males, but not females, exposed born from a pregnancy complicated by GDM had an increased risk of being overweight by 5 years of age [91]. The increase in macrosomia at birth and adiposity in childhood in males, may increase their risk of developing non-communicable metabolic diseases later in life. Interestingly, mothers carrying male fetuses have been found to have an increased risk of developing GDM, compared to mothers carrying female fetuses, highlighting that some pregnancy complications are impacted by fetal sex [92]. Overall, these studies have further highlighted that fetal sex is a crucial consideration in the DOHaD field of study and understanding specifically how male and female fetuses adapt to environmental stress, especially the stresses in conditions of nutrient overabundance is of increasing importance.

While the impacts of maternal obesity on offspring metabolic health may likely be mediated by a poor maternal diet overabundant in saturated FA species, the impacts of

maternal diabetes on fetal development are likely due to maternal hyperglycemia. In fact, children born to diabetic women who maintained appropriate glycemic control throughout gestation have been found to have reduced birthweight and improved neonatal outcomes compared to children born to diabetic mothers with poor glycemic control [93,94]. Thus, maintaining appropriate glycemic control and preventing maternal hyperglycemia in diabetic pregnancies may be essential in limiting impacts to offspring metabolic health.

Overall, investigations into the impacts of obesity and maternal DM on offspring metabolic health have revealed that nutrient overabundance (i.e. dietary fats in obesity, and glucose in DM) is an important factor in the *in utero* programming of offspring metabolic health.

1.4 The Developmental Origins of Health and Disease and the placenta

The placenta is a transient organ composed of a heterogeneous population of cells that facilitates hormone production, fetal immunity and all gaseous, nutrient and waste transport between maternal and fetal circulation. It consists of two distinct but important populations of placental trophoblast cells (extravillous trophoblasts (EVTs) and villous trophoblasts) that arise from the outer trophoblast layer of the pre-implantation blastocyst, as well as the fetal extraembryonic mesoderm and fetal placental blood vessels. EVT cells are responsible for invading into the uterine decidual tissue to establish the maternofetal blood connection (by remodeling uterine spiral arteries) as well as act to anchor chorionic villi to the uterine wall (**Figure 1-1a**). In contrast, the villous trophoblast cells of the chorionic villi act as a transport layer and comprise the physical barrier between maternal blood supply (facilitated by maternal spiral arteries emptying into the intervillous space) and fetal circulation (**Figure 1-1a**). The villous trophoblast layer is comprised of two unique cell populations: underlying progenitor cytotrophoblast (CT) cells and fused multi-nucleated (differentiated) syncytiotrophoblast (SCT) cells [95] (**Figure 1-1b**). The SCT cells of the villous trophoblast layer arise following the differentiation and fusion of progenitor CT cells.

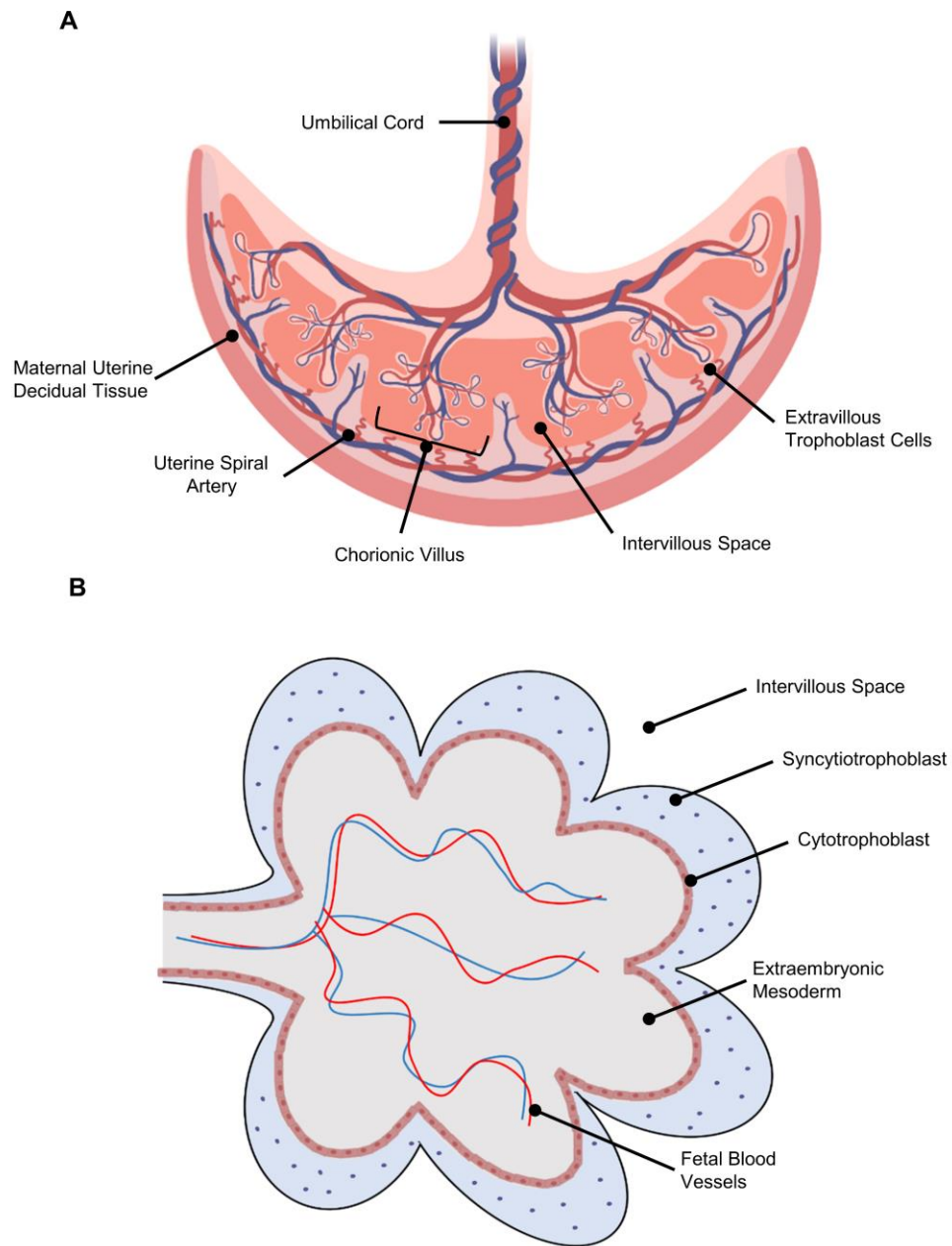


Figure 1-1 Structure of the human placenta.

Illustration showing (A) a sagittal cross-section of the mature human placenta, and (B) a magnified view of the placenta chorionic villus highlighting the location of cytotrophoblasts and syncytiotrophoblast cells. Created with biorender.com.

Maintenance of normal physiological function of the placenta is vital for proper fetal development, and impairments in placental growth, development, and function in obese and diabetic pregnancies are thought to underlie the *in utero* programming of offspring metabolic disease [96–99]. For example, placentae from obese pregnancies have morphological abnormalities including immature chorionic villi structures, and an increased placental-to-fetus weight ratio (a marker of placental insufficiency or a poorly functioning placenta) [100,101]. Additionally, maternal gestational obesity is often associated with increased inflammation in placental tissues highlighted by increased pro-inflammatory cytokine abundance (e.g. TNF α , IL-6) and macrophage accumulation that can be detected as early as mid-gestation [102–104]. NHP models of gestational obesity have likewise demonstrated reduced placental and uterine blood perfusion and increased placental inflammation with maternal obesity [105,106]. However, these impairments in obese NHP placentae were improved with a diet-reversal from a high-fat diet to a healthy control diet [105], overall suggesting that a poor maternal diet in obese pregnancies facilitates the development of offspring metabolic health complications by impairing the function of the placenta.

Morphological abnormalities have likewise been described in pregnancies complicated with pre-existing DM or GDM. Specifically, DM during pregnancy has been associated with increased intervillous space volume, increased placental vascularization as well as an increased placental-to-fetal weight ratio [107–110]. Interestingly, metformin (an insulin sensitizing drug) treatment has been linked with improved placental development in some GDM pregnancies [111], which highlights that impaired maternal glucose metabolism and hyperglycemia may underlie placental abnormalities in diabetic pregnancies. Overall, these data highlight that maternal nutrient environment is a key regulator of placental development.

Notably, placental abnormalities from obese and diabetic pregnancies have also been demonstrated to be influenced by fetal sex. For example, in obese pregnancies, female but not male placentae were found to have increased rates of chorionic villitis, an inflammatory placental lesion [112]. In contrast, male placentae have been found to have impaired anti-oxidant capacity in response to maternal obesity, which has been thought to

promote the development of pregnancy complications and adverse outcomes [113]. These studies may highlight that the molecular mechanisms that underlie aberrant *in utero* programming in response to maternal adiposity is dependent on the sex of the fetus.

In diabetic pregnancies, female placentae display altered microRNA signatures (associated with endoplasmic reticulum protein processing; proteoglycan synthesis; and Hippo signaling) suggestive of an increased responsiveness to the nutrient excessive environment of GDM [114]. This sex-specific difference especially in diabetic pregnancies may highlight an underlying mechanism in the female placenta that may act in an adaptive manner to protect the female fetus from an adverse hyperglycemic *in utero* environment. More importantly, these sex-specific differences in placental function may help explain the reduced rates of pregnancy complications and macrosomia in female fetuses in diabetic pregnancies [36,90]. Future investigations are needed to highlight how fetal sex impacts placental development, and function in order to better understand how the placenta regulates *in utero* programming of non-communicable metabolic disease.

1.4.1 Placental metabolic impairments in adverse maternal environments

In addition to facilitating morphological and structural alterations in the placenta, maternal obesity and diabetes also negatively impacts metabolic and nutrient processing functions in the CT and SCT cells of the placental villous trophoblast layer [115–118]. As CT and SCT cells are directly responsible for materno-fetal nutrient transport, alterations to the metabolic functions in these cells may impact nutrient transport to the fetus and directly underlie the *in utero* programming of metabolic disease. Specifically, impairments in placental handling of glucose and dietary fats highlighted by alterations in the transport, storage and oxidation of these nutrients has been documented in obese and diabetic pregnancies. Understanding how maternal obesity, maternal dietary fat consumption, maternal DM, and maternal hyperglycemia individually modulate these important placental nutrient processing functions and elucidating what these changes mean for the developing fetus, will provide a better understanding of the placental mechanisms that facilitate early-onset metabolic diseases in the exposed offspring.

As the placenta is discarded at the end of pregnancy, the endpoint impacts of maternal obesity and DM on placental nutrient processing functions can be explored by analyzing term placental lysates. Moreover, examining term placentae may also allow researchers to determine how maternal dietary interventions in obesity and appropriate glycemic control in diabetes influence placental metabolic functions. For example, CT cells have been cultured from term human placentae following planned, non-labouring Caesarean-section births and utilized to examine placental metabolic function in obese pregnancies with and without a dietary intervention [119,120]. Additionally, the isolated effects of individual nutrients (fats and glucose) on placental metabolic processes can be examined using immortalized villous trophoblast cell lines (including BeWo, JAR and JEG-3 cells) that are available for commercial purchase. The BeWo choriocarcinoma cell line in particular, has been demonstrated as a viable model of placental barrier function and has been extensively utilized to examine the isolated effects that individual PUFA species have on placental lipid processing [121,122]. Overall, the use of placental cell lines such as the BeWo trophoblast cell line can allow for insight into how different dietary FA species and hyperglycemia independently impact placental metabolism and nutrient handling.

1.4.2 Mechanisms of fatty acid and glucose transport in the placenta

The human placenta has an extensive ability to uptake lipid species and shuttle them and their metabolic byproducts into fetal circulation. Proteomic analysis of term primary human trophoblast (PHTs) has revealed that the placenta expresses lipid transport proteins on both the apical microvillous (maternal-facing) and basolateral (fetal-facing) membranes [123]. Specifically, Fatty Acid Transport Proteins 1, 2 and 4 (FATP1, FATP2, FATP4); Fatty Acid Binding Proteins 1 and 3 (FABP1, FABP3) as well as Fatty Acid Translocase (FAT/CD36) are expressed in the human placenta [123–126]. In addition, isolated PHTs have demonstrated activity of Lipoprotein Lipase (LPL) indicating that lipid species packaged as TGs in lipoproteins (VLDL particles) can be processed by the placenta [127,128]. Lipase enzymes such as LPL are responsible for cleaving TG species in VLDL particles to release free FAs so that they can then be

imported into the placenta by facilitative transport via the FATPs, FABPs and FAT/CD36 [129].

The FATPs as well as FAT/CD36 are localized on both the basolateral and apical placental membranes and are involved in transporting a wide range of FA species across the placenta [123,130]. The presence of these transporters on both apical and basal placental membranes suggests a bidirectional transfer of non-esterified fatty acids (NEFAs) can occur to respond to the changing nutrient demands of both mother and developing fetus [123,130]. In contrast, FABP transporters that demonstrate preferential binding for PUFA species are largely localized to the maternal-facing apical membranes of the placenta [58,64]. This may suggest that PUFA species are transported unidirectionally across the placenta into the fetal circulation in order to support and prioritize proper fetal brain development [123,131]. Similar to PHTs, the BeWo cell line has been demonstrated to uptake and transport dietary NEFA species [132]. Specifically, this cell line has been shown to express the lipid transporters: FATP1, FATP4, FAT/CD36 as well as FABP1 and FABP3 [132,133]. Although caution must be taken with interpretation of data from immortalized cell lines, since BeWo cells express the same lipid transport proteins as PHTs they may represent a viable model for studying placental barrier function and lipid transport,

In addition to facilitating the transfer of lipid species to the developing fetus, the placenta also has a high capacity to transport glucose from mother to fetus. In total, the placenta has been shown to express multiple glucose transporter (GLUT) isoforms including: GLUT1, GLUT3, GLUT4, GLUT8, GLUT9, GLUT10, and GLUT12 [134–138]. The GLUT1 isoform is the highest expressed GLUT isoform in placenta, highlighting its specific importance in facilitating trans-placental glucose transport [136,137]. Additional work has demonstrated GLUT1 is largely localized to the maternal-facing apical membrane of SCT cells which suggests that GLUT1 expression on the fetal-facing placental basal membrane is a rate-limiting factor in transplacental glucose transport [135,136]. Further, GLUT1 expression increases from the first trimester and remain elevated throughout the duration of gestation, highlighting that materno-fetal glucose transfer increases as pregnancy progresses to support fetal growth and

development [136]. The BeWo trophoblast cell line also expresses GLUT1, GLUT3 and GLUT8 isoforms [139–141]. Further studies have demonstrated an asymmetric distribution of GLUT1 expression between apical and basal membrane in BeWo trophoblasts, as well as that induction of syncytialization with 8-Br-cAMP in BeWo trophoblasts increases GLUT1 expression [140,142]. These studies suggest that the BeWo trophoblast cell line may additionally represent a viable model for studying placental glucose transport and metabolism. Thus, BeWo trophoblasts may be useful in elucidating placental responses to independent dietary fat overabundance and hyperglycemia.

1.4.2.1 Maternal obesity and placental nutrient transport

Maternal obesity during pregnancy has been associated with an altered expression and activity of lipid transporters in the placenta. Specifically, an increase in the activity of LPL and mRNA expression of FAT/CD36 in conjunction with diminished mRNA levels of FATP1, FATP4 and FABP3 as well as reduced protein expression of FABP3 have been observed with increased maternal adiposity [127,128]. These alterations in placental nutrient transporter expression have ultimately been associated with reduced placental uptake of important omega-6 PUFA species such as linoleic acid [127], which could overall impact important fetal growth processes including brain development. Overall, the observed increases in the activity and expression of placental LPL and FAT/CD36 may facilitate increased lipid transport into fetal circulation and could potentially explain the increased prevalence of LGA offspring in obese pregnancies. In contrast, the specific reduction in the expression of FATP and FABP transporters may reflect that the placenta is attempting to modulate transplacental lipid transport under conditions of lipid overload to prevent fetal lipid toxicity. The notion that the placenta is able to modulate materno-fetal lipid transfer in response to nutritional state is supported by recent NHP experiments that identified increased protein expression of FATP and FABP transporters under conditions of maternal nutrient restriction [143].

The relative influences that individual dietary FAs have on obesity-mediated altered placenta lipid transport can help predict how maternal diet interventions may impact fetal metabolic disease. While almost one-third of the total lipid consumption of

pregnant women is saturated fats, current research into the effects of individual NEFA supplementation on placental lipid transport has largely emphasized the effects of dietary PUFAs. Cell culture experiments conducted with the BeWo cell line have found that a 24 hour exposure to 100 μ M concentrations of individual unsaturated NEFAs (Oleate, DHA, and Arachidonic Acid (AA)) has no influence on placental FATP expression [132]. Similarly, there were no significant alterations in FATP expression in PHTs from women who took DHA supplements during the third trimester [144]. PUFAs may in contrast, have an ability to alter the expression of FABP transporters within the placenta and specifically AA has been found to increase the expression of FABP3 in BeWo cells following 24 hours in culture [133]. Increased expression of FABP3 in AA-treated BeWo cells may be reflective of the preferential transport of PUFA species by placental FABPs [58,64]. Future research must increasingly focus on the effects of saturated dietary fats to elucidate if a maternal saturated fat overconsumption independent of body composition leads to increased materno-fetal lipid transport via LPL and FAT/CD36 mediated transport. Furthermore, understanding the molecular mechanisms that potentially regulate this increased materno-fetal lipid transport could lead to the development of pharmacological inhibitors to better modulate in utero growth.

Overall, maternal obesity has largely not been associated with alterations in the expression or protein abundance of GLUT1 transport proteins [145–147], although some studies have shown reductions in placental GLUT1 expression in the obese placenta [148]. Overall, these data suggest that increased maternal adiposity has limited impacts on trans-placental glucose transport. However, current research has not investigated the direct impacts of dietary FA species on placental expression of GLUT transport proteins, and these interactions need to be elucidated.

1.4.2.2 The impacts of maternal diabetes mellitus on placental nutrient transport

In contrast to obese pregnancies, diabetic pregnancies have been associated with relatively limited alterations in the expression of placental FATP and FABP transporters. Specifically, studies have found no alterations in the protein abundance or mRNA levels of LPL, FAT/CD36, FATP2, and FATP4 in Type 1 diabetic and GDM pregnancies [149–

152]. However, increased placental LPL activity has been highlighted in Type 1 diabetic pregnancies, despite no alterations in LPL protein abundance, potentially indicating that post-translational modifications regulate LPL activity [151]. Additionally, the expression of endothelial lipase (EL) and hormone-sensitive lipase (HSL) is elevated in placentas from Type 1 diabetic and GDM pregnancies [150,153]. Interestingly, the increased expression of EL and HSL is more profound in women with poor glycemic control, suggesting that maternal hyperglycemia directly modulates placental expression of these enzymes [150]. The increased activity of LPL and increased expression of EL and HSL in uncontrolled diabetic pregnancies may, like in obese pregnancies, facilitate increased placental lipid uptake by increasing free FA concentrations at the placental barrier, and may in turn underlie the increased risk of offspring being born LGA [84,85]. Placental term explants from uncomplicated healthy pregnancies cultured under hyperglycemia for 18 hours, however, were not found to have altered expression of EL, LPL, FAT/CD36, FATP2 or FATP4 [149]. The limited impacts of hyperglycemia on placental EL expression in culture may simply be due to the limited duration of high glucose exposure [149]. Currently, there is limited insight into how independent hyperglycemia impacts lipid transport mechanisms in placental cell line models such as BeWo trophoblasts.

Maternal DM during pregnancy has also been linked with alterations in placental glucose transport mechanisms. Specifically, pre-gestational diabetes and GDM have been associated with increased basal membrane (but not apical membrane) GLUT1 expression leading to approximately a 40-60% increase in glucose transport across the fetal-facing membrane [154,155]. Interestingly, these differences in GLUT1 expression between diabetic and control pregnancies were evident despite the diabetic groups displaying normal glycated-hemoglobin (HbA1c) levels indicative of appropriate glycemic control at term [154]. It is important to note however, that some studies have presented conflicting data and have described no alterations to placental GLUT1 expression in response to maternal GDM [156], indicating that the mechanisms underlying GDM-mediated alterations to placental glucose transport remain poorly understood. Overall, as correlations have been found between basal-membrane GLUT1 density and offspring birthweight [147], increased placental expression of GLUT1 may underlie the

development of fetal macrosomia, and in turn the development of later life metabolic health complications in offspring exposed to DM [84,85].

Studies utilizing PHT culture systems, have highlighted that exposure to independent hyperglycemia (20-25 mM for 48 hours) is associated with reduced placental glucose transport, and reduced GLUT1 mRNA and protein abundance compared to euglycemic cultured controls [157]. Further work from this research group additionally highlighted that a 48 hour hyperglycemia exposure was associated with increased internalization of GLUT1 transporters that may facilitate their previously observed reductions in glucose transport [158]. Overall, these data highlighted that hyperglycemia is an important regulator of placental glucose transport. However, the differences between the impacts of hyperglycemia in vitro (reduced GLUT1 expression and increased GLUT1 internalization) and the impacts of diabetes in vivo (increased basal membrane GLUT1 expression) still need to be investigated and understood.

1.4.3 Placental nutrient storage

The villous trophoblast cells of the placenta not only have the capability to uptake and transfer NEFAs from maternal circulation to the fetus, but also to store them as lipid droplets for future metabolic needs [159–161]. Analysis of the activity of FA transport proteins on placental membranes has indicated that placental lipid up take is greater on maternal facing membranes than on fetal-facing membranes, highlighting that placental lipid storage and/or metabolism is an important aspect of placental lipid processing [161]. In fact, both CT and SCT cells accumulate lipid droplets, and the lipid droplet abundance and volume has been reported to be similar in these cells at term [162]. Interestingly however, studies examining PHTs treated with fluorescently-labelled FA substrates have found that only CT cells, and not SCT cells, exhibit FA esterification activity leading to increased lipid droplet abundance [162–164]. Reduced lipid droplet synthesis in SCT cells was associated with decreased expression of lipid metabolism genes including Glycerol-3-Phosphate Acyltransferase 3 (GPAT3), an enzyme involved in TG formation [162]. These data may highlight that transcriptional regulation directly underlies the differences in lipid droplet synthesis between differentiated SCT cells and progenitor CT cells. Additionally, placental villous trophoblast cells have been found to express Fatty

Acid Synthase (FASN), highlighting that de novo lipogenesis may also contribute to placental lipid droplet formation. However, the activity of enzymes involved in FA synthesis have been found to be low in term placentae [165,166], suggesting that these pathways may be of little importance in placental lipid handling.

Similar to placental lipid transporters, placental GLUT transporters are more prevalent on maternal-facing apical placental membranes than on fetal-facing basal membranes [135,136], suggesting that nutrient storage may also be an important aspect of placental glucose processing. In fact, placental trophoblasts store large quantities of glycogen [167–169], further highlighting that nutrient storage is an important component of overall placental nutrient handling. Interestingly, CT cells are the predominant area for glycogen storage in the placenta [167,168]. Since these cells are also the predominant area for new lipid storage in the placenta, these cells may be especially important in placental nutrient processing, as has recently been proposed [163].

Overall, placental nutrient stores are thought to be a mechanism by which the placenta modulates materno-fetal nutrient transport in order to control fetal growth trajectories [169–171]. Thus, any alterations in placental villous trophoblast nutrient storage mechanisms in response to adverse maternal nutrient environments (such as those in obese and diabetic pregnancies) may lead to aberrant trans-placental nutrient transport and facilitate the in utero programming of fetal metabolic disease. As with nutrient transport, the impacts of maternal obesity, and DM as well as the independent impacts of dietary FA and hyperglycemia can be examined through the use of term placental lysates, in conjunction with cultured PHTs, term placental explants, and placental cell line systems.

1.4.3.1 The impacts of obesity, and maternal diet on placental nutrient storage

Maternal gestational obesity has been well demonstrated to alter placental lipid storage resulting in a pathological accumulation of lipid droplets (steatosis) at term [116,165,172,173]. Analysis of the composition of these lipid droplets has demonstrated that saturated FAs and MUFAs are the predominate lipid species that are stored in the

obese placenta and may indicate increased supply of saturated FA and MUFA species to the placental in obese pregnancies [174]. Further underlying this increased TG accumulation in obese pregnancies is altered placental metabolic processing of FA species via desaturation [175]. FA desaturation refers to the enzymatic introduction of a new double bond in the carbon backbone of FA species, increasing the units of unsaturation in the FA. In the placenta, an important mediator of FA desaturation is the enzyme stearoyl-CoA desaturase-1 (SCD1) which introduces a new double bond into palmitate or stearate producing the MUFA species palmitoleate and oleate, respectively [176]. Previously, maternal obesity has been demonstrated to increase placental mRNA expression of SCD1, that may highlight an increased formation of MUFA species in the obese placenta [116]. As MUFA species have been found to be preferentially localized to lipid droplets in the placenta [177], increased SCD1 expression in obese placenta may underlie previously observed increases in TG accumulation. It is important to note however, that conflicting reports have highlighted reduced SCD1 activity in obese placenta, overall resulting in decreased placental palmitoleate synthesis [178]. The mechanisms by which maternal obesity, and maternal dietary fat consumption impact placental SCD1 expression and activity, and how these changes related to placental lipid accumulation requires further investigation. The human placenta has also been found to express isoforms of Fatty Acid Desaturase 1 (FADS1) and Fatty Acid Desaturase 2 (FADS2) which introduce double bonds into a variety of PUFA species [179,180], although the activity of these enzymes is low in placental tissues [181,182].

Studies examining the impacts of independent dietary FAs on PHTs and BeWo trophoblast cells have highlighted that oleate (a dietary MUFA) is highly lipogenic in trophoblasts leading to increased TG abundance [132,183]. Interestingly, co-culture of PHT cells with both oleate and palmitate (a dietary saturated FA) was associated with reduced TG formation versus oleate-alone exposure [183]. Overall, these data highlight that dietary FA species regulate placental lipid storage both independently and in combination and may reflect that altered fat supply to the placenta facilitates the development of steatosis in obese pregnancies. In fact, dietary intervention studies in obese pregnancies, have highlighted that altering maternal dietary fat intake can modulate placental lipid accumulation. Specifically, maternal dietary supplementation with omega-

3 PUFAs decreases placental lipid accumulation at term in obese pregnancies [165]. Further, human population data indicates that obese women from pacific regions such as Hawaii who naturally consume greater levels of omega-3 rich fatty foods such as fish have less severe placental steatosis than obese women from landlocked areas such as Ohio who generally consume diets less plentiful in omega-3 fats [116,184]. However, as previously stated, lipid esterification is an important regulator of transplacental lipid transport. Thus, an improvement in placental steatosis with omega-3 PUFA supplements without correcting an underlying maternal overconsumption of saturated fats may be harmful to the fetus through increasing transplacental saturated FA transport. In fact, there may be an increased risk of offspring being born LGA in pregnancies that are supplemented with omega-3 PUFA, which itself may promote the development of later life metabolic disease [185,186]. Overall, a simple dietary supplementation may not be sufficient to improve adverse fetal outcomes, and a more rigorous dietary intervention that also addresses maternal saturated fat and MUFA consumption may be required.

While the impacts of maternal obesity on placental lipid storage have been thoroughly explored, the impacts of obesity on glycogen storage in the human placenta have not been well documented [187]. However, in rodent models maternal high-fat feeding induced obesity has been associated with increased placental glycogen accumulation [188], which may further highlight aberrant placental nutrient storage in obese pregnancies. Overall, the direct influence of maternal obesity and dietary fat consumption on placental glycogen synthesis, and how this may relate to materno-fetal glucose transport remains not well defined.

1.4.3.2 Maternal diabetes mellitus and placental nutrient storage

Maternal pre-gestational Type 1 DM, and maternal GDM have also been highlighted increase TG and lipid droplet accumulation in the placenta at term [118,150,189–191]. Interestingly, placental expression of SCD1 is elevated in GDM pregnancies, further highlighting the potential role of FA desaturation in facilitating placental lipid accumulation [189]. However, it is important to note that additional examinations of placental steatosis in diabetic pregnancies have highlighted that increased placental TG abundance only occurs in women with GDM and a BMI>30, but

not in women with pre-gestational Type 1 and Type 2 DM, or GDM and a BMI<30 [149]. The differences in placental lipid accumulation in these reports may be due to differences in glycemic control between study populations.

Independent hyperglycemia has also been demonstrated to be an independent regulator of placental lipid storage. Specifically, placental explants from healthy uncomplicated pregnancies were found to have increased rates of FA esterification, and increased TG accumulation when cultured under hyperglycemic conditions [149,191]. However, additional analyses have demonstrated that glucose overabundance does not increase placental TG content to the extent that oleate exposure does, suggesting that glucose is less lipogenic in placental trophoblasts than dietary MUFAs [192]. These data, nonetheless, highlight that maternal hyperglycemia in diabetic pregnancies is an important regulator of placental lipid storage and TG content.

Maternal pre-gestational DM and GDM are also well associated with increased glycogen accumulation at term in both humans and in rodent models [190,193–196]. More importantly, data from both human and rat studies have highlighted that increased placental glycogen accumulation is associated with poor maternal glycemic control, suggesting that increased glucose supply to the placenta directly induces glucose storage as glycogen [193,194]. This increased glycogen content in response to maternal hyperglycemia may serve to modulate trans-placental glucose transport, potentially in an effort to reduce fetal overgrowth, as has previously been hypothesized [170]. However, the investigations into the direct impacts of elevated glucose levels on placental glycogen storage using PHT and placental cell line culture systems are limited [197,198]. For example, a study by Schmon *et al.* (1991) did not find differences in PHT glycogen abundance after 4 days of high glucose exposure. The lack of glucose-mediated impacts on glycogen content may arise as this study utilized differentiated SCT cells, which are not a predominant site of placental glycogen storage [167,168]. In contrast, Pattillo *et al.* (1971) has described increased glycogen accumulation in BeWo trophoblast cells cultured under high glucose conditions. Overall, the mechanisms underlying glycogen synthesis and storage in response to nutrient overload are poorly understood.

1.4.4 Placental mitochondrial function and nutrient oxidation

Mitochondria are important organelles responsible for cellular energy production and homeostasis in the placenta [199,200]. For example, the inner mitochondrial matrix contains important metabolic enzymes involved in the citric acid cycle (or tricarboxylic acid cycle (TCA cycle)) that are utilized to generate the co-factors NADH and FADH₂ from acetyl-CoA [201] (**Figure 1-2**). The cellular acetyl-CoA utilized in the TCA cycle in the placenta is the product of glucose and fatty acid metabolism, via glycolysis and β -oxidation, respectively [201]. In brief, glycolysis is a metabolic process that occurs in the cytosol, whereby one six-carbon glucose molecule is broken down and converted into 2 three-carbon pyruvate molecules [202]. The newly synthesized pyruvate can then be processed anaerobically via Lactate Dehydrogenase (LDH) to form the metabolite lactate [202]. Additionally, pyruvate can be processed inside the mitochondrial matrix via the Pyruvate Dehydrogenase (PDH) complex to produce acetyl-CoA necessary for the TCA cycle [203] (**Figure 1-2**). The process of FA β -oxidation is discussed in depth in Section 1.4.4.1. Additionally, the amino acid glutamine is an important oxidative fuel in placental trophoblasts [204]. Once in the mitochondrial matrix glutamine is metabolized to glutamate via the enzyme glutaminase, and subsequently to α -ketoglutarate via the enzyme glutamate dehydrogenase [204] (**Figure 1-2**). The generated α -ketoglutarate then directly feeds into the TCA cycle to generate NADH and FADH₂.

Ultimately, the NADH and FADH₂ generated by the TCA cycle act as electron donors for the Electron Transport Chain (ETC) complexes on the inner mitochondrial membrane [205]. The shuttling of electrons through the first 4 ETC complexes (ETC complex I-IV) and ultimately to oxygen (the terminal electron acceptor) generates a proton gradient across the inner mitochondrial membrane that is then utilized by the final ETC complex (complex V or ATP synthase) to generate the cellular energy carrying molecule adenosine triphosphate (ATP) [205] (**Figure 1-2**). This process is also known as oxidative phosphorylation or mitochondrial respiration. ATP is subsequently utilized in a variety of important cellular processes in the placenta, including the synthesis of proteins, hormones, nucleic acids, and glycogen, as well as transplacental nutrient transport [206–208].

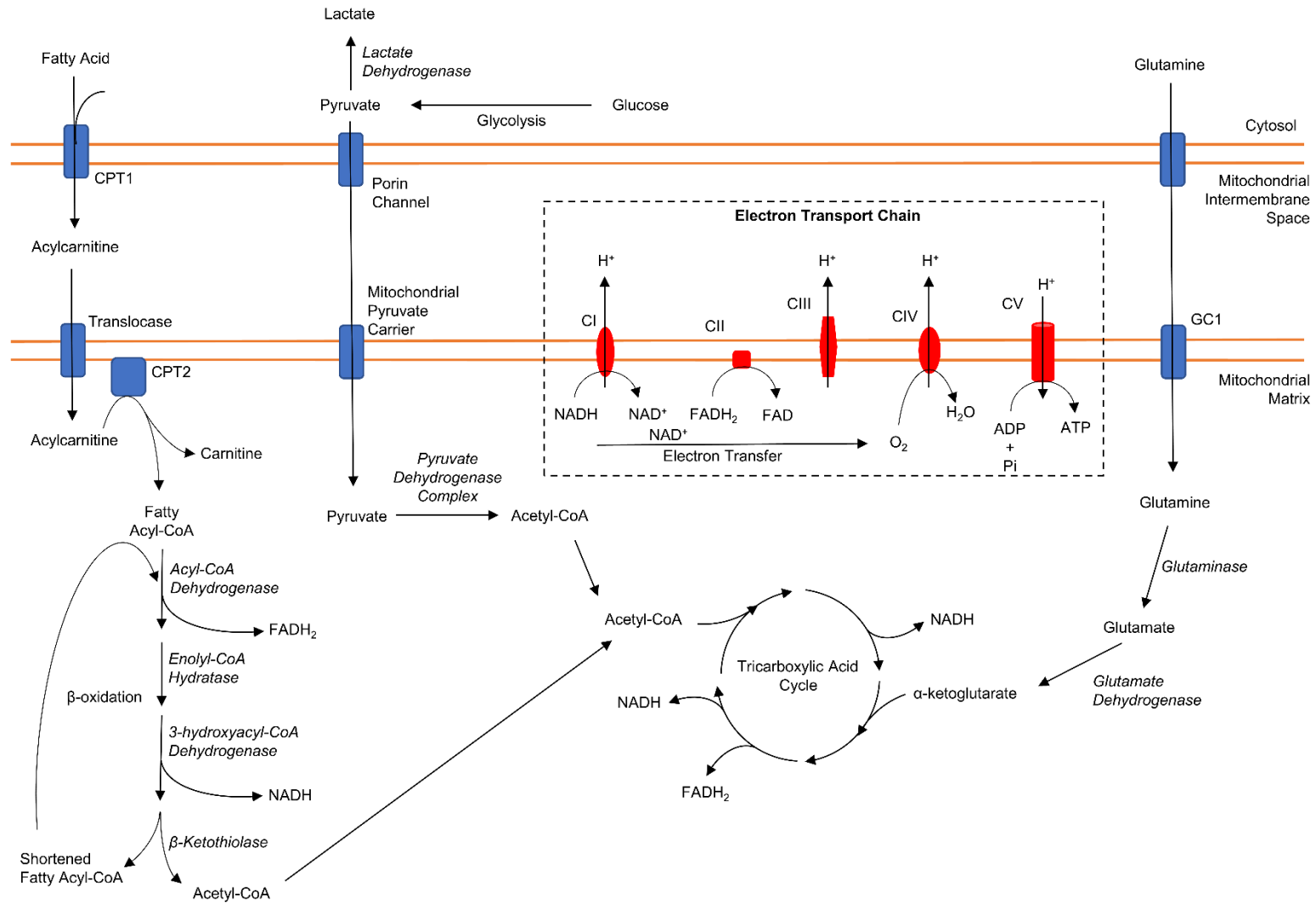


Figure 1-2 Schematic overview of mitochondrial nutrient oxidation.

Interestingly, recent studies have highlighted that progenitor CT cells display greater mitochondrial respiratory activity than differentiated SCT cells, further highlighting the importance of CT cells in placental nutrient processing [118,163,209,210]. More importantly, adverse maternal metabolic environments in obese and diabetic pregnancies impair placental mitochondrial function. For example, maternal gestational obesity has been linked with an overall reduction in mitochondrial ETC activity (mitochondrial oxidative function) in term PHT cultures leading to reduced placental ATP levels [115,211]. Notably, the expression of miR-210 (a marker of mitochondrial dysfunction) is only elevated in the placentae of female fetuses from obese pregnancies, potentially highlighting sex-dependent impacts of maternal environment on placental mitochondrial function [212]. These sex-specific changes may underlie the previously observed macrosomia only in female offspring of human obese pregnancies [37]. Further targeted investigations of ETC complex activity in term placenta lysates has also demonstrated specific impairments in complex I and complex II activity in the obese placenta [117]. However, the direct impacts of maternal dietary fat consumption and individual dietary FA species on placental mitochondrial respiratory activity and ETC complex function are poorly understood.

PHTs cultured from GDM pregnancies also display similar impairments in mitochondrial respiratory activity leading to reduced ATP production [118,210,213]. These impairments in mitochondrial activity in PHTs from GDM pregnancies were shown to be restricted to CT cells, and not SCT cells, further demonstrating the importance of these progenitor trophoblasts in regulating the overall metabolic function of the placenta [118]. Further, women with GDM and a BMI>30 were found to have morphological abnormalities in placental mitochondria that may specifically underlie altered mitochondrial respiratory activity [214]. In addition to GDM, women with pre-gestational DM have also been found to have impaired ETC complex function at term [117]. Specifically reduced activities of ETC complexes I, II, and II were observed in term placental lysates from type 1 DM pregnancies and reduced activities of ETC complexes II and II were observed in term placental lysates from type 2 DM pregnancies [117]. Previously, independent hyperglycemia has been demonstrated to stimulate BeWo

trophoblast mitochondrial dehydrogenase activity and decrease JAR and JEG-3 placental trophoblast mitochondrial dehydrogenase activity following 24 hours of high glucose exposure when analyzed by endpoint tetrazolium salt assay [215]. These data suggest that hyperglycemia is an independent regulator of placental mitochondrial function. However, targeted functional analysis of mitochondrial respiratory activity in PHTs cultured under high glucose conditions revealed no hyperglycemia-mediated impairments to mitochondrial function [118].

Overall, these data demonstrate that placental mitochondrial respiratory impairments are highly prevalent in obese and diabetic pregnancies. These impairments in placental mitochondrial respiration may have vast consequences on global placental functions and may be of great importance in the placental programming of fetal metabolic disease. However, underlying mechanisms regulating placental mitochondrial respiration in response to dietary FAs and glucose need to be elucidated to better understand the impacts of maternal obesity and DM on placental mitochondrial function.

1.4.4.1 Placental β -oxidation

In addition to impacting placental mitochondrial function via impacting oxidative ATP production, maternal obesity and DM have been highlighted to impact placental mitochondrial FA oxidation (β -oxidation). Alterations in this important mitochondrial function in obese and diabetic pregnancies may not only impact placental ATP production but also alter transplacental lipid transport, and subsequently impact fetal growth and development.

As previously mentioned, β -oxidation is the process by which FA species are catabolized into acetyl-CoA that is utilized to regenerate NADH and FADH₂ (**Figure 1-2**). The first step of β -oxidation is the dehydrogenation of an acyl-CoA species and is catalyzed by an acyl-CoA dehydrogenase enzyme. There are multiple isoforms of this enzyme, each of which is responsible for initiating β -oxidation of acyl-CoA species of a different length. Specifically, medium-chain acyl-CoA dehydrogenase (MCAD) has an optimal activity with FA chains containing 8 carbon atoms; long-chain acyl-CoA dehydrogenase (LCAD) has optimal activity with 12-carbon FAs; and very long-chain

acyl-CoA dehydrogenase (VLCAD) is most active with 16-carbon FAs [216]. Next, enoyl-CoA hydratase catalyzes the hydration of the newly formed Trans carbon double bond. Subsequently, 3-hydroxyacyl-CoA dehydrogenase converts the newly formed hydroxyl group to a keto functional group. Two isoforms of 3-hydroxyacyl-CoA dehydrogenase, SCHAD and LCHAD, catalyze reactions derived from short-chain and long-chain FAs respectively [216]. Finally, β -ketothiolase—which has the short and long-chain isoforms, SKAT and LKAT—cleaves the carbon chain to generate a shortened acyl-CoA molecule and a new molecule of acetyl-CoA [216]. Under normal physiological conditions, complete β -oxidation occurs whereby all carbon atoms in the FA backbone are converted into acetyl-CoA molecules that are oxidized for ATP production [95,96]. However, under pathological conditions such as lipid overload, mitochondrial β -oxidation may become incomplete resulting in accumulation of shortened chain acyl-CoA molecules within the mitochondrial matrix that may then be exported into circulation [217,218].

However, in order to undergo β -oxidation, the FA-derived acyl-CoA molecule must be first transported into the mitochondrial matrix through a carrier-mediated process. Acyl-CoA molecules are conjugated to l-carnitine, an amino acid-derived molecule, in the cell cytosol through an enzymatic process via Carnitine Palmitoyltransferase I (CPT1) at the outer mitochondrial membrane. The acylcarnitine molecules are then shuttled into the intermembrane space where the protein transporter translocase shuttles the molecule into the mitochondrial matrix. Finally, Carnitine Palmitoyl Transferase II (CPT2) catalyzes the hydrolysis of the acyl-carnitine enabling the free FA molecule to undergo β -oxidation. While the majority of circulating maternal carnitine can be attributed to dietary sources, tissues including the placenta can synthesize l-carnitine from precursor amino acids [219,220].

Immunohistochemical staining of isolated placental cells and western blot protein analysis of term and early gestation human placental explants has revealed that villous trophoblast cells express enzyme isoforms for all enzymatic steps in the mitochondrial β -oxidation pathway. Both SCT and CT cells express the Acyl-CoA dehydrogenase isoforms VLCAD, LCAD, and MCAD; enoyl-CoA hydratase; the 3-hydroxyacyl-CoA

dehydrogenase enzyme isoforms SCHAD, and LCHAD; as well as the 3-ketoacyl-CoA thiolase enzyme isoforms LKAT, and SKAT [221–223]. Notably, the expression levels of these β -oxidation enzymes within placental explants are similar to that of skeletal muscle—a tissue known to be highly dependent on β -oxidation for ATP production—highlighting that FA oxidation is critical for placental function [221]. Additionally, the ability of placental mitochondria to utilize lipid substrates for ATP production varies over gestation [223]. Specifically, mid gestational placental explants display an elevated expression of mitochondrial β -oxidation enzymes compared to term samples, suggesting that the capacity of the placenta to utilize FA as a metabolic substrate may diminish as pregnancy progresses [223].

1.4.4.2 Maternal obesity, and β -oxidation

Independently, maternal gestational obesity has been shown to impede the ability of term placental mitochondria to oxidize FA species for ATP production [116,224]. Decreased intra-placental concentrations of acylcarnitine species (a marker of β -oxidation) combined with an overall reduction in mitochondrial content within term obese placentae suggests that this aberrant maternal environment can negatively impact placental β -oxidation activity [116]. However, while β -oxidation primarily occurs within the mitochondria, placental peroxisomes have also been found to express enzymes for FA oxidation [120,225,226]. Specifically, the enzymes involved in peroxisomal β -oxidation are acyl-CoA oxidases (ACOX), D-bifunctional protein (DBP) and 3-ketoacyl-CoA thiolases [225,227]. In brief, peroxisomal β -oxidation shortens long-chain FA species into acetyl-CoA and short-chain acyl-CoAs such as octanoyl-CoA which can then be exported into the mitochondria in a CTP1 independent manner for further oxidation [225,227]. More importantly, environmental cues such as fatty acid overabundance in obesity are associated with increases in both the size and number of peroxisomes [116,228]. Additionally, maternal obesity has been linked increased mRNA expression of peroxisomal β -oxidation enzymes, suggesting that peroxisomal β -oxidation is a major component of placental lipid handling in obese pregnancies [116]. Obese placentae were further found to have greater rates of oxidation of radio-labelled palmitate following treatment with etomoxir (a mitochondrial β -oxidation inhibitor) than non-obese placentae

highlighting that increases in peroxisomal β -oxidation may act to modulate lipid oxidation in obese pregnancies with poor mitochondrial function [116]. Overall, these results suggest that the balance between mitochondrial and peroxisomal β -oxidation in the placenta is disrupted by obesity.

Maternal diet has also been identified to impact placental lipid oxidative function in some obese women. Specifically, obese Hawaiian women, who consume the Pacific diet, have similar mRNA expression levels of mitochondrial and peroxisomal β -oxidation enzymes as lean Hawaiian women [184]. This may suggest that the increased PUFA content of the Pacific diet could moderate the balance between mitochondrial and peroxisomal lipid oxidation. In contrast however, dietary omega-3 PUFA supplementation in obese pregnancies from landlocked areas (Ohio) was not linked to alterations in mRNA expression of mitochondrial and peroxisomal β -oxidative enzymes although these dietary supplements alleviated placental steatosis [165]. Additionally, omega-3 PUFA supplements did not alter [^3H]palmitate oxidation rates in cultured villous trophoblast cells from otherwise healthy obese Ohioan women [165]. While PUFA supplementation studies have highlighted some favourable outcomes, further investigation of the impact upon mitochondrial and peroxisomal β -oxidation pathways is warranted.

An illustration summarizing the impacts of maternal obesity and dietary interventions on placental nutrient processing is available in **Figure 1-3**.

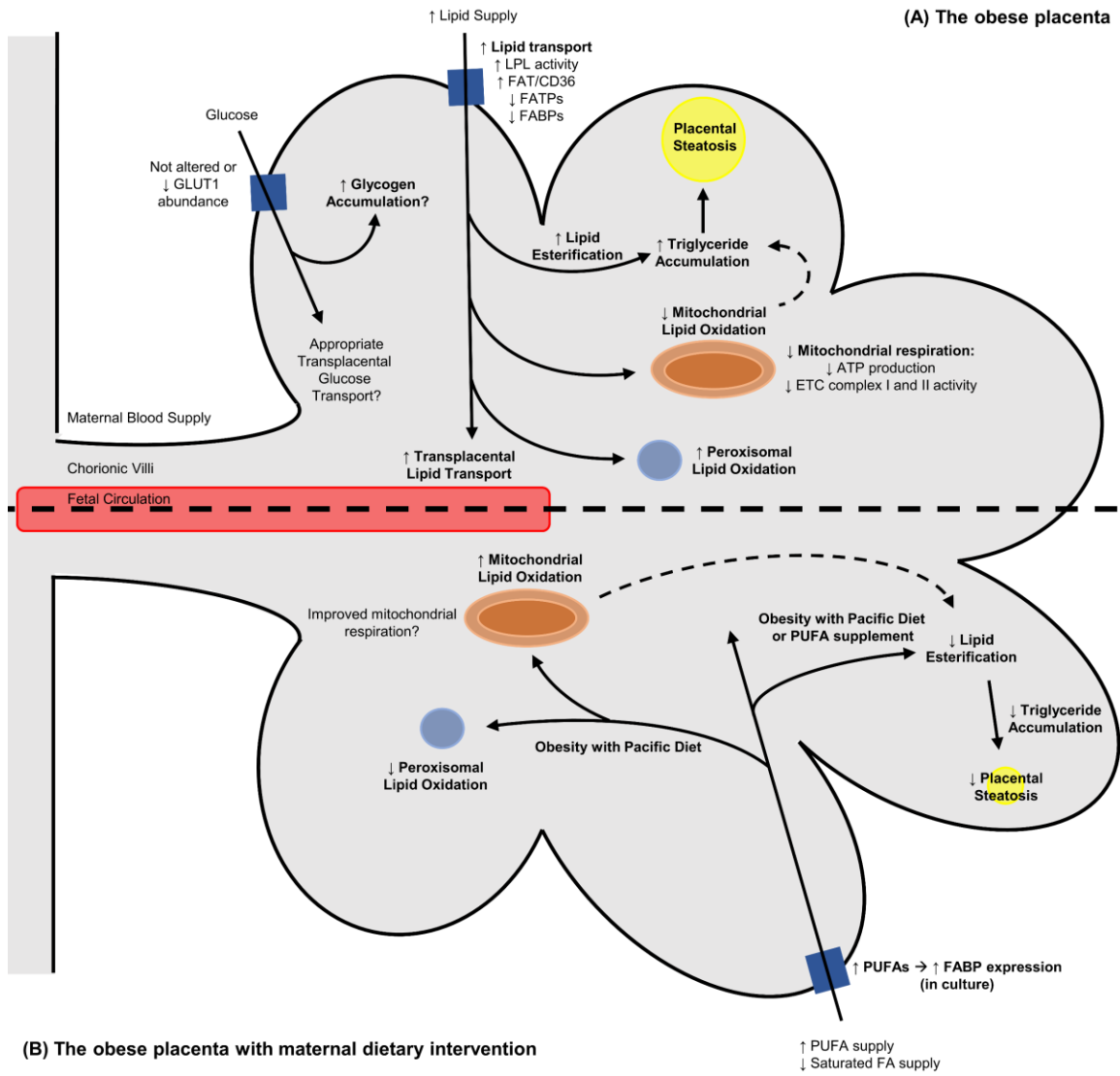


Figure 1-3 Summary illustration of the alterations to placental villous trophoblast nutrient processing and mitochondrial function under conditions of (A) maternal obesity and (B) maternal obesity with maternal dietary intervention.

Maternal gestational obesity has been associated with increased transplacental lipid transport (mediated by increased LPL activity and increased FAT/CD36 expression), increased placental lipid esterification and lipid droplet formation as well as decreased placental mitochondrial β -oxidation with concomitant increased peroxisomal β -oxidation. Additionally, term placental villous trophoblasts from obese pregnancies have been found to have impaired mitochondrial respiratory activity with specific underlying impairments in the activities of ETC complexes I and II. These changes are understood to be important in utero insults that program the development of early-life metabolic disease in the offspring from obesity-exposed pregnancies. An improved maternal diet in obese pregnancies, such as with consumption of a 'pacific diet' or use of dietary PUFA supplements, has been associated with reduced placental steatosis and improved placental β -oxidative function (increased mitochondrial β -oxidation with simultaneous decreased peroxisomal β -oxidation). These changes highlight that maternal dietary fat intake is an important regulator of placental nutrient processing and suggests that a poor maternal diet underlies the development aberrant placental metabolic function in obese pregnancies.

1.4.4.3 Maternal diabetes mellitus and placental β -oxidation

Maternal DM during pregnancy, much like maternal obesity, is associated with impaired placental β -oxidation processing. Specifically, cultured term placental explants from both laboring vaginal deliveries and non-laboring cesarean section deliveries from GDM pregnancies have been shown to have reduced [^3H]palmitate oxidation compared to explants from healthy control pregnancies [191,229]. Independent hyperglycemia exposure was subsequently demonstrated to decrease [^3H]palmitate oxidation rates, and CPT1 activity in cultured explants from healthy control pregnancies, highlighting that diabetic hyperglycemia may directly impair placental β -oxidation [191]. Interestingly, placental explants cultured with CPT1 agonists (resulting in increased β -oxidation) in conjunction with hyperglycemia have reduced placental TG accumulation compared to explants cultured with hyperglycemia alone [149]. These data suggest that decreased placental β -oxidation is also implicated in the development of placental steatosis in response to elevated glucose supply [149].

An illustration summarizing the impacts of maternal DM and independent glucose exposure on placental nutrient processing is available in **Figure 1-4**.

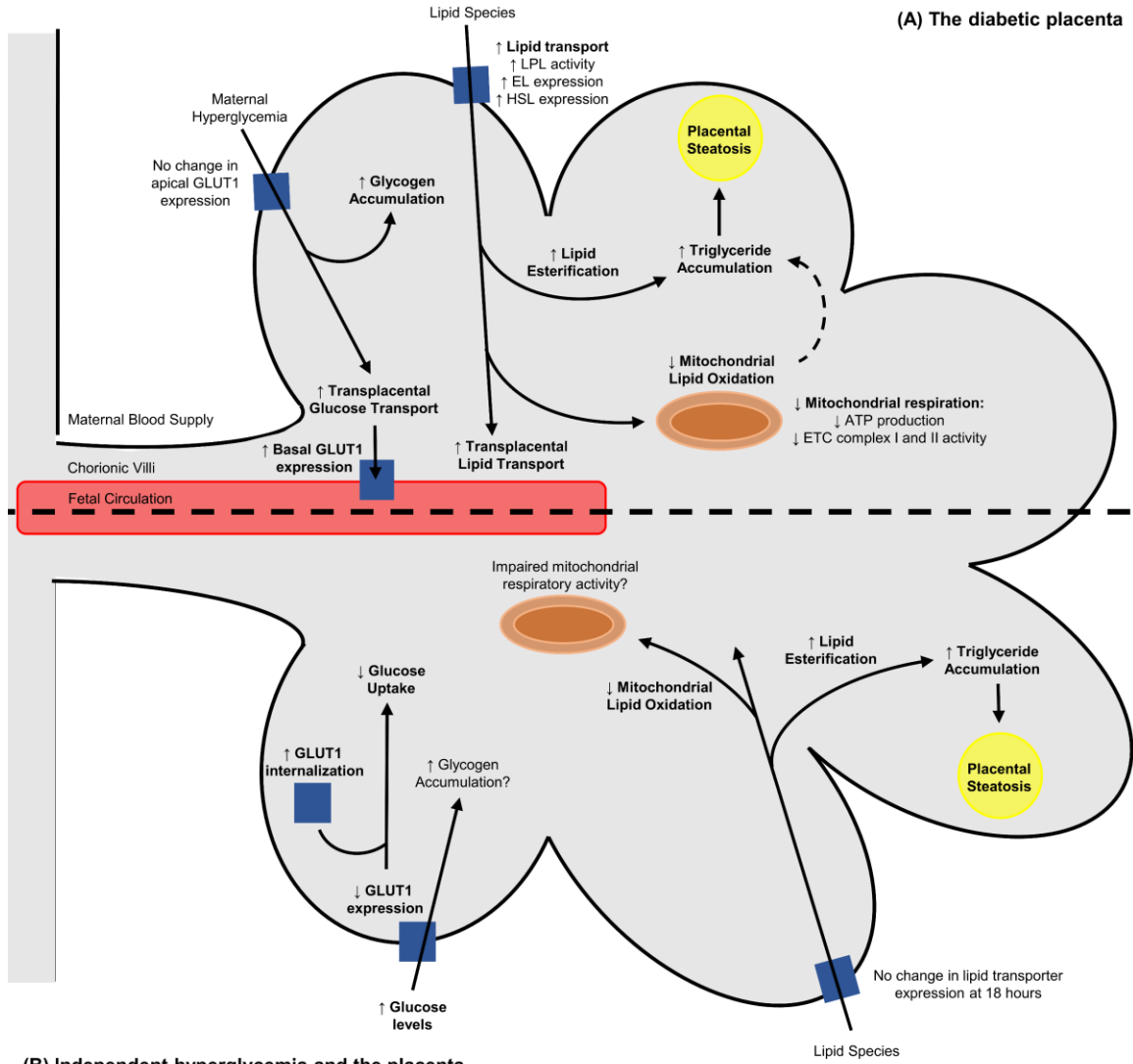


Figure 1-4 Summary illustration of the alterations to placental villous trophoblast nutrient processing and mitochondrial function under conditions of (A) maternal diabetes mellitus and (B) hyperglycemia in culture conditions.

Maternal diabetes mellitus has been associated with increased basal membrane GLUT1 protein abundance and increased glycogen content. Further, diabetic placentae exhibit increased lipid esterification, and placental steatosis in conjunction with reduced β -oxidation activity. Diabetic placenta mitochondrial have also been found to have impaired mitochondrial respiratory activity highlighted by an underlying impairment in the functions of ETC complexes I and II. These changes in placental nutrient oxidation and processing are thought to mediate pathological transplacental nutrient transport, ultimately impacting fetal growth and increasing the risk of offspring metabolic disease. High glucose exposure in cultured *ex vivo* placental preparations and *in vitro* placental cell line systems has subsequently highlighted that increased glucose levels independently regulates placental nutrient storage (e.g., glycogen and triglycerides), nutrient transport, and nutrient oxidation. Thus, maternal hyperglycemia in diabetic pregnancies may directly facilitate the observed impairments in placental development and function.

1.4.4.4 Acylcarnitines as biomarkers of placental β -oxidative function

Overall, adverse intrauterine environments resulting from maternal obesity and diabetes have been linked with impaired β -oxidative activity in the placenta. Interestingly, placental β -oxidation biomarker signatures may have future utility in clinical diagnostic tests to assess placental function in real time throughout gestation. One potential method to quantify placental β -oxidative function in obese and diabetic pregnancies may be through examining the acylcarnitine profiles of maternal blood products. Previously, analysis of differences in acylcarnitine profiles has been utilized to predict the presence of aberrant metabolic function in tissues including cardiac and skeletal muscle [230–234]. As previously highlighted, obesity is associated with reduced placental acylcarnitine abundance [116]. Thus, analyzing maternal blood acylcarnitine profiles specifically in obese pregnancies may allow for the real-time identification of aberrant placental mitochondrial β -oxidative function.

Acylcarnitine profiles have previously been examined as potential biomarkers for the early-detection of other placental diseases such as pre-eclampsia [235,236]. Specifically, potential acylcarnitine biomarkers for the early detection of pre-eclampsia were found in both maternal serum and plasma [235,236]. In addition, acylcarnitines have also been examined as potential non-invasive biomarkers to examine placental metabolic function under conditions of maternal obesity [116,237,238]. Notably however, maternal acylcarnitine profiles differ based upon the blood fraction that they are isolated from. For example, increases in some short chain acylcarnitine species were reported in maternal serum with increasing BMI [237], while no differences were found in acylcarnitine profiles in maternal plasma [238]. As this field of investigation develops, these blood fraction dependent differences in acylcarnitine profiles will need to be considered in order accurately assess placental metabolic function.

Overall, acylcarnitine analysis represents an emerging field in placenta physiology. Analysis of differences within these profiles in obese and diabetic women may allow clinicians to diagnose placental mitochondrial dysfunctions early in the gestational period, prior to onset of clinical disease. In turn, acylcarnitine biomarkers may

allow clinicians to monitor the impacts of dietary interventions and stringent glycemic control regimens on placental lipid handling during gestational period and subsequently modulate the course of treatment, if needed, to limit the risks of offspring developing disease in later life.

1.5 Omic analyses and the placenta

Recently, large datasets generated using omics based research approaches have been utilized to elucidate the underlying mechanisms governing placental development and function [239–241]. In a biological context omics generally refers to examining something in its entirety [242]. For example, transcriptomics examines all expressed ribonucleic acid (RNA) species, such as messenger RNA (mRNA), and highlights global gene expression in a tissue or cell. Metabolomics, on the other hand, refers to the study of small polar metabolite species that are the endpoint products of biological metabolic processes. The metabolome of a given tissue or cell culture system is thought to be a measure of the overall cell or tissue phenotype [243–245]. In addition, lipidome readouts highlight global cellular polar and neutral lipid species profiles and is a relatively recent development in omics research [246]. It is important to note that these readouts have previously been utilized to identify markers associated with metabolic dysfunction in other organs including cardiac [247,248] and hepatic [249,250] systems. In the pregnancy field, these important hypothesis-generating tools have been utilized to help elucidate how fetal sex impacts baseline placental metabolism in healthy pregnancies [251,252]. These omics based approaches have also been utilized to provide detailed insight into how an aberrant maternal environment disrupts normal physiological function of the placenta [253]. While each of these omics based approaches has been demonstrated to be useful on their own, recent studies have also highlighted that integrating or combining these readouts can provide a more in depth understanding of the underlying regulation of important biological functions [241,254,255].

In the context of maternal obesity and diabetes during pregnancy, omics based analyses have allowed for a thorough understanding of underlying mechanisms that underlie the development of impaired placental function. For example, transcriptomic signatures have highlighted mechanisms involved in inflammation, lipid metabolic

processing, and nutrient transport that are dysregulated in the obese and diabetic placenta [256–260]. Excitingly, some of the markers (such as increased mRNA expression of *IGKV2D-28* and *PTPRG*) have been proposed to have utility as diagnostic biomarkers that may enable clinicians to recognize early-onset GDM more easily [261]. Additionally, lipidomic and metabolomic analyses have highlighted that maternal obesity and GDM are associated with an altered placental lipid profile that may be implicated in altered trans-placental lipid transport and subsequently altered fetal growth and development [128,262–266]. Omics based analyses have also previously been used to elucidate underlying mechanisms involved in placental responses to PUFA supplementation in obese pregnancies [267]. For example, PUFA supplementation was found to increase markers of proliferation in placental cells that, interestingly, were also directly correlated with offspring birthweight [267]. These data may highlight that increased proliferation of placental trophoblasts directly underlies the increased risk of offspring being born LGA in obese pregnancies treated with dietary PUFA supplementation [185,186]. Overall, omic based analyses have great potential to allow researchers to better understand the regulation of placental function in response to overabundant nutrient supplies and may highlight important placental pathways that may be targeted in future investigations that aim to modulate or improve dysregulated placental metabolism.

1.6 Thesis overview, rationale, and objectives

Maternal diet is an important regulator not only of fetal metabolic health outcomes, but also of the nutrient processing functions, and overall metabolism of the placenta. Increasingly, women of reproductive ages consume a diet that may not be optimal for successful pregnancy outcomes. These diets are characterized by high processed sugar and saturated fat intake and are clinically associated with maternal obesity and GDM development. Analysis of circulating NEFA levels in pregnant women has highlighted that palmitate (hereafter PA), and oleate (hereafter OA) are the most abundant circulating FA species in the third trimester, but more importantly, that the circulating levels of these dietary FA species are elevated in both obese and GDM pregnancies [268,269]. Since PA and OA are the most abundant FA species in the typical “Westernized Diet”, these FA species themselves may be a link between poor maternal

diet and aberrant placental function [63,65,270,271]. However, the independent and combined impacts of dietary PA and OA in isolation on placental trophoblast metabolic and mitochondrial function remains ill defined. This information is critical improve our understanding of their potential contribution to placental dysfunction.

Likewise, maternal diabetes negatively regulates placental metabolic function, however these negative outcomes may be facilitated by poor maternal glycemic control. Additional, *in vitro* analyses using PHT and placental cell line systems have demonstrated that hyperglycemia can also affect placental functions including nutrient storage and transport, which in themselves may directly impact other aspects of placental oxidative metabolism. However, the direct impacts of independent hyperglycemia on important aspects of placental metabolic function including mitochondrial respiratory activity and the regulation of nutrient storage remains poorly understood.

Thus, the collective aim of the work presented here was to further characterize the direct and independent impacts of dietary FA overabundance and hyperglycemia on BeWo trophoblast cell oxidative metabolism and nutrient storage. We specifically sought to examine metabolic function, and nutrient storage using a combination of functional readouts and endpoint analyses in both progenitor BeWo CT cells and differentiated BeWo SCT cells. Furthermore, as CT cells have been highlighted to be the more metabolically active villous trophoblast cell type, we additionally aimed to utilize a multi-omics approach to further elucidate the underlying mechanisms governing placental responses to nutrient overabundance in these progenitor cells. The governing hypothesis of this thesis is *increased nutrient abundance will impact placental metabolic function specifically highlighted by altered nutrient storage, impaired mitochondrial respiratory activity, as well as an altered transcriptomic, metabolomic, and lipidomic profile representative of dysfunctional metabolism.*

1.6.1 Chapter 2 – Objectives and hypothesis

1. Develop an *in vitro* cell culture protocol to examine prolonged PA and OA exposure in BeWo CT and SCT trophoblast cells

2. Quantify mitochondrial respiration and metabolic enzyme activities in PA and OA exposed BeWo trophoblast cells using functional readouts

In Chapter 2, it was postulated that *a prolonged exposure to the dietary NEFAs PA and OA both independently and in combination would impair mitochondrial function in BeWo CT and SCT cells.*

1.6.2 Chapter 3 – Objectives and hypothesis

1. Characterize mitochondrial respiration and metabolic enzyme activity in BeWo CT and SCT cells exposed to independent hyperglycemia using functional assays
2. Investigate the underlying mechanisms regulating nutrient storage in high glucose exposed BeWo CT and SCT cells
3. Utilize a multi-omic approach combining transcriptomics, untargeted metabolomics, and untargeted lipidomics to elucidate underlying mechanisms governing altered metabolic processing in BeWo CT cells exposed to hyperglycemia.

In Chapter 3, it was postulated that *hyperglycemic culture conditions would be associated with increased nutrient storage and impaired mitochondrial respiratory function in BeWo CT and SCT cells, in association with altered transcriptome, metabolome, and lipidome signatures in BeWo CT cells indicative of altered metabolic function.*

1.6.3 Chapter 4 – Objectives and hypothesis

1. Examine FA and neutral lipid profiles in both progenitor BeWo CT cells and differentiated BeWo SCT cells using targeted lipidomic analyses
2. Utilize transcriptomics, in conjunction with untargeted metabolomics and lipidomics in BeWo CT cells to characterize the underlying mechanisms governing placental responses to dietary FA overabundance

In Chapter 4, it was postulated that *exposure to elevated levels of dietary NEFA would alter BeWo trophoblast lipid profiles, highlighted by increased TG abundance, and increased FA elongation and desaturation.* It was additionally postulated that

dietary-FA treated BeWo CT cells would display altered transcriptomic, metabolomic and lipidomic profiles indicative of altered lipid processing.

1.7 References

- [1] P.M. Catalano, E.D. Tyzbir, N.M. Roman, S.B. Amini, E.A.H. Sims, Longitudinal changes in insulin release and insulin resistance in nonobese pregnant women, *Am. J. Obstet. Gynecol.* 165 (1991) 1667–1672. doi:10.1016/0002-9378(91)90012-G.
- [2] G. Desoye, m. O. Schweditsch, k. P. Pfeiffer, R. Zechner, g. M. Kostner, Correlation of Hormones with Lipid and Lipoprotein Levels During Normal Pregnancy and Postpartum*, *J. Clin. Endocrinol. Metab.* 64 (1987) 704–712. doi:10.1210/jcem-64-4-704.
- [3] B. Musial, O.R. Vaughan, D.S. Fernandez-Twinn, P. Voshol, S.E. Ozanne, A.L. Fowden, A.N. Sferruzzi-Perri, A Western-style obesogenic diet alters maternal metabolic physiology with consequences for fetal nutrient acquisition in mice, *J. Physiol.* 595 (2017) 4875–4892. doi:10.1113/JP273684.
- [4] P.P. Silveira, A.K. Portella, M.Z. Goldani, M.A. Barbieri, Developmental origins of health and disease (DOHaD), *J. Pediatr. (Rio. J.)* 83 (2007) 494–504. doi:10.2223/JPED.1728.
- [5] P. Wadhwa, C. Buss, S. Entringer, J. Swanson, Developmental Origins of Health and Disease: Brief History of the Approach and Current Focus on Epigenetic Mechanisms, *Semin. Reprod. Med.* 27 (2009) 358–368. doi:10.1055/s-0029-1237424.
- [6] A. Forsdahl, Are poor living conditions in childhood and adolescence an important risk factor for arteriosclerotic heart disease?, *J. Epidemiol. Community Heal.* 31 (1977) 91–95. doi:10.1136/jech.31.2.91.
- [7] P.C. Lisboa, E. de Oliveira, E.G. de Moura, Obesity and Endocrine Dysfunction Programmed by Maternal Smoking in Pregnancy and Lactation, *Front. Physiol.* 3 (2012). doi:10.3389/fphys.2012.00437.
- [8] J.M. Rogers, Smoking and pregnancy: Epigenetics and developmental origins of the metabolic syndrome, *Birth Defects Res.* 111 (2019) 1259–1269. doi:10.1002/bdr2.1550.
- [9] P. Casanello, E.A. Herrera, B.J. Krause, Epigenetic Programming of Cardiovascular Disease by Perinatal Hypoxia and Fetal Growth Restriction, in: *Hypoxia Hum. Dis.*, InTech, 2017. doi:10.5772/66740.
- [10] M.M. Aljunaidy, J.S. Morton, C.-L.M. Cooke, S.T. Davidge, Prenatal hypoxia and placental oxidative stress: linkages to developmental origins of cardiovascular disease, *Am. J. Physiol. Integr. Comp. Physiol.* 313 (2017) R395–R399. doi:10.1152/ajpregu.00245.2017.
- [11] K.A. Bailey, Developmental Origins of Adult Disease, in: *Syst. Biol. Toxicol.*

- Environ. Heal., Elsevier, 2015: pp. 239–253. doi:10.1016/B978-0-12-801564-3.00011-0.
- [12] J.C. King, Maternal Obesity, Metabolism, and Pregnancy Outcomes, *Annu. Rev. Nutr.* 26 (2006) 271–291. doi:10.1146/annurev.nutr.24.012003.132249.
- [13] G. Wu, F.W. Bazer, T. a Cudd, C.J. Meininger, T.E. Spencer, Recent Advances in Nutritional Sciences Maternal Nutrition and Fetal, *Amino Acids.* (2004) 2169–2172. <http://jn.nutrition.org/content/134/9/2169.full.pdf>.
- [14] C. Maric-Bilkan, M. Symonds, S. Ozanne, B.T. Alexander, Impact of Maternal Obesity and Diabetes on Long-Term Health of the Offspring, *Exp. Diabetes Res.* 2011 (2011) 1–2. doi:10.1155/2011/163438.
- [15] Obesity: preventing and managing the global epidemic. Report of a WHO consultation., *World Health Organ. Tech. Rep. Ser.* (2000) 1-253. <http://www.ncbi.nlm.nih.gov/pubmed/11234459>.
- [16] S.D. McDonald, Z. Han, S. Mulla, J. Beyene, Overweight and obesity in mothers and risk of preterm birth and low birth weight infants: systematic review and meta-analyses, *BMJ.* 341 (2010) c3428–c3428. doi:10.1136/bmj.c3428.
- [17] Z. Yu, S. Han, J. Zhu, X. Sun, C. Ji, X. Guo, Pre-Pregnancy Body Mass Index in Relation to Infant Birth Weight and Offspring Overweight/Obesity: A Systematic Review and Meta-Analysis, *PLoS One.* 8 (2013) e61627. doi:10.1371/journal.pone.0061627.
- [18] V.M.F. da Silveira, B.L. Horta, [Birth weight and metabolic syndrome in adults: meta-analysis]., *Rev. Saude Publica.* 42 (2008) 10–8. doi:10.1590/s0034-89102008000100002.
- [19] C.M. Boney, A. Verma, R. Tucker, B.R. Vohr, Metabolic syndrome in childhood: association with birth weight, maternal obesity, and gestational diabetes mellitus., *Pediatrics.* 115 (2005) e290-6. doi:10.1542/peds.2004-1808.
- [20] R.C. Whitaker, Predicting Preschooler Obesity at Birth: The Role of Maternal Obesity in Early Pregnancy, *Pediatrics.* 114 (2004) e29–e36. doi:10.1542/peds.114.1.e29.
- [21] M.J.R. Heerwagen, M.R. Miller, L.A. Barbour, J.E. Friedman, Maternal obesity and fetal metabolic programming: a fertile epigenetic soil, *AJP Regul. Integr. Comp. Physiol.* 299 (2010) R711–R722. doi:10.1152/ajpregu.00310.2010.
- [22] L. Williams, Y. Seki, P.M. Vuguin, M.J. Charron, Animal models of in utero exposure to a high fat diet: A review, *Biochim. Biophys. Acta - Mol. Basis Dis.* 1842 (2014) 507–519. doi:10.1016/j.bbadis.2013.07.006.
- [23] H.N. Jones, L.A. Woollett, N. Barbour, P.D. Prasad, T.L. Powell, T. Jansson,

- High-fat diet before and during pregnancy causes marked up-regulation of placental nutrient transport and fetal overgrowth in C57/BL6 mice, *FASEB J.* 23 (2009) 271–278. doi:10.1096/fj.08-116889.
- [24] M. Srinivasan, Maternal high-fat diet consumption results in fetal malprogramming predisposing to the onset of metabolic syndrome-like phenotype in adulthood, *AJP Endocrinol. Metab.* 291 (2006) E792–E799. doi:10.1152/ajpendo.00078.2006.
- [25] M. Li, D.M. Sloboda, M.H. Vickers, Maternal Obesity and Developmental Programming of Metabolic Disorders in Offspring: Evidence from Animal Models, *Exp. Diabetes Res.* 2011 (2011) 1–9. doi:10.1155/2011/592408.
- [26] M.M. Elahi, F.R. Cagampang, D. Mukhtar, F.W. Anthony, S.K. Ohri, M.A. Hanson, Long-term maternal high-fat feeding from weaning through pregnancy and lactation predisposes offspring to hypertension, raised plasma lipids and fatty liver in mice, *Br. J. Nutr.* 102 (2009) 514. doi:10.1017/S000711450820749X.
- [27] G.J. Howie, D.M. Sloboda, T. Kamal, M.H. Vickers, Maternal nutritional history predicts obesity in adult offspring independent of postnatal diet, *J. Physiol.* 587 (2009) 905–915. doi:10.1113/jphysiol.2008.163477.
- [28] A.-M. Samuelsson, P.A. Matthews, M. Argenton, M.R. Christie, J.M. McConnell, E.H.J.M. Jansen, A.H. Piersma, S.E. Ozanne, D.F. Twinn, C. Remacle, A. Rowleson, L. Poston, P.D. Taylor, Diet-induced obesity in female mice leads to offspring hyperphagia, adiposity, hypertension, and insulin resistance: a novel murine model of developmental programming., *Hypertens. (Dallas, Tex. 1979)*. 51 (2008) 383–92. doi:10.1161/HYPERTENSIONAHA.107.101477.
- [29] K.G.M.M. Alberti, P. Zimmet, J. Shaw, The metabolic syndrome—a new worldwide definition, *Lancet.* 366 (2005) 1059–1062. doi:10.1016/S0140-6736(05)67402-8.
- [30] J. Rkhezay-Jaf, J.F. O’Dowd, C.J. Stocker, Maternal Obesity and the Fetal Origins of the Metabolic Syndrome, *Curr. Cardiovasc. Risk Rep.* 6 (2012) 487–495. doi:10.1007/s12170-012-0257-x.
- [31] N.M. Long, D.C. Rule, N. Tuersunjiang, P.W. Nathanielsz, S.P. Ford, Maternal Obesity in Sheep Increases Fatty Acid Synthesis, Upregulates Nutrient Transporters, and Increases Adiposity in Adult Male Offspring after a Feeding Challenge, *PLoS One.* 10 (2015) e0122152. doi:10.1371/journal.pone.0122152.
- [32] L.K. Philp, B.S. Muhlhausler, A. Janovska, G.A. Wittert, J.A. Duffield, I.C. McMillen, Maternal overnutrition suppresses the phosphorylation of 5'-AMP-activated protein kinase in liver, but not skeletal muscle, in the fetal and neonatal sheep, *Am. J. Physiol. Integr. Comp. Physiol.* 295 (2008) R1982–R1990. doi:10.1152/ajpregu.90492.2008.

- [33] N. Tuersunjiang, J.F. Odhiambo, N.M. Long, D.R. Shasa, P.W. Nathanielsz, S.P. Ford, Diet reduction to requirements in obese/overfed ewes from early gestation prevents glucose/insulin dysregulation and returns fetal adiposity and organ development to control levels, *Am. J. Physiol. Metab.* 305 (2013) E868–E878. doi:10.1152/ajpendo.00117.2013.
- [34] C.E. McCurdy, J.M. Bishop, S.M. Williams, B.E. Grayson, M.S. Smith, J.E. Friedman, K.L. Grove, Maternal high-fat diet triggers lipotoxicity in the fetal livers of nonhuman primates, *J. Clin. Invest.* 119 (2009) 323–335. doi:10.1172/JCI32661.
- [35] L.D. Pound, S.M. Comstock, K.L. Grove, Consumption of a Western-style diet during pregnancy impairs offspring islet vascularization in a Japanese macaque model, *Am. J. Physiol. Metab.* 307 (2014) E115–E123. doi:10.1152/ajpendo.00131.2014.
- [36] B.E. Lingwood, A.M. Henry, M.C. D’Emden, A.-M. Fullerton, R.H. Mortimer, P.B. Colditz, K.-A. Lê Cao, L.K. Callaway, Determinants of Body Fat in Infants of Women With Gestational Diabetes Mellitus Differ With Fetal Sex, *Diabetes Care.* 34 (2011) 2581–2585. doi:10.2337/dc11-0728.
- [37] D. Mitanchez, S. Jacqueminet, J. Nizard, M.-L. Tanguy, C. Ciangura, J.-M. Lacorte, C. De Carne, L. Foix L’Hélias, P. Chavatte-Palmer, M.-A. Charles, M. Dommergues, Effect of maternal obesity on birthweight and neonatal fat mass: A prospective clinical trial, *PLoS One.* 12 (2017) e0181307. doi:10.1371/journal.pone.0181307.
- [38] F. Ornellas, V.S. Mello, C.A. Mandarim-de-Lacerda, M.B. Aguila, Sexual dimorphism in fat distribution and metabolic profile in mice offspring from diet-induced obese mothers, *Life Sci.* 93 (2013) 454–463. doi:10.1016/j.lfs.2013.08.005.
- [39] E. Zambrano, T. Sosa-Larios, L. Calzada, C.A. Ibáñez, C.A. Mendoza-Rodríguez, A. Morales, S. Morimoto, Decreased basal insulin secretion from pancreatic islets of pups in a rat model of maternal obesity, *J. Endocrinol.* 231 (2016) 49–57. doi:10.1530/JOE-16-0321.
- [40] S. Lecoutre, B. Deracinois, C. Laborie, D. Eberlé, C. Guinez, P.E. Panchenko, J. Lesage, D. Vieau, C. Junien, A. Gabory, C. Breton, Depot- and sex-specific effects of maternal obesity in offspring’s adipose tissue, *J. Endocrinol.* 230 (2016) 39–53. doi:10.1530/JOE-16-0037.
- [41] Trends in adult body-mass index in 200 countries from 1975 to 2014: a pooled analysis of 1698 population-based measurement studies with 19·2 million participants, *Lancet.* 387 (2016) 1377–1396. doi:10.1016/S0140-6736(16)30054-X.
- [42] Statistics Canada, Women in Canada: A gender-based statistical report (89-503-

- X); 2012-2013 Canadian Health Measures Survey, custom tabulation, (2013).
- [43] S.R. Wesolowski, C.M. Mulligan, R.C. Janssen, P.R. Baker, B.C. Bergman, A. D'Alessandro, T. Nemkov, K.N. Maclean, H. Jiang, T.A. Dean, D.L. Takahashi, P. Kievit, C.E. McCurdy, K.M. Aagaard, J.E. Friedman, Switching obese mothers to a healthy diet improves fetal hypoxemia, hepatic metabolites, and lipotoxicity in non-human primates, *Mol. Metab.* 18 (2018) 25–41. doi:10.1016/j.molmet.2018.09.008.
- [44] E. Zambrano, P.M. Martínez-Samayoa, G.L. Rodríguez-González, P.W. Nathanielsz, RAPID REPORT: Dietary intervention prior to pregnancy reverses metabolic programming in male offspring of obese rats, *J. Physiol.* 588 (2010) 1791–1799. doi:10.1113/jphysiol.2010.190033.
- [45] I.E. Sasson, A.P. Vitins, M.A. Mainigi, K.H. Moley, R.A. Simmons, Pre-gestational vs gestational exposure to maternal obesity differentially programs the offspring in mice, *Diabetologia.* 58 (2014) 615–624. doi:10.1007/s00125-014-3466-7.
- [46] S.J. Borengasser, P. Kang, J. Faske, H. Gomez-Acevedo, M.L. Blackburn, T.M. Badger, K. Shankar, High Fat Diet and In Utero Exposure to Maternal Obesity Disrupts Circadian Rhythm and Leads to Metabolic Programming of Liver in Rat Offspring, *PLoS One.* 9 (2014) e84209. doi:10.1371/journal.pone.0084209.
- [47] S.J. Borengasser, J. Faske, P. Kang, M.L. Blackburn, T.M. Badger, K. Shankar, In utero exposure to prepregnancy maternal obesity and postweaning high-fat diet impair regulators of mitochondrial dynamics in rat placenta and offspring, *Physiol. Genomics.* 46 (2014) 841–850. doi:10.1152/physiolgenomics.00059.2014.
- [48] A.M. Swanson, A.L. David, Animal models of fetal growth restriction: Considerations for translational medicine, *Placenta.* 36 (2015) 623–630. doi:10.1016/j.placenta.2015.03.003.
- [49] J.L. Morrison, K.J. Botting, J.R.T. Darby, A.L. David, R.M. Dyson, K.L. Gatford, C. Gray, E.A. Herrera, J.J. Hirst, B. Kim, K.L. Kind, B.J. Krause, S.G. Matthews, H.K. Palliser, T.R.H. Regnault, B.S. Richardson, A. Sasaki, L.P. Thompson, M.J. Berry, Guinea pig models for translation of the developmental origins of health and disease hypothesis into the clinic, *J. Physiol.* 596 (2018) 5535–5569. doi:10.1113/JP274948.
- [50] M.G.J. Gademan, M. Vermeulen, A.J.J.M. Oostvogels, T.J. Roseboom, T.L.S. Visscher, M. van Eijsden, M.T.B. Twickler, T.G.M. Vrijkotte, Maternal Prepregnancy BMI and Lipid Profile during Early Pregnancy Are Independently Associated with Offspring's Body Composition at Age 5–6 Years: The ABCD Study, *PLoS One.* 9 (2014) e94594. doi:10.1371/journal.pone.0094594.
- [51] A.E. Jones, M. Stolinski, R.D. Smith, J.L. Murphy, S.A. Wootton, Effect of fatty acid chain length and saturation on the gastrointestinal handling and metabolic

- disposal of dietary fatty acids in women, *Br. J. Nutr.* 81 (1999) 37–44. doi:10.1017/S0007114599000124.
- [52] A. Julibert, M. del M. Bibiloni, J.A. Tur, Dietary fat intake and metabolic syndrome in adults: A systematic review, *Nutr. Metab. Cardiovasc. Dis.* 29 (2019) 887–905. doi:10.1016/j.numecd.2019.05.055.
- [53] R.P. Mensink, P.L. Zock, A.D.M. Kester, M.B. Katan, Effects of dietary fatty acids and carbohydrates on the ratio of serum total to HDL cholesterol and on serum lipids and apolipoproteins: a meta-analysis of 60 controlled trials., *Am. J. Clin. Nutr.* 77 (2003) 1146–55. doi:11778166.
- [54] C.B. Dias, N. Amigo, L.G. Wood, X. Correig, M.L. Garg, Effect of diets rich in either saturated fat or n-6 polyunsaturated fatty acids and supplemented with long-chain n-3 polyunsaturated fatty acids on plasma lipoprotein profiles, *Eur. J. Clin. Nutr.* 71 (2017) 1297–1302. doi:10.1038/ejcn.2017.56.
- [55] H.E. Bays, A.P. Tighe, R. Sadovsky, M.H. Davidson, Prescription omega-3 fatty acids and their lipid effects: physiologic mechanisms of action and clinical implications, *Expert Rev. Cardiovasc. Ther.* 6 (2008) 391–409. doi:10.1586/14779072.6.3.391.
- [56] K.R. Feingold, *Introduction to Lipids and Lipoproteins*, 2000. <http://www.ncbi.nlm.nih.gov/pubmed/26247089>.
- [57] J. Delarue, C. LeFoll, C. Corporeau, D. Lucas, n-3 long chain polyunsaturated fatty acids: a nutritional tool to prevent insulin resistance associated to type 2 diabetes and obesity?, *Reprod. Nutr. Dev.* 44 (2004) 289–299. doi:10.1051/rnd:2004033.
- [58] Y.B. Lombardo, G. Hein, A. Chicco, Metabolic syndrome: Effects of n-3 PUFAs on a model of dyslipidemia, insulin resistance and adiposity, *Lipids.* 42 (2007) 427–437. doi:10.1007/s11745-007-3039-3.
- [59] Y.S. Diniz, A.C. Cicogna, C.R. Padovani, L.S. Santana, L.A. Faine, E.L.B. Novelli, Diets rich in saturated and polyunsaturated fatty acids: metabolic shifting and cardiac health., *Nutrition.* 20 (2004) 230–4. doi:10.1016/j.nut.2003.10.012.
- [60] Y.-M. Dong, Y. Li, H. Ning, C. Wang, J.-R. Liu, C.-H. Sun, High dietary intake of medium-chain fatty acids during pregnancy in rats prevents later-life obesity in their offspring., *J. Nutr. Biochem.* 22 (2011) 791–7. doi:10.1016/j.jnutbio.2010.07.006.
- [61] P.C. de Velasco, G. Chicaybam, D.M. Ramos-Filho, R.M.A.R. dos Santos, C. Mairink, F.L.C. Sardinha, T. El-Bacha, A. Galina, M. das G. Tavares-do-Carmo, Maternal intake of trans-unsaturated or interesterified fatty acids during pregnancy and lactation modifies mitochondrial bioenergetics in the liver of adult offspring in mice, *Br. J. Nutr.* (2017) 1–12. doi:10.1017/S0007114517001817.

- [62] M. Makrides, Is there a dietary requirement for DHA in pregnancy?, *Prostaglandins Leukot. Essent. Fat. Acids.* 81 (2009) 171–174. doi:10.1016/j.plefa.2009.05.005.
- [63] C. Savard, S. Lemieux, S. Weisnagel, B. Fontaine-Bisson, C. Gagnon, J. Robitaille, A.-S. Morisset, Trimester-Specific Dietary Intakes in a Sample of French-Canadian Pregnant Women in Comparison with National Nutritional Guidelines, *Nutrients.* 10 (2018) 768. doi:10.3390/nu10060768.
- [64] V. Watts, H. Rockett, H. Baer, J. Leppert, G. Colditz, Assessing Diet Quality in a Population of Low-Income Pregnant Women: A Comparison Between Native Americans and Whites, *Matern. Child Health J.* 11 (2007) 127–136. doi:10.1007/s10995-006-0155-2.
- [65] J. Denomme, K.D. Stark, B.J. Holub, Directly quantitated dietary (n-3) fatty acid intakes of pregnant Canadian women are lower than current dietary recommendations., *J. Nutr.* 135 (2005) 206–11. doi:135/2/206 [pii].
- [66] A.M. Siega-Riz, L.M. Bodnar, D.A. Savitz, What are pregnant women eating? Nutrient and food group differences by race, *Am. J. Obstet. Gynecol.* 186 (2002) 480–486. doi:10.1067/mob.2002.121078.
- [67] S.M. Innis, S.L. Elias, Intakes of essential n-6 and n-3 polyunsaturated fatty acids among pregnant Canadian women., *Am. J. Clin. Nutr.* 77 (2003) 473–8. <http://www.ncbi.nlm.nih.gov/pubmed/12540410>.
- [68] M.E. Bianco, J.L. Josefson, Hyperglycemia During Pregnancy and Long-Term Offspring Outcomes, *Curr. Diab. Rep.* 19 (2019) 143. doi:10.1007/s11892-019-1267-6.
- [69] T. Vilmi-Kerälä, O. Palomäki, M. Vainio, J. Uotila, A. Palomäki, The risk of metabolic syndrome after gestational diabetes mellitus – a hospital-based cohort study, *Diabetol. Metab. Syndr.* 7 (2015) 43. doi:10.1186/s13098-015-0038-z.
- [70] P.M. Catalano, The impact of gestational diabetes and maternal obesity on the mother and her offspring, *J. Dev. Orig. Health Dis.* 1 (2010) 208–215. doi:10.1017/S2040174410000115.
- [71] Y. Yang, Z. Wang, M. Mo, X. Muyiduli, S. Wang, M. Li, S. Jiang, Y. Wu, B. Shao, Y. Shen, Y. Yu, The association of gestational diabetes mellitus with fetal birth weight, *J. Diabetes Complications.* 32 (2018) 635–642. doi:10.1016/j.jdiacomp.2018.04.008.
- [72] D.A. Doherty, E.F. Magann, J. Francis, J.C. Morrison, J.P. Newnham, Pre-pregnancy body mass index and pregnancy outcomes, *Int. J. Gynecol. Obstet.* 95 (2006) 242–247. doi:10.1016/j.ijgo.2006.06.021.
- [73] I.-W. Yen, C.-N. Lee, M.-W. Lin, K.-C. Fan, J.-N. Wei, K.-Y. Chen, S.-C. Chen,

- Y.-Y. Tai, C.-H. Kuo, C.-H. Lin, C.-Y. Hsu, L.-M. Chuang, S.-Y. Lin, H.-Y. Li, Overweight and obesity are associated with clustering of metabolic risk factors in early pregnancy and the risk of GDM, *PLoS One*. 14 (2019) e0225978. doi:10.1371/journal.pone.0225978.
- [74] P.M. Catalano, H.D. McIntyre, J.K. Cruickshank, D.R. McCance, A.R. Dyer, B.E. Metzger, L.P. Lowe, E.R. Trimble, D.R. Coustan, D.R. Hadden, B. Persson, M. Hod, J.J.N. Oats, The Hyperglycemia and Adverse Pregnancy Outcome Study: Associations of GDM and obesity with pregnancy outcomes, *Diabetes Care*. 35 (2012) 780–786. doi:10.2337/dc11-1790.
- [75] G.R. Babu, R. Deepa, M.G. Lewis, E. Lobo, A. Krishnan, Y. Ana, J.G. Katon, D.A. Enquobahrie, O.A. Arah, S. Kinra, G. Murthy, Do Gestational Obesity and Gestational Diabetes Have an Independent Effect on Neonatal Adiposity? Results of Mediation Analysis from a Cohort Study in South India, *Clin. Epidemiol.* Volume 11 (2019) 1067–1080. doi:10.2147/CLEP.S222726.
- [76] D.K. Tobias, C. Zhang, J. Chavarro, K. Bowers, J. Rich-Edwards, B. Rosner, D. Mozaffarian, F.B. Hu, Prepregnancy adherence to dietary patterns and lower risk of gestational diabetes mellitus, *Am. J. Clin. Nutr.* 96 (2012) 289–295. doi:10.3945/ajcn.111.028266.
- [77] Z. Paknahad, A. Fallah, A.R. Moravejolahkami, Maternal Dietary Patterns and Their Association with Pregnancy Outcomes, *Clin. Nutr. Res.* 8 (2019) 64. doi:10.7762/cnr.2019.8.1.64.
- [78] M. Mizgier, G. Jarzabek-Bielecka, K. Mruczyk, Maternal diet and gestational diabetes mellitus development, *J. Matern. Neonatal Med.* 34 (2021) 77–86. doi:10.1080/14767058.2019.1598364.
- [79] D.C. Berry, K. Boggess, Q.B. Johnson, Management of Pregnant Women with Type 2 Diabetes Mellitus and the Consequences of Fetal Programming in Their Offspring, *Curr. Diab. Rep.* 16 (2016) 36. doi:10.1007/s11892-016-0733-7.
- [80] T.D. Clausen, E.R. Mathiesen, T. Hansen, O. Pedersen, D.M. Jensen, J. Lauenborg, L. Schmidt, P. Damm, Overweight and the Metabolic Syndrome in Adult Offspring of Women with Diet-Treated Gestational Diabetes Mellitus or Type 1 Diabetes, *J. Clin. Endocrinol. Metab.* 94 (2009) 2464–2470. doi:10.1210/jc.2009-0305.
- [81] S. Rodrigues, A.M. Ferris, R. Pérez-Escamilla, J.R. Backstrand, Obesity among offspring of women with type 1 diabetes., *Clin. Invest. Med.* 21 (1998) 258–66. <http://www.ncbi.nlm.nih.gov/pubmed/9885760>.
- [82] Z. Vlachová, B. Bytoft, S. Knorr, T.D. Clausen, R.B. Jensen, E.R. Mathiesen, K. Højlund, P. Ovesen, H. Beck-Nielsen, C.H. Gravholt, P. Damm, D.M. Jensen, Increased metabolic risk in adolescent offspring of mothers with type 1 diabetes: the EPICOM study, *Diabetologia*. 58 (2015) 1454–1463. doi:10.1007/s00125-015-

3589-5.

- [83] R.S. Lindsay, S.M. Nelson, J.D. Walker, S.A. Greene, G. Milne, N. Sattar, D.W. Pearson, Programming of Adiposity in Offspring of Mothers With Type 1 Diabetes at Age 7 Years, *Diabetes Care*. 33 (2010) 1080–1085. doi:10.2337/dc09-1766.
- [84] M. Jolly, The causes and effects of fetal macrosomia in mothers with type 1 diabetes, *J. Clin. Pathol.* 53 (2000) 889–889. doi:10.1136/jcp.53.12.889.
- [85] J. Yves, V. Valerie, V.H. Katrien, M. Guy, Birth Weight in Type 1 Diabetic Pregnancy, *Obstet. Gynecol. Int.* 2010 (2010) 1–4. doi:10.1155/2010/397623.
- [86] S.M. Steculorum, S.G. Bouret, Maternal Diabetes Compromises the Organization of Hypothalamic Feeding Circuits and Impairs Leptin Sensitivity in Offspring, *Endocrinology*. 152 (2011) 4171–4179. doi:10.1210/en.2011-1279.
- [87] I. López-Soldado, E. Herrera, Different Diabetogenic Response to Moderate Doses of Streptozotocin in Pregnant Rats, and Its Long-Term Consequences in the Offspring, *Exp. Diabetes Res.* 4 (2003) 107–118. doi:10.1155/EDR.2003.107.
- [88] K. Holemans, L. Aerts, F.A. Van Assche, Evidence for an insulin resistance in the adult offspring of pregnant streptozotocin-diabetic rats, *Diabetologia*. 34 (1991) 81–85. doi:10.1007/BF00500377.
- [89] N.L. Gelardi, R.E. Rapoza, B.T. Jackson, G.J. Piasecki, R.M. Cowett, Streptozotocin Induced Gestational Diabetes in the Sheep, *Pediatr. Res.* 45 (1999) 282A-282A. doi:10.1203/00006450-199904020-01679.
- [90] M. Persson, H. Fadl, Perinatal outcome in relation to fetal sex in offspring to mothers with pre-gestational and gestational diabetes-a population-based study, *Diabet. Med.* 31 (2014) 1047–1054. doi:10.1111/dme.12479.
- [91] N. Le Moullec, A. Fianu, O. Maillard, E. Chazelle, N. Naty, C. Schneebeli, P. Gérardin, L. Huiart, M.-A. Charles, F. Favier, Sexual dimorphism in the association between gestational diabetes mellitus and overweight in offspring at 5-7 years: The OBEGEST cohort study, *PLoS One*. 13 (2018) e0195531. doi:10.1371/journal.pone.0195531.
- [92] R. Retnakaran, C.K. Kramer, C. Ye, S. Kew, A.J. Hanley, P.W. Connelly, M. Sermer, B. Zinman, Fetal Sex and Maternal Risk of Gestational Diabetes Mellitus: The Impact of Having a Boy, *Diabetes Care*. 38 (2015) 844–851. doi:10.2337/dc14-2551.
- [93] B. Buhary, O. Almohareb, N. Aljohani, S. Alzahrani, S. Elkaissi, S. Sherbeeni, A. Almaghami, M. Almalki, Glycemic control and pregnancy outcomes in patients with diabetes in pregnancy: A retrospective study, *Indian J. Endocrinol. Metab.* 20 (2016) 481. doi:10.4103/2230-8210.183478.

- [94] T. Chivese, M.C. Haynes, H. van Zyl, U. Kyriacos, N.S. Levitt, S.A. Norris, The influence of maternal blood glucose during pregnancy on weight outcomes at birth and preschool age in offspring exposed to hyperglycemia first detected during pregnancy, in a South African cohort, *PLoS One*. 16 (2021) e0258894. doi:10.1371/journal.pone.0258894.
- [95] N.M. Gude, C.T. Roberts, B. Kalionis, R.G. King, Growth and function of the normal human placenta., *Thromb. Res.* 114 (2004) 397–407. doi:10.1016/j.thromres.2004.06.038.
- [96] A. Tarrade, P. Panchenko, C. Junien, A. Gabory, Placental contribution to nutritional programming of health and diseases: epigenetics and sexual dimorphism, *J. Exp. Biol.* 218 (2015) 50–58. doi:10.1242/jeb.110320.
- [97] K.L. Thornburg, P.F. O’Tierney, S. Louey, Review: The Placenta is a Programming Agent for Cardiovascular Disease, *Placenta*. 31 (2010) S54–S59. doi:10.1016/j.placenta.2010.01.002.
- [98] T. Jansson, T.L. Powell, Role of the placenta in fetal programming: underlying mechanisms and potential interventional approaches, *Clin. Sci.* 113 (2007) 1–13. doi:10.1042/CS20060339.
- [99] K.M. Godfrey, The Role of the Placenta in Fetal Programming—A Review, *Placenta*. 23 (2002) S20–S27. doi:10.1053/plac.2002.0773.
- [100] C. Loardi, M. Falchetti, F. Prefumo, F. Facchetti, T. Frusca, Placental morphology in pregnancies associated with pregravid obesity, *J. Matern. Neonatal Med.* (2015) 1–6. doi:10.3109/14767058.2015.1094792.
- [101] L. Huang, J. Liu, L. Feng, Y. Chen, J. Zhang, W. Wang, Maternal prepregnancy obesity is associated with higher risk of placental pathological lesions, *Placenta*. 35 (2014) 563–569. doi:10.1016/j.placenta.2014.05.006.
- [102] M.J. Zhu, M. Du, P.W. Nathanielsz, S.P. Ford, Maternal obesity up-regulates inflammatory signaling pathways and enhances cytokine expression in the mid-gestation sheep placenta, *Placenta*. 31 (2010) 387–391. doi:10.1016/j.placenta.2010.02.002.
- [103] K.A. Roberts, S.C. Riley, R.M. Reynolds, S. Barr, M. Evans, A. Statham, K. Hor, H.N. Jabbour, J.E. Norman, F.C. Denison, Placental structure and inflammation in pregnancies associated with obesity, *Placenta*. 32 (2011) 247–254. doi:10.1016/j.placenta.2010.12.023.
- [104] J.C. Challier, S. Basu, T. Bintein, J. Minium, K. Hotmire, P.M. Catalano, S. Hauguel-de Mouzon, Obesity in Pregnancy Stimulates Macrophage Accumulation and Inflammation in the Placenta, *Placenta*. 29 (2008) 274–281. doi:10.1016/j.placenta.2007.12.010.

- [105] J.A. Salati, V.H.J. Roberts, M.C. Schabel, J.O. Lo, C.D. Kroenke, K.S. Lewandowski, J.R. Lindner, K.L. Grove, A.E. Frias, Maternal high-fat diet reversal improves placental hemodynamics in a nonhuman primate model of diet-induced obesity, *Int. J. Obes.* 43 (2019) 906–916. doi:10.1038/s41366-018-0145-7.
- [106] A.E. Frias, T.K. Morgan, A.E. Evans, J. Rasanen, K.Y. Oh, K.L. Thornburg, K.L. Grove, Maternal High-Fat Diet Disturbs Uteroplacental Hemodynamics and Increases the Frequency of Stillbirth in a Nonhuman Primate Model of Excess Nutrition, *Endocrinology.* 152 (2011) 2456–2464. doi:10.1210/en.2010-1332.
- [107] S.M. Nelson, P.M. Coan, G.J. Burton, R.S. Lindsay, Placental Structure in Type 1 Diabetes, *Diabetes.* 58 (2009) 2634–2641. doi:10.2337/db09-0739.
- [108] I. Carrasco-Wong, A. Moller, F.R. Giachini, V. V. Lima, F. Toledo, J. Stojanova, L. Sobrevia, S. San Martín, Placental structure in gestational diabetes mellitus, *Biochim. Biophys. Acta - Mol. Basis Dis.* 1866 (2020) 165535. doi:10.1016/j.bbadis.2019.165535.
- [109] M. Kadivar, M.E. Khamseh, M. Malek, A. Khajavi, A.H. Noohi, L. Najafi, Histomorphological changes of the placenta and umbilical cord in pregnancies complicated by gestational diabetes mellitus, *Placenta.* 97 (2020) 71–78. doi:10.1016/j.placenta.2020.06.018.
- [110] M. Jirkovská, T. Kučera, J. Kaláb, M. Jadrníček, V. Niedobová, J. Janáček, L. Kubínová, M. Moravcová, Z. Žizka, V. Krejčí, The branching pattern of villous capillaries and structural changes of placental terminal villi in type 1 diabetes mellitus, *Placenta.* 33 (2012) 343–351. doi:10.1016/j.placenta.2012.01.014.
- [111] R. Arshad, M.A. Kanpurwala, N. Karim, J.A. Hassan, Effects of Diet and Metformin on placental morphology in Gestational Diabetes Mellitus, *Pakistan J. Med. Sci.* 32 (2016). doi:10.12669/pjms.326.10872.
- [112] S.M. Leon-Garcia, H.A. Roeder, K.K. Nelson, X. Liao, D.P. Pizzo, L.C. Laurent, M.M. Parast, D.Y. LaCoursiere, Maternal obesity and sex-specific differences in placental pathology, *Placenta.* 38 (2016) 33–40. doi:10.1016/j.placenta.2015.12.006.
- [113] L. Evans, L. Myatt, Sexual dimorphism in the effect of maternal obesity on antioxidant defense mechanisms in the human placenta, *Placenta.* 51 (2017) 64–69. doi:10.1016/j.placenta.2017.02.004.
- [114] J. Strutz, S. Cvitic, H. Hackl, K. Kashofer, H.M. Appel, A. Thüringer, G. Desoye, P. Koolwijk, U. Hiden, Gestational diabetes alters microRNA signatures in human fetoplacental endothelial cells depending on fetal sex, *Clin. Sci.* 132 (2018) 2437–2449. doi:10.1042/CS20180825.
- [115] J. Mele, S. Muralimanoharan, A. Maloyan, L. Myatt, Impaired mitochondrial function in human placenta with increased maternal adiposity., *Am. J. Physiol.*

- Endocrinol. Metab. 307 (2014) E419-25. doi:10.1152/ajpendo.00025.2014.
- [116] V. Calabuig-Navarro, M. Haghiac, J. Minium, P. Glazebrook, G.C. Ranasinghe, C. Hoppel, S. Hauguel de-Mouzon, P. Catalano, P. O'Tierney-Ginn, Effect of Maternal Obesity on Placental Lipid Metabolism, *Endocrinology*. 158 (2017) 2543–2555. doi:10.1210/en.2017-00152.
- [117] R. Hastie, M. Lappas, The effect of pre-existing maternal obesity and diabetes on placental mitochondrial content and electron transport chain activity., *Placenta*. 35 (2014) 673–83. doi:10.1016/j.placenta.2014.06.368.
- [118] A.M. Valent, H. Choi, K.S. Kolahi, K.L. Thornburg, Hyperglycemia and gestational diabetes suppress placental glycolysis and mitochondrial function and alter lipid processing, *FASEB J*. 35 (2021). doi:10.1096/fj.202000326RR.
- [119] L. Li, D.J. Schust, Isolation, purification and in vitro differentiation of cytotrophoblast cells from human term placenta, *Reprod. Biol. Endocrinol*. 13 (2015) 71. doi:10.1186/s12958-015-0070-8.
- [120] H. Mendez-Figueroa, E.K. Chien, H. Ji, N.L. Nesbitt, S.S. Bharathi, E. Goetzman, Effects of labor on placental fatty acid β oxidation, *J. Matern. Neonatal Med*. 26 (2013) 150–154. doi:10.3109/14767058.2012.722721.
- [121] S.A. Nersisyan, M.Y. Shkurnikov, E.N. Knyazev, Factors Involved in miRNA Processing Change Its Expression Level during Imitation of Hypoxia in BeWo b30 Cells., *Dokl. Biochem. Biophys*. 493 (2020) 205–207. doi:10.1134/S1607672920040110.
- [122] C.. Abaidoo, M.A. Warren, P.W. Andrews, K.A. Boateng, A Quantitative Assessment of the Morphological Characteristics of BeWo Cells as an in vitro Model of Human Trophoblast Cells, *Int. J. Morphol*. 28 (2010) 1047–1058. doi:10.4067/S0717-95022010000400011.
- [123] F.M. Campbell, P.G. Bush, J.H. Veerkamp, A.K. Dutta-Roy, Detection and cellular localization of plasma membrane-associated and cytoplasmic fatty acid-binding proteins in human placenta, *Placenta*. 19 (1998) 409–415. doi:10.1016/S0143-4004(98)90081-9.
- [124] E. Larqué, H. Demmelmair, M. Klingler, S. De Jonge, B. Bondy, B. Koletzko, Expression pattern of fatty acid transport protein-1 (FATP-1), FATP-4 and heart-fatty acid binding protein (H-FABP) genes in human term placenta, *Early Hum. Dev*. 82 (2006) 697–701. doi:10.1016/j.earlhumdev.2006.02.001.
- [125] P. Haggarty, J. Ashton, M. Joynson, D.R. Abramovich, K. Page, Effect of Maternal Polyunsaturated Fatty Acid Concentration on Transport by the Human Placenta, *Biol. Neonate*. 75 (1999) 350–359. doi:10.1159/000014115.
- [126] A.K. Duttaroy, S. Basak, Maternal dietary fatty acids and their roles in human

- placental development, Prostaglandins, Leukot. Essent. Fat. Acids. 155 (2020) 102080. doi:10.1016/j.plefa.2020.102080.
- [127] E. Dubé, A. Gravel, C. Martin, G. Desparois, I. Moussa, M. Ethier-Chiasson, J.-C. Forest, Y. Giguère, A. Masse, J. Lafond, Modulation of Fatty Acid Transport and Metabolism by Maternal Obesity in the Human Full-Term Placenta, *Biol. Reprod.* 87 (2012). doi:10.1095/biolreprod.111.098095.
- [128] M.T. Segura, H. Demmelmair, S. Krauss-Etschmann, P. Nathan, S. Dehmel, M.C. Padilla, R. Rueda, B. Koletzko, C. Campoy, Maternal BMI and gestational diabetes alter placental lipid transporters and fatty acid composition, *Placenta.* 57 (2017) 144–151. doi:10.1016/j.placenta.2017.07.001.
- [129] M.J.R. Heerwagen, D.L. Gumina, T.L. Hernandez, R.E. Van Pelt, A.W. Kramer, R.C. Janssen, D.R. Jensen, T.L. Powell, J.E. Friedman, V.D. Winn, L.A. Barbour, Placental lipoprotein lipase activity is positively associated with newborn adiposity, *Placenta.* 64 (2018) 53–60. doi:10.1016/j.placenta.2018.03.001.
- [130] N. Walker, P. Filis, U. Soffientini, M. Bellingham, P.J. O’Shaughnessy, P.A. Fowler, Placental transporter localization and expression in the Human: the importance of species, sex, and gestational age differences†, *Biol. Reprod.* 96 (2017) 733–742. doi:10.1093/biolre/iox012.
- [131] A. Gil-Sánchez, Mechanisms involved in the selective transfer of long chain polyunsaturated fatty acids to the fetus, *Front. Genet.* 2 (2011). doi:10.3389/fgene.2011.00057.
- [132] K.A.R. Tobin, G.M. Johnsen, A.C. Staff, A.K. Duttaroy, Long-chain Polyunsaturated Fatty Acid Transport across Human Placental Choriocarcinoma (BeWo) Cells, *Placenta.* 30 (2009) 41–47. doi:10.1016/j.placenta.2008.10.007.
- [133] C. Leroy, K.A.R. Tobin, S. Basak, A. Cathrine Staff, A.K. Duttaroy, Fatty acid-binding protein3 expression in BeWo cells, a human placental choriocarcinoma cell line, *Prostaglandins, Leukot. Essent. Fat. Acids.* 120 (2017) 1–7. doi:10.1016/j.plefa.2017.04.002.
- [134] N.P. Illsley, M.U. Baumann, Human placental glucose transport in fetoplacental growth and metabolism, *Biochim. Biophys. Acta - Mol. Basis Dis.* 1866 (2020) 165359. doi:10.1016/j.bbadis.2018.12.010.
- [135] M.U. Baumann, S. Deborde, N.P. Illsley, Placental Glucose Transfer and Fetal Growth, *Endocrine.* 19 (2002) 13–22. doi:10.1385/ENDO:19:1:13.
- [136] T. Jansson, M. Wennergren, N.P. Illsley, Glucose transporter protein expression in human placenta throughout gestation and in intrauterine growth retardation., *J. Clin. Endocrinol. Metab.* 77 (1993) 1554–1562. doi:10.1210/jcem.77.6.8263141.
- [137] L.F. Barrosa, D.L. Yudilevich, S.M. Jarvis, N. Beaumont, S.A. Baldwin,

- Quantitation and immunolocalization of glucose transporters in the human placenta, *Placenta*. 16 (1995) 623–633. doi:10.1016/0143-4004(95)90031-4.
- [138] N.P. Illsley, CURRENT TOPIC: Glucose Transporters in the Human Placenta, *Placenta*. 21 (2000) 14–22. doi:10.1053/plac.1999.0448.
- [139] H.N. Jones, T. Crombleholme, M. Habli, Adenoviral-Mediated Placental Gene Transfer of IGF-1 Corrects Placental Insufficiency via Enhanced Placental Glucose Transport Mechanisms, *PLoS One*. 8 (2013) e74632. doi:10.1371/journal.pone.0074632.
- [140] P.A. Vardhana, N.P. Illsley, Transepithelial Glucose Transport and Metabolism in BeWo Choriocarcinoma Cells, *Placenta*. 23 (2002) 653–660. doi:10.1053/plac.2002.0857.
- [141] S.W. Shah, H. Zhao, S.Y. Low, H.J. Mcardle, H.S. Hundal, Characterization of Glucose Transport and Glucose Transporters in the Human Choriocarcinoma Cell Line, BeWo, *Placenta*. 20 (1999) 651–659. doi:10.1053/plac.1999.0437.
- [142] K. Ogura, M. Sakata, Y. Okamoto, Y. Yasui, C. Tadokoro, Y. Yoshimoto, M. Yamaguchi, H. Kurachi, T. Maeda, Y. Murata, 8-bromo-cyclicAMP stimulates glucose transporter-1 expression in a human choriocarcinoma cell line, *J. Endocrinol.* 164 (2000) 171–178. doi:10.1677/joe.0.1640171.
- [143] S.S. Chassen, V. Ferchaud-Roucher, C. Palmer, C. Li, T. Jansson, P.W. Nathanielsz, T.L. Powell, Placental fatty acid transport across late gestation in a baboon model of intrauterine growth restriction, *J. Physiol.* (2020) JP279398. doi:10.1113/JP279398.
- [144] E. Larqué, S. Krauss-Etschmann, C. Campoy, D. Hartl, J. Linde, M. Klingler, H. Demmelmair, A. Caño, A. Gil, B. Bondy, B. Koletzko, Docosahexaenoic acid supply in pregnancy affects placental expression of fatty acid transport proteins, *Am. J. Clin. Nutr.* 84 (2006) 853–861. doi:10.1093/ajcn/84.4.853.
- [145] M. Colomiere, M. Permezel, C. Riley, G. Desoye, M. Lappas, Defective insulin signaling in placenta from pregnancies complicated by gestational diabetes mellitus, *Eur. J. Endocrinol.* 160 (2009) 567–578. doi:10.1530/EJE-09-0031.
- [146] K.E. Brett, Z.M. Ferraro, M. Holcik, K.B. Adamo, Placenta nutrient transport-related gene expression: the impact of maternal obesity and excessive gestational weight gain, *J. Matern. Neonatal Med.* 29 (2016) 1399–1405. doi:10.3109/14767058.2015.1049522.
- [147] O. Acosta, V.I. Ramirez, S. Lager, F. Gaccioli, D.J. Dudley, T.L. Powell, T. Jansson, Increased glucose and placental GLUT-1 in large infants of obese nondiabetic mothers, *Am. J. Obstet. Gynecol.* 212 (2015) 227.e1-227.e7. doi:10.1016/j.ajog.2014.08.009.

- [148] P. Nogues, E. Dos Santos, A. Couturier-Tarrade, P. Berveiller, L. Arnould, E. Lamy, S. Grassin-Delyle, F. Vialard, M.-N. Dieudonne, Maternal Obesity Influences Placental Nutrient Transport, Inflammatory Status, and Morphology in Human Term Placenta, *J. Clin. Endocrinol. Metab.* 106 (2021) 1880–1896. doi:10.1210/clinem/dgaa660.
- [149] C.H. Hulme, A. Nicolaou, S.A. Murphy, A.E.P. Heazell, J.E. Myers, M. Westwood, The effect of high glucose on lipid metabolism in the human placenta, *Sci. Rep.* 9 (2019) 14114. doi:10.1038/s41598-019-50626-x.
- [150] M.L.S. Lindegaard, P. Damm, E.R. Mathiesen, L.B. Nielsen, Placental triglyceride accumulation in maternal type 1 diabetes is associated with increased lipase gene expression, *J. Lipid Res.* 47 (2006) 2581–2588. doi:10.1194/jlr.M600236-JLR200.
- [151] A.L. Magnusson, I.J. Waterman, M. Wennergren, T. Jansson, T.L. Powell, Triglyceride Hydrolase Activities and Expression of Fatty Acid Binding Proteins in the Human Placenta in Pregnancies Complicated by Intrauterine Growth Restriction and Diabetes, *J. Clin. Endocrinol. Metab.* 89 (2004) 4607–4614. doi:10.1210/jc.2003-032234.
- [152] H.L. Barrett, M.H. Kubala, K. Scholz Romero, K.J. Denny, T.M. Woodruff, H.D. McIntyre, L.K. Callaway, M.D. Nitert, Placental Lipases in Pregnancies Complicated by Gestational Diabetes Mellitus (GDM), *PLoS One.* 9 (2014) e104826. doi:10.1371/journal.pone.0104826.
- [153] M. Gauster, U. Hiden, M. van Poppel, S. Frank, C. Wadsack, S. Hauguel-de Mouzon, G. Desoye, Dysregulation of Placental Endothelial Lipase in Obese Women With Gestational Diabetes Mellitus, *Diabetes.* 60 (2011) 2457–2464. doi:10.2337/db10-1434.
- [154] K. Gaither, A.N. Quraishi, N.P. Illsley, Diabetes Alters the Expression and Activity of the Human Placental GLUT1 Glucose Transporter 1, *J. Clin. Endocrinol. Metab.* 84 (1999) 695–701. doi:10.1210/jcem.84.2.5438.
- [155] T. Jansson, M. Wennergren, T.L. Powell, Placental glucose transport and GLUT 1 expression in insulin-dependent diabetes, *Am. J. Obstet. Gynecol.* 180 (1999) 163–168. doi:10.1016/S0002-9378(99)70169-9.
- [156] T. Jansson, Y. Ekstrand, M. Wennergren, T.L. Powell, Placental glucose transport in gestational diabetes mellitus, *Am. J. Obstet. Gynecol.* 184 (2001) 111–116. doi:10.1067/mob.2001.108075.
- [157] T. Hahn, S. Barth, U. Weiss, W. Mosgoeller, G. Desoye, Sustained hyperglycemia in vitro down-regulates the GLUT1 glucose transport system of cultured human term placental trophoblast: a mechanism to protect fetal development? 1, *FASEB J.* 12 (1998) 1221–1231. doi:10.1096/fasebj.12.12.1221.
- [158] T. Hahn, D. Hahn, A. Blaschitz, E.T. Korgun, G. Desoye, G. Dohr,

- Hyperglycaemia-induced subcellular redistribution of GLUT1 glucose transporters in cultured human term placental trophoblast cells, *Diabetologia*. 43 (2000) 173–180. doi:10.1007/s001250050026.
- [159] A.J. Szabo, R. de Lellis, R.D. Grimaldi, Triglyceride synthesis by the human placenta, *Am. J. Obstet. Gynecol.* 115 (1973) 257–262. doi:10.1016/0002-9378(73)90295-0.
- [160] A.N. Pathmaperuma, P. Maña, S.N. Cheung, K. Kugathas, A. Josiah, M.E. Koina, A. Broomfield, V. Delghingaro-Augusto, D.A. Ellwood, J.E. Dahlstrom, Fatty acids alter glycerolipid metabolism and induce lipid droplet formation, syncytialisation and cytokine production in human trophoblasts with minimal glucose effect or interaction, *Placenta*. 31 (2010) 230–239. doi:10.1016/j.placenta.2009.12.013.
- [161] S. Perazzolo, B. Hirschmugl, C. Wadsack, G. Desoye, R.M. Lewis, B.G. Sengers, The influence of placental metabolism on fatty acid transfer to the fetus, *J. Lipid Res.* 58 (2017) 443–454. doi:10.1194/jlr.P072355.
- [162] K. Kolahi, S. Louey, O. Varlamov, K. Thornburg, Real-time tracking of BODIPY-C12 long-chain fatty acid in human term placenta reveals unique lipid dynamics in cytotrophoblast cells, *PLoS One*. 11 (2016) 1–23. doi:10.1371/journal.pone.0153522.
- [163] K. Kolahi, A. Valent, K.L. Thornburg, Cytotrophoblast, Not Syncytiotrophoblast, Dominates Glycolysis and Oxidative Phosphorylation in Human Term Placenta., *Sci. Rep.* (2017) 1–12. doi:10.1038/srep42941.
- [164] K.S. Kolahi, A.M. Valent, K.L. Thornburg, Real-time microscopic assessment of fatty acid uptake kinetics in the human term placenta, *Placenta*. 72–73 (2018) 1–9. doi:10.1016/j.placenta.2018.07.014.
- [165] V. Calabuig-Navarro, M. Puchowicz, P. Glazebrook, M. Haghiac, J. Minium, P. Catalano, S. Hauguel deMouzon, P. O’Tierney-Ginn, Effect of ω -3 supplementation on placental lipid metabolism in overweight and obese women., *Am. J. Clin. Nutr.* 103 (2016) 1064–72. doi:10.3945/ajcn.115.124651.
- [166] Y.Z. Diamant, N. Mayorek, S. Neuman, E. Shafrir, Enzymes of glucose and fatty acid metabolism in early and term human placenta, *Am. J. Obstet. Gynecol.* 121 (1975) 58–61. doi:10.1016/0002-9378(75)90975-8.
- [167] G.B. Wislocki, H.S. Bennett, The histology and cytology of the human and monkey placenta, with special reference to the trophoblast, *Am. J. Anat.* 73 (1943) 335–449. doi:10.1002/aja.1000730303.
- [168] P. Georgiades, A.C. Ferguson-Smith, G.J. Burton, Comparative Developmental Anatomy of the Murine and Human Definitive Placentae, *Placenta*. 23 (2002) 3–19. doi:10.1053/plac.2001.0738.

- [169] S.J. Tunster, E.D. Watson, A.L. Fowden, G.J. Burton, Placental glycogen stores and fetal growth: insights from genetic mouse models, *Reproduction*. 159 (2020) R213–R235. doi:10.1530/REP-20-0007.
- [170] G. Desoye, E.T. Korgun, N. Ghaffari-Tabrizi, T. Hahn, Is fetal macrosomia in adequately controlled diabetic women the result of a placental defect? – a hypothesis, *J. Matern. Neonatal Med.* 11 (2002) 258–261. doi:10.1080/jmf.11.4.258.261.
- [171] E. Larqué, H. Demmelmair, A. Gil-Sánchez, M.T. Prieto-Sánchez, J.E. Blanco, A. Pagán, F.L. Faber, S. Zamora, J.J. Parrilla, B. Koletzko, Placental transfer of fatty acids and fetal implications, *Am. J. Clin. Nutr.* 94 (2011) 1908S-1913S. doi:10.3945/ajcn.110.001230.
- [172] E. Margariti, M. Deutsch, S. Manolakopoulos, G. Kafri, D. Tiniakos, G.V. Papatheodoridis, Non-alcoholic fatty liver disease (nafld) may develop in patients with normal body mass index (BMI), *J. Hepatol.* 54 (2011) S340. doi:10.1016/S0168-8278(11)60854-4.
- [173] I. Cetin, F. Parisi, C. Berti, C. Mandò, G. Desoye, Placental fatty acid transport in maternal obesity, *J. Dev. Orig. Health Dis.* 3 (2012) 409–414. doi:10.1017/S2040174412000414.
- [174] A. Gázquez, O. Uhl, M. Ruíz-Palacios, C. Gill, N. Patel, B. Koletzko, L. Poston, E. Larqué, Placental lipid droplet composition: Effect of a lifestyle intervention (UPBEAT) in obese pregnant women, *Biochim. Biophys. Acta - Mol. Cell Biol. Lipids.* 1863 (2018) 998–1005. doi:10.1016/j.bbalip.2018.04.020.
- [175] A.D. Attie, R.M. Krauss, M.P. Gray-Keller, A. Brownlie, M. Miyazaki, J.J. Kastelein, A.J. Lusis, A.F.H. Stalenhoef, J.P. Stoehr, M.R. Hayden, J.M. Ntambi, Relationship between stearoyl-CoA desaturase activity and plasma triglycerides in human and mouse hypertriglyceridemia, *J. Lipid Res.* 43 (2002) 1899–1907. doi:10.1194/jlr.M200189-JLR200.
- [176] M.T. Flowers, J.M. Ntambi, Role of stearoyl-coenzyme A desaturase in regulating lipid metabolism, *Curr. Opin. Lipidol.* 19 (2008) 248–256. doi:10.1097/MOL.0b013e3282f9b54d.
- [177] O.C. Watkins, M.O. Islam, P. Selvam, R.A. Pillai, A. Cazenave-Gassiot, A.K. Bendt, N. Karnani, K.M. Godfrey, R.M. Lewis, M.R. Wenk, S.-Y. Chan, Metabolism of ¹³C-Labeled Fatty Acids in Term Human Placental Explants by Liquid Chromatography–Mass Spectrometry, *Endocrinology*. 160 (2019) 1394–1408. doi:10.1210/en.2018-01020.
- [178] V. Ferchaud-Roucher, K. Barner, T. Jansson, T.L. Powell, Maternal obesity results in decreased syncytiotrophoblast synthesis of palmitoleic acid, a fatty acid with anti-inflammatory and insulin-sensitizing properties, *FASEB J.* 33 (2019) 6643–6654. doi:10.1096/fj.201802444R.

- [179] H.P. Cho, M. Nakamura, S.D. Clarke, Cloning, Expression, and Fatty Acid Regulation of the Human Δ -5 Desaturase, *J. Biol. Chem.* 274 (1999) 37335–37339. doi:10.1074/jbc.274.52.37335.
- [180] A. Rani, P. Chavan-Gautam, S. Mehendale, G. Wagh, N.S. Mani, S. Joshi, Region-specific changes in the mRNA and protein expression of LCPUFA biosynthesis enzymes and transporters in the placenta of women with preeclampsia, *Placenta*. 95 (2020) 33–43. doi:10.1016/j.placenta.2020.04.013.
- [181] J. Chambaz, D. Ravel, M.-C. Manier, D. Pepin, N. Mulliez, G. Bereziat, Essential Fatty Acids Interconversion in the Human Fetal Liver, *Neonatology*. 47 (1985) 136–140. doi:10.1159/000242104.
- [182] M. Crawford, Placental delivery of arachidonic and docosahexaenoic acids: implications for the lipid nutrition of preterm infants, *Am. J. Clin. Nutr.* 71 (2000) 275S–284S. doi:10.1093/ajcn/71.1.275S.
- [183] B.N. Colvin, M.S. Longtine, B. Chen, M.L. Costa, D.M. Nelson, Oleate attenuates palmitate-induced endoplasmic reticulum stress and apoptosis in placental trophoblasts, *Reproduction*. 153 (2017) 369–380. doi:10.1530/REP-16-0576.
- [184] F.L. Alvarado, V. Calabuig-Navarro, M. Haghiac, M. Puchowicz, P.-J.S. Tsai, P. O'Tierney-Ginn, Maternal obesity is not associated with placental lipid accumulation in women with high omega-3 fatty acid levels, *Placenta*. 69 (2018) 96–101. doi:10.1016/j.placenta.2018.07.016.
- [185] P. Middleton, J.C. Gomersall, J.F. Gould, E. Shepherd, S.F. Olsen, M. Makrides, Omega-3 fatty acid addition during pregnancy, *Cochrane Database Syst. Rev.* (2018). doi:10.1002/14651858.CD003402.pub3.
- [186] R.K. Vinding, J. Stokholm, A. Sevelsted, B.L. Chawes, K. Bønnelykke, M. Barman, B. Jacobsson, H. Bisgaard, Fish Oil Supplementation in Pregnancy Increases Gestational Age, Size for Gestational Age, and Birth Weight in Infants: A Randomized Controlled Trial, *J. Nutr.* 149 (2019) 628–634. doi:10.1093/jn/nxy204.
- [187] L.K. Akison, M.D. Nitert, V.L. Clifton, K.M. Moritz, D.G. Simmons, Review: Alterations in placental glycogen deposition in complicated pregnancies: Current preclinical and clinical evidence, *Placenta*. 54 (2017) 52–58. doi:10.1016/j.placenta.2017.01.114.
- [188] J. Nam, E. Greenwald, C. Jack-Roberts, T.T. Ajeeb, O. V. Malysheva, M.A. Caudill, K. Axen, A. Saxena, E. Semernina, K. Nanobashvili, X. Jiang, Choline prevents fetal overgrowth and normalizes placental fatty acid and glucose metabolism in a mouse model of maternal obesity, *J. Nutr. Biochem.* 49 (2017) 80–88. doi:10.1016/j.jnutbio.2017.08.004.
- [189] M. Balachandiran, Z. Bobby, G. Dorairajan, S.E. Jacob, V. Gladwin, V.

- Vinayagam, R.M. Packirisamy, Placental Accumulation of Triacylglycerols in Gestational Diabetes Mellitus and Its Association with Altered Fetal Growth are Related to the Differential Expressions of Proteins of Lipid Metabolism, *Exp. Clin. Endocrinol. Diabetes*. 129 (2021) 803–812. doi:10.1055/a-1017-3182.
- [190] Y.Z. Diamant, B.E. Metzger, N. Freinkel, E. Shafir, Placental lipid and glycogen content in human and experimental diabetes mellitus, *Am. J. Obstet. Gynecol.* 144 (1982) 5–11. doi:10.1016/0002-9378(82)90385-4.
- [191] F. Visiedo, F. Bugatto, V. Sánchez, I. Cózar-Castellano, J.L. Bartha, G. Perdomo, High glucose levels reduce fatty acid oxidation and increase triglyceride accumulation in human placenta, *Am. J. Physiol. Metab.* 305 (2013) E205–E212. doi:10.1152/ajpendo.00032.2013.
- [192] T. Radaelli, J. Lepercq, A. Varastehpour, S. Basu, P.M. Catalano, S. Hauguel-De Mouzon, Differential regulation of genes for fetoplacental lipid pathways in pregnancy with gestational and type 1 diabetes mellitus, *Am. J. Obstet. Gynecol.* 201 (2009) 209.e1-209.e10. doi:10.1016/j.ajog.2009.04.019.
- [193] E. Shafir, V. Barash, Placental glycogen metabolism in diabetic pregnancy., *Isr. J. Med. Sci.* 27 (n.d.) 449–61. doi:1835720.
- [194] N.Y. Abdelhalim, M.H. Shehata, H.N. Gadallah, W.M. Sayed, A.A. Othman, Morphological and ultrastructural changes in the placenta of the diabetic pregnant Egyptian women, *Acta Histochem.* 120 (2018) 490–503. doi:10.1016/j.acthis.2018.05.008.
- [195] U. Cirkel, W. Burkart, E. Stähler, R. Buchholz, Effects of alloxan-induced diabetes mellitus on the metabolism of the rat placenta, *Arch. Gynecol.* 237 (1986) 155–163. doi:10.1007/BF02133859.
- [196] S.G. Gabbe, L.M. Demers, R.O. Greep, C.A. Vilee, Placental Glycogen Metabolism in Diabetes Mellitus, *Diabetes*. 21 (1972) 1185–1191. doi:10.2337/diab.21.12.1185.
- [197] B. SCHMON, M. HARTMANN, C.J. JONES, G. DESOYE, Insulin and Glucose Do not Affect the Glycogen Content in Isolated and Cultured Trophoblast Cells of Human Term Placenta, *J. Clin. Endocrinol. Metab.* 73 (1991) 888–893. doi:10.1210/jcem-73-4-888.
- [198] R.A. Pattillo, R.O. Husa, J.C. Garancis, Glycogen metabolism in human hormone-producing trophoblastic cells in continuous culture, *In Vitro*. 7 (1971) 59–67. doi:10.1007/BF02628263.
- [199] I.L.M.H. Aye, C.E. Aiken, D.S. Charnock-Jones, G.C.S. Smith, Placental energy metabolism in health and disease—significance of development and implications for preeclampsia, *Am. J. Obstet. Gynecol.* (2020). doi:10.1016/j.ajog.2020.11.005.

- [200] Z. Cheng, M. Ristow, Mitochondria and Metabolic Homeostasis, *Antioxid. Redox Signal.* 19 (2013) 240–242. doi:10.1089/ars.2013.5255.
- [201] M. Akram, Citric Acid Cycle and Role of its Intermediates in Metabolism, *Cell Biochem. Biophys.* 68 (2014) 475–478. doi:10.1007/s12013-013-9750-1.
- [202] X. Li, J. Gu, Q. Zhou, Review of aerobic glycolysis and its key enzymes - new targets for lung cancer therapy, *Thorac. Cancer.* 6 (2015) 17–24. doi:10.1111/1759-7714.12148.
- [203] M.S. Patel, T.E. Roche, Molecular biology and biochemistry of pyruvate dehydrogenase complexes 1, *FASEB J.* 4 (1990) 3224–3233. doi:10.1096/fasebj.4.14.2227213.
- [204] Y. Wang, M. Bucher, L. Myatt, Use of Glucose, Glutamine, and Fatty Acids for Trophoblast Respiration in Lean Women, Women With Obesity, and Women With Gestational Diabetes, *J. Clin. Endocrinol. Metab.* 104 (2019) 4178–4187. doi:10.1210/jc.2019-00166.
- [205] D. Nolfi-Donagan, A. Braganza, S. Shiva, Mitochondrial electron transport chain: Oxidative phosphorylation, oxidant production, and methods of measurement, *Redox Biol.* 37 (2020) 101674. doi:10.1016/j.redox.2020.101674.
- [206] A.N. Sferruzzi-Perri, J.S. Higgins, O.R. Vaughan, A.J. Murray, A.L. Fowden, Placental mitochondria adapt developmentally and in response to hypoxia to support fetal growth, *Proc. Natl. Acad. Sci.* 116 (2019) 1621–1626. doi:10.1073/pnas.1816056116.
- [207] A. Blanco, G. Blanco, Carbohydrate Metabolism, in: *Med. Biochem.*, Elsevier, 2017: pp. 283–323. doi:10.1016/B978-0-12-803550-4.00014-8.
- [208] H. Strid, T.L. Powell, ATP-Dependent Ca²⁺ Transport Is Up-Regulated during Third Trimester in Human Syncytiotrophoblast Basal Membranes, *Pediatr. Res.* 48 (2000) 58–63. doi:10.1203/00006450-200007000-00012.
- [209] J.J. Fisher, D.R. McKeating, J.S. Cuffe, T. Bianco-Miotto, O.J. Holland, A. V. Perkins, Proteomic Analysis of Placental Mitochondria Following Trophoblast Differentiation, *Front. Physiol.* 10 (2019). doi:10.3389/fphys.2019.01536.
- [210] J.J. Fisher, C.L. Vanderpeet, L.A. Bartho, D.R. McKeating, J.S.M. Cuffe, O.J. Holland, A. V. Perkins, Mitochondrial dysfunction in placental trophoblast cells experiencing gestational diabetes mellitus, *J. Physiol.* 599 (2021) 1291–1305. doi:10.1113/JP280593.
- [211] A. Maloyan, J. Mele, S. Muralimanoharan, L. Myatt, Placental metabolic flexibility is affected by maternal obesity, *Placenta.* 45 (2016) 69. doi:10.1016/j.placenta.2016.06.031.

- [212] S. Muralimanoharan, C. Guo, L. Myatt, A. Maloyan, Sexual dimorphism in miR-210 expression and mitochondrial dysfunction in the placenta with maternal obesity, *Int. J. Obes.* 39 (2015) 1274–1281. doi:10.1038/ijo.2015.45.
- [213] S. Muralimanoharan, A. Maloyan, L. Myatt, Mitochondrial function and glucose metabolism in the placenta with gestational diabetes mellitus: role of miR-143., *Clin. Sci. (Lond)*. 130 (2016) 931–41. doi:10.1042/CS20160076.
- [214] C. Mandò, G.M. Anelli, C. Novielli, P. Panina-Bordignon, M. Massari, M.I. Mazzocco, I. Cetin, Impact of Obesity and Hyperglycemia on Placental Mitochondria, *Oxid. Med. Cell. Longev.* 2018 (2018) 1–10. doi:10.1155/2018/2378189.
- [215] U. Weiss, M. Cervar, P. Puerstner, O. Schmut, J. Haas, R. Mauschitz, G. Arikian, G. Desoye, Hyperglycaemia in vitro alters the proliferation and mitochondrial activity of the choriocarcinoma cell lines BeWo, JAR and JEG-3 as models for human first-trimester trophoblast, *Diabetologia*. 44 (2001) 209–219. doi:10.1007/s001250051601.
- [216] P.S. Shekhawat, D. Matern, A.W. Strauss, Fetal Fatty Acid Oxidation Disorders, Their Effect on Maternal Health and Neonatal Outcome: Impact of Expanded Newborn Screening on Their Diagnosis and Management, *Pediatr. Res.* 57 (2005) 78R-86R. doi:10.1203/01.PDR.0000159631.63843.3E.
- [217] K.H. Moore, J.F. Radloff, F.E. Hull, C.C. Sweeley, Incomplete fatty acid oxidation by ischemic heart: beta-hydroxy fatty acid production., *Am. J. Physiol.* 239 (1980) H257-65.
- [218] J.M. Rutkowski, T.A. Knotts, K.D. Ono-Moore, C.S. McCain, S. Huang, D. Schneider, S. Singh, S.H. Adams, D.H. Hwang, Acylcarnitines activate proinflammatory signaling pathways., *Am. J. Physiol. Endocrinol. Metab.* 306 (2014) E1378-87. doi:10.1152/ajpendo.00656.2013.
- [219] N. Oey, N. Vanvliet, F. Wijburg, R. Wanders, T. Attiebitach, F. Vaz, l-Carnitine is Synthesized in the Human Fetal–Placental Unit: Potential Roles in Placental and Fetal Metabolism, *Placenta*. 27 (2006) 841–846. doi:10.1016/j.placenta.2005.10.002.
- [220] F.M. Vaz, R.J.A. Wanders, Carnitine biosynthesis in mammals, *Biochem. J.* 361 (2002) 417–429. doi:10.1042/bj3610417.
- [221] P. Shekhawat, M.J. Bennett, Y. Sadovsky, D.M. Nelson, D. Rakheja, A.W. Strauss, Human placenta metabolizes fatty acids: implications for fetal fatty acid oxidation disorders and maternal liver diseases, *Am. J. Physiol. - Endocrinol. Metab.* 284 (2003) E1098–E1105. doi:10.1152/ajpendo.00481.2002.
- [222] N.A. Oey, M.E.J. Den Boer, J.P.N. Ruiter, R.J.A. Wanders, M. Duran, H.R. Waterham, K. Boer, J.A.M. van der Post, F.A. Wijburg, High activity of fatty acid

- oxidation enzymes in human placenta: Implications for fetal-maternal disease, *J. Inherit. Metab. Dis.* 26 (2003) 385. doi:10.1023/A:1025163204165.
- [223] D. Rakheja, M.J. Bennett, B.M. Foster, R. Domiati-Saad, B.B. Rogers, Evidence for Fatty Acid Oxidation in Human Placenta, and the Relationship of Fatty Acid Oxidation Enzyme Activities with Gestational Age, *Placenta*. 23 (2002) 447–450. doi:10.1053/plac.2002.0808.
- [224] K.E. Boyle, Z.W. Patinkin, A.L.B. Shapiro, C. Bader, L. Vanderlinden, K. Kechris, R.C. Janssen, R.J. Ford, B.K. Smith, G.R. Steinberg, E.J. Davidson, I. V. Yang, D. Dabelea, J.E. Friedman, Maternal obesity alters fatty acid oxidation, AMPK activity, and associated DNA methylation in mesenchymal stem cells from human infants, *Mol. Metab.* 6 (2017) 1503–1516. doi:10.1016/j.molmet.2017.08.012.
- [225] R.J.A. Wanders, H.R. Waterham, S. Ferdinandusse, Metabolic Interplay between Peroxisomes and Other Subcellular Organelles Including Mitochondria and the Endoplasmic Reticulum, *Front. Cell Dev. Biol.* 3 (2016). doi:10.3389/fcell.2015.00083.
- [226] T. Hashimoto, Peroxisomal beta-oxidation enzymes., *Cell Biochem. Biophys.* 32 Spring (2000) 63–72. doi:10.1385/cbb:32:1-3:63.
- [227] P.P. Van Veldhoven, Biochemistry and genetics of inherited disorders of peroxisomal fatty acid metabolism, *J. Lipid Res.* 51 (2010) 2863–2895. doi:10.1194/jlr.R005959.
- [228] T.-Y. Huang, D. Zheng, R.C. Hickner, J.J. Brault, R.N. Cortright, Peroxisomal gene and protein expression increase in response to a high-lipid challenge in human skeletal muscle, *Metabolism*. 98 (2019) 53–61. doi:10.1016/j.metabol.2019.06.009.
- [229] F. Visiedo, F. Bugatto, R. Quintero-Prado, I. Cózar-Castellano, J.L. Bartha, G. Perdomo, Glucose and Fatty Acid Metabolism in Placental Explants From Pregnancies Complicated With Gestational Diabetes Mellitus, *Reprod. Sci.* 22 (2015) 798–801. doi:10.1177/1933719114561558.
- [230] T.R. Koves, J.R. Ussher, R.C. Noland, D. Slentz, M. Mosedale, O. Ilkayeva, J. Bain, R. Stevens, J.R.B. Dyck, C.B. Newgard, G.D. Lopaschuk, D.M. Muoio, Mitochondrial Overload and Incomplete Fatty Acid Oxidation Contribute to Skeletal Muscle Insulin Resistance, *Cell Metab.* 7 (2008) 45–56. doi:10.1016/j.cmet.2007.10.013.
- [231] P.R. Baker, K.E. Boyle, T.R. Koves, O.R. Ilkayeva, D.M. Muoio, J.A. Houmard, J.E. Friedman, Metabolomic analysis reveals altered skeletal muscle amino acid and fatty acid handling in obese humans., *Obesity (Silver Spring)*. 23 (2015) 981–988. doi:10.1002/oby.21046.

- [232] P.R. Baker, Z. Patinkin, A.L. Shapiro, B.A. De La Houssaye, M. Woontner, K.E. Boyle, L. Vanderlinden, D. Dabelea, J.E. Friedman, Maternal obesity and increased neonatal adiposity correspond with altered infant mesenchymal stem cell metabolism., *JCI Insight*. 2 (2017). doi:10.1172/jci.insight.94200.
- [233] M. Ruiz, F. Labarthe, A. Fortier, B. Bouchard, J. Thompson Legault, V. Bolduc, O. Rigal, J. Chen, A. Ducharme, P.A. Crawford, J.-C. Tardif, C. Des Rosiers, Circulating acylcarnitine profile in human heart failure: a surrogate of fatty acid metabolic dysregulation in mitochondria and beyond., *Am. J. Physiol. Heart Circ. Physiol.* 313 (2017) H768–H781. doi:10.1152/ajpheart.00820.2016.
- [234] A.T. Turer, R.D. Stevens, J.R. Bain, M.J. Muehlbauer, J. van der Westhuizen, J.P. Mathew, D.A. Schwinn, D.D. Glower, C.B. Newgard, M. V Podgoreanu, Metabolomic profiling reveals distinct patterns of myocardial substrate use in humans with coronary artery disease or left ventricular dysfunction during surgical ischemia/reperfusion., *Circulation*. 119 (2009) 1736–46. doi:10.1161/CIRCULATIONAHA.108.816116.
- [235] I.G.I. Thiele, K.E. Niezen-Koning, A.H. van Gennip, J.G. Aarnoudse, Increased Plasma Carnitine Concentrations in Preeclampsia, *Obstet. Gynecol.* 103 (2004) 876–880. doi:10.1097/01.AOG.0000125699.60416.03.
- [236] M.P.H. Koster, R.J. Vreeken, A.C. Harms, A.D. Dane, S. Kuc, P.C.J.I. Schielen, T. Hankemeier, R. Berger, G.H.A. Visser, J.L.A. Pennings, First-Trimester Serum Acylcarnitine Levels to Predict Preeclampsia: A Metabolomics Approach, *Dis. Markers*. 2015 (2015) 1–8. doi:10.1155/2015/857108.
- [237] K. Ryckman, B. Donovan, D. Fleener, B. Bedell, K. Borowski, Pregnancy-Related Changes of Amino Acid and Acylcarnitine Concentrations: The Impact of Obesity, *Am. J. Perinatol. Reports*. 06 (2016) e329–e336. doi:10.1055/s-0036-1592414.
- [238] C. Hellmuth, K.L. Lindsay, O. Uhl, C. Buss, P.D. Wadhwa, B. Koletzko, S. Entringer, Association of maternal prepregnancy BMI with metabolomic profile across gestation, *Int. J. Obes.* 41 (2017) 159–169. doi:10.1038/ijo.2016.153.
- [239] A. Jaremek, M.J. Jeyarajah, G. Jaju Bhattad, S.J. Renaud, Omics Approaches to Study Formation and Function of Human Placental Syncytiotrophoblast, *Front. Cell Dev. Biol.* 9 (2021). doi:10.3389/fcell.2021.674162.
- [240] S. Mohammad, J. Bhattacharjee, T. Vasanthan, C.S. Harris, S.A. Bainbridge, K.B. Adamo, Metabolomics to understand placental biology: Where are we now?, *Tissue Cell*. 73 (2021) 101663. doi:10.1016/j.tice.2021.101663.
- [241] B.-K. Lee, J. Kim, Integrating High-Throughput Approaches and in vitro Human Trophoblast Models to Decipher Mechanisms Underlying Early Human Placenta Development, *Front. Cell Dev. Biol.* 9 (2021). doi:10.3389/fcell.2021.673065.
- [242] S. Nalbantoglu, A. Karadag, Introductory Chapter: Insight into the OMICS

- Technologies and Molecular Medicine, in: *Mol. Med.*, IntechOpen, 2019. doi:10.5772/intechopen.86450.
- [243] L.M. Raamsdonk, B. Teusink, D. Broadhurst, N. Zhang, A. Hayes, M.C. Walsh, J.A. Berden, K.M. Brindle, D.B. Kell, J.J. Rowland, H. V. Westerhoff, K. van Dam, S.G. Oliver, A functional genomics strategy that uses metabolome data to reveal the phenotype of silent mutations, *Nat. Biotechnol.* 19 (2001) 45–50. doi:10.1038/83496.
- [244] C. Guijas, J.R. Montenegro-Burke, B. Warth, M.E. Spilker, G. Siuzdak, Metabolomics activity screening for identifying metabolites that modulate phenotype, *Nat. Biotechnol.* 36 (2018) 316–320. doi:10.1038/nbt.4101.
- [245] O. Fiehn, Metabolomics--the link between genotypes and phenotypes., *Plant Mol. Biol.* 48 (2002) 155–71. <http://www.ncbi.nlm.nih.gov/pubmed/11860207>.
- [246] K. Yang, X. Han, Lipidomics: Techniques, Applications, and Outcomes Related to Biomedical Sciences, *Trends Biochem. Sci.* 41 (2016) 954–969. doi:10.1016/j.tibs.2016.08.010.
- [247] S. Doran, M. Arif, S. Lam, A. Bayraktar, H. Turkez, M. Uhlen, J. Boren, A. Mardinoglu, Multi-omics approaches for revealing the complexity of cardiovascular disease, *Brief. Bioinform.* 22 (2021). doi:10.1093/bib/bbab061.
- [248] P. Leon-Mimila, J. Wang, A. Huertas-Vazquez, Relevance of Multi-Omics Studies in Cardiovascular Diseases, *Front. Cardiovasc. Med.* 6 (2019). doi:10.3389/fcvm.2019.00091.
- [249] L. Niu, K. Sulek, C.G. Vasilopoulou, A. Santos, N.J. Wewer Albrechtsen, S. Rasmussen, F. Meier, M. Mann, Defining NASH from a Multi-Omics Systems Biology Perspective, *J. Clin. Med.* 10 (2021) 4673. doi:10.3390/jcm10204673.
- [250] W. Wruck, K. Kashofer, S. Rehman, A. Daskalaki, D. Berg, E. Gralka, J. Jozefczuk, K. Drews, V. Pandey, C. Regenbrecht, C. Wierling, P. Turano, U. Korf, K. Zatloukal, H. Lehrach, H. V. Westerhoff, J. Adjaye, Multi-omic profiles of human non-alcoholic fatty liver disease tissue highlight heterogenic phenotypes, *Sci. Data.* 2 (2015) 150068. doi:10.1038/sdata.2015.68.
- [251] S. Gong, U. Sovio, I.L.M.H. Aye, F. Gaccioli, J. Dopierala, M.D. Johnson, A.M. Wood, E. Cook, B.J. Jenkins, A. Koulman, R.A. Casero, M. Constância, D.S. Charnock-Jones, G.C.S. Smith, Placental polyamine metabolism differs by fetal sex, fetal growth restriction, and preeclampsia, *JCI Insight.* 3 (2018). doi:10.1172/jci.insight.120723.
- [252] M. Saoi, K.M. Kennedy, W. Gohir, D.M. Sloboda, P. Britz-McKibbin, Placental Metabolomics for Assessment of Sex-specific Differences in Fetal Development During Normal Gestation, *Sci. Rep.* 10 (2020) 9399. doi:10.1038/s41598-020-66222-3.

- [253] C.S. Rosenfeld, Transcriptomics and Other Omics Approaches to Investigate Effects of Xenobiotics on the Placenta, *Front. Cell Dev. Biol.* 9 (2021). doi:10.3389/fcell.2021.723656.
- [254] C.H. Hulme, A. Stevens, W. Dunn, A.E.P. Heazell, K. Hollywood, P. Begley, M. Westwood, J.E. Myers, Identification of the functional pathways altered by placental cell exposure to high glucose: lessons from the transcript and metabolite interactome, *Sci. Rep.* 8 (2018) 5270. doi:10.1038/s41598-018-22535-y.
- [255] Y. Hasin, M. Seldin, A. Lusic, Multi-omics approaches to disease, *Genome Biol.* 18 (2017) 83. doi:10.1186/s13059-017-1215-1.
- [256] S. Altmäe, M.T. Segura, F.J. Esteban, S. Bartel, P. Brandi, M. Irmeler, J. Beckers, H. Demmelmair, C. López-Sabater, B. Koletzko, S. Krauss-Etschmann, C. Campoy, Maternal Pre-Pregnancy Obesity Is Associated with Altered Placental Transcriptome, *PLoS One.* 12 (2017) e0169223. doi:10.1371/journal.pone.0169223.
- [257] J. Saben, F. Lindsey, Y. Zhong, K. Thakali, T.M. Badger, A. Andres, H. Gomez-Acevedo, K. Shankar, Maternal obesity is associated with a lipotoxic placental environment, *Placenta.* 35 (2014) 171–177. doi:10.1016/j.placenta.2014.01.003.
- [258] S. Sureshchandra, N.E. Marshall, R.M. Wilson, T. Barr, M. Rais, J.Q. Purnell, K.L. Thornburg, I. Messaoudi, Inflammatory Determinants of Pregravid Obesity in Placenta and Peripheral Blood, *Front. Physiol.* 9 (2018). doi:10.3389/fphys.2018.01089.
- [259] L. Tang, P. Li, L. Li, Whole transcriptome expression profiles in placenta samples from women with gestational diabetes mellitus, *J. Diabetes Investig.* 11 (2020) 1307–1317. doi:10.1111/jdi.13250.
- [260] T. Radaelli, A. Varastehpour, P. Catalano, S. Hauguel-de Mouzon, Gestational Diabetes Induces Placental Genes for Chronic Stress and Inflammatory Pathways, *Diabetes.* 52 (2003) 2951–2958. doi:10.2337/diabetes.52.12.2951.
- [261] M.R.B. Pineda-Cortel, J.A.A. Bunag, T.P. Mamerto, M.F.B. Abulencia, Differential gene expression and network-based analyses of the placental transcriptome reveal distinct potential biomarkers for gestational diabetes mellitus, *Diabetes Res. Clin. Pract.* 180 (2021) 109046. doi:10.1016/j.diabres.2021.109046.
- [262] L. Myatt, E. Wang, K. Stratton, L. Bramer, B.-J. Webb-Robertson, J. Kyle, K. Burnum-Johnson, Changes in Placental Lipidomics with Obesity and Gestational Diabetes: Sexual Dimorphism, *Placenta.* 83 (2019) e44–e45. doi:10.1016/j.placenta.2019.06.145.
- [263] O. Uhl, H. Demmelmair, M.T. Segura, J. Florido, R. Rueda, C. Campoy, B. Koletzko, Effects of obesity and gestational diabetes mellitus on placental phospholipids, *Diabetes Res. Clin. Pract.* 109 (2015) 364–371.

doi:10.1016/j.diabres.2015.05.032.

- [264] S. Furse, D.S. Fernandez-Twinn, B. Jenkins, C.L. Meek, H.E.L. Williams, G.C.S. Smith, D.S. Charnock-Jones, S.E. Ozanne, A. Koulman, A high-throughput platform for detailed lipidomic analysis of a range of mouse and human tissues, *Anal. Bioanal. Chem.* 412 (2020) 2851–2862. doi:10.1007/s00216-020-02511-0.
- [265] C. Fattuoni, C. Mandò, F. Palmas, G.M. Anelli, C. Novielli, E. Parejo Laudicina, V.M. Savasi, L. Barberini, A. Dessì, R. Pintus, V. Fanos, A. Noto, I. Cetin, Preliminary metabolomics analysis of placenta in maternal obesity, *Placenta*. 61 (2018) 89–95. doi:10.1016/j.placenta.2017.11.014.
- [266] Y. Yang, Z. Pan, F. Guo, H. Wang, W. Long, H. Wang, B. Yu, Placental metabolic profiling in gestational diabetes mellitus: An important role of fatty acids, *J. Clin. Lab. Anal.* 35 (2021). doi:10.1002/jcla.24096.
- [267] E.-M. Sedlmeier, S. Brunner, D. Much, P. Pagel, S.E. Ulbrich, H.H. Meyer, U. Amann-Gassner, H. Hauner, B.L. Bader, Human placental transcriptome shows sexually dimorphic gene expression and responsiveness to maternal dietary n-3 long-chain polyunsaturated fatty acid intervention during pregnancy, *BMC Genomics*. 15 (2014) 941. doi:10.1186/1471-2164-15-941.
- [268] X. Chen, T.O. Scholl, M. Leskiw, J. Savaille, T.P. Stein, Differences in maternal circulating fatty acid composition and dietary fat intake in women with gestational diabetes mellitus or mild gestational hyperglycemia, *Diabetes Care*. 33 (2010) 2049–2054. doi:10.2337/dc10-0693.
- [269] P.M. Villa, H. Laivuori, E. Kajantie, R. Kaaja, Free fatty acid profiles in preeclampsia, *Prostaglandins, Leukot. Essent. Fat. Acids*. 81 (2009) 17–21. doi:10.1016/j.plefa.2009.05.002.
- [270] D. Iggman, U. Risérus, Role of different dietary saturated fatty acids for cardiometabolic risk, *Clin. Lipidol.* 6 (2011) 209–223. doi:10.2217/clp.11.7.
- [271] C.L. Kien, J.Y. Bunn, R. Stevens, J. Bain, O. Ikayeva, K. Crain, T.R. Koves, D.M. Muoio, Dietary intake of palmitate and oleate has broad impact on systemic and tissue lipid profiles in humans, *Am. J. Clin. Nutr.* 99 (2014) 436–445. doi:10.3945/ajcn.113.070557.

Chapter 2

2 Syncytialization and prolonged exposure to palmitate impacts BeWo respiration

A version of this chapter has been published:

Easton ZJW, Delhaes F, Mathers K, Zhao L, Vanderboor CMG, and Regnault TRH.
Syncytialization and prolonged exposure to palmitate impacts BeWo respiration.
Reproduction. 2021;161: 73–88. doi:10.1530/REP-19-0433

Reproduced with permission from Bioscientifica Ltd (Appendix B)

2.1 Introduction

The prevalence of obesity in women of reproductive age has been increasing worldwide over the past several decades, and approximately 40 million pregnant women globally are obese [1–3]. Additional reports have indicated that a majority of women of reproductive age have a hip-to-waist ratio (WHR) indicative of a high risk for metabolic disease development [4,5]. Increased body mass, obesity and elevated WHR prior to and during pregnancy have not only been associated with negative health impacts for the mother, but also with impaired metabolic health outcomes in the offspring [6–11]. For example, children born to mothers who were overweight or obese throughout the gestational period have an increased risk of developing metabolic complications such as type 2 diabetes mellitus and obesity compared to children born to mothers with lean body compositions [10]. Of greater concern, these children develop these “adult-associated” metabolic diseases as early as four years of age, and the prevalence of pediatric metabolic syndrome appears to be increasing [8,12,13].

The origin of early onset development of adult-associated diseases is the result of aberrant *in utero* programming of fetal metabolism potentially induced by maternal obesity-mediated alterations to placental mitochondrial function [14–16]. Specifically, due to their close proximity to maternal blood, trophoblast cells within the placental chorionic villi may be important in facilitating the adverse effects observed with increased maternal adiposity [9,17]. In fact, the large multinuclear syncytiotrophoblast (SCT) cells, and underlying progenitor cytotrophoblast (CT) cells that comprise the chorionic villi in obese pregnancies have been found to display decreased mitochondrial respiratory activity (oxidative phosphorylation) as well as reduced cellular ATP content [17–19]. Obesity-associated impairments in placental mitochondrial function have also been identified through analysis of enzymes within mitochondrial energy production pathways. Specifically, the activity of citrate synthase (CS; a proxy measurement of total cellular mitochondrial content) as well as the protein abundance and enzyme activity of electron transport chain (ETC) complex I (NADH Dehydrogenase) and complex II (Succinate Dehydrogenase) are decreased in villous trophoblast cells from term obese placentae, [19,20]. Since progenitor CT and differentiated SCT cells form the materno-

fetal interface and regulate nutrient and gaseous exchange between mother and developing fetus, obesity-mediated mitochondrial dysfunction within these cell types may alter transplacental nutrient transfer such that fetoplacental development becomes pathological [21].

Recently however, analysis of dietary patterns in Westernized populations have discussed a link between poor diet and metabolic health risks [22,23]. For example, adherence to an unhealthy diet during gestation has been found to promote the development of Gestational Diabetes Mellitus (GDM) [24–26], which in itself has been found to promote poor metabolic health outcomes in the exposed offspring [27–30]. Studies analyzing gestational diet composition have demonstrated that many pregnant women consume diets that are calorie-dense, but nutrient lacking and high in saturated and monounsaturated fatty acids [31–34]. These reports are concerning as consumption of a poor diet during gestation has been identified to facilitate the progression of placental metabolic impairments that ultimately lead to the development metabolic disease in the exposed offspring. For example, a pre-gestational diet-reversal from a high fat diet (HFD) to healthy control diet in obese non-human primates has been associated with improved placental vascular function as well as improvements in fetal metabolic health [35–38]. As these diet reversal studies altered maternal fat intake to improve placental and fetal metabolic health, dietary fatty acids (FA) themselves may be important in mediating adverse outcomes in obese pregnancies.

Specific analysis of fasting blood lipid levels in pregnant populations revealed that pregnancies complicated by maternal obesity and GDM display hyperlipidemia and increased circulating levels of the saturated FA palmitate (C16:0, PA) and the monounsaturated FA oleate (C18:1 cis 9, OA) [39–41]. As circulating PA and OA levels have previously been found to be impacted by diet composition [42,43], these data suggest that PA and OA are overabundant in the diets of women with pregnancies complicated by obesity and GDM. It is important to note that increased PA levels have been demonstrated to independently induce mitochondrial damage and impair mitochondrial oxidative function leading to decreased ATP content in a number of cell culture systems [44–46].

Collectively these data could indicate that placental mitochondrial impairments are the result of dietary FA overabundance, and that changes in maternal diet and fat intake alone may have effects on placental function and ultimately offspring metabolic health. However, the underlying independent effects of dietary saturated and monounsaturated NEFAs in mediating these phenotypes remains uncertain. The objective of this study was to examine the direct prolonged effects of PA and OA on placental CT and SCT mitochondrial metabolism. It was postulated that a prolonged exposure to the dietary NEFAs PA and OA both independently and in combination would impair mitochondrial function in BeWo CT and SCT cells.

2.2 Materials and Methods:

2.2.1 Materials

All chemicals were purchased from Millipore Sigma (Oakville, Canada) unless otherwise indicated.

2.2.2 Cell culture conditions

BeWo cells are a choriocarcinoma-derived immortalized cell line that are representative system of villous trophoblast cells of the human placenta and have been previously utilized to examine human villous trophoblast metabolic function [47,48]. Under basal conditions these cells are proliferative and CT-like, and when cultured with a cAMP analogue (8-Br-cAMP) they differentiate into SCT-like cells that secrete human chorionic gonadotropin (hCG) [49,50]. In the current study, BeWo cells were utilized as a model to examine the independent effects of dietary NEFAs as these cells are isolated from effects of maternal body composition and gestational diet.

BeWo cells (CCL-98) were purchased from the American Type Culture Collection (ATCC; Cedarlane Labs, Burlington, Canada) and cultured in F12K media (Gibco, ThermoFisher, Missasauga, Canada) supplemented with 1% Penicillin-Streptomycin (Invitrogen, ThermoFisher, Mississauga, Canada) and 10% Fetal Bovine Serum (Gibco). Cells were maintained at 37 °C in 5% CO₂/95% atmospheric air and used between passages 5-11 for all experiments. For each experiment, BeWo CT cells were

plated at stated specific experimental densities and allowed to adhere to cell culture plates overnight prior to NEFA treatment. For all NEFA treatments, fats were conjugated 2:1 (molar ratio) to FA free bovine serum albumin (BSA). NEFA medias were heated at 37°C for at least 30 mins prior to media changes to ensure equilibrium state of FA-BSA complexes [51]. Media supplemented with 0.3% BSA was used for control cultures in all experiments (BSA-ctrl). For SCT differentiation, 250 μ M 8-Br-cAMP was added to experimental cell culture media at 24H and 48H. Media in all experimental conditions were replenished every 24H. A schematic showing the experimental timeline is shown in **Figure 2-1**.

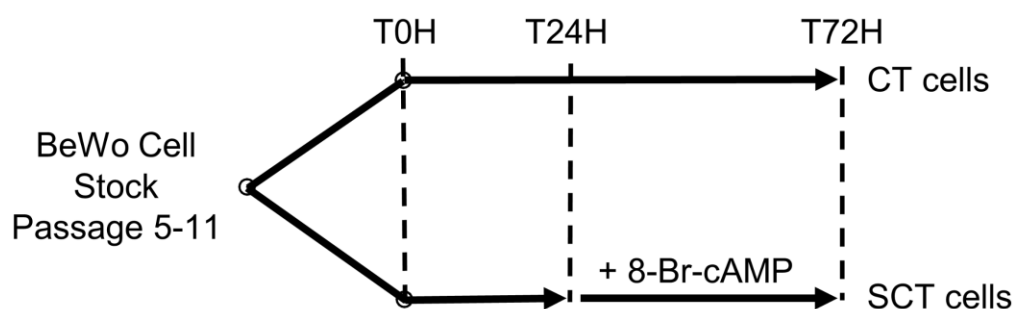


Figure 2-1 Cell culture timeline for BeWo cell NEFA-treatments

BeWo cells were plated and allowed to adhere overnight prior to NEFA-treatment initiation at T0H. At T24H 250 μ M 8-Br-cAMP or a vehicle control was added to the cell culture plates to allocate cells to either CT or SCT cell type. All metabolic activity assays and cell collections were performed at T72H.

2.2.3 Cell viability

Cell viability in response to increasing concentrations (0-200 μ M) of PA, OA, and a 1:1 ratio of PA and OA (P/O) conjugated 2:1 (molar ratio) to BSA was assessed via the CellTiter-Fluor live-cell protease activity assay (Promega Corporation, Madison, WI, USA). BeWo cells were plated at 1×10^4 cells/well in 96-well opaque walled plates, and viability was assessed at 72H for both CT and SCT cell types as per the manufacturer's instructions, using a SpectraMax M5 plate reader (Molecular Devices, San Jose, CA, USA).

2.2.4 Immunofluorescent analysis of BeWo syncytialization

To assess the syncytialization of NEFA-treated BeWo cultures, percent fusion of each treatment group was determined via zona occludens-1 (ZO-1) immunofluorescent cell imaging [52]. In brief, BeWo cells were plated at a density of 1.4×10^5 cells/well on glass coverslips coated with laminin ($2 \mu\text{g}/\text{cm}^2$) in 6-well cell culture plates and cultured for 72H with 100 μ M of PA, OA or P/O conjugated 2:1 (molar ratio) to BSA. At 72H cells were washed once with Phosphate Buffered Saline (PBS) and fixed with 1:1 methanol:acetone for 30 mins at -20°C . Fixed cells were washed with PBS and permeabilized with 0.3% Triton-X 100 in PBS for 5 mins. Coverslips were then washed three times with PBS and blocked with 10% goat serum (abcam, Toronto, Canada) in PBS (blocking buffer). Coverslips were then incubated with ZO-1 antibody (1:200 dilution in blocking buffer; catalog No. 33-9100, Invitrogen) for 1 hour at room temperature. After washing with PBS three times coverslips were incubated with donkey anti-mouse IgG secondary antibody, Alexa Fluor 594 (1:2000 dilution in blocking buffer; Catalog No. R37115, Invitrogen) for 1 hour at room temperature. Coverslips were then washed 3 more times in PBS and mounted on slides using Fluoroshield with DAPI. Immunofluorescent images were then captured using the Zeiss Axioimager Z1 microscope (Carl Zeiss AG, Oberkochen, Germany) at the Biotron Integrated Microscopy Facility, Biotron Research Centre, Western University, London, Ontario, Canada. Nuclei and fused BeWo cells were then counted using ZEN software (Carl Zeiss AG), and percent fusion calculated as the percentage of total counted cells lacking ZO-1 expression.

2.2.5 Quantitative-PCR analysis of BeWo syncytialization

Relative mRNA transcript abundance of the genes encoding the beta subunit of human chorionic gonadotropin beta (*CGB*), and Ovo Like Transcriptional Repressor 1 (*OVOLI*) were used as an indirect quantification of BeWo syncytialization following NEFA-treatment. Cells were plated at a density of 2×10^5 cells/well 6-well plates and treated with 100 μ M NEFAs as described above. Total RNA was then extracted via phenol-chloroform extraction using TRIzol reagent (Invitrogen) as per the manufacturer's specifications. Isolated RNA was then reverse transcribed using random decamer primers and M-MLV reverse transcriptase (Invitrogen) and RT-qPCR was subsequently performed using the CFX384 Real Time System (BioRad, Mississauga, Canada).

Target *CGB* primer sequences were obtained from Malhotra *et al.*, (2015); primer sequences for *OVOLI* were obtained from Kusama *et al.*, (2018); and primers for the reference genes β -actin (*ACTB*) and Proteasome 20S subunit Beta 6 (*PSMB6*) were designed using the NCBI/Primer-BLAST tool (**Table 2-1**). Amplification of target gene expression was reported as fold change relative to control CT cells using the $2^{-\Delta\Delta Ct}$ method with the ΔCt of each treatment condition being assessed as $Ct(target) - \text{Geometric mean of } Ct(ACTB) \text{ and } Ct(PSMB6)$.

Table 2-1 Forward and reverse primer sequences used for quantitative Real-Time PCR measurement of BeWo cell syncytialization.

Gene	Accession No.	Annealing Temperature (°C)	Primer Sequences	Efficiency
<i>ACTB</i>	NM_001101.4	60	F – GTTGCTATCCAGGCTGTGCT R – AGGTAGTCAGTCAGGTCCCG	109.0%
<i>PSMB6</i>	NM_002798	60	F – CGGGAAGACCTGATGGCGGGA R – TCCCGGAGCCTCCAATGGCAA	107.1%
<i>CGB</i>	Malhotra <i>et al</i> (2015) [53]	60	F – CCCCTTGACCTGTGATGACC R – TATGTGGGAGGATCGGGGT	101.1%
<i>OVOLI</i>	Kusama <i>et al</i> (2018) [54]	60	F – AGACATGGGCCACTTGACAG R – AGGTGAACAGGTCTCCACTG	99.5 %

2.2.6 Quantification of apoptosis

The activation state of pro-apoptotic pathways in BeWo CT and SCT cells in response to 100 μM NEFA treatments was assessed via caspase-3/7 activity at 72H. Cells were plated at a density of 1×10^4 cells/well in opaque walled 96-well plates and treated with 100 μM NEFAs as described above. Live cell caspase 3/7 activity was determined at 72H utilizing the Caspase-Glo 3/7 Assay (Promega Corporation) as per manufacturer's instructions. BeWo CT cells treated with 100 μM of each rotenone (ETC complex I inhibitor) and antimycin A (ETC complex II inhibitor) were utilized as a positive control for upregulation of pro-apoptotic pathways [55].

2.2.7 Optimization of Seahorse XF assay protocols

BeWo cells were plated at the determined optimal density of 7.5×10^3 cells/well in Seahorse XF24 V7PS cell culture microplates (Agilent Technologies, Santa Clara, CA, USA) coated with $9 \mu\text{g}/\text{cm}^2$ collagen I (Gibco). The optimal concentration of the ATP synthase inhibitor oligomycin (1.5 $\mu\text{g}/\text{mL}$) was determined as per manufacturer's instructions. The mitochondrial uncoupler dinitrophenol (DNP; 50 μM) was utilized to measure maximal mitochondrial respiratory activity. Attempts to follow the manufacturer's recommended uncoupler FCCP resulted in unstable and declining OCR measurements. Previous reports have identified that progesterone, which is secreted by BeWo cells, recouples FCCP uncoupled mitochondria, but not DNP uncoupled mitochondria, and the optimization of DNP in our system produced the required stable OCR increase to measure maximal respiratory rate [56,57]. The complex I inhibitor rotenone (0.5 μM), complex II inhibitor antimycin A (0.5 μM), D-glucose (10 mM), and 2-deoxy-D-glucose (50 mM) were used as per manufacturer's recommendation.

2.2.8 BeWo cell oxidative function

The optimized Mitochondrial (Mito) Stress Test was utilized to quantify the oxidative function of NEFA-treated (100 μM) BeWo CTs and SCTs. At the 72H timepoint the culture medium exchanged with Mito Stress Test assay media (Seahorse XF base media (Agilent Technologies) supplemented with 10 mM D-glucose, 2 mM sodium pyruvate, and 2 mM L-glutamine (Gibco, ThermoFisher, Mississauga, Canada),

pH 7.4), and cells were incubated at 37°C in 100% atmospheric air for 45 mins. Following basal OCR readings subsequent injections of oligomycin; DNP; and rotenone combined with antimycin A were utilized to measure parameters of mitochondrial respiratory function. A representative Seahorse XF Mito Stress Test Tracing is available in **Figure 2-2**.

Following the Mito Stress Test assay, cells were lysed via freeze-thaw method in Seahorse assay media and total DNA was quantified using Hoechst dye fluorescence [58,59]. Briefly, cell lysates were mixed with 2x Hoechst Dye assay mix (0.0324 mM Hoechst 33342 Dye (Pierce, ThermoFisher Scientific, Mississauga, Canada), 2 M NaCl, 50 mM NaH₂PO₄, pH 7.4), fluorescence (360 nm excitation, 460 nm emission) was then measured, and DNA content was determined via standard curve.

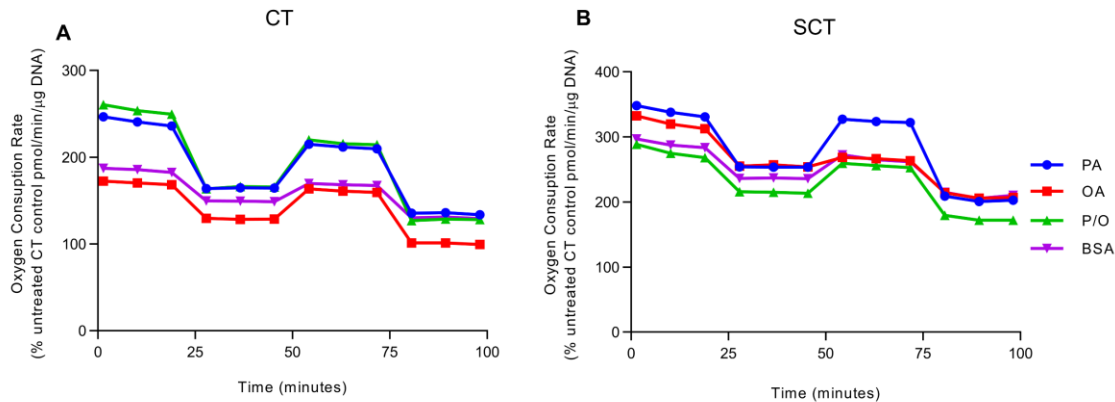


Figure 2-2 Representative Seahorse Mito Stress Test assay tracings.

Representative tracing of Oxygen Consumption Rate (OCR) throughout experimental assay for NEFA-treated (**A**) BeWo CT cells and (**B**) BeWo SCT cells from the Mito Stress Test. Data is represented as mean OCR of each group in technical duplicate from one experiment and presented as percent CT untreated control.

2.2.9 BeWo cell glycolytic function

The optimized Glycolysis Stress Test was utilized to quantify the glycolytic function of NEFA-treated (100 μ M) BeWo CTs and SCTs. At 72H culture media was exchanged with Glycolysis Stress Test assay media (Seahorse XF base media supplemented with 2 mM L-glutamine, pH 7.4), and cells were incubated at 37°C in 100% atmospheric air for 45 mins. Following basal Extracellular Acidification Rate (ECAR) readings, injections of D-glucose; oligomycin; and 2-Deoxy-D-glucose were utilized to measure parameters of glycolysis function. A representative Seahorse XF Glycolysis Stress Test Tracing is available in **Figure 2-3**. ECAR readings were normalized to total DNA content as described above.

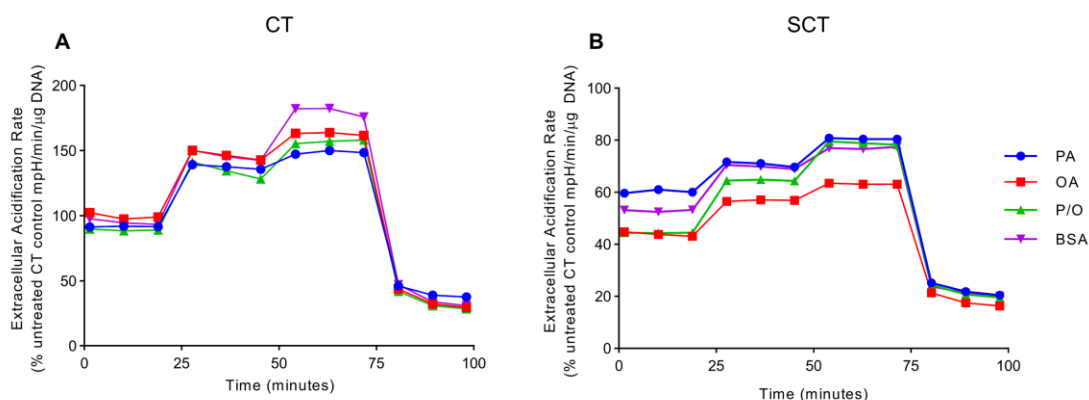


Figure 2-3 Representative Seahorse Glycolysis Stress Test assay tracings

Representative tracing of Extracellular Acidification Rate (ECAR) throughout experimental assay for NEFA-treated (A) BeWo CT cells and (B) BeWo SCT cells from the Glycolysis Stress Test. Data is represented as mean ECAR of each group in technical duplicate from one experiment and presented as percent CT untreated control.

2.2.10 Immunoblot analysis

BeWo cells were plated at 1×10^6 in 100mm cell culture plates and cultured with NEFAs (100 μ M) as described. Total protein was collected with radioimmunoprecipitation assay (RIPA) buffer containing protease inhibitors (leupeptin and aprotinin (1 μ g/mL each; Bioshop, Burlington, Canada); and phenylmethylsulfonyl fluoride (PMSF, 1mM, Bioshop)) and phosphatase inhibitors (sodium orthovanadate (1 mM), New England Biolabs; and sodium fluoride (25 mM), Bioshop). The lysates were sonicated with 5 bursts at 30% output (MISONIX: Ultrasonic liquid processor) and centrifuged at 12,000g at 4°C for 15 mins. The supernatant was collected, and protein concentration was quantified via Bicinchoninic Acid (BCA) assay (Pierce, ThermoFisher Scientific).

Protein abundance was then determined via immunoblotting. Proteins were separated by molecular weight on sodium dodecyl sulfate polyacrylamide gels (10-15% acrylamide) and transferred to Immobilon polyvinylidene fluoride (PVDF) membrane (EMD Millipore, Fisher Scientific). Transfer of proteins was confirmed with Ponceau-S stain (0.1% Ponceau-S in 0.5% acetic acid), and ponceau band density was imaged with a ChemiDoc Imager (BioRad) for total lane protein normalization. Respective primary antibodies and horseradish peroxidase-labelled secondary antibodies were used to visualize proteins of interest (**Table 2-2**). Protein bands were imaged with Clarity western ECL substrate (BioRad) on a ChemiDoc. Protein band density was analyzed with ImageLab software (BioRad) and protein abundance was normalized to total lane protein [60]. Representative full-length uncropped blots highlighting the specificity of utilized antibodies is available in **Supplementary Figure 1** (doi.org/10.5683/SP3/XMPKOK).

Table 2-2 Specifications of antibodies utilized in immunoblotting experiments, and the protein mass loaded for each protein target

Protein Target	Source	Dilution	Blocking solution	Protein Loaded	Heat (°C)	Company	Catalogue No.
Human Mitoprofile	Mouse Monoclonal	1:1000	5% Milk	35 µg	37	ABCAM	ab110411
Lactate Dehydrogenase	Rabbit Polyclonal	1:1000	5% Milk	20 µg	95	Cell Signaling Technologies	2012
Pyruvate Dehydrogenase	Rabbit Polyclonal	1:1000	5% Milk	20 µg	95	Cell Signaling Technologies	3205
PDH-E1α (pSer ²³²)	Rabbit Polyclonal	1:1000	5% BSA	10 µg	37	EMD Millipore	AP1063-50µG
PDH Kinase 1	Rabbit Monoclonal	1:1000	5% BSA	20 µg	95	Cell Signaling Technologies	3820
CPT1a	Rabbit Polyclonal	1:1000	5% milk	10 µg	37	Cell Signaling Technologies	4691P
4-Hydroxynonenal	Rabbit Polyclonal	1:1000	5% milk	15 µg	95	ABCAM	ab46545
Nitrotyrosine	Mouse Monoclonal	1:1500	5% BSA	15 µg	95	Santa Cruz Biotechnology	sc-32757
Anti-Rabbit Secondary	Goat	1:10,000	-	-	-	Cell Signaling Technologies	7074
Anti-Mouse Secondary	Horse	1:10,000	-	-	-	Cell Signaling Technologies	7076

2.2.11 Metabolic enzyme activity assays

Full step-by-step experimental protocols for the enzyme activity assays utilized in Chapter 2 are available in the Supplementary Materials (doi.org/10.5683/SP3/ZTN4ZR).

2.2.11.1 ETC complex I and II activity

ETC complex I and II was assessed as previously described and adapted for use with cell culture lysates [61]. BeWo cells were plated at a density of 4×10^5 cells/well in 60mm plates and collected by scraping. Cells were lysed in ETC lysis buffer (250 mM sucrose, 5 mM HEPES, 100 μ g/mL saponin) containing protease and phosphatase inhibitors (as described above), centrifuged at 5000 g for 5 mins at 4°C and resuspended in Phosphate buffer (25 mM K_2HPO_4). Enzyme assays were performed at 37°C using a SpectraMax plate spectrophotometer (Molecular Devices) in a 96-well plate. Enzyme activities were expressed relative to total protein concentration for each cell lysate (determined by BCA assay).

Complex I activity was assessed as rate of NADH oxidation (measured at 340 nm) following the addition of cell lysate (approximately 15 μ g total protein) to assay buffer (25 mM KH_2PO_4 , 2.5 mg/mL BSA, 0.13 mM NADH, 2 mM KCN, 2 μ g/mL antimycin A, 65 μ M CoQ_1). Complex I activity was calculated from the difference between rates with and without rotenone (10 μ M) to account for non-specific NADH oxidation.

Complex II activity was assessed as rate of DCPIP oxidation (measured at 600 nm) following addition of CoQ_1 (100 μ M) to assay mix containing cell lysate (approximately 10 μ g total protein) in assay buffer (25 mM KH_2PO_4 , 20 mM monosodium succinate, 50 μ M DCPIP, 2 mM KCN, 2 μ g/mL antimycin A, 2 μ g/mL rotenone).

2.2.11.2 Lactate Dehydrogenase and Citrate Synthase activity

Lactate dehydrogenase (LDH) and CS activity were assessed as previously described and adapted for use with cell culture lysates [62,63]. BeWo cells were plated at

a density of 4×10^5 cells/well in 60 mm cell culture dishes collected by scraping at 72H. Cells were subsequently lysed in glycerol lysis buffer (20 mM Na_2HPO_4 , 0.5 mM EDTA, 0.1% Triton X-100, 0.2% BSA, 50% glycerol) containing protease and phosphatase inhibitors (as described above) and stored at -80°C until analyzed [64]. Assays were performed at 37°C using a 96-well plate. Enzyme activity rates were normalized to total protein content of cell lysates determined via BCA assay.

LDH activity was assessed as the rate of NADH oxidation (measured at 340 nm) following addition of cell lysate (corresponding to approximately 1 μg total protein) to assay buffer (0.2 mM NADH, 1mM sodium pyruvate).

CS activity was assessed as rate of Ellman's reagent (DTNB) consumption (measured at 412 nm), following addition of oxaloacetate (0.33 mM) to assay mix containing cell lysate (approximately 30 μg total protein) in assay buffer (0.15 mM acetyl CoA, 0.15 mM DTNB).

2.2.11.3 Analysis of total Pyruvate Dehydrogenase activity and PDHE1-subunit activity

Total PDH activity was assessed at 72H using the PDH Activity Assay Kit (Millipore Sigma). In brief, BeWo cells were plated at a density of 4×10^5 cells/well in 60mm cell culture plates and treated with NEFAs as previously described. At 72H cells were lysed in 400 μL of the provided lysis buffer and 50 μL of cell lysate was mixed with an equal volume of assay mix and PDH enzyme activity was assessed as per the provided kit instructions.

The activity of the PDH-E1 enzyme subunit was assessed as previously described and modified for use with the BeWo cell line [65]. BeWo cells were plated at a density of 4×10^5 cells/well in 60mm plates and treated with NEFAs as previously described. At 72H cells were collected by scraping and were lysed by sonication with 10 bursts at 15% output (MISONIX: Ultrasonic liquid processor) in 50 mM K_2HPO_4 buffer containing protease and phosphatase inhibitors. PDH-E1 enzyme activity was assessed at 37°C using a SpectraMax plate spectrophotometer (Molecular Devices) in a 96-well plate, as the rate of DCPIP oxidation (measured at 600 nm) following the addition of cell lysate

(approximately 20 μ g total protein) to assay buffer (50 mM KH_2PO_4 , 1 mM MgCl_2 , 0.2 mM thymine pyrophosphate, 0.1 mM DCPIP, 2 mM sodium pyruvate). Enzyme activities were expressed relative to total protein concentration for each cell lysate (determined by BCA assay).

2.2.12 Statistical Analysis

A Randomized Block Design One-Way ANOVA and Dunnett's Multiple Comparisons Test of raw fluorescence values was utilized to compare cell viabilities of BeWo cells treated with each NEFA to respective differentiation state BSA-alone control. BeWo percent fusion data, as well as the Mito Stress Test parameters of Spare Respiratory Capacity and Coupling Efficiency (expressed as percent basal OCR) and the Glycolysis Stress Test parameter of Reserve Capacity (expressed as percent ECAR) were log-transformed and statistically analyzed via Two-Way ANOVA (2WA) and Bonferroni's Multiple Comparisons. A Randomized Block Design 2WA and Sidak's Multiple Comparisons Test using raw data was utilized to analyze statistical differences in the relative CGB mRNA transcript abundance; live-cell caspase 3/7 activity; protein abundance; metabolic enzyme activities; as well as all other Seahorse Mito Stress Test and Glycolysis Stress Test parameters between the NEFA-treatment groups for the BeWo CT and SCT cells [66]. Data were then expressed as percent of untreated CT control (basal F12K media) for visualization in figures. All statistical analyses were performed with GraphPad Prism 8 (GraphPad Software, San Diego, CA, USA).

2.2.13 Supplementary materials

Supplementary materials including step-by-step enzyme activity assay protocols (doi.org/10.5683/SP3/ZTN4ZR), and full-length representative immunoblot images (doi.org/10.5683/SP3/XMPKOK) have been uploaded to a publicly available data repository and can be accessed via the indicated Digital Object Identifier (DOI) webpage addresses.

2.3 Results

2.3.1 Characterization of BeWo CT and SCT cells treated with NEFAs

Cell viability of BeWo CT and SCT cells following a prolonged (72H) NEFA treatment was assessed to ensure that subsequent mitochondrial activity measurements were not confounded by a potential stress activated cell death program. A 100 μ M NEFA treatment (PA, OA, and P/O) did not impact BeWo cell viability in either CT or SCT cells relative to BSA-alone treated controls at T72H (**Table 2-3**, n=4/group).

Table 2-3 Cell viability of NEFA-treated BeWo CT and SCT cells

NEFA Treatment (μ M)		CT Cell Viability (% CT F12K)	SCT Cell Viability (% SCT F12K)
BSA Control		-	72.35 \pm 2.61
PA	50	86.83 \pm 3.56	87.08 \pm 9.46 *
	100	77.34 \pm 4.92	61.40 \pm 12.14
	200	55.03 \pm 10.31*	45.32 \pm 16.53
OA	50	88.10 \pm 4.93	73.70 \pm 9.62 *
	100	72.97 \pm 6.13	59.02 \pm 10.18
	200	48.78 \pm 10.19*	34.54 \pm 11.59*
P/O	50	85.57 \pm 4.39	70.27 \pm 10.72 *
	100	76.37 \pm 6.09	57.92 \pm 9.71
	200	57.87 \pm 10.59*	40.18 \pm 14.48

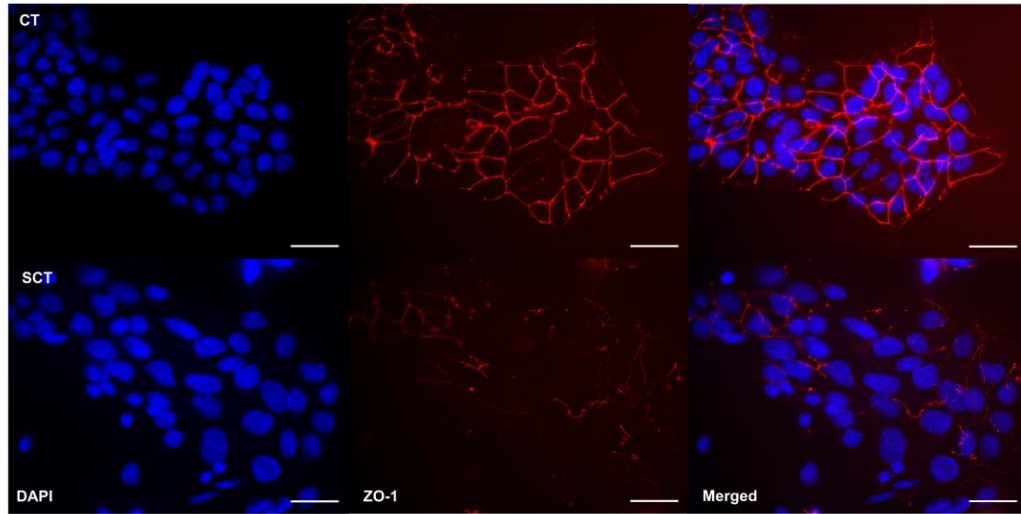
Data are mean \pm SEM. * denotes significantly different cell viability relative to respective differentiation state BSA-control (n=4/group).

BeWo cells treated with 8-Br-cAMP displayed decreased ZO-1 protein expression and increased cell fusion (mean 78% fusion) compared to CT cells (mean 15% fusion) (**Figure 2-4 A,B**; 2WA: differentiation state p<0.001, n=3/group). Additionally, BeWo cells treated with 8-Br-cAMP displayed elevated CGB (mean expression 86-fold higher) and OVOL1 (mean expression 9-fold higher) mRNA abundance (23-85 fold higher expression) consistent with the differentiation process (**Figure 2-4 C,D**; 2WA: differentiation state p<0.01, n=5/group)

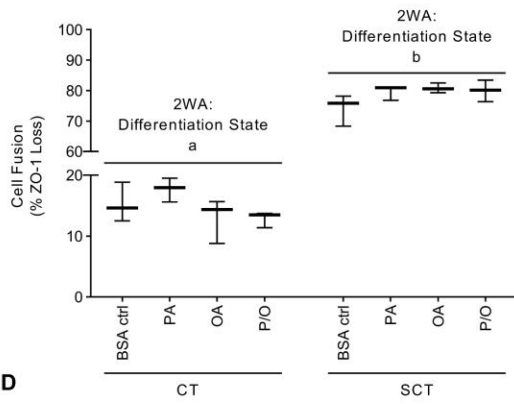
The 100 μ M NEFA treatments were additionally not associated with altered BeWo fusion in either CT and SCT cells as measured with ZO-1 expression (**Figure 2-4 A,B**). Further, these 100 μ M treatments did not significantly alter the mRNA abundance of CGB or OVOL1 (markers of syncytialization in BeWo cells) within the CT and SCT cells (**Figure 2-4 C,D**).

Additionally, in each NEFA-treatment there was no significant difference in live-cell caspase 3/7 activity compared to respective differentiation state BSA-control sample (**Figure 2-4 E**; n=5/group).

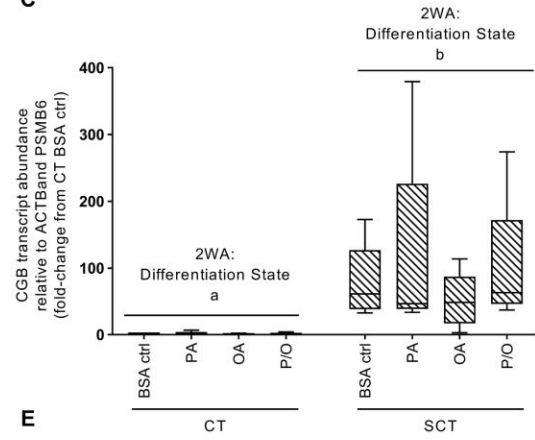
A



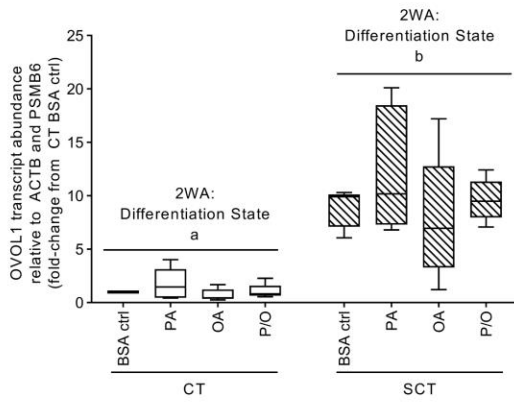
B



C



D



E

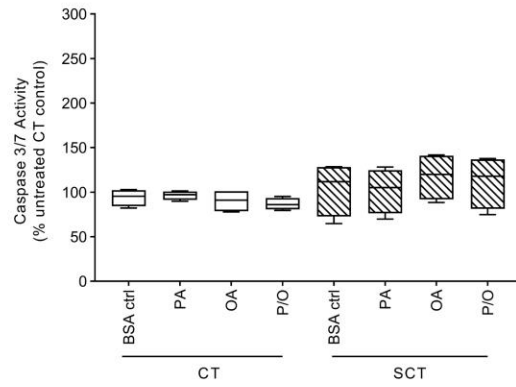


Figure 2-4 100 μ M of PA, OA or P/O does not negatively impact BeWo cell syncytialization or upregulate pro-apoptotic pathways at 72H.

(A) Representative ZO-1, DAPI and merged immunofluorescent images of BeWo CT and SCT cells (scale bar = 50 μ m); (B) Percent fusion of NEFA-treated BeWo CT and SCT cells; data is expressed as percentage of nuclei lacking ZO-1 staining. Relative mRNA abundance of (C) *CGB* and (D) *OVOLI* in NEFA-treated BeWo CT and SCT cells; RT-qPCR data is presented as the fold-change of target mRNA abundance compared to CT BSA ctrl samples relative to the geometric mean of ACTB and PMSB6 mRNA abundance. (E) Live-cell caspase activity of NEFA-treated BeWo CT and SCT cells; data is presented as percent untreated CT control luminescence values (B n=3/group; C-E n=5/group; different letters denote statistical significance $p < 0.05$; B percent fusion data was log transformed and analyzed via two-way ANOVA (2WA); C,D relative mRNA abundance data was analyzed via randomized-block 2WA).

2.3.2 The impact of prolonged NEFA exposure upon respiratory activity of BeWo cells

BeWo CT cells treated with PA (100 μ M) and P/O (containing 50 μ M PA) for 72H exhibited a significant increase in basal mitochondrial activity compared to control CT samples (**Figure 2-5 A**, 2WA: NEFA treatment $p < 0.01$, $n = 5$ /group). Under DNP-stimulated conditions CT cells exposed to PA and P/O exhibited a significant increase in OCR compared to BSA-alone treated CT cells (**Figure 2-5 B**, 2WA: NEFA Treatment $p < 0.05$, $n = 5$ /group). Conversely, BeWo SCT cells displayed diminished respiratory activity and had significantly lower OCR under basal and DNP-stimulated conditions compared to BeWo CT cells (**Figure 2-5 A-B**, 2WA differentiation state $p < 0.05$). This diminished respiratory activity observed in BeWo SCT cells was associated with a significant reduction in spare respiratory capacity (**Figure 2-5 D**, 2WA differentiation state $p < 0.001$, $n = 5$ /group). No differences in BeWo cell proton leak or coupling efficiency was observed with differentiation state or NEFA-treatment (**Figure 2-5 C,E**, $n = 5$ /group)

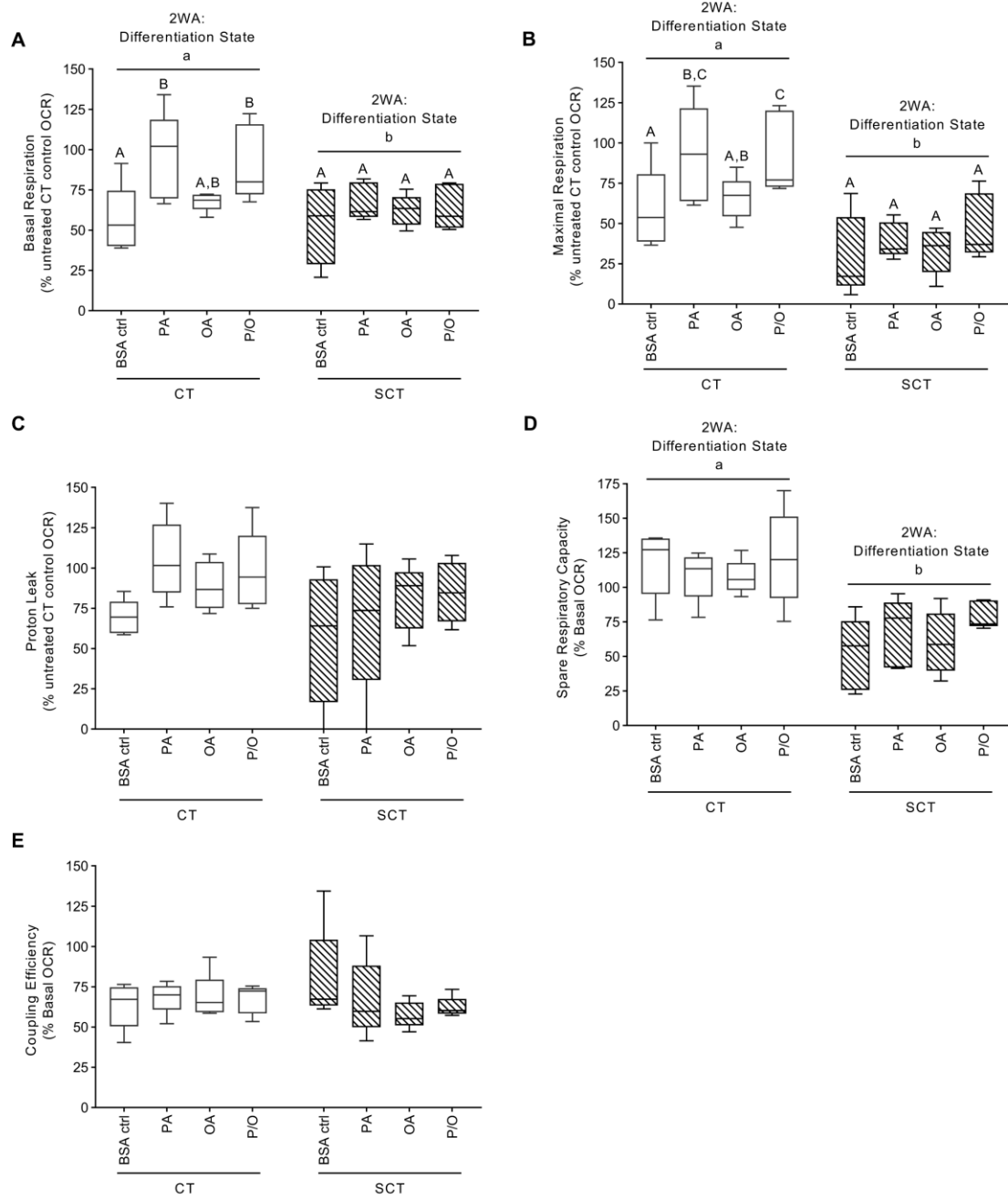


Figure 2-5 Mitochondrial respiratory activity of BeWo cells following prolonged NEFA treatment.

Oxygen Consumption Rate (OCR) of experimental media was measured under basal conditions and following subsequent injections of: Oligomycin (1.5 $\mu\text{g/mL}$); Dinitrophenol (50 μM); and Rotenone and Antimycin A (0.5 μM each) to calculate the **(A)** Basal Respiration, **(B)** Maximal Respiration, **(C)** Proton Leak, **(D)** Spare Respiratory Capacity, and **(E)** Coupling Efficiency in NEFA-treated BeWo CT and SCT cells (n=5/group). **(A, B, C)** Statistical analysis was performed on DNA-normalized OCR rates via Two-Way Randomized Block ANOVA, Sidak's multiple comparisons Test; **(D, E)** percent basal OCR was log transformed and analyzed via Two-Way ANOVA. **(A, B, C)** Respiratory activity data is expressed as OCR normalized to total DNA content and presented as percent CT untreated control; **(D, E)** data is represented as percent basal OCR for each condition. Different letters denote statistical significance ($p < 0.05$, $n = 5/\text{group}$).

2.3.3 Glycolytic function in BeWo cells is unaltered with NEFA treatments

Basal glycolysis, maximum glycolysis, glycolytic reserve capacity, and non-glycolytic acidification were not impacted after cells were differentiated to SCT cells and were unaltered with NEFA treatment (**Table 2-4**, n=5/group).

Table 2-4 NEFA treatments did not affect the glycolytic activities of BeWo CT or SCT cells

Differentiation State	Treatment	Basal Glycolysis ¹	Max Glycolysis ¹	Reserve Glycolytic Capacity ²	Non-Glycolytic Acidification ¹
CT	BSA Ctrl	86.14 ± 10.71	72.19 ± 8.22	120.80 ± 6.79	84.25 10.01
	PA	89.99 ± 6.20	81.61 ± 5.62	134.30 ± 6.77	91.31 8.53
	OA	97.59 ± 11.09	86.11 ± 11.81	129.50 ± 11.57	87.72 11.08
	P/O	89.26 ± 6.19	85.82 ± 5.47	142.90 ± 6.68	91.90 7.33
SCT	BSA Ctrl	83.53 ± 7.97	67.04 ± 6.54	115.50 ± 4.48	117.70 9.16
	PA	81.91 ± 14.13	66.57 ± 11.47	137.00 ± 27.10	104.90 13.76
	OA	83.51 ± 11.90	67.32 ± 8.49	118.40 ± 13.33	105.00 9.36
	P/O	75.55 ± 8.19	65.30 ± 6.97	131.30 ± 7.73	98.36 8.68

Data are mean ± SEM (n=5/group). Data are presented as ¹% untreated CT ECAR, and ²% Basal Glycolysis

2.3.4 NEFA impact upon electron transport chain complex protein abundance and activity

BeWo CT cells treated with PA (100 μ M) and P/O (containing 50 μ M PA) for 72H exhibited a significant increase in basal mitochondrial activity compared to control CT samples (**Figure 2-5 A**, 2WA: NEFA treatment $p < 0.01$, $n = 5/\text{group}$). Under DNP-stimulated conditions CT cells exposed to PA and P/O exhibited a significant increase in OCR compared to BSA-alone treated CT cells (**Figure 2-5 B**, 2WA: NEFA Treatment $p < 0.05$, $n = 5/\text{group}$). Conversely, BeWo SCT cells displayed diminished respiratory activity and had significantly lower OCR under basal and DNP-stimulated conditions compared to BeWo CT cells (**Figure 2-5 A-B**, 2WA differentiation state $p < 0.05$). This diminished respiratory activity observed in BeWo SCT cells was associated with a significant reduction in spare respiratory capacity (**Figure 2-5 D**, 2WA differentiation state $p < 0.001$, $n = 5/\text{group}$). No differences in BeWo cell proton leak or coupling efficiency was observed with differentiation state or NEFA-treatment (**Figure 2-5 C,E**, $n = 5/\text{group}$).

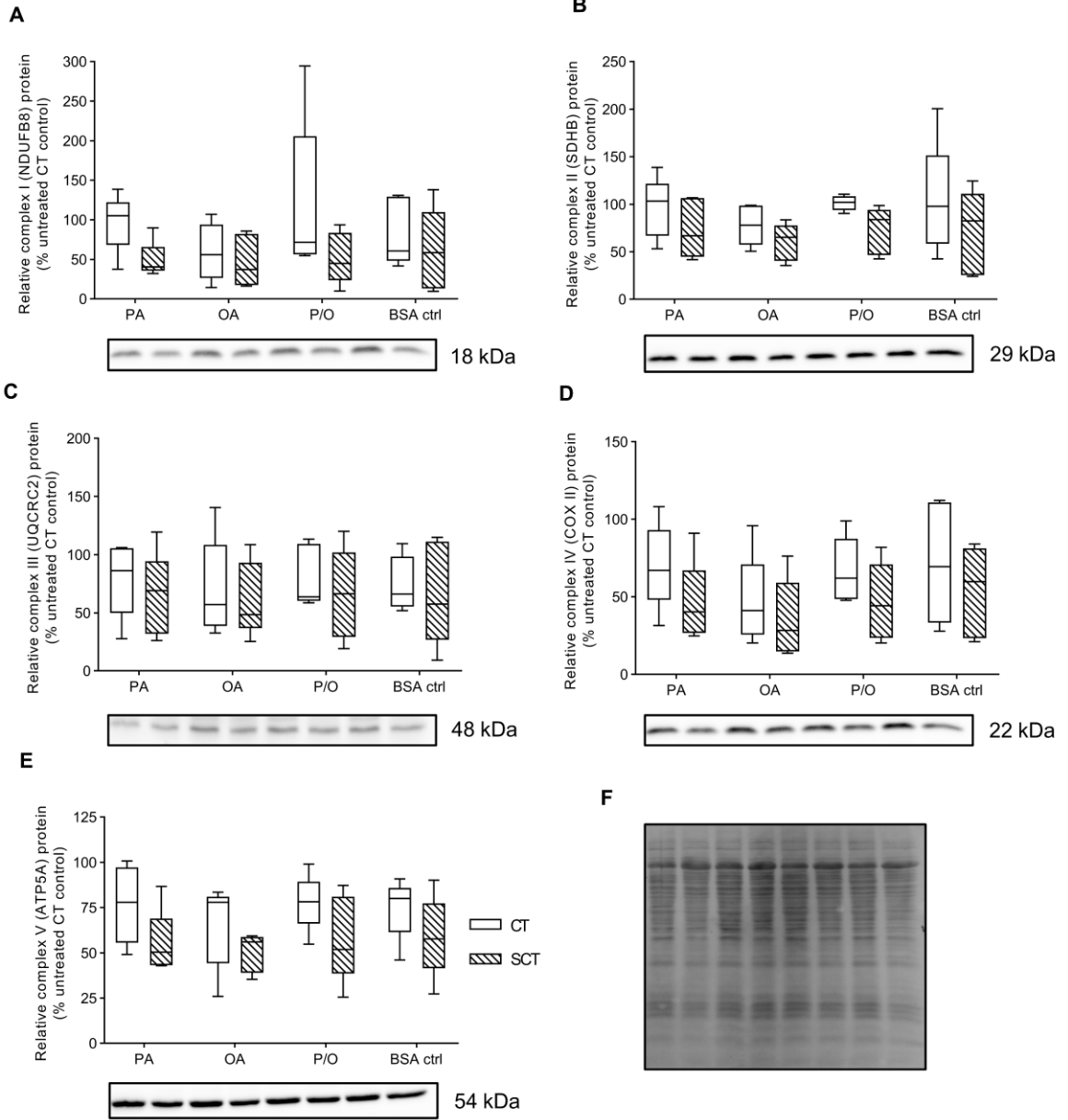


Figure 2-6 Prolonged NEFA treatment did not affect BeWo Electron Transport Chain complex protein abundance.

Relative protein abundance of (A) complex I (NDUFB8 subunit) (B) complex II (SDHB subunit) (C) complex III (UQCRC2 subunit) (D) complex IV (COX II subunit), and (E) complex V (ATP5A subunit) of the Electron Transport Chain was determined at T72H via immunoblotting. (F) Representative ponceau image used to quantify total lane protein. Data is presented as percent untreated CT control for each experimental replicate (n=5/group). Full-length representative western blot images are available in **Supplementary Figure 1** (doi.org/10.5683/SP3/XMPKOK).

2.3.5 The impact of prolonged NEFA exposure on metabolic enzyme activity

LDH activity was not significantly altered with differentiation state or NEFA-treatment (**Table 2-5**, n=5/group). BeWo SCT cells exhibited a significantly increased PDH-E1 subunit activity compared to CT cells (**Table 2-5**). However, BeWo SCT cells displayed a significantly reduced rate of total PDH enzyme activity compared to CT cells (**Table 2-5**; 2WA differentiation state $p < 0.01$). Additionally, BeWo CT cells treated with PA had a significantly reduced total PDH enzyme activity compared to BSA-alone treated CT controls (**Table 2-5**; 2WA differentiation state $p < 0.05$). There was no differentiation state or NEFA dependent alteration in citrate synthase enzyme activity in BeWo cells (**Table 2-5**).

Table 2-5 Maximal activity rates of mitochondrial enzymes in NEFA-treated BeWo CT and SCT cells.

Differentiation State	Treatment	Citrate Synthase	ETC Complex I	ETC Complex II	Lactate Dehydrogenase	PDH-E1 subunit	Pyruvate Dehydrogenase
(% untreated CT U/mg protein)							
CT	BSA Ctrl	116.20 ± 22.37	120.7 ± 7.71	113.8 ± 13.71	163.20 ± 45.50	99.23 ± 6.37	105.04 ± 6.93 a
	PA	93.62 ± 15.00	98.00 ± 10.03	98.99 ± 19.80	109.80 ± 14.41	101.72 ± 3.83	86.78 ± 10.96 b
	OA	85.31 ± 14.22	100.00 ± 5.59	94.46 ± 17.77	104.90 ± 19.23	102.84 ± 16.80	112.01 ± 10.41 a
	P/O	90.34 ± 5.44	106.20 ± 10.32	93.67 ± 17.50	133.60 ± 31.71	118.96 ± 21.97	99.56 ± 7.37 ab
SCT	BSA Ctrl	60.68 ± 6.01	191.50 ± 31.49 a	61.76 ± 13.75	79.25 ± 18.77	260.45 ± 41.81	84.66 ± 4.99
	PA	49.80 ± 4.60	183.10 ± 25.80 a	62.05 ± 15.57	79.54 ± 16.18	246.35 ± 20.16	88.20 ± 9.06
	OA	39.80 ± 4.74	129.2 ± 13.85 ab	51.88 ± 17.79	73.79 ± 17.63	222.28 ± 19.02	80.33 ± 3.51
	P/O	63.52 ± 4.14	103.60 ± 17.77 b	58.96 ± 8.20	78.59 ± 13.26	233.78 ± 57.00	81.68 ± 8.10
*Differentiation state difference		NS	*	*	NS	*	*

Data are mean ± SEM. * denotes a differentiation state dependent difference in enzyme activity between BeWo CT and SCT cells (n=5/group). Different letters denote significant differences between NEFA treatments within a differentiation state.

2.3.6 Oxidative State in unaltered in NEFA-treated BeWo cells

There were no differences in the protein expression of 4-Hydroxynonenal (4-HNE) and 3-Nitrotyrosine, markers of oxidative stress and nitrative stress respectively, with prolonged NEFA treatment or differentiation in BeWo cells (**Figure 2-7 A,B**, n=5/group).

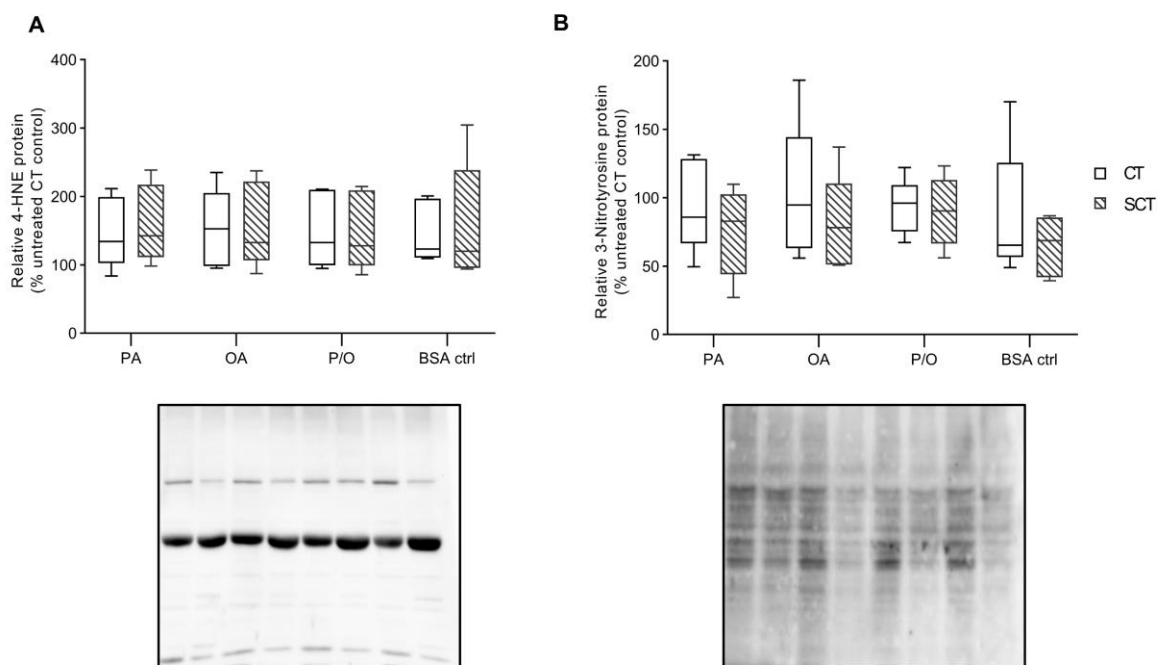


Figure 2-7 Prolonged NEFA treatment does not alter oxidative state of BeWo cells.

Relative Protein abundance of **(A)** 4-Hydroxynonenal (4-HNE) and **(B)** 3-Nitrotyrosine was determined in NEFA-treated BeWo CT and SCT cells at 72H via immunoblotting. Data is presented as relative protein density normalized to total lane protein density and expressed as percent CT untreated control protein abundance (n=5/group).

2.3.7 The impact of prolonged NEFA exposure on metabolic enzyme expression

There was a differentiation state dependent expression pattern in Pyruvate Dehydrogenase (PDH) in both its unphosphorylated and phosphorylated (pPDH) form. BeWo SCT cells displayed significantly reduced relative abundances of both PDH and pPDH (**Figure 2-8 A,B**; 2WA differentiation state $p < 0.05$, $n = 5/\text{group}$), however the ratio of pPDH:PDH (**Figure 2-8 C**, $n = 5/\text{group}$) was not significantly altered between differentiation states. No differentiation state or NEFA-treatment specific differences were found in the relative protein abundances of either LDH or carnitine palmitoyltransferase 1a (CPT1a) in BeWo cells (**Figure 2-8 D,E**, $n = 5/\text{group}$).

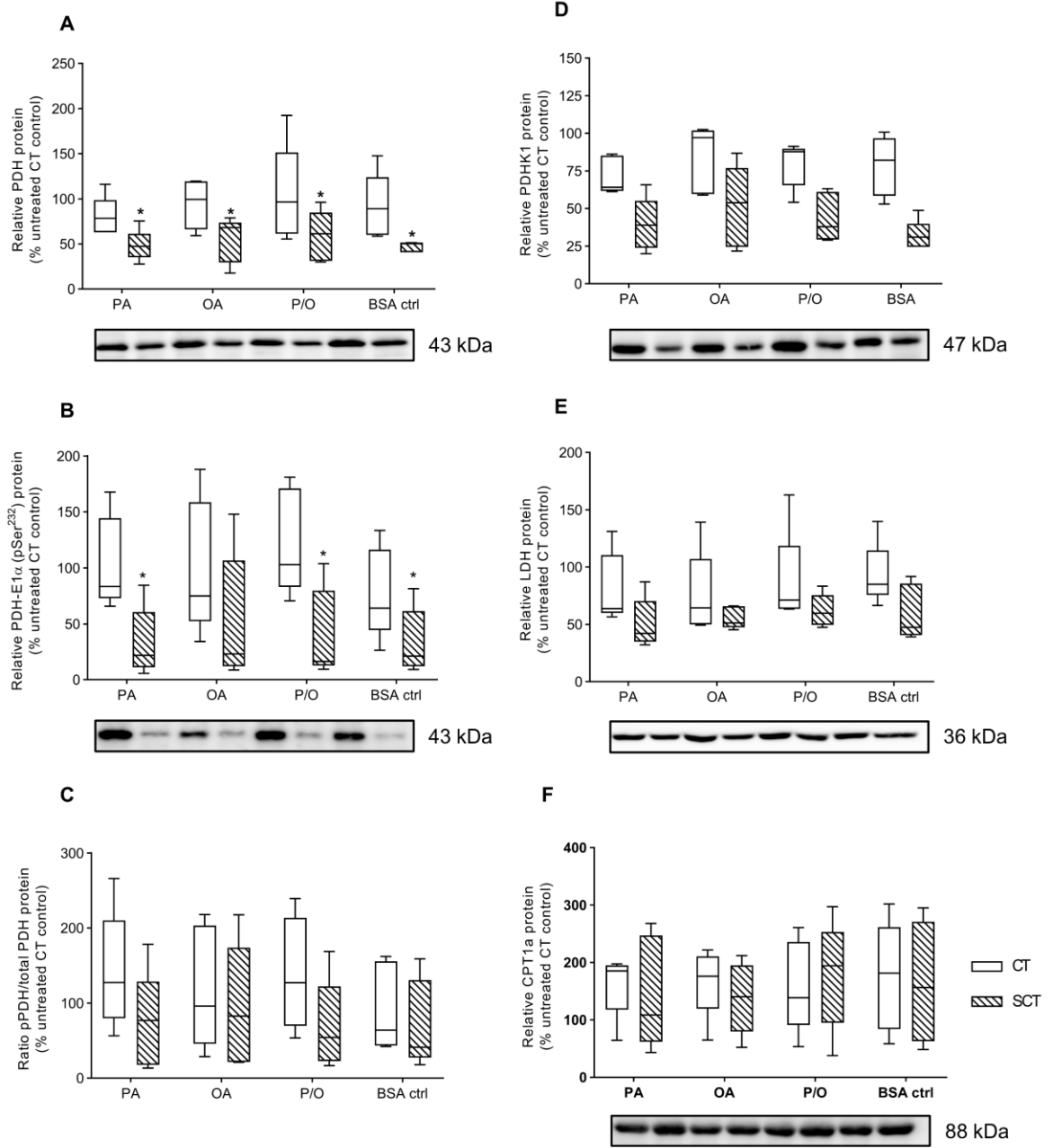


Figure 2-8 Prolonged NEFA treatments did not affect protein expression of enzymes involved in mitochondrial uptake of pyruvate or long-chain fatty acid species.

Relative protein abundance of (A) Pyruvate Dehydrogenase (PDH), (B) PDH-E1 α (pSer²³²) (pPDH), (C) the pPDH/PDH ratio, (D) Pyruvate Dehydrogenase Kinase-1 (PDHK1) (E) Lactate Dehydrogenase (LDH), and (F) CPT1a was determined in NEFA-treated BeWo CT and SCT cells at 72H via immunoblotting. Data is presented as percent CT untreated control (n=5/group). Uncropped representative western blot images are available in **Supplementary Figure 1** (doi.org/10.5683/SP3/XMPKOK).

2.4 Discussion

The current study aimed to characterize the metabolic function and mitochondrial respiratory activity in a model of the differentiating human villous trophoblast following a prolonged (72 hour) NEFA challenge. To confirm that mitochondrial respiratory activity and metabolic function was examined using a stable population of cells we analyzed cell viability, CT-to-SCT differentiation potential and apoptotic state of the treated cells. Our experiments demonstrated that NEFA treatments exceeding 200 μM produced large variances in cell viability, which is consistent with previous observations in primary human trophoblast culture systems [67]. A treatment of 100 μM of PA, OA and P/O was found to not impact BeWo cell syncytialization or upregulate pro-apoptotic pathways, yielding a stable cell culture system in which mitochondrial function could be examined. Additionally, the 100 μM of PA and OA used in this current study also aligned with published human third trimester fasting circulating lipid levels under conditions of maternal obesity and GDM highlighting a physiological relevance of the utilized NEFA treatment [39].

2.4.1 Differentiation and BeWo Metabolic Function

BeWo cells displayed a significant reduction in mitochondrial respiratory activity (Mito Stress Test readouts) following 8-Br-cAMP induced differentiation to SCT cells. These reductions in basal and maximal respiration rates were consistent with previous reports in human primary trophoblast (PHT) cell culture systems, which demonstrated that SCT cells are less metabolically active than progenitor CT cells [68]. More strikingly, we observed these similarities despite the BeWo cells in our culture system fusing at rates around 60%, further supporting that diminished mitochondrial oxidative function is an important physiological marker of placental syncytialization.

This study provides novel insight into dynamic changes in the activity of individual ETC complexes during CT differentiation in SCT. Specifically, we observed significant differences in complex I and complex II activity between CT and SCT cell types that were independent of alterations in mitochondrial biomass as assessed by CS enzyme activity. The decreased complex II activity observed in BeWo SCT cells may

allude to a biochemical mechanism that potentially explains the overall reduction in respiratory activity observed in syncytialized BeWo cells.

Additionally, the BeWo SCT cells in our study may exhibit a diminished oxidative metabolism of pyruvate substrates as evidenced by reduced protein expression and enzyme activity of total Pyruvate Dehydrogenase (PDH). These data may indicate an overall decrease in the conversion of glycolysis-derived pyruvate to acetyl-CoA in BeWo SCTs and may further highlight the mechanism by which oxidative energy production is suppressed in differentiated SCT cells. However, future studies are needed to elucidate if similar mechanisms govern the reduction in mitochondrial function in the differentiated SCT cell populations in both BeWo cells and isolated primary trophoblasts.

2.4.2 NEFAs and BeWo Metabolic Function

The current study demonstrated a novel NEFA-induced increase mitochondrial respiratory activity in PA and P/O-treated BeWo CT cells under basal and DNP-stimulated (maximal) conditions of the Mito Stress Test that was not associated with any specific alterations in the individual enzyme activities of ETC complexes I and II. Previously, an overall reduction in mitochondrial respiratory activity has been reported as an indication of mitochondrial dysfunction in term placentae [19]. However, increases in mitochondrial respiratory activity have also been described as a preliminary marker of mitochondrial failure in disease states that are linked to an ultimate mitochondrial dysfunction [69,70]. In particular, mitochondrial dysfunction induced in hepatocytes under conditions of Non-alcoholic fatty liver disease (NAFLD) has been suggested to be the result of an initial increase in mitochondrial respiratory activity stimulated by increased saturated FA supply that in turn promotes increased Reactive Oxygen Species (ROS) production, and ultimately, oxidative damage to mitochondria [69,71]. We speculate that the increases in respiratory activity observed in the PA and P/O-treated BeWo CT cultures may be indicative of an early timepoint of mitochondrial dysfunction in the villous trophoblast, mirroring these other reports with an activation of mitochondrial respiration prior to an ultimate failure.

In many other culture systems PA exposures have been demonstrated to increase ROS production leading to cellular oxidative stress [72–74]. As oxidative stress has additionally been identified as a marker of metabolic dysfunction in the term obese placenta, we speculate that the increased respiratory activity observed in PA and P/O-treated BeWo CT cells in this study could over time increase ROS production and lead to oxidative stress [75,76]. However, at the 72H timepoint utilized in the current study there were no indications of oxidative stress in any of the treatments, as evidenced by immunoblots for total abundance of 3-nitrotyrosine and 4-HNE. Further studies are needed to investigate if continued exposure of BeWo CT cells to the selected physiologically relevant PA treatment will lead to ROS-induced mitochondrial oxidative damage and ultimately impaired mitochondrial respiration.

It is important to note that OA has previously been shown to elicit anti-oxidant capabilities and rescue mitochondrial function in muscle and pancreatic beta-cells treated with high levels of saturated fats [45,77]. Thus, the co-culture of OA with PA (P/O) over longer timepoints may prevent the accumulation of PA-stimulated ROS and could preserve villous trophoblast mitochondrial function as has been observed in other systems.

While this study has demonstrated the impacts of a prolonged PA exposure, and differentiation state on placental cell metabolic function, the use of the immortalized BeWo cell line may limit the conclusions that can be drawn as they may confer properties not observed in primary culture or other *ex vivo* systems. Having said that, the use of a cell line model of the villous trophoblast in the current study allowed for the analysis of the effects of lipid exposure in isolation from factors of maternal body composition and gestational diet. Specifically, the BeWo choriocarcinoma cell line enabled us to analyze the metabolic function of SCTs differentiated under constant exposure to elevated dietary-NEFAs, analogous to that of a differentiating trophoblast throughout gestation in an obese or GDM pregnancy, but independent to non-dietary obesogenic and diabetic environmental components [78–80]. However, future studies still need to examine if prolonged NEFA challenge at physiologically relevant levels can lead to similar early markers of mitochondrial dysfunction in primary-derived trophoblast cultures. However,

the use of trophoblasts from early gestational periods may be required in these future works to develop a primary culture model that, similar to this study, is independent from the influence of maternal body composition and gestational diet.

2.4.3 Conclusion

The current study aimed to characterize the mitochondrial function and respiratory activity in a model of the differentiating human villous trophoblast following a prolonged (72 hour) NEFA challenge. Differentiated BeWo SCT cells displayed a reduced basal and maximal mitochondrial respiratory activity, similar to that previously observed in primary trophoblast culture. Additionally, this study highlighted that an isolated and prolonged exposure to physiological levels of dietary-NEFAs, independent from factors of maternal body composition, increases villous trophoblast cell mitochondrial respiratory activity. The observed increases in basal and maximal respiratory activity in response to PA and P/O treatments in this study may be indicative of an early phenotype of placental mitochondrial impairment that may later trigger oxidative damage to the mitochondria. Overall, this study highlights dietary fats independently modulate villous trophoblast mitochondrial function, and further demonstrates that maternal diet composition is an important regulator of the adverse placental outcomes that underlie the development of metabolic disease in the offspring.

2.5 References

- [1] C. Chen, X. Xu, Y. Yan, Estimated global overweight and obesity burden in pregnant women based on panel data model, *PLoS One*. 13 (2018) e0202183. doi:10.1371/journal.pone.0202183.
- [2] B.M. Popkin, C.M. Doak, The Obesity Epidemic Is a Worldwide Phenomenon, *Nutr. Rev.* 56 (2009) 106–114. doi:10.1111/j.1753-4887.1998.tb01722.x.
- [3] N.P. Deputy, B. Dub, A.J. Sharma, Prevalence and Trends in Prepregnancy Normal Weight — 48 States, New York City, and District of Columbia, 2011–2015, *MMWR. Morb. Mortal. Wkly. Rep.* 66 (2018) 1402–1407. doi:10.15585/mmwr.mm665152a3.
- [4] Statistics Canada, Women in Canada: A gender-based statistical report (89-503-X); 2012-2013 Canadian Health Measures Survey, custom tabulation, (2013).
- [5] S. Czernichow, A.-P. Kengne, R.R. Huxley, G.D. Batty, B. de Galan, D. Grobbee, A. Pillai, S. Zoungas, M. Marre, M. Woodward, B. Neal, J. Chalmers, Comparison of waist-to-hip ratio and other obesity indices as predictors of cardiovascular disease risk in people with type-2 diabetes: a prospective cohort study from ADVANCE, *Eur. J. Cardiovasc. Prev. Rehabil.* 18 (2011) 312–319. doi:10.1097/HJR.0b013e32833c1aa3.
- [6] R.C. Whitaker, Predicting Preschooler Obesity at Birth: The Role of Maternal Obesity in Early Pregnancy, *Pediatrics*. 114 (2004) e29–e36. doi:10.1542/peds.114.1.e29.
- [7] M.J.R. Heerwagen, M.R. Miller, L.A. Barbour, J.E. Friedman, Maternal obesity and fetal metabolic programming: a fertile epigenetic soil, *AJP Regul. Integr. Comp. Physiol.* 299 (2010) R711–R722. doi:10.1152/ajpregu.00310.2010.
- [8] C.M. Boney, A. Verma, R. Tucker, B.R. Vohr, Metabolic syndrome in childhood: association with birth weight, maternal obesity, and gestational diabetes mellitus., *Pediatrics*. 115 (2005) e290-6. doi:10.1542/peds.2004-1808.
- [9] S.J. Borengasser, P. Kang, J. Faske, H. Gomez-Acevedo, M.L. Blackburn, T.M. Badger, K. Shankar, High Fat Diet and In Utero Exposure to Maternal Obesity Disrupts Circadian Rhythm and Leads to Metabolic Programming of Liver in Rat Offspring, *PLoS One*. 9 (2014) e84209. doi:10.1371/journal.pone.0084209.
- [10] E.L. Sullivan, K.L. Grove, Metabolic Imprinting in Obesity, in: *Front. Eat. Weight Regul.*, KARGER, Basel, 2009: pp. 186–194. doi:10.1159/000264406.
- [11] M. McDonnold, L. Mele, L. Myatt, J. Hauth, K. Leveno, U. Reddy, B. Mercer, Waist-to-Hip Ratio versus Body Mass Index as Predictor of Obesity-Related Pregnancy Outcomes, *Am. J. Perinatol.* 33 (2016) 618–624. doi:10.1055/s-0035-1569986.

- [12] R. Weiss, A.A. Bremer, R.H. Lustig, What is metabolic syndrome, and why are children getting it?, *Ann. N. Y. Acad. Sci.* 1281 (2013) 123–140. doi:10.1111/nyas.12030.
- [13] S. Poyrazoglu, F. Bas, F. Darendeliler, Metabolic syndrome in young people, *Curr. Opin. Endocrinol. Diabetes Obes.* 21 (2014) 56–63. doi:10.1097/01.med.0000436414.90240.2c.
- [14] S.J. Borengasser, J. Faske, P. Kang, M.L. Blackburn, T.M. Badger, K. Shankar, In utero exposure to prepregnancy maternal obesity and postweaning high-fat diet impair regulators of mitochondrial dynamics in rat placenta and offspring, *Physiol. Genomics.* 46 (2014) 841–850. doi:10.1152/physiolgenomics.00059.2014.
- [15] L. Myatt, Placental adaptive responses and fetal programming, *J. Physiol.* 572 (2006) 25–30. doi:10.1113/jphysiol.2006.104968.
- [16] K.L. Thornburg, P.F. O’Tierney, S. Louey, Review: The Placenta is a Programming Agent for Cardiovascular Disease, *Placenta.* 31 (2010) S54–S59. doi:10.1016/j.placenta.2010.01.002.
- [17] A. Maloyan, J. Mele, S. Muralimanoharan, L. Myatt, Placental metabolic flexibility is affected by maternal obesity, *Placenta.* 45 (2016) 69. doi:10.1016/j.placenta.2016.06.031.
- [18] K.E. Ireland, A. Maloyan, L. Myatt, Melatonin Improves Mitochondrial Respiration in Syncytiotrophoblasts From Placentas of Obese Women, *Reprod. Sci.* 25 (2018) 120–130. doi:10.1177/1933719117704908.
- [19] J. Mele, S. Muralimanoharan, A. Maloyan, L. Myatt, Impaired mitochondrial function in human placenta with increased maternal adiposity., *Am. J. Physiol. Endocrinol. Metab.* 307 (2014) E419–25. doi:10.1152/ajpendo.00025.2014.
- [20] R. Hastie, M. Lappas, The effect of pre-existing maternal obesity and diabetes on placental mitochondrial content and electron transport chain activity., *Placenta.* 35 (2014) 673–83. doi:10.1016/j.placenta.2014.06.368.
- [21] N.M. Gude, C.T. Roberts, B. Kalionis, R.G. King, Growth and function of the normal human placenta., *Thromb. Res.* 114 (2004) 397–407. doi:10.1016/j.thromres.2004.06.038.
- [22] K. Osadnik, T. Osadnik, M. Lonnie, M. Lejawa, R. Reguła, M. Fronczek, M. Gawlita, L. Wądołowska, M. Gąsior, N. Pawlas, Metabolically healthy obese and metabolic syndrome of the lean: the importance of diet quality. Analysis of MAGNETIC cohort, *Nutr. J.* 19 (2020) 19. doi:10.1186/s12937-020-00532-0.
- [23] B.M. Popkin, Global nutrition dynamics: the world is shifting rapidly toward a diet linked with noncommunicable diseases, *Am. J. Clin. Nutr.* 84 (2006) 289–298. doi:10.1093/ajcn/84.2.289.

- [24] D.K. Tobias, C. Zhang, J. Chavarro, K. Bowers, J. Rich-Edwards, B. Rosner, D. Mozaffarian, F.B. Hu, Prepregnancy adherence to dietary patterns and lower risk of gestational diabetes mellitus, *Am. J. Clin. Nutr.* 96 (2012) 289–295. doi:10.3945/ajcn.111.028266.
- [25] Z. Paknahad, A. Fallah, A.R. Moravejolahkami, Maternal Dietary Patterns and Their Association with Pregnancy Outcomes, *Clin. Nutr. Res.* 8 (2019) 64. doi:10.7762/cnr.2019.8.1.64.
- [26] M. Mizgier, G. Jarzabek-Bielecka, K. Mruczyk, Maternal diet and gestational diabetes mellitus development, *J. Matern. Neonatal Med.* 34 (2021) 77–86. doi:10.1080/14767058.2019.1598364.
- [27] M.E. Bianco, J.L. Josefson, Hyperglycemia During Pregnancy and Long-Term Offspring Outcomes, *Curr. Diab. Rep.* 19 (2019) 143. doi:10.1007/s11892-019-1267-6.
- [28] T. Vilmi-Kerälä, O. Palomäki, M. Vainio, J. Uotila, A. Palomäki, The risk of metabolic syndrome after gestational diabetes mellitus – a hospital-based cohort study, *Diabetol. Metab. Syndr.* 7 (2015) 43. doi:10.1186/s13098-015-0038-z.
- [29] P.M. Catalano, The impact of gestational diabetes and maternal obesity on the mother and her offspring, *J. Dev. Orig. Health Dis.* 1 (2010) 208–215. doi:10.1017/S2040174410000115.
- [30] Y. Yang, Z. Wang, M. Mo, X. Muyiduli, S. Wang, M. Li, S. Jiang, Y. Wu, B. Shao, Y. Shen, Y. Yu, The association of gestational diabetes mellitus with fetal birth weight, *J. Diabetes Complications.* 32 (2018) 635–642. doi:10.1016/j.jdiacomp.2018.04.008.
- [31] C. Savard, S. Lemieux, S. Weisnagel, B. Fontaine-Bisson, C. Gagnon, J. Robitaille, A.-S. Morisset, Trimester-Specific Dietary Intakes in a Sample of French-Canadian Pregnant Women in Comparison with National Nutritional Guidelines, *Nutrients.* 10 (2018) 768. doi:10.3390/nu10060768.
- [32] V. Watts, H. Rockett, H. Baer, J. Leppert, G. Colditz, Assessing Diet Quality in a Population of Low-Income Pregnant Women: A Comparison Between Native Americans and Whites, *Matern. Child Health J.* 11 (2007) 127–136. doi:10.1007/s10995-006-0155-2.
- [33] J. Denomme, K.D. Stark, B.J. Holub, Directly quantitated dietary (n-3) fatty acid intakes of pregnant Canadian women are lower than current dietary recommendations., *J. Nutr.* 135 (2005) 206–11. doi:135/2/206 [pii].
- [34] A.M. Siega-Riz, L.M. Bodnar, D.A. Savitz, What are pregnant women eating? Nutrient and food group differences by race, *Am. J. Obstet. Gynecol.* 186 (2002) 480–486. doi:10.1067/mob.2002.121078.

- [35] C.E. McCurdy, J.M. Bishop, S.M. Williams, B.E. Grayson, M.S. Smith, J.E. Friedman, K.L. Grove, Maternal high-fat diet triggers lipotoxicity in the fetal livers of nonhuman primates, *J. Clin. Invest.* 119 (2009) 323–335. doi:10.1172/JCI32661.
- [36] S.R. Wesolowski, C.M. Mulligan, R.C. Janssen, P.R. Baker, B.C. Bergman, A. D'Alessandro, T. Nemkov, K.N. Maclean, H. Jiang, T.A. Dean, D.L. Takahashi, P. Kievit, C.E. McCurdy, K.M. Aagaard, J.E. Friedman, Switching obese mothers to a healthy diet improves fetal hypoxemia, hepatic metabolites, and lipotoxicity in non-human primates, *Mol. Metab.* 18 (2018) 25–41. doi:10.1016/j.molmet.2018.09.008.
- [37] J.A. Salati, V.H.J. Roberts, M.C. Schabel, J.O. Lo, C.D. Kroenke, K.S. Lewandowski, J.R. Lindner, K.L. Grove, A.E. Frias, Maternal high-fat diet reversal improves placental hemodynamics in a nonhuman primate model of diet-induced obesity, *Int. J. Obes.* 43 (2019) 906–916. doi:10.1038/s41366-018-0145-7.
- [38] L.D. Pound, S.M. Comstock, K.L. Grove, Consumption of a Western-style diet during pregnancy impairs offspring islet vascularization in a Japanese macaque model, *Am. J. Physiol. Metab.* 307 (2014) E115–E123. doi:10.1152/ajpendo.00131.2014.
- [39] X. Chen, T.O. Scholl, M. Leskiw, J. Savaille, T.P. Stein, Differences in maternal circulating fatty acid composition and dietary fat intake in women with gestational diabetes mellitus or mild gestational hyperglycemia, *Diabetes Care.* 33 (2010) 2049–2054. doi:10.2337/dc10-0693.
- [40] E.S. Gordon, Non-Esterified Fatty Acids in the Blood of Obese and Lean Subjects, *Am. J. Clin. Nutr.* 8 (1960) 740–747. doi:10.1093/ajcn/8.5.740.
- [41] H. Merzouk, M. Meghelli-Bouchenak, B. Loukidi, J. Prost, J. Belleville, Impaired Serum Lipids and Lipoproteins in Fetal Macrosomia Related to Maternal Obesity, *Neonatology.* 77 (2000) 17–24. doi:10.1159/000014190.
- [42] C.L. Kien, J.Y. Bunn, R. Stevens, J. Bain, O. Ikayeva, K. Crain, T.R. Koves, D.M. Muoio, Dietary intake of palmitate and oleate has broad impact on systemic and tissue lipid profiles in humans, *Am. J. Clin. Nutr.* 99 (2014) 436–445. doi:10.3945/ajcn.113.070557.
- [43] C.L. Kien, K.I. Everingham, R.D. Stevens, N.K. Fukagawa, D.M. Muoio, Short-Term Effects of Dietary Fatty Acids on Muscle Lipid Composition and Serum Acylcarnitine Profile in Human Subjects, *Obesity.* 19 (2011) 305–311. doi:10.1038/oby.2010.135.
- [44] B. Kwon, H.-K. Lee, H.W. Querfurth, Oleate prevents palmitate-induced mitochondrial dysfunction, insulin resistance and inflammatory signaling in neuronal cells, *Biochim. Biophys. Acta - Mol. Cell Res.* 1843 (2014) 1402–1413. doi:10.1016/j.bbamcr.2014.04.004.

- [45] L. Yuzefovych, G. Wilson, L. Rachek, Different effects of oleate vs. palmitate on mitochondrial function, apoptosis, and insulin signaling in L6 skeletal muscle cells: role of oxidative stress, *Am. J. Physiol. Metab.* 299 (2010) E1096–E1105. doi:10.1152/ajpendo.00238.2010.
- [46] N. Itami, K. Shirasuna, T. Kuwayama, H. Iwata, Palmitic acid induces ceramide accumulation, mitochondrial protein hyperacetylation, and mitochondrial dysfunction in porcine oocytes†, *Biol. Reprod.* 98 (2018) 644–653. doi:10.1093/biolre/ioy023.
- [47] C.H. Hulme, A. Stevens, W. Dunn, A.E.P. Heazell, K. Hollywood, P. Begley, M. Westwood, J.E. Myers, Identification of the functional pathways altered by placental cell exposure to high glucose: lessons from the transcript and metabolite interactome, *Sci. Rep.* 8 (2018) 5270. doi:10.1038/s41598-018-22535-y.
- [48] K.A.R. Tobin, G.M. Johnsen, A.C. Staff, A.K. Duttaroy, Long-chain Polyunsaturated Fatty Acid Transport across Human Placental Choriocarcinoma (BeWo) Cells, *Placenta.* 30 (2009) 41–47. doi:10.1016/j.placenta.2008.10.007.
- [49] K. Ogura, M. Sakata, Y. Okamoto, Y. Yasui, C. Tadokoro, Y. Yoshimoto, M. Yamaguchi, H. Kurachi, T. Maeda, Y. Murata, 8-bromo-cyclicAMP stimulates glucose transporter-1 expression in a human choriocarcinoma cell line., *J. Endocrinol.* 164 (2000) 171–8. <http://www.ncbi.nlm.nih.gov/pubmed/10657852>.
- [50] B. Wice, D. Menton, H. Geuze, A.L. Schwartz, Modulators of cyclic AMP metabolism induce syncytiotrophoblast formation in vitro, *Exp. Cell Res.* 186 (1990) 306–316. doi:10.1016/0014-4827(90)90310-7.
- [51] D.K.T. Pang, Z. Nong, B.G. Sutherland, C.G. Sawyez, D.L. Robson, J. Toma, J.G. Pickering, N.M. Borradaile, Niacin promotes revascularization and recovery of limb function in diet-induced obese mice with peripheral ischemia, *Pharmacol. Res. Perspect.* 4 (2016) e00233. doi:10.1002/prp2.233.
- [52] C. Tang, L. Tang, X. Wu, W. Xiong, H. Ruan, M. Hussain, J. Wu, C. Zou, X. Wu, Glioma-associated Oncogene 2 Is Essential for Trophoblastic Fusion by Forming a Transcriptional Complex with Glial Cell Missing-a, *J. Biol. Chem.* 291 (2016) 5611–5622. doi:10.1074/jbc.M115.700336.
- [53] S.S. Malhotra, P. Suman, S. Kumar Gupta, Alpha or beta human chorionic gonadotropin knockdown decrease BeWo cell fusion by down-regulating PKA and CREB activation, *Sci. Rep.* 5 (2015) 11210. doi:10.1038/srep11210.
- [54] K. Kusama, R. Bai, K. Imakawa, Regulation of human trophoblast cell syncytialization by transcription factors STAT5B and NR4A3, *J. Cell. Biochem.* 119 (2018) 4918–4927. doi:10.1002/jcb.26721.
- [55] E.J. Wolvetang, K.L. Johnson, K. Krauer, S.J. Ralph, A.W. Linnane, Mitochondrial respiratory chain inhibitors induce apoptosis, *FEBS Lett.* 339

(1994) 40–44. doi:10.1016/0014-5793(94)80380-3.

- [56] A.A. Starkov, R.A. Simonyan, V.I. Dedukhova, S.E. Mansurova, L.A. Palamarchuk, V.P. Skulachev, Regulation of the energy coupling in mitochondria by some steroid and thyroid hormones, *Biochim. Biophys. Acta - Bioenerg.* 1318 (1997) 173–183. doi:10.1016/S0005-2728(96)00135-1.
- [57] U. Jeschke, D.-U. Richter, B.-M. Möbius, V. Briese, I. Mylonas, K. Friese, Stimulation of progesterone, estradiol and cortisol in trophoblast tumor bewo cells by glycodeclin A N-glycans., *Anticancer Res.* 27 (2007) 2101–8. <http://www.ncbi.nlm.nih.gov/pubmed/17649829>.
- [58] T.R. Downs, W.W. Wilfinger, Fluorometric quantification of DNA in cells and tissue., *Anal. Biochem.* 131 (1983) 538–47. <http://www.ncbi.nlm.nih.gov/pubmed/6193739>.
- [59] C. Muschet, G. Möller, C. Prehn, M.H. de Angelis, J. Adamski, J. Tokarz, Removing the bottlenecks of cell culture metabolomics: fast normalization procedure, correlation of metabolites to cell number, and impact of the cell harvesting method, *Metabolomics.* 12 (2016) 151. doi:10.1007/s11306-016-1104-8.
- [60] J.S. Thacker, D.H. Yeung, W.R. Staines, J.G. Mielke, Total protein or high-abundance protein: Which offers the best loading control for Western blotting?, *Anal. Biochem.* 496 (2016) 76–78. doi:10.1016/j.ab.2015.11.022.
- [61] D.M. Kirby, D.R. Thorburn, D.M. Turnbull, R.W. Taylor, Biochemical assays of respiratory chain complex activity., *Methods Cell Biol.* 80 (2007) 93–119. doi:10.1016/S0091-679X(06)80004-X.
- [62] R. Davies, K.E. Mathers, A.D. Hume, K. Bremer, Y. Wang, C.D. Moyes, Hybridization in Sunfish Influences the Muscle Metabolic Phenotype, *Physiol. Biochem. Zool.* 85 (2012) 321–331. doi:10.1086/666058.
- [63] K.E. Mathers, J.F. Staples, Saponin-permeabilization is not a viable alternative to isolated mitochondria for assessing oxidative metabolism in hibernation, *Biol. Open.* 4 (2015) 858–864. doi:10.1242/bio.011544.
- [64] E.R. Price, J.T. McFarlan, C.G. Guglielmo, Preparing for Migration? The Effects of Photoperiod and Exercise on Muscle Oxidative Enzymes, Lipid Transporters, and Phospholipids in White-Crowned Sparrows, *Physiol. Biochem. Zool.* 83 (2010) 252–262. doi:10.1086/605394.
- [65] C.-J. Ke, Y.-H. He, H.-W. He, X. Yang, R. Li, J. Yuan, A new spectrophotometric assay for measuring pyruvate dehydrogenase complex activity: a comparative evaluation, *Anal. Methods.* 6 (2014) 6381–6388. doi:10.1039/C4AY00804A.
- [66] M. Lew, Good statistical practice in pharmacology Problem 2, *Br. J. Pharmacol.*

- 152 (2009) 299–303. doi:10.1038/sj.bjp.0707372.
- [67] B.N. Colvin, M.S. Longtine, B. Chen, M.L. Costa, D.M. Nelson, Oleate attenuates palmitate-induced endoplasmic reticulum stress and apoptosis in placental trophoblasts, *Reproduction*. 153 (2017) 369–380. doi:10.1530/REP-16-0576.
- [68] K. Kolahi, A. Valent, K.L. Thornburg, Cytotrophoblast, Not Syncytiotrophoblast, Dominates Glycolysis and Oxidative Phosphorylation in Human Term Placenta., *Sci. Rep.* (2017) 1–12. doi:10.1038/srep42941.
- [69] N.E. Sunny, E.J. Parks, J.D. Browning, S.C. Burgess, Excessive Hepatic Mitochondrial TCA Cycle and Gluconeogenesis in Humans with Nonalcoholic Fatty Liver Disease, *Cell Metab.* 14 (2011) 804–810. doi:10.1016/j.cmet.2011.11.004.
- [70] C.M. Palmeira, F.M.L. Ferreira, D.L. Santos, R. Ceiça, K. Suzuki, M.S. Santos, Higher efficiency of the liver phosphorylative system in diabetic Goto-Kakizaki (GK) rats, *FEBS Lett.* 458 (1999) 103–106. doi:10.1016/S0014-5793(99)01144-8.
- [71] Y. Wei, R.S. Rector, J.P. Thyfault, J.A. Ibdah, Nonalcoholic fatty liver disease and mitochondrial dysfunction, *World J. Gastroenterol.* 14 (2008) 193. doi:10.3748/wjg.14.193.
- [72] T. Koyama, S. Kume, D. Koya, S. Araki, K. Isshiki, M. Chin-Kanasaki, T. Sugimoto, M. Haneda, T. Sugaya, A. Kashiwagi, H. Maegawa, T. Uzu, SIRT3 attenuates palmitate-induced ROS production and inflammation in proximal tubular cells, *Free Radic. Biol. Med.* 51 (2011) 1258–1267. doi:10.1016/j.freeradbiomed.2011.05.028.
- [73] J. Liu, F. Chang, F. Li, H. Fu, J. Wang, S. Zhang, J. Zhao, D. Yin, Palmitate promotes autophagy and apoptosis through ROS-dependent JNK and p38 MAPK, *Biochem. Biophys. Res. Commun.* 463 (2015) 262–267. doi:10.1016/j.bbrc.2015.05.042.
- [74] T.A. Miller, N.K. LeBrasseur, G.M. Cote, M.P. Trucillo, D.R. Pimentel, Y. Ido, N.B. Ruderman, D.B. Sawyer, Oleate prevents palmitate-induced cytotoxic stress in cardiac myocytes, *Biochem. Biophys. Res. Commun.* 336 (2005) 309–315. doi:10.1016/j.bbrc.2005.08.088.
- [75] N. Malti, H. Merzouk, S.A. Merzouk, B. Loukidi, N. Karaouzene, A. Malti, M. Narce, Oxidative stress and maternal obesity: Feto-placental unit interaction, *Placenta*. 35 (2014) 411–416. doi:10.1016/j.placenta.2014.03.010.
- [76] V.H.J. Roberts, J. Smith, S.A. McLea, A.B. Heizer, J.L. Richardson, L. Myatt, Effect of Increasing Maternal Body Mass Index on Oxidative and Nitrate Stress in The Human Placenta, *Placenta*. 30 (2009) 169–175. doi:10.1016/j.placenta.2008.11.019.

- [77] D. Sommerweiss, T. Gorski, S. Richter, A. Garten, W. Kiess, Oleate rescues INS-1E β -cells from palmitate-induced apoptosis by preventing activation of the unfolded protein response, *Biochem. Biophys. Res. Commun.* 441 (2013) 770–776. doi:10.1016/j.bbrc.2013.10.130.
- [78] C.. Abaidoo, M.A. Warren, P.W. Andrews, K.A. Boateng, A Quantitative Assessment of the Morphological Characteristics of BeWo Cells as an in vitro Model of Human Trophoblast Cells, *Int. J. Morphol.* 28 (2010) 1047–1058. doi:10.4067/S0717-95022010000400011.
- [79] T.M. Mayhew, Villous trophoblast of human placenta: a coherent view of its turnover, repair and contributions to villous development and maturation., *Histol. Histopathol.* 16 (2001) 1213–24. doi:10.14670/HH-16.1213.
- [80] B. Huppertz, J.C.P. Kingdom, Apoptosis in the Trophoblast—Role of Apoptosis in Placental Morphogenesis, *J. Soc. Gynecol. Investig.* 11 (2004) 353–362. doi:10.1016/j.jsg.2004.06.002.

Chapter 3

3 The impact of hyperglycemia upon BeWo trophoblast cell metabolic function: A multi-OMICS and functional metabolic analysis

This chapter is a version of a manuscript submitted for publication entitled “The impact of hyperglycemia upon BeWo trophoblast cell metabolic function: A multi-OMICS and functional metabolic analysis”

3.1 Introduction

The rates of diabetes mellitus (DM) during pregnancy have increased substantially over the past several decades [1]. It is currently estimated that up to 1 in 10 pregnancies worldwide are impacted by maternal DM [2,3], however these rates may be even higher in certain at risk demographics such as in Indigenous populations [4]. These increases are particularly concerning as maternal DM during pregnancy, regardless of whether it is pre-existing (such as in type 1 DM or type 2 DM) or develops during gestation (gestational DM (GDM)), is associated with a multitude of poor fetal health outcomes [5–8]. Specifically, children exposed to DM during intrauterine development have been found to be at a greater risk of developing non-communicable diseases such as obesity, metabolic syndrome, and impaired insulin sensitivity early in their lives [5,9–12]. Understanding the underlying mechanisms that link maternal DM during pregnancy to the development of non-communicable diseases in offspring is critical to develop appropriate prenatal clinical management practices that help reduce health risks to the next generations.

As the placenta is responsible for nutrient, gas, and waste exchange between mother and fetus, specific alterations in the function of this organ may underlie the intrauterine programming of metabolic disorders in DM-exposed offspring. Unsurprisingly, morphological, and functional abnormalities have been found to be highly prevalent in placentae of diabetic pregnancies [13,14]. For example, diabetic placentae are often heavier [15–17] and display increased glycogen and triglyceride content [18–23], that is suggestive of altered nutrient storage and processing by the placenta and subsequently altered nutrient delivery to the developing fetus. This increase in nutrient storage in DM placentae has been thought to modulate trans-placental nutrient transport and fetal growth trajectories [24,25]. Additionally, the progenitor cytotrophoblasts (CT) and differentiated syncytiotrophoblasts (SCT) cells of the placenta villous trophoblast layer (cells that form the materno-fetal exchange barrier and are a primary site for placental energy (ATP) production) have impaired mitochondrial function in response to maternal DM that may further impact placental nutrient handling [26]. In particular, cultured primary CT and SCT cells from GDM pregnancies display

reduced basal and maximal mitochondrial respiratory (oxidative) activity compared to non-diabetic control trophoblasts [27,28]. Additionally, pre-existing DM has been found to impact the activities of individual placental Electron Transport Chain (ETC) complexes in whole placental lysates, highlighted by reduced complex I, II and III activities in type 1 DM placentae, and reduced complex II and III activity in type 2 DM placentae [29]. Overall, these studies suggest that impaired placental nutrient storage and mitochondrial oxidative function may be implicated in the development of metabolic diseases in DM-exposed offspring.

Previous work with placental cell lines and *ex vivo* placental explant preparations have demonstrated that hyperglycemia (a hallmark symptom of both pre-existing and gestationally-developed DM) is an important regulator of placental metabolic function. For example, explants from uncomplicated pregnancies display altered metabolic processing of lipids when cultured under hyperglycemic (HG) conditions (25 mM glucose) for only 18 hours [22]. Further reports have highlighted transcriptomic and metabolomic markers indicative of altered lipid metabolism, β -oxidation, and glycolysis functions in BeWo CT cells cultured under HG-conditions (25 mM) for 48 hours [30]. Independent hyperglycemia (30 mM glucose for 72h) has also been linked to increased Reactive Oxygen Species (ROS) generation in BeWo CTs [31], which directly promotes mitochondrial oxidative damage [32,33].

These reports have suggested that hyperglycemia independently facilitates the development of aberrant placental metabolic function in diabetic pregnancies. However, the direct and independent impacts of hyperglycemia on placental mitochondrial respiratory (oxidative) function are poorly understood. It is important to note that elevated glucose levels (25 mM for 48h) have also been associated with altered mitochondrial activity in BeWo CT cells when assessed by endpoint tetrazolium salt (MTT) assay [34]. However, an interrogation of mitochondrial respiratory activity of HG-exposed trophoblast cells using recently developed real-time functional readouts (such as the Seahorse XF Analyzer), as has been performed with DM-exposed Primary Human Trophoblasts (PHT), [27–29] is warranted. In addition, the direct impacts of hyperglycemia on glycogen and lipid nutrient stores of placental trophoblasts and the

underlying mechanisms governing placental nutrient storage in HG-conditions are not well defined. Thus, the first objective of the current study was to characterize the impacts of independent hyperglycemia on placental mitochondrial respiratory activity and nutrient storage by evaluating both progenitor BeWo CTs and differentiated BeWo SCTs following a relatively prolonged 72-hour HG (25 mM) exposure.

Recently, the integration of transcriptomics, metabolomics, and lipidomics has been identified as a useful method to elucidate cellular mechanisms that underlie pathological placental development in pre-clinical models [30,35,36]. Thus, the second objective of this study was to utilize a multi-omics research approach to thoroughly characterize the underlying mechanisms leading to altered metabolic function specifically in high-glucose exposed BeWo progenitor CT cells. Overall, it was postulated that HG-culture conditions would be associated with increased nutrient storage and impaired mitochondrial respiratory function in BeWo CT and SCT cells, in association with altered transcriptome, metabolome, and lipidome signatures in BeWo CT cells indicative of altered metabolic function.

3.2 Materials and methods

3.2.1 Materials

All materials were purchased from Millipore Sigma (Oakville, Canada) unless otherwise specified.

3.2.2 Cell culture conditions

BeWo (CCL-98) trophoblast cells were purchased from the American Type Culture Collection (ATCC; Cedarlane Labs, Burlington, Canada). Cells were cultured in F12K media (Gibco, ThermoFisher Scientific, Mississauga, Canada) as recommended by the ATCC, and supplemented with 10% Fetal Bovine Serum (Gibco) and 1% Penicillin-Streptomycin (Invitrogen, ThermoFisher Scientific, Mississauga, Canada). All cells were utilized between passages 5-15 and were maintained at 37°C and 5% CO₂/95% atmospheric air.

The F12K media contained 7 mM of glucose, a relatively physiological glucose level, and was utilized for low-glucose (LG) controls. F12K media was supplemented to 25 mM glucose for hyperglycemic (HG) culture treatments as previously utilized with BeWo trophoblasts [30,34]. BeWo trophoblasts cells were plated in LG F12K media at the specifically stated experimental densities and allowed to adhere to cell culture plates overnight before being treated with HG culture media. Cell media was replenished every 24 hours. At T24h and T48h subsets of BeWo trophoblasts were treated with 250 μ M 8-Br-cAMP to induce differentiation from cytotrophoblast-like (CT) cells to SCT cells. Cell cultures were collected after 72 hours of high glucose exposure. A schematic of the HG culture protocol is available in **Figure 3-1**.

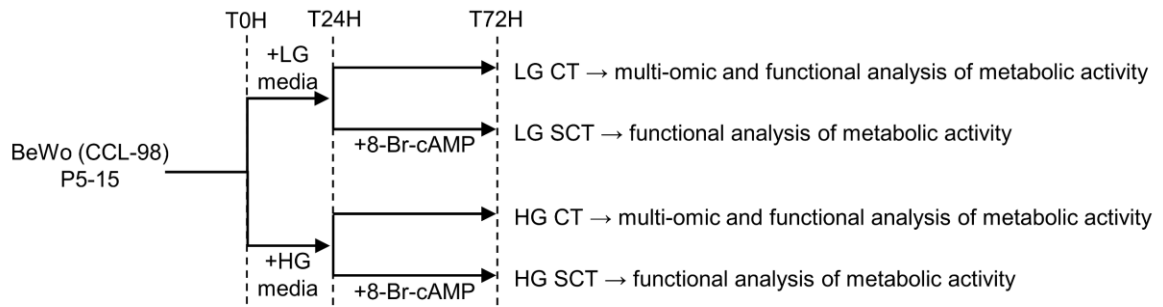


Figure 3-1 Schematic of 72-hour hyperglycemic cell culture protocol.

BeWo trophoblasts were plated in F12K media and allowed to adhere to culture plates overnight. At T0H cells were treated with low glucose (LG, 7 mM) or hyperglycemic (HG, 25 mM) supplemented F12K media. At T24H subsets of BeWo trophoblasts were treated with 250 μ M 8-Br-cAMP to induce CT-to-SCT differentiation. Cell media was replenished every 24 hours and cells were collected at T72H for analysis of metabolic function.

3.2.3 Cell viability

BeWo trophoblasts were plated at 7.5×10^3 cells/well in black walled 96-well cell culture plates and cultured as described. At T72h cell viability of both CT and SCT cultures was assessed via the CellTiter-Fluor cell viability assay (Promega Corporation, Madison WI, USA) as per manufacturer's instructions.

3.2.4 Immunofluorescent analysis of BeWo syncytialization

To determine the potential of HG culture conditions to impact the ability of BeWo trophoblasts to differentiate into SCT cells, cell fusion of 8-Br-cAMP stimulated cells (expressed as percent loss of the tight junction protein zona occludens-1 (ZO-1)) was examined. In brief, BeWo cells were plated at 1.4×10^5 cells/well in 6-well plates containing coverslips coated with laminin ($2 \mu\text{g}/\text{cm}^2$) and grown under HG conditions as described. Cellular expression of ZO-1 was then examined via immunofluorescent microscopy as previously detailed in chapter 2 [37].

3.2.5 RT-qPCR analysis of BeWo syncytialization

The expression of the transcription factor Ovo Like Transcriptional Repressor 1 (*OVOLI*) as well as human chorionic gonadotropin subunit beta (*CGB*) was additionally analyzed to ensure cell fusion in 8-Br-cAMP stimulated BeWo cells was associated with increased expression of syncytialization-related genes. In brief, BeWo trophoblasts were plated at 3.5×10^5 cells/plate in 60mm cell culture plates and cultured as described above. At T72h cells were collected in TRIzol reagent (Invitrogen), and total RNA was extracted as per the manufacturer's protocol. RNA integrity was assessed via formaldehyde gel electrophoresis, and RNA concentration was quantified by Nanodrop Spectrophotometer 2000 (NanoDrop Technologies, Inc., Wilmington, DE, USA). RNA ($2 \mu\text{g}$) was then reverse transcribed with the High-Capacity cDNA Reverse Transcription Kit (Applied Biosystems; ThermoFisher Scientific). RT-qPCR was then performed via the CFX384 Real Time system (Bio-Rad, Mississauga, Canada). Relative gene expression of *OVOLI* [38] and *CGB* [39] was then determined using the $\Delta\Delta\text{Ct}$ method with the geometric mean of *PSMB6* and *ACTB* utilized as a reference. Primer sequences and their efficiencies are available in **Table 3-1**.

Table 3-1 Forward and reverse primer sequences used for quantitative Real-Time PCR analysis of BeWo cell syncytialization

Gene	Accession No.	Annealing Temperature (°C)	Primer Sequences	Efficiency
<i>ACTB</i>	NM_001101.4	60	F – GTTGCTATCCAGGCTGTGCT R - AGGTAGTCAGTCAGGTCCCG	92.6%
<i>PSMB6</i>	NM_002798	60	F – CGGGAAGACCTGATGGCGGGA R - TCCCGGAGCCTCCAATGGCAAA	108.4%
<i>CGB</i>	Malhotra <i>et al</i> (2015) [39]	60	F – CCCCTTGACCTGTGATGACC R – TATTGTGGGAGGATCGGGGT	105.3%
<i>OVOL1</i>	Kusama <i>et al</i> (2018) [38]	60	F – AGACATGGGCCACTTGACAG R – AGGTGAACAGGTCTCCACTG	101.1%

3.2.6 Quantifying BeWo cell oxidative function

BeWo cells were plated at 7.5×10^3 cells/well in Seahorse XF24 V7PS plates and cultured under LG and HG conditions as described above. At T72h mitochondrial activity was assessed using the Seahorse XF Mito Stress Test, as previously optimized for BeWo trophoblast cells [37]. In brief, oxygen consumption rate (OCR) of cell culture media was quantified as a proxy measure of mitochondrial respiratory activity. Subsequent injections of oligomycin (1.5 $\mu\text{g/mL}$), dinitrophenol (DNP, 50 μM) and Rotenone and Antimycin A (0.5 μM each) were used to interrogate the basal respiration, maximal respiration, proton leak, spare respiratory capacity, and coupling efficiency parameters of mitochondrial respiratory activity. OCR measures were normalized to cellular DNA content using Hoechst dye fluorescence as described in Chapter 2 [37].

3.2.7 Quantifying BeWo cell glycolytic function

BeWo cells were plated at 7.5×10^3 cells/well in Seahorse XF24 V7PS plates and cultured under LG and HG conditions as described above. At T72h glycolytic activity was assessed via the Seahorse XF Glycolysis Stress Test, as previously optimized for BeWo trophoblasts [37]. In brief, Extracellular Acidification Rate (ECAR) of cell culture media was assessed to quantify glycolytic activity in BeWo trophoblasts. Injections of glucose (10 mM), oligomycin (1.5 $\mu\text{g/mL}$) and 2-deoxyglucose (50 mM) were utilized to interrogate the basal glycolytic rate, maximal glycolytic rate, glycolytic reserve, and non-glycolytic acidification parameters of glycolytic function. ECAR data was normalized to cellular DNA content using Hoechst dye fluorescence as previously described [37].

Representative tracings of the Seahorse XF Mito Stress Test and Glycolysis Stress Test for LG and HG-cultured BeWo trophoblast cells are available in **Figure 3-2**.

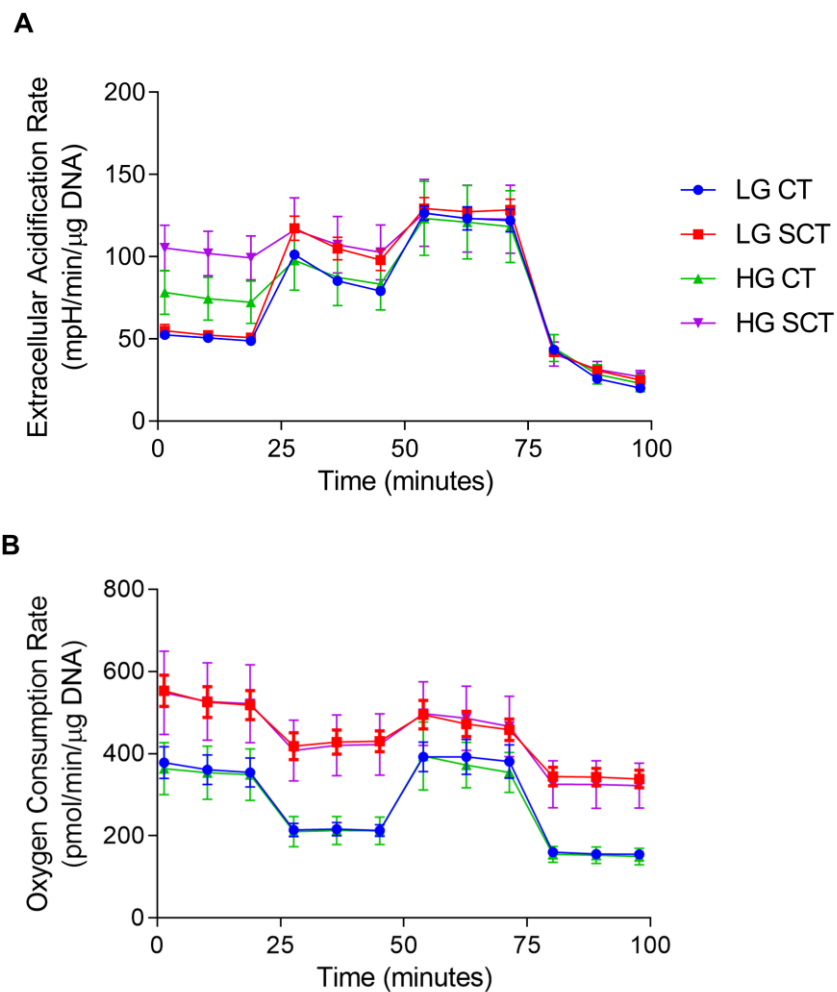


Figure 3-2 Representative tracings of the Seahorse XF Mito Stress Test and Glycolysis Stress Test in LG and HG-cultured BeWo trophoblasts.

(A) Representative Seahorse XF Mito Stress Test assay tracings; data is presented as mean Oxygen Consumption Rate (OCR) \pm SEM of the technical replicates of each treatment group from one experiment. (B) Representative Seahorse XF Glycolysis Stress Test assay tracings; data is presented as mean Extracellular Acidification Rate (ECAR) \pm SEM of the technical replicates of each treatment group from one experiment.

3.2.8 Immunoblot analysis

BeWo trophoblasts were plated at 9.5×10^5 cells/plate in 100 mm cell culture dishes and cultured under LG and HG conditions as described. At T72h cells were washed once in ice-cold PBS and subsequently lysed in radioimmunoprecipitation assay (RIPA) buffer supplemented with protease and phosphatase inhibitors as described in chapter 2 [37]. Protein concentrations were then adjusted to $2 \mu\text{g}/\mu\text{L}$ in Laemmli loading buffer (62.5 mM Tris-Cl (pH 6.8); 2% SDS 10% glycerol; 0.002% bromophenol blue; 4% β -mercaptoethanol).

The relative abundance of target proteins was then determined via SDS-PAGE gel electrophoresis. In brief, protein lysates were separated with on acrylamide gels (10-15%), and separated proteins were transfer to polyvinylidene fluoride (PVDF) membranes (EMD Millipore, Fisher Scientific). Total lane protein was then determined via Ponceau stain (0.1% Ponceau-S in 5% acetic acid) and utilized to normalize densitometry values. PVDF membranes were blocked in 5% dry-milk protein or 5% Bovine Serum Albumin (BSA, BioShop Canada Inc., Burlington, Canada) and membranes were incubated overnight at 4°C with respective antibody solutions (**Table 3-2**). Membranes were then washed 3 times with Tris-buffered Saline with 0.1% Tween-20 (TBST) and incubated with respective secondary antibodies for 1 hour at room temperature (**Table 3-2**). Membranes were washed 3 more times in TBST and imaged on a ChemiDoc Imager (Bio-Rad) using Clarity western ECL substrate (Bio-Rad). Protein band abundance and total lane protein (ponceau) were quantified with Image-Lab Software (Bio-Rad). Representative uncropped images of immunoblot images highlighting antibody specificity are available in **Supplementary Figures 2 and 3** (doi.org/10.5683/SP3/XMPKOK).

Table 3-2 Specifications of antibodies utilized in immunoblotting experiments, and the protein mass loaded for each protein target

Protein Target	Source	Dilution	Blocking solution	Protein Loaded	Heat (°C)	Company	Catalogue No.
Human Mitoprofile	Mouse Monoclonal	1:1000	5% Milk	35 µg	37	ABCAM	ab110411
Glycogen Synthase	Rabbit Polyclonal	1:1000	5% BSA	25 µg	95	Cell Signaling Technologies	3893
pSer ⁶⁴¹ Glycogen Synthase	Rabbit Polyclonal	1:1000	5% BSA	20 µg	95	Cell Signaling Technologies	3891
GSK3-β	Rabbit Monoclonal	1:1000	5% BSA	25 µg	95	Cell Signaling Technologies	9315
pSer ⁹ GSK3-β	Rabbit Monoclonal	1:1000	5% BSA	20 µg	95	Cell Signaling Technologies	9323
ACSL1	Rabbit Polyclonal	1:500	5% BSA	12.5 µg	95	Cell Signaling Technologies	4047
Fatty Acid Synthase	Rabbit Monoclonal	1:1000	5% BSA	15 µg	95	Cell Signaling Technologies	3180
OPA1	Rabbit Monoclonal	1:1000	5% BSA	15 µg	95	Cell Signaling Technologies	67589
DRP1	Rabbit Monoclonal	1:1000	5% BSA	15 µg	95	Cell Signaling Technologies	8570
pSER616 DRP1	Rabbit Monoclonal	1:1000	5% BSA	12.5 µg	95	Cell Signaling Technologies	4494
GLUT1	Mouse Monoclonal	1:1000	5% BSA	15 µg	20	EMD Millipore	mabs132
Anti-Rabbit Secondary	Goat	1:10,000	-	-	-	Cell Signaling Technologies	7074
Anti-Mouse Secondary	Horse	1:10,000	-	-	-	Cell Signaling Technologies	7076

3.2.9 Enzyme activity assays

Full step-by-step experimental protocols for the enzyme activity assays utilized in Chapter 3 are available in the Supplementary Materials (doi.org/10.5683/SP3/ZTN4ZR).

3.2.9.1 ETC complex I and II activity

BeWo trophoblasts were plated at 3.5×10^5 cells/plate in 60mm cell culture dishes and cultured under LG and HG conditions as described. At T72h cells were washed once with PBS and detached from cell culture plates by scraping. Cells were then pelleted (400g, 5 mins), snap frozen in liquid nitrogen and stored at -80°C until analyzed. Cell pellets were subsequently lysed and complex I activity was assessed as the rate of rotenone-sensitive NADH oxidation, and complex II activity was assessed as the rate of DCPIP oxidation as previously detailed in Chapter 2 [37]. ETC complex activity assays were normalized to cell lysate protein content via Bicinchoninic Acid (BCA) assay (Pierce, ThermoFisher Scientific) as per manufacturer's instructions.

3.2.9.2 Quantifying metabolic enzyme activities

BeWo trophoblasts were plated at 3.5×10^5 cells/plate in 60mm cell culture dishes and cultured under LG and HG conditions as detailed above. To examine the enzyme activities of Lactate Dehydrogenase (LDH) and Citrate Synthase (CS), cells were collected by scraping and lysed in glycerol lysis buffer (20 mM Na_2HPO_4 , 0.5 mM EDTA, 0.1% Triton X-100, 0.2% BSA, 50% glycerol) containing protease and phosphatase inhibitors as previously described [37,40]. LDH activity was assessed as the rate of NADH oxidation, and CS activity was assessed as the rate of Ellman's reagent consumption as detailed in Chapter 2 [37]. The enzyme activity of LDH and CS were normalized to cell lysate protein content via BCA assay.

Additional BeWo cultures were collected to analyze the activity of the E1 (rate-limiting) subunit of the Pyruvate Dehydrogenase (PDH) complex. PDH-E1 subunit was assessed on freshly collected BeWo cells as the rate of DCPIP oxidation and normalized to protein content via BCA assay as detailed in Chapter 2 [37].

3.2.10 Analysis of nutrient storage

BeWo trophoblasts were plated at 3.5×10^5 cells/plate in 60mm cell culture dishes and cultured under LG and HG conditions. At T72h cells were washed with PBS and collected into fresh PBS (1.5 mL) by scraping. Cells were then pelleted (400g, 5 minutes) and the PBS was aspirated.

To determine cellular glycogen content, the cell pellets were lysed in 200 μ L ddH₂O and samples were boiled for 10 minutes to inactivate cell enzymes. Samples were stored at -20°C until glycogen content was analyzed. Samples were diluted 5-fold and glycogen content was analyzed via the Glycogen Assay Kit (ABCAM, ab65620) as per manufacturer's protocol. Glycogen content was then normalized to cell lysate protein content via BCA assay.

To determine cellular triglyceride accumulation, the collected cell pellets were snap frozen in liquid nitrogen and stored at -80°C until analyzed. Cells were then lysed, and cellular triglyceride content was analyzed via the Triglyceride Assay Kit (ABCAM, ab178780) as per kit instructions. Triglyceride content was normalized to cell lysate protein content measured by a BCA assay.

3.2.11 Transcriptomic analysis of gene expression changes

BeWo CT cells were plated at 3.5×10^5 cells/plate in 60 mm cell culture dishes and grown under LG and HG culture conditions as described. At T72h cells were washed once with PBS and collected in 900 μ L TRIzol Reagent and stored at -80°C. Samples were then shipped to the Genome Québec Innovation Centre for transcriptomic analysis via Clariom S mRNA microarray. Automated RNA extraction was completed via QIAcube Connect (Qiagen, Toronto, Canada). RNA content was then quantified via NanoDrop Spectrophotometer 2000 (Nanodrop Technologies, Inc) and RNA integrity was determined by Bioanalyzer 2100 (Agilent Technologies, Waldbronn, Germany). All extracted RNA samples had an RNA Integrity Number (RIN) greater than 9.5. RNA was then processed via the Affymetrix Whole Transcript 2 workflow and analyzed using a Clariom S human mRNA microarray. In brief, sense-stranded cDNA was synthesized from 100 ng total RNA, and subsequently fragmented, and labelled with the GeneChip

WT Terminal Labeling Kit (ThermoFisher Scientific) as per manufacturer's instructions. Labelled DNA was then hybridized to Clariom S human GeneChips (ThermoFisher Scientific) and incubated at 45°C in the GeneChip Hybridization oven 640 (Affymetrix, ThermoFisher Scientific) for 17 hours at 60 rpm. GeneChips were washed using GeneChip Hybridization Wash and Stain Kit (ThermoFisher Scientific) according to manufacturer's specifications. Microarray chips were scanned on a GeneChip scanner 3000 (ThermoFisher Scientific).

Microarray data was then analyzed via Transcriptome Analysis Console v4.0 (ThermoFisher Scientific), and raw data was normalized using the Robust Multiple-Array Averaging (RMA) method. HG-treated samples were paired with respective LG-control for each cell collection for analysis. Genes with a $\geq \pm 1.3$ fold-change (FC) vs LG-control and raw-p < 0.05 were determined to be differentially expressed. The list of differentially expressed genes was then imported into WebGestalt for gene ontology (GO) analysis and analysis of functional pathways using the Wikipathways database. Biological processes and functional pathways were determined to be significantly enriched with and a False Discovery Rate (FDR) $p < 0.05$.

3.2.12 RT-qPCR validation of differentially expressed genes identified by mRNA microarray

RT-qPCR was utilized to validate differentially expressed genes involved in metabolic pathways that were highlighted by the mRNA microarray. The RNA utilized for the microarray was returned by Genome Québec and 2 µg was reverse transcribed as described above. The CT samples previously utilized to examine expression of syncytialization-related genes were additionally utilized to validate the differentially expressed genes identified in the microarray. RT-qPCR was then performed and analyzed using the $\Delta\Delta C_t$ with the geometric mean of *ACTB* and *PSMB6* used as a reference. Primer sequences of validated targets and their efficiencies are available in **Table 3-3**.

Table 3-3 Forward and reverse primer sequences used for quantitative Real-Time PCR mRNA microarray validation

Gene	Accession No.	Annealing Temperature (°C)	Forward Sequence (5'-3')	Efficiency
------	---------------	----------------------------	--------------------------	------------

ACTB	NM_001101.4	60	F – GTTGCTATCCAGGCTGTGCT R – AGGTAGTCAGTCAGGTCCCG	92.6%
PSMB6	NM_002798	60	F – CGGGAAGACCTGATGGCGGGA R – TCCCGGAGCCTCCAATGGCAAA	108.4%
SLC27A2	NM_003645.4	60	F – ACTTCTGGAACCACAGGTCTTC R – TCATCTGCCTTCAATCCGCTT	107.2%
HSD11B2	NM_000196.4	60	F – GGCTGCTTCAAGACAGAGTCAG R – GCTCGATGTAGTCCTTGCCG	100.9%
ACSL1	NM_001995.5	60	F – AGTCAATCCTTGCCCAGATGA R – ATCCGGTTCAGCAGTCTTGG	103.8%
RPS6KA5	NM_001322232.2	60	F – GTGCCTGCACCATTAAAGCC R – AGCAACAAAGGAATAGCCCTGA	95.0%
HK2	NM_000189.5	60	F – ACGCCAAAATCACGTCTCCG R – AGAGATACTGGTCAACCTTCTGC	98.8%

3.2.13 Cell culture collections for metabolomic and lipidomic profiling of BeWo CT cells

BeWo trophoblasts were plated at a density of 2×10^6 cells/plate in 150mm cell culture plates and cultured under LG and HG-conditions as described. At T72h cell media was aspirated and the cells were washed three times with cold PBS. Pre-cooled methanol (-20°C) was then added to quench cellular metabolic processes. Cells were then scraped and collected into microcentrifuge tubes, and the methanol was evaporated with a gentle flow of nitrogen gas. Samples were then frozen at -80°C and were subsequently lyophilized to remove any residual moisture.

The samples were then sent to The Metabolomics Innovation Centre (Edmonton, Canada) for subsequent metabolomics and lipidomics analysis via a High-Performance Chemical Isotope Labelling (HP CIL) liquid chromatography mass spectrometry (LC-MS) approach [41,42]. Samples were reconstituted in 50% methanol and freeze-thaw cycles were utilized to lyse the cells. The lysed samples were then centrifuged at 16000 g at 4°C for 10 mins, and 300 μL of resultant supernatant was transferred to a fresh tube for metabolomic profiling, while the remaining supernatant and cell pellets were utilized for lipidomic profiling.

3.2.14 Untargeted metabolomic profiling

The collected supernatants for metabolomic analysis were dried down and re-dissolved in 41 μL of water. The total concentrations of metabolite were then determined

via the NovaMT Sample Normalization kit (Edmonton, Alberta). Water was added to adjust all the concentrations of samples to 2 mM. The samples were split into five aliquots for respective labeling methods. Each of the individual samples was labeled by ^{12}C -DnsCl, base activated ^{12}C -DnsCl, ^{12}C -DmPA Br, and ^{12}C -DnsHz, for amine-/phenol-, hydroxyl-, carboxyl, and carbonyl- metabolomic profiling, respectively [43]. A pooled sample was generated by mixing of each individual sample and labeled by ^{13}C -reagent, accordingly. After mixing the each of ^{12}C -labeled individual sample with ^{13}C -labeled pool by equal volume, the mixtures were injected onto LC-MS for analysis. The LC-MS system was the Agilent 1290 LC (Agilent Technologies) linked to the Bruker Impact II QTOF Mass Spectrometer (Bruker Corporation, Billerica, US). LC-MS data was then exported to .csv files with Bruker DataAnalysis 4.4 (Bruker Corporation), the exported data were then uploaded to IsoMS pro v1.2.7 for data quality check and data processing.

Metabolite peak pairs were then identified using a three-tier approach, as previously described [43]. In tier 1, peak pairs were identified by searching against a labelled metabolite library (CIL library) based on accurate mass and retention time. In tier 2, the remaining peak pairs were matched by searching against a linked identity library (LI library), containing predicted retention time and accurate mass information. In tier 3, the rest of peak pairs were matched by searching against MyCompoundID (MCID) library, containing accurate mass information of metabolites and their predicted products

Metabolites with $\geq \pm 1.5$ FC and raw- $p < 0.05$ vs LG CT were determined to be differentially abundant in the HG-cultured BeWo CT cells. Subsequent pathway analysis (Homo sapiens KEGG library) was performed using MetaboAnalyst v5.0 to elucidate the biological impacts of the differentially abundant metabolites identified in tiers 1 and 2. Pathways with an FDR $p < 0.05$ were determined to be significantly enriched.

3.2.15 Untargeted lipidomic profiling

For lipidomic profiling, the remaining supernatant and cell pellets were processed using a modified Folch liquid-liquid lipid extraction protocol, as previously detailed [44]. In brief, samples were vortexed with 5 μL Splash Lipidomix Mass Spec Standard and methanol for 20s, and subsequently vortexed for an additionally 20s following additions

of dichloromethane. Samples were then incubated at room temperature for 10 mins before being centrifuged at 16,000g for 10 mins at 4°C. An aliquot of the resulting organic layer was then dried using a SpeedVac. The resulting dried material was resuspended in 15 µL of 10 mM ammonium formate in methanol:acetonitrile:water (50:40:10 v/v/v), vortexed for 1 min then diluted with 135 µL 10 mM ammonium formate in 95% isopropanol. A pooled mixture of all extracts was then prepared for quality control (QC) samples that were injected into the mass spectrometer every 7 runs to monitor instrument performance. Liquid Chromatography with tandem Mass Spectrometry (LC-MS/MS) was then performed in both positive and negative ion modes using a ThermoFisher Dionex UltiMate 3000 UHPLC machine (ThermoFisher Scientific) with a Water BEH C18 Column (Manufacturer Information; 5 cm × 2.1 mm with 1.7 µm particles) coupled with a Bruker Impact II QTOF Mass Spectrometer. Each sample was analyzed in technical duplicate. Data from each of the positive and negative ion mode runs were combined for each unique sample into a single feature-intensity table.

A three-tier approach was utilized to identify MS/MS lipid-species peaks. In tiers 1 and 2 positive MS/MS identification was performed by searching the MS Dial LipidBlast database, the Human Metabolome database, and the MassBank of North America LC-MS/MS, while lipid species in tier 3 were MS identified with the LipidMaps database [44,45]. For tier 1 identifications cutoffs of: MS/MS match score ≥ 500 ; precursor m/z error ≤ 5 mDa were utilized. For tier 2 identifications cutoffs of: MS/MS match score ≥ 100 ; precursor m/z error ≤ 5 mDa were utilized. Finally, in tier 3, lipid species were putatively identified by mass match with m/z error ≤ 5 mDa.

Identified features were combined and feature intensity normalized to the internal mass spectrometry standards. Normalized feature intensities were then imported in MetaboAnalyst v5.0 for statistical analysis. Lipid species were filtered if their relative standard deviation (RSD; SD/mean) was greater than 30% in QC samples. Lipid species in each NEFA treatment condition with $\geq \pm 1.5$ FC and raw p-value < 0.05 versus BSA control samples were considered to be differentially abundant.

3.2.16 Statistical analysis for non-omic experiments

Data collected as a percentage (percent loss of ZO-1 staining data, spare respiratory capacity, coupling efficiency, and glycolytic reserve) were log-transformed and analyzed via Two-Way ANOVA (2WA) and Bonferroni's Multiple Comparisons post-hoc test. A Randomized Block Design 2WA and Sidak's Multiple Comparisons Test was utilized to analyze relative mRNA transcript abundances; relative protein abundances; metabolic activity assay parameters; and nutrient storage data, using raw experimental data from each experimental replicate blocked together, as previously described [46]. These data were then expressed as percent of LG CT control for visualization in figures. Statistical analysis was performed with GraphPad Prism 8 Software (GraphPad Software, San Diego, CA, USA). A paired T-test was utilized to analyze gene FC data between HG and LG BeWo CT cells in the RT-qPCR validation of the microarray.

3.2.17 Supplementary data and materials

Microarray data are available on the National Center for Biotechnology Information (NCBI) Gene Expression Omnibus (GEO) database (GSE190025). Supplementary materials including detailed enzyme activity assay protocols (doi.org/10.5683/SP3/ZTN4ZR), and supplementary tables and figures (doi.org/10.5683/SP3/XMPKOK) have been uploaded to a publicly available data repository and can be accessed via the indicated Digital Object Identifier (DOI) webpage addresses. Metabolomic and lipidomic peak-pair data are available in Supplementary Tables 3 and 5, respectively.

3.3 Results

3.3.1 Characterization of BeWo viability and differentiation under high glucose culture conditions

HG culture conditions were associated with a mean 7% and 10% reduction in cell viability in BeWo CT and SCT cells respectively (**Figure 3-3**; $p < 0.01$; $n = 6$ /group). It is important to note that these viability data were consistent with previously reported values in BeWo trophoblasts and PHTs cultured under hyperglycemia (25 mM glucose) for 48h [30,47], and highlights that a more prolonged 72H HG-culture protocol does not impact the stability of cultured BeWo trophoblasts cells. Additionally, BeWo SCT cells displayed lower viability relative to BeWo CT cells consistent with trophoblast cells becoming less proliferative while undergoing syncytialization (**Figure 3-3**; $p < 0.001$).

BeWo SCT cultures displayed a greater loss of ZO-1 protein expression (and thus increased cell fusion) compared to BeWo CT cultures (**Figure 3-4 A,B**; $p < 0.0001$, $n = 4$ /group). However, HG-culture conditions had no impact on ZO-1 protein expression in BeWo trophoblast cells (**Figure 3-4 A,B**).

BeWo SCT cultures additionally displayed increased relative transcript abundance of the syncytialization-associated transcription factor *OVOLI* (**Figure 3-4 C**; $p < 0.01$, $n = 5$ /group) as well as the syncytialization-associated hormone *CGB* (**Figure 3-4 D**; $p < 0.01$, $n = 5$ /group). HG culture conditions in BeWo SCT cells was additionally associated with an increased transcript abundance of *CGB* compared to LG BeWo SCT cells (**Figure 3-4 D**; $p < 0.05$; 2WA: Interaction $p < 0.05$).

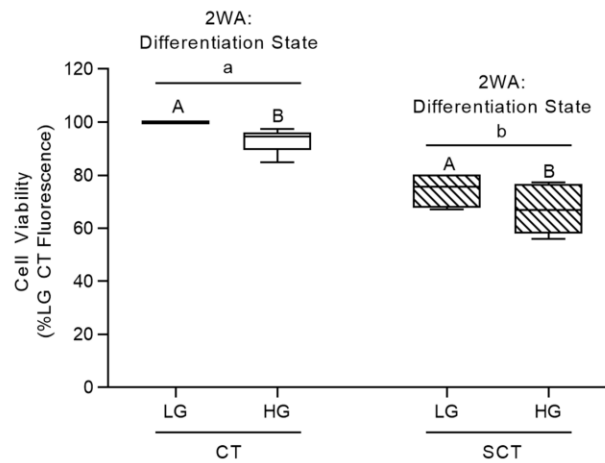


Figure 3-3 Viability of BeWo trophoblasts cultured under hyperglycemic (HG) conditions for 72h.

BeWo trophoblasts were cultured for 72H under HG culture conditions as described, and cell viability was assessed via the CellTiter-Flour cell viability assay. Data is presented as percent of LG CT cell viability (n=6/group). Raw cell viability fluorescence data was analyzed via Two-Way Randomized block design ANOVA (2WA). Different lower-case letters denote differentiation state-dependent differences in viability, and different upper-case letter denote differences in viability within each differentiation state (p<0.05).

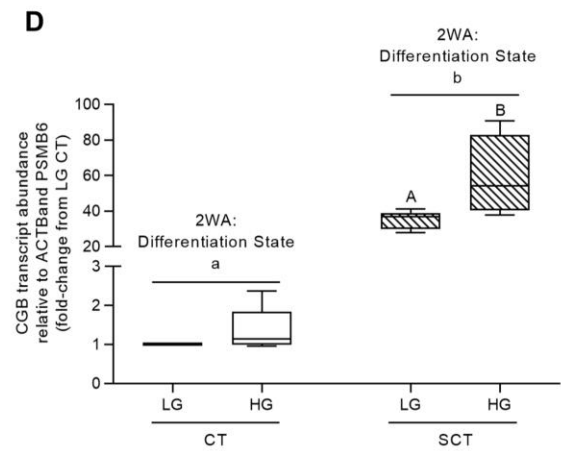
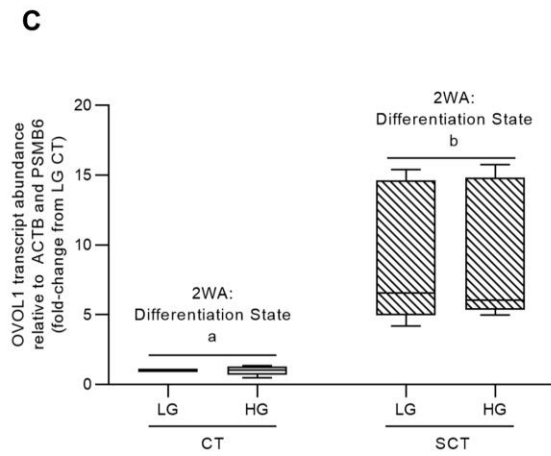
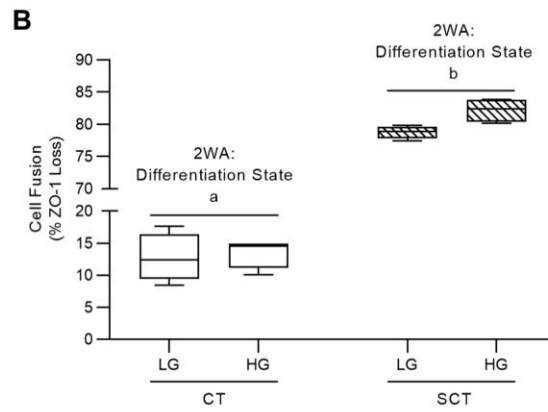
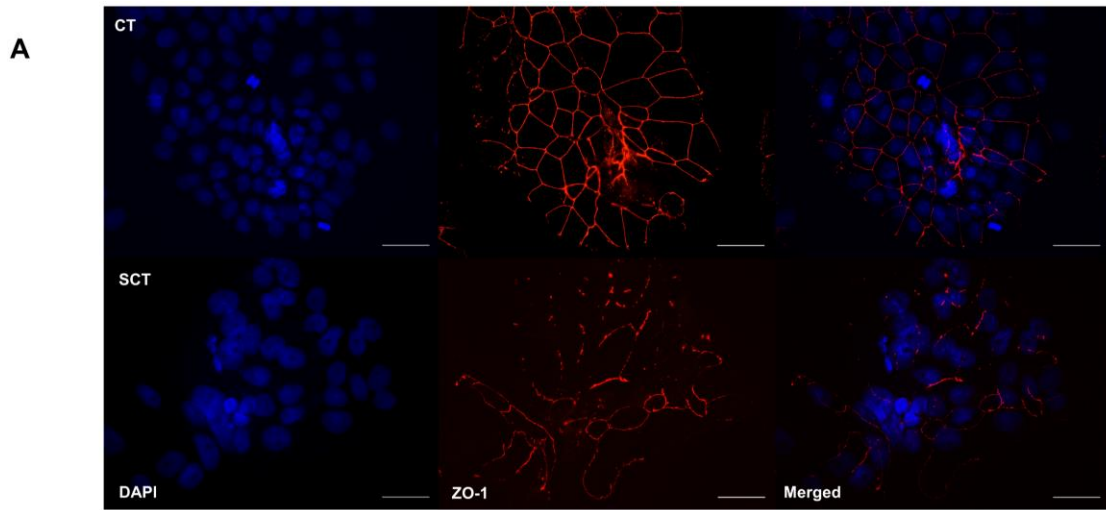


Figure 3-4 Hyperglycemic (HG) culture conditions do not impact BeWo SCT cell fusion but are associated with increased CGB transcript abundance at 72h.

(A) Representative DAPI (blue); Zona occludens-1 (ZO1; red) and merged immunofluorescent images (scale bar = 50 μ m) of BeWo CT and SCT cells. (B) Percent fusion of HG-cultured BeWo trophoblasts. Percent fusion data was log-transformed and analyzed via Two-Way Anova (2WA); data is expressed as the percentage of cells lacking ZO-1 expression (n=4/group). BeWo cell syncytialization was additionally analyzed via quantifying mRNA transcript abundance of the syncytialization markers (C) OVOL1 and (D) CGB. Transcript abundance data was analyzed via Randomized Block 2WA and Sidak's multiple comparisons test; data is present as transcript fold-change versus LG CT cultures (n=5/group). Different lower-case letters denote statistical differences between differentiation states, and different upper-case letter denote differences between LG and HG treatments within each respective differentiation state (p<0.05).

3.3.2 BeWo mitochondrial respiratory and glycolytic activity

High glucose culture conditions did not impact any of the parameters of mitochondrial respiratory function as assessed by the Seahorse XF Mito Stress Test (**Table 3-4**; n=5/group). However, BeWo syncytialization was associated with reduced Spare Respiratory Capacity (**Table 3-4**; p<0.0001) and reduced Coupling Efficiency (**Table 3-4**; p<0.01) independent of culture glucose level.

The parameters of glycolytic function as measured with the Seahorse XF Glycolysis Stress Test were not impacted by BeWo syncytialization, or by HG culture conditions (**Table 3-5**; n=5/group).

Table 3-4 Syncytialization but not HG culture conditions impacts BeWo trophoblast mitochondrial respiratory activity

Differentiation State	Treatment	Basal Respiration ¹	Maximal Respiration ¹	Proton Leak ¹	Spare Respiratory Capacity ²	Coupling Efficiency ²
CT	LG	199.70 ± 39.08	249.10 ± 43.78	55.48 ± 8.45	129.00 ± 5.30	70.38 ± 3.34
	HG	173.40 ± 24.69	221.30 ± 36.78	46.72 ± 3.76	125.50 ± 6.79	70.58 ± 4.59
SCT	LG	173.00 ± 7.96	154.40 ± 11.97	78.20 ± 7.38	89.02 ± 5.68	55.04 ± 2.99
	HG	177.5 ± 19.07	168.30 ± 18.27	75.88 ± 12.12	95.76 ± 5.83	57.30 ± 3.80
*Differentiation state difference		NS	NS	NS	*	*

Data are mean ± SEM (n=5/group). * denotes a differentiation state dependent difference in mitochondrial respiratory activity between BeWo CT and SCT cells. ¹Data are OCR/μg DNA; ²Data are % Basal OCR

Table 3-5 HG culture conditions do not impact BeWo trophoblast glycolytic activity

Differentiation State	Treatment	Basal glycolytic Rate ¹	Max Glycolytic Rate ¹	Reserve Glycolytic Capacity ²	Non-Glycolytic Acidification ¹
CT	LG	75.71 ± 15.38	101.4 ± 20.92	133.8 ± 1.14	19.26 ± 4.43
	HG	67.54 ± 7.30	88.23 ± 11.82	129.5 ± 4.08	18.38 ± 3.10
SCT	LG	69.21 ± 12.67	84.45 ± 14.55	123.5 ± 3.70	20.50 ± 3.39
	HG	77.38 ± 6.78	88.01 ± 8.17	113.6 ± 1.45	23.30 ± 2.45
*Differentiation state difference		NS	NS	*	NS

Data are mean ± SEM (n=5/group). * denotes a differentiation state dependent difference in glycolytic activity between BeWo CT and SCT cells. ¹Data are ECAR/μg DNA; ²Data are % Basal Glycolysis

3.3.3 The impact of high glucose and syncytialization upon BeWo ETC complex protein abundance and activity

High glucose levels did not impact protein abundance of ETC complex subunits in BeWo trophoblasts (**Figure 3-5 A-E**; n=4-5/group). Likewise, the HG-culture conditions did not affect ETC complex I or II activity in BeWo trophoblasts (**Table 3-6**, n=6/group).

However, BeWo syncytialization was associated with reduced ETC complex IV Cytochrome c oxidase subunit II (COXII) relative protein abundance in both LG and HG cultures (**Figure 3-5 D**; $p < 0.05$). Additionally, BeWo SCT cells displayed reduced activity of ETC complex II compared to CT cells independent of culture glucose level (**Table 3-6**; $p < 0.001$).

3.3.4 Metabolic enzyme activity and HG-cultured BeWo trophoblasts

BeWo SCT cells displayed increased activity of the PDH-E1 subunit compared to BeWo CT cells regardless of glucose level (**Table 3-6**; $p < 0.01$, n=6/group). Additionally, high glucose levels did not impact the activities of the PDH-E1 subunit, citrate synthase or lactate dehydrogenase (LDH) in BeWo CT and SCT cells (**Table 3-6**, n=5-6/group). Syncytialization additionally did not affect the enzyme activities of CS or LDH in BeWo trophoblasts (**Table 3-6**).

Table 3-6 Syncytialization but not HG-culture media impacts BeWo metabolic enzyme activity and individual ETC complex activity

Differentiation State	Treatment	Citrate Synthase	ETC complex I	ETC complex II (U/mg protein)	Lactate Dehydrogenase	PDH-E1 subunit
CT	LG	0.0126 ± 0.0034	0.0354 ± 0.0040	0.0470 ± 0.0036	2.821 ± 0.277	0.0046 ± 0.0006
	HG	0.0134 ± 0.0033	0.0413 ± 0.0052	0.0448 ± 0.0039	3.095 ± 0.391	0.0041 ± 0.0005
SCT	LG	0.0080 ± 0.0020	0.0722 ± 0.0208	0.0321 ± 0.0035	3.589 ± 0.312	0.0090 ± 0.0012
	HG	0.0070 ± 0.0015	0.0709 ± 0.0217	0.0330 ± 0.0039	3.504 ± 0.359	0.0098 ± 0.0014
*Differentiation state difference		NS	NS	*	NS	*

Data are mean ± SEM (n=5-6/group). * denotes a differentiation state dependent difference in enzyme activity between BeWo CT and SCT cells.

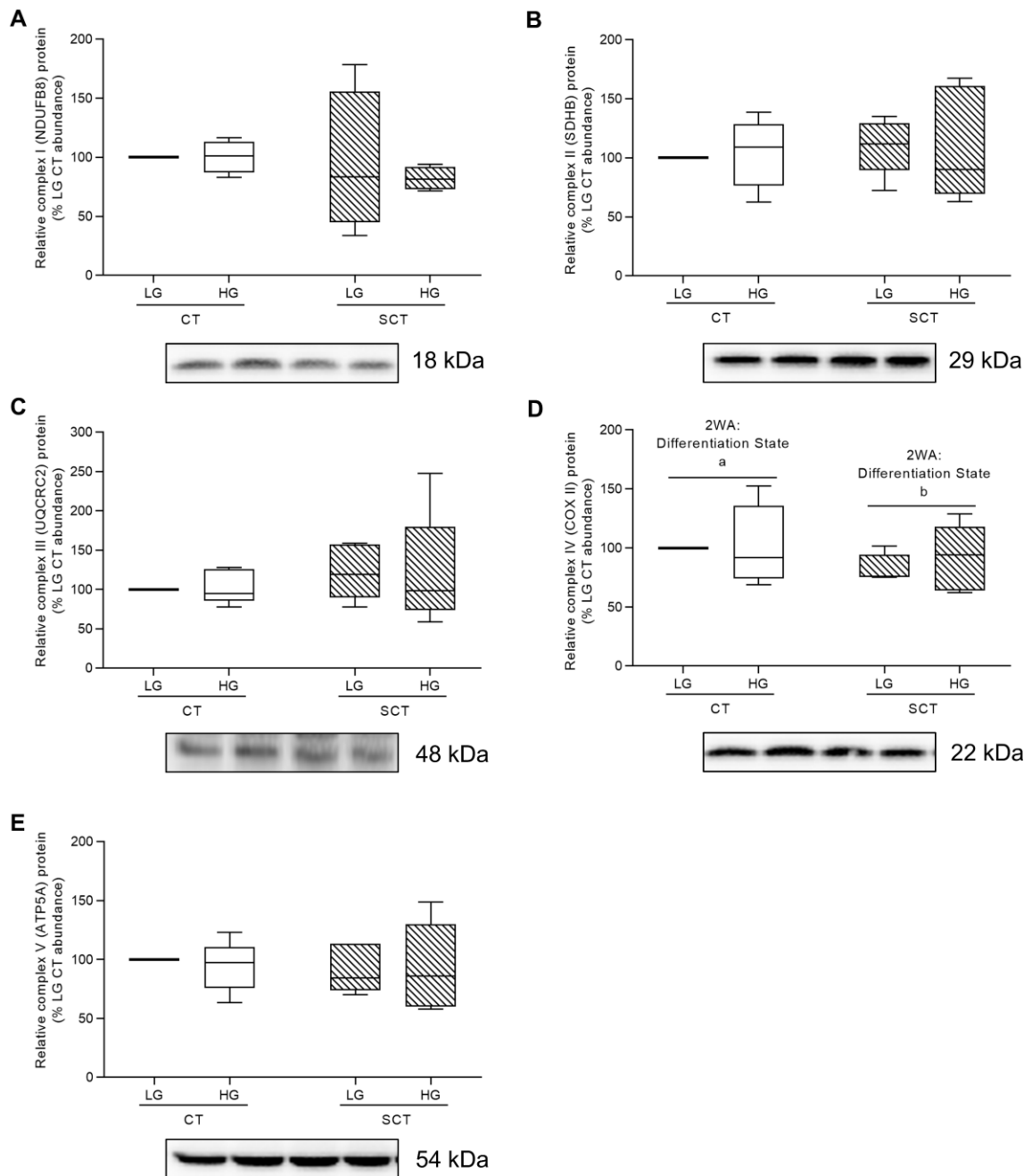


Figure 3-5 Hyperglycemic (HG) culture conditions do not impact protein expression of Electron Transport Chain (ETC) complexes in BeWo trophoblasts.

Relative protein abundance of (A) complex I (NDUFB8 subunit) (B) complex II (SDHB subunit) (C) complex III (UQCRC2 subunit) (D) complex IV (COX II subunit), and (E) complex V (ATP5A subunit) of the ETC in HG-cultured BeWo trophoblasts. Different lower-case letters denote differentiation state-dependent differences in ETC complex protein abundance (n=4-5/group; Two-Way Randomized Block ANOVA (2WA)). ETC complex protein band density was normalized to total lane protein (ponceau) for statistical analysis and the data is presented as percent of LG CT protein abundance for visualization. Full-length representative western blot images are available in **Supplementary Figure 2** (doi.org/10.5683/SP3/XMPKOK).

3.3.5 HG-cultured BeWo trophoblast mitochondrial fission and fusion dynamics

Regardless of glucose level BeWo SCT cells displayed increased relative protein abundance of the mitochondrial fission marker DRP1 in conjunction with decreased relative protein levels of the mitochondrial fusion marker OPA1 compared to progenitor BeWo CT cells (**Figure 3-6 A,C**; $p < 0.05$, $n = 5/\text{group}$).

HG culture conditions additionally did not impact total protein abundance of OPA1 and DRP1 in BeWo trophoblasts (**Figure 3-6 A,C**; $p > 0.05$). However, there was a trend towards increased pSER⁶¹⁶ phosphorylation of DRP1 in HG-cultured BeWo trophoblasts (**Figure 3-6 B**; $p = 0.0632$, $n = 5/\text{group}$) as well as reduced pSER⁶¹⁶ DRP1 phosphorylation in syncytialized BeWo trophoblasts (**Figure 3-6 B**; $p = 0.0924$).

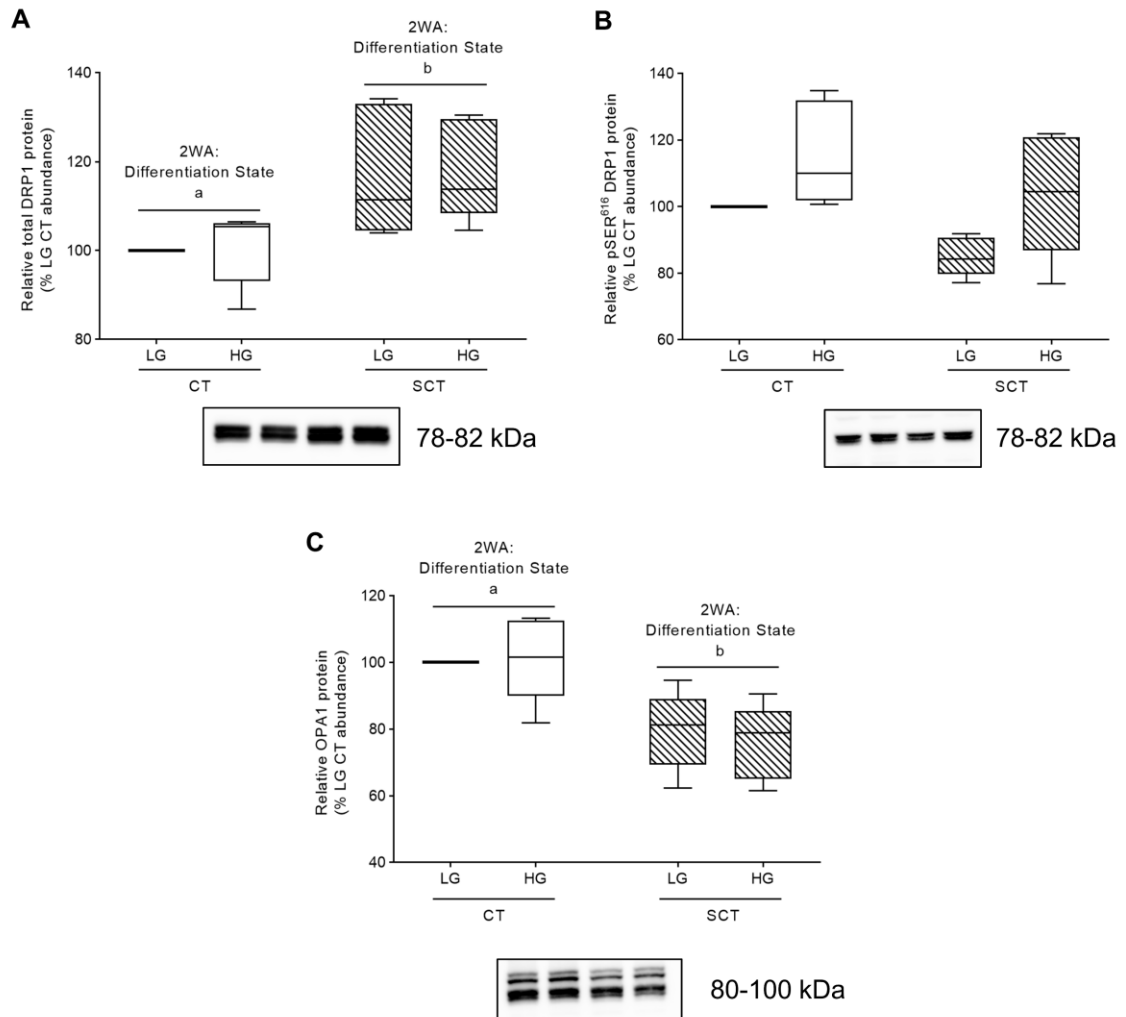


Figure 3-6 Syncytialization impacts mitochondrial dynamics in BeWo trophoblasts.

Relative protein abundance of (A) total DRP1 (B) pSER⁶¹⁶ DRP1 (C) OPA1 in HG and LG cultured BeWo trophoblasts. Different lower-case letters denote differentiation state-dependent differences in relative protein abundance (n=5/group; Two-Way Randomized Block ANOVA (2WA)). Protein band density was normalized to total lane protein (ponceau) for statistical analysis and the data is presented as percent of LG CT abundance for visualization. Uncropped representative western blot images are available in **Supplementary Figure 3** (doi.org/10.5683/SP3/XMPKOK).

3.3.6 HG culture conditions impact glycogen storage in BeWo trophoblasts

HG culture conditions in both BeWo CT and SCT cells increased cellular glycogen content compared to respective differentiation state LG cultures (**Figure 3-7 A**; $p < 0.0001$; $n = 4/\text{group}$). Furthermore, the glycogen content in BeWo CT cultures was greater than that of the SCT cultures (**Figure 3-7 A**; $p < 0.0001$). In addition, BeWo SCT cells displayed increased GLUT1 protein abundance compared to BeWo CT cells (**Figure 3-7 B**; $p < 0.05$), however, no glucose-dependent impacts to GLUT1 protein abundance were observed.

However, HG culture conditions reduced relative glycogen synthase protein abundance in both BeWo CT and SCT cells (**Figure 3-7 C**; $p < 0.05$, $n = 5/\text{group}$). HG cultured BeWo CT and SCT cells subsequently displayed increased relative abundance of phosphorylated (pSer⁶⁴¹) glycogen synthase (**Figure 3-7 D**; $p < 0.01$, $n = 5/\text{group}$), and differentiated BeWo SCT cells displayed increased phosphorylated (pSer⁶⁴¹) glycogen synthase levels relative to CT cultures (**Figure 3-7 D**; $p < 0.01$, $n = 5/\text{group}$).

Furthermore, differentiated BeWo SCT cells were found to have increased protein levels of both Glycogen synthase kinase 3 beta (GSK3 β) and phosphorylated (pSer⁹) GSK3 β relative to BeWo CT cultures (**Figure 3-7 E-F**; $n = 5/\text{group}$). However, HG culture conditions were not associated with alterations in the relative protein abundance of GSK3 β and phosphorylated (pSer⁹) GSK3 β (**Figure 3-7 E-F**; $p > 0.05$, $n = 5/\text{group}$).

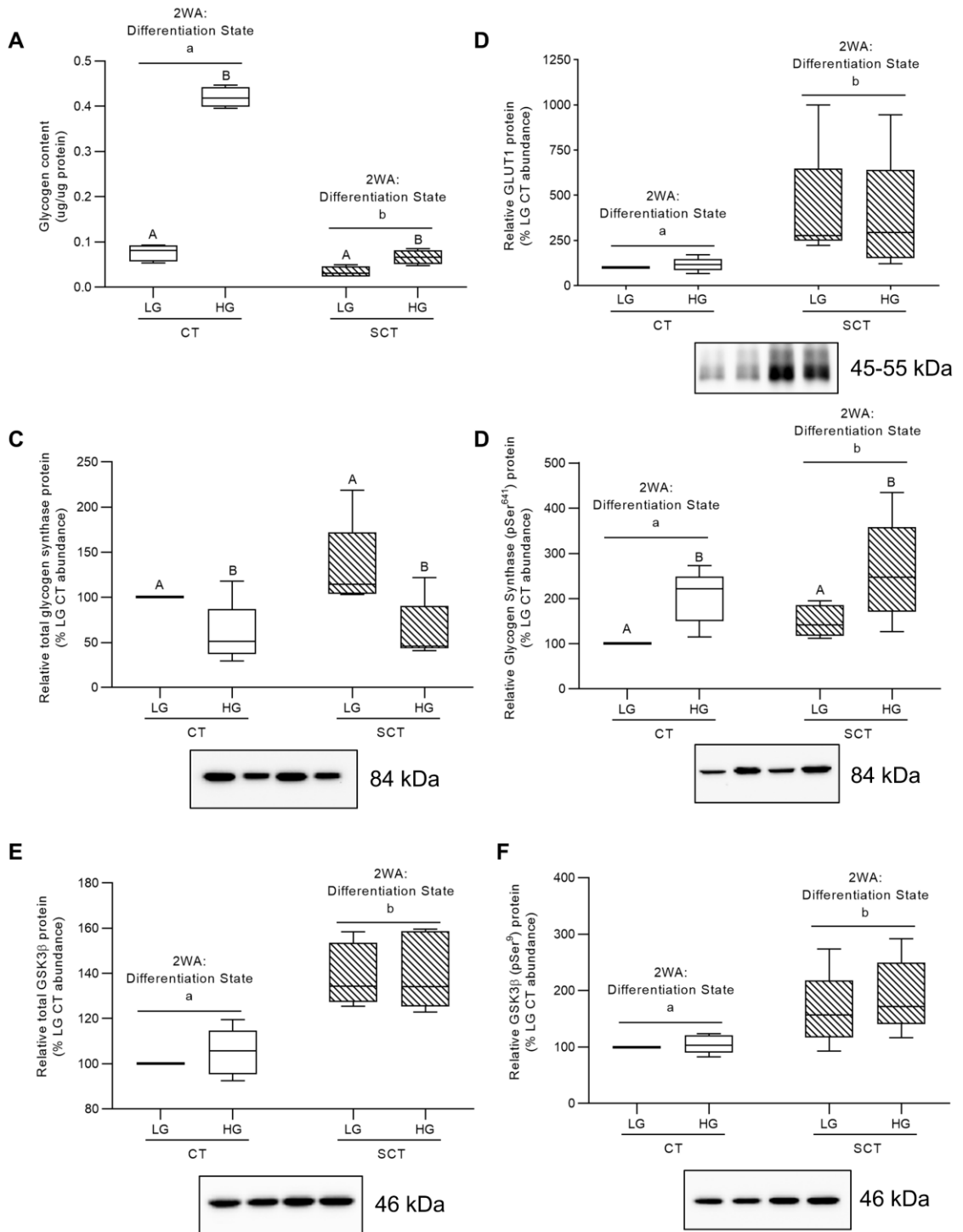


Figure 3-7 Hyperglycemic (HG) culture conditions impact glycogen storage and regulation in BeWo trophoblasts.

(A) Glycogen content and relative protein abundance of (B) GLUT1 (C) glycogen synthase; (D) pSer⁶⁴¹ glycogen synthase; (E) GSK3 β ; (F) pSer⁹ GSK3 β in HG-treated BeWo trophoblasts at T72H. Different lower-case letters denote differentiation state-dependent differences in protein abundance, and different upper-case letters denote glucose-level dependent differences within a differentiation state (Randomized-Block Two-Way ANOVA (2WA), and Sidak's multiple comparisons test, $p < 0.05$). Glycogen content data are presented as protein normalized glycogen abundance (μg glycogen per μg protein; $n=4/\text{group}$). Protein band density was normalized to total lane protein (ponceau) for statistical analysis and the data is presented as percent of LG CT abundance for visualization ($n=5/\text{group}$). Uncropped representative western blot images are available in **Supplementary Figure 3** (doi.org/10.5683/SP3/XMPKOK).

3.3.7 HG culture conditions increases TG abundance in BeWo CT cells

HG culture conditions were associated with increased triglyceride accumulation in BeWo CT cells, but not in BeWo SCT cells (**Figure 3-8 A**; $p < 0.01$, $n = 4/\text{group}$). Furthermore, BeWo syncytialization and HG culture conditions did not impact the relative abundance of ACSL1 protein, although there was a trend towards increased expression in both differentiated BeWo SCT cells and in HG-treated BeWo trophoblasts (**Figure 3-8 B**; 2WA: glucose level $p = 0.0894$; 2WA: differentiation state $p = 0.0695$, $n = 5/\text{group}$). Finally, syncytialization and HG culture conditions did not impact the relative abundance of fatty acid synthase (FASN) in BeWo trophoblasts (**Figure 3-8 C**).

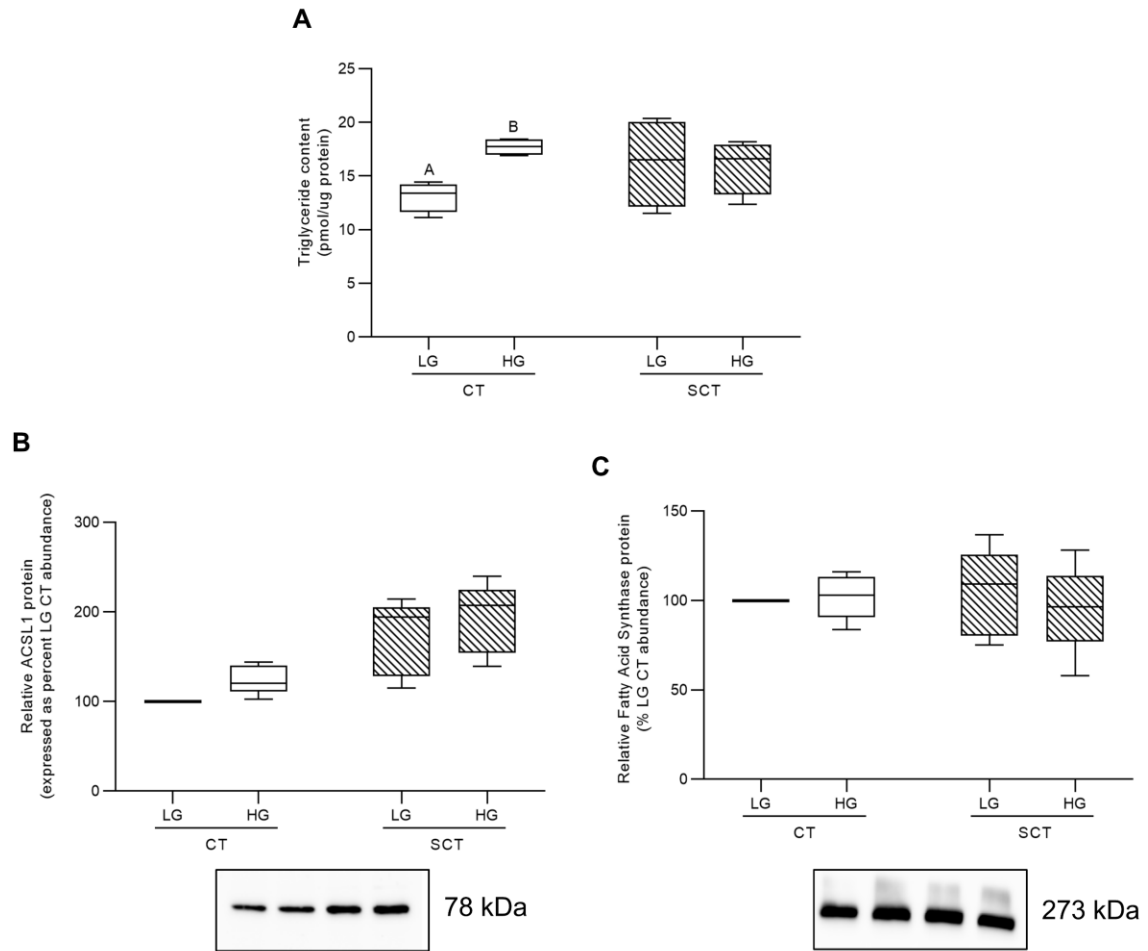


Figure 3-8 Hyperglycemic (HG) culture conditions impact triglyceride content in BeWo CT cells.

(A) Triglyceride content and relative protein abundance of (B) ACSL1, and (C) FASN in HG-treated BeWo trophoblasts at T72H relative abundance. Different upper-case letters denote differences between LG and HG treatments within each respective differentiation state (Two-Way Randomized Block ANOVA; Sidak's multiple comparisons test, $p < 0.05$). TG content data is presented as protein normalized TG abundance (pmol TG per μg protein; $n=4/\text{group}$). Protein band density was normalized to total lane protein (ponceau) for statistical analysis and the data is presented as percent of LG CT abundance for visualization ($n=5/\text{group}$). Uncropped representative western blot images are available in **Supplementary Figure 3** (doi.org/10.5683/SP3/XMPKOK).

3.3.8 Transcriptomic profiling of HG-cultured BeWo CT cells

HG-cultured BeWo CT cells displayed 197 differentially expressed genes (75 upregulated, 122 down-regulated) compared to LG BeWo CT cells ($\geq \pm 1.3$ FC vs LG CT; raw-p < 0.05, n=5/group). A summary of the differentially expressed genes between LG and HG-cultured BeWo CT cells is available in **Supplementary Table 1** (doi.org/10.5683/SP3/XMPKOK). A 3D principal component analysis (PCA) plot (**Figure 3-9 A**), volcano plot (**Figure 3-9 B**) and 2D hierarchical clustering heatmap (**Figure 3-10**) were constructed to visualize the degree of gene expression differences between LG and HG cultured BeWo CT cells.

At the FC cut-offs selected, the differentially expressed genes were not associated with significant enrichment in gene ontology (GO) biological processes (**Figure 3-11 A**). Functional pathway analysis with WikiPathways revealed that the Overview of Nanoparticle Effects Pathway was significantly enriched in the HG-cultured BeWo CT cells (**Figure 3-11** ; FDR < 0.05). The differentially expressed genes involved in this pathway were: *CCND3* (-1.41 FC), *IL6* (-1.39 FC), *PTGS1* (-1.31 FC), and *PTK2* (-1.40 FC).

As there were no enriched metabolism-related pathways, individual differentially expressed genes involved in cellular metabolic processes were individually identified and selected for validation via RT-qPCR. Specifically, *ACSL1*, *RPS6KA5*, *HSD11B2*, *HK2* and *SLC27A2* were selected for validation (**Figure 3-11 C**, n=8/group). The altered expression of *ACSL1* (+1.36 FC in the microarray; +1.369 FC in the RT-qPCR validation); *RPS6KA5* (+1.32 FC in the microarray; +1.304 FC in the RT-qPCR validation); and *HSD11B2* (+1.35 FC in the microarray; +1.463 FC in the RT-qPCR validation) in HG-cultured BeWo CT cells were validated via RT-qPCR. (**Figure 3-11 C**) While not significant, the expression of *HK2* was found slightly reduced in HG BeWo CT cultures via RT-qPCR (-1.152 FC vs LG BeWo CT cells). The differential expression of *SLC27A2* in HG-cultured BeWo CT cells could not be validated via RT-qPCR (**Figure 3-11 C**).

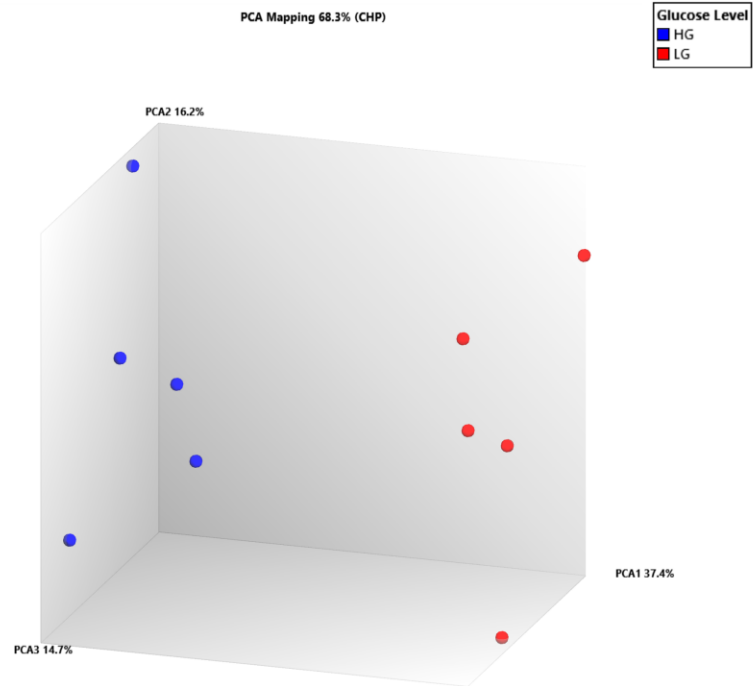
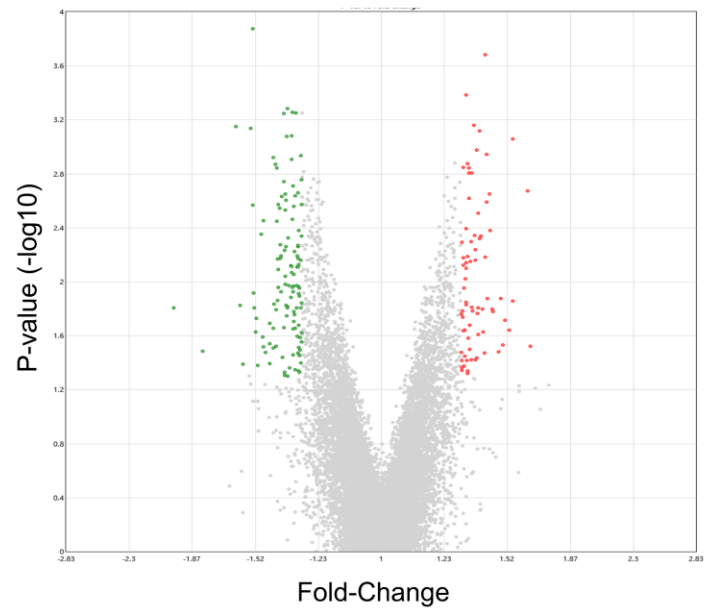
A**B**

Figure 3-9 Principal Component Analysis (PCA) and volcano plot visualization of differentially expressed genes between low-glucose (LG) and hyperglycemic (HG) cultured BeWo CT cells.

(A) An unsupervised PCA plot was constructed to visualize the degree of separation in transcriptomic profiles between LG (red dots) and HG (blue dots) cultured BeWo CT cells

(B) The volcano plot was generated to visualize differentially expressed genes in HG-cultured BeWo CT cells ($\geq \pm 1.3$ fold-change, $p < 0.05$, $n = 5/\text{group}$). The x-axis indicated fold-changes vs LG BeWo CTs, and the y-axis indicates the p-value ($-\log_{10}$). The green dots represent statistically significant down-regulated genes, and the red dots represent statistically significant upregulated genes in HG-cultured BeWo CT cells.

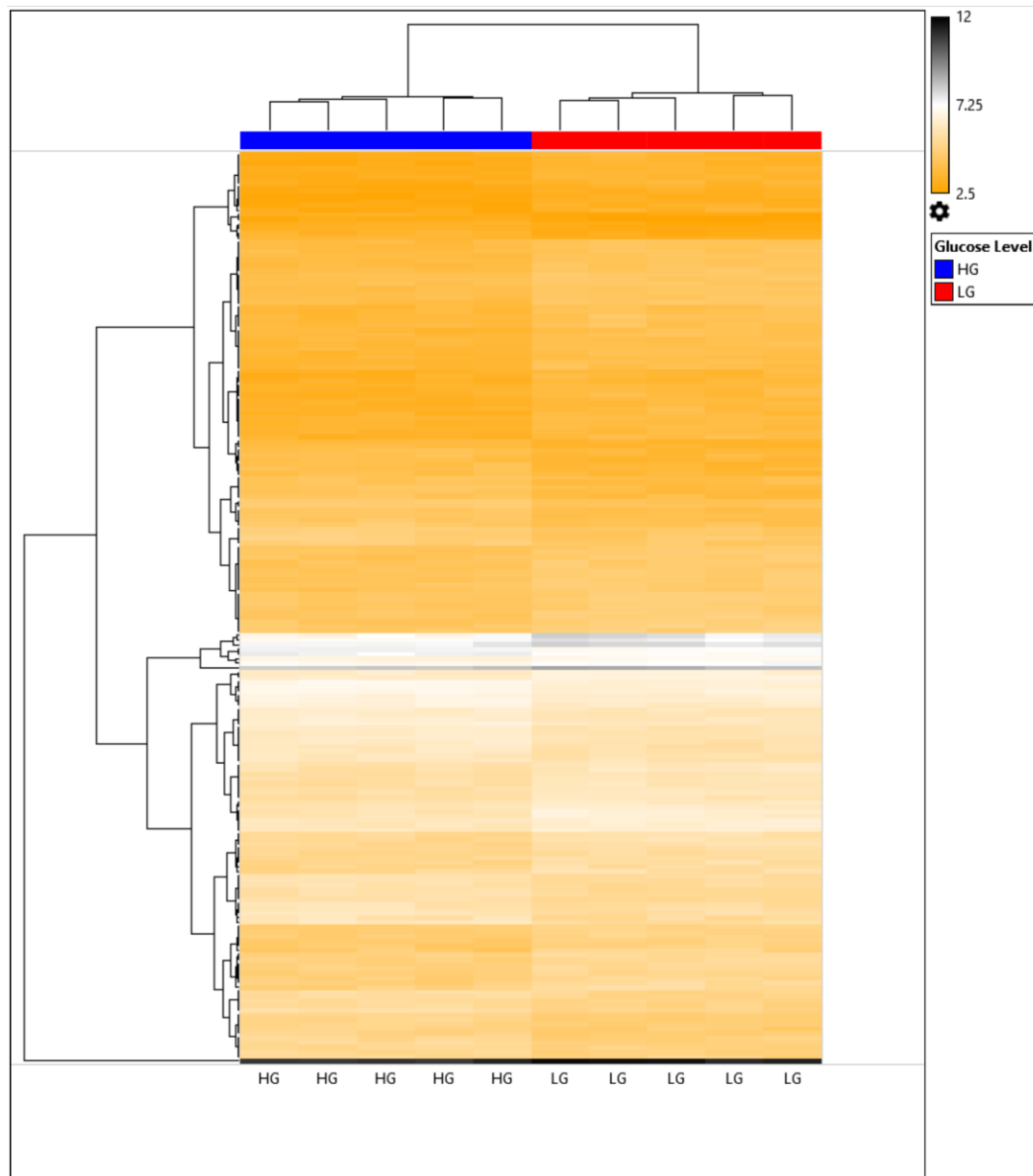


Figure 3-10 Heat map visualization of differentially expressed genes in hyperglycemic (HG) cultured BeWo CT cells.

Each column of the heat map represents an individual sample, with blue columns representing HG-cultured BeWo CT cells and the red columns representing low-glucose (LG) cultured BeWo CT cells. Each row represents an individual differentially expressed gene. Gene expression intensity is color coded with orange representing low-expression genes and black representing high-expression genes.

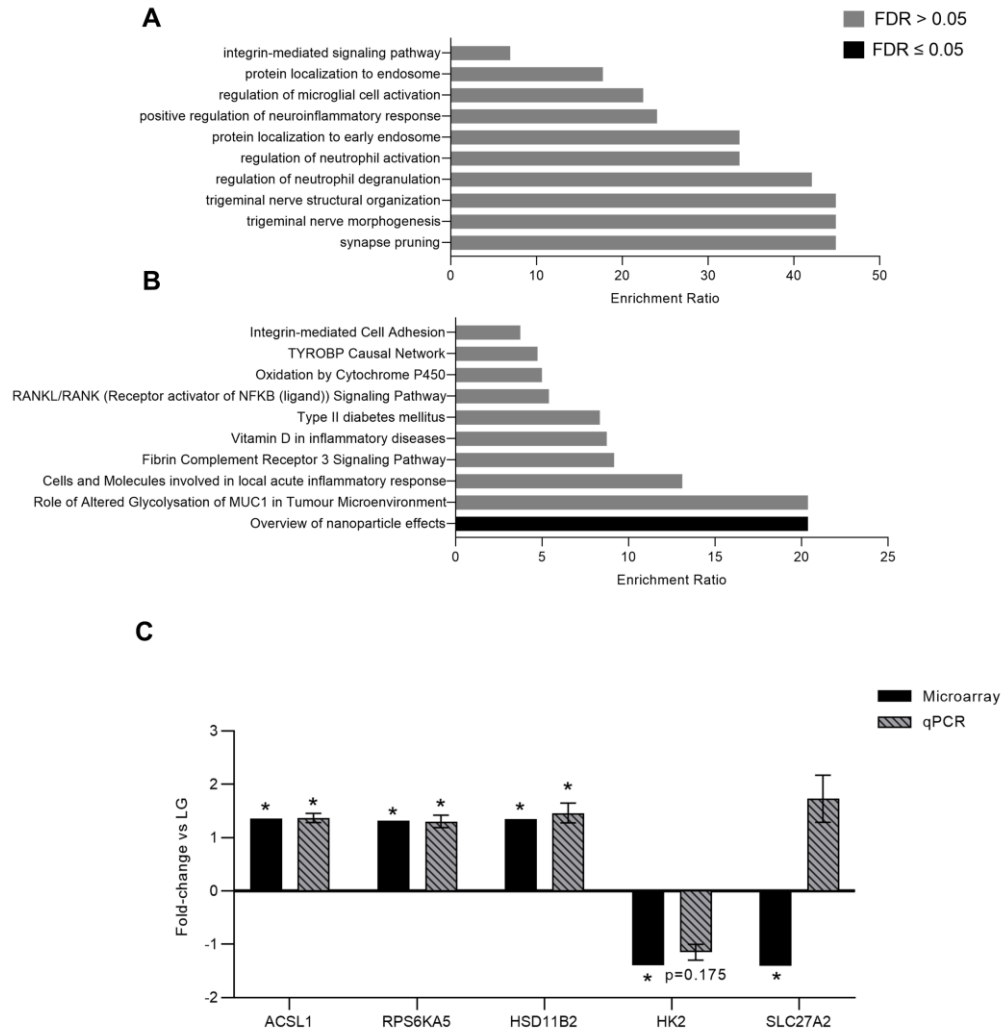


Figure 3-11 Pathway analysis of differentially expressed genes and RT-qPCR validation of microarray gene changes.

Webgestalt was utilized to examine significantly enriched pathways of the differentially expressed genes identified in the Clariom S mRNA microarray. **(A)** Top 10 Geneontology biological pathways and **(B)** top 10 Wikipathways functional pathways enriched in the differentially expressed genes. Black bars represent significantly enriched pathways (FDR $p < 0.05$) and grey bars represent pathways that were not significantly enriched in the gene set (FDR $p > 0.05$). **(C)** RT-qPCR was utilized to validate differentially expressed genes identified in the microarray. Data was analyzed via paired t-test ($n=8/\text{group}$), and data expressed as fold-change vs LG BeWo CT (mean \pm SEM). Down-regulated genes ratios were inversed and expressed as a negative (e.g 0.5-fold is expressed as a minus-2 fold-change).

3.3.9 Impacts of HG culture conditions on the metabolome of BeWo CT cells

On average 6541 ± 42 (mean \pm SD) metabolite peak pairs were measured in each sample. A summary of the metabolites identified in all tiers, and LG and HG-cultured BeWo CT cell metabolite peak-pair data is available in **Supplementary Table 2** (doi.org/10.5683/SP3/XMPKOK). Of these peak pairs, 179 were positively identified in tier 1 and 602 peak pairs were identified with high confidence in tier 2. Of these identified peak pairs, 7 from tier 1 and 116 from tier 2 were found to be differentially abundant ($\geq \pm 1.5$ FC, raw- $p < 0.05$, $n = 5$ /group) between HG and LG cultured BeWo CT cells. A list of all differentially abundant metabolites between LG and HG-cultured BeWo CT cells is available in **Supplementary Table 3** (doi.org/10.5683/SP3/XMPKOK).

The degree of differences in metabolite profiles between HG and LG-cultured BeWo CT cells was visualized by unsupervised principal component analysis (PCA) plot as well as supervised partial least squares discriminant analysis (PLS-DA) scores plot (**Figure 3-12 A,B**). Differentially abundant metabolites were subsequently visualized via volcano plot and heat map (**Figure 3-13 A,B**).

Pathway analysis revealed that the glycolysis/gluconeogenesis (highlighted by significantly increased lactate levels, and significantly decreased acetaldehyde levels); pyruvate metabolism (highlighted by increased lactate (+2.72 FC) levels, and decreased acetaldehyde (-1.20 FC) levels); drug metabolism – cytochrome P450 (highlighted by increased 2-hydroxyiminostilbene (+2.52 FC) and 3-carbamoyl-2-phenylpropionic acid (+5.42 FC) levels); ascorbate and aldarate metabolism (highlighted by increased L-gulonolactone (+2.46 FC) levels); riboflavin metabolism (highlighted by increased riboflavin (+3.68 FC) levels); fatty acid biosynthesis (highlighted by increased malonate (+3.74 FC) levels); as well as synthesis and degradation of ketone bodies (highlighted by increased (R)-3-hydroxybutanoate (+1.60 FC) levels) pathways were significantly enriched in HG-cultured BeWo CT cells (FDR-corrected $p < 0.05$). A scatterplot of the pathway nodes and summary of the differentially abundant metabolites within each pathway is available in **Figure 3-14**.

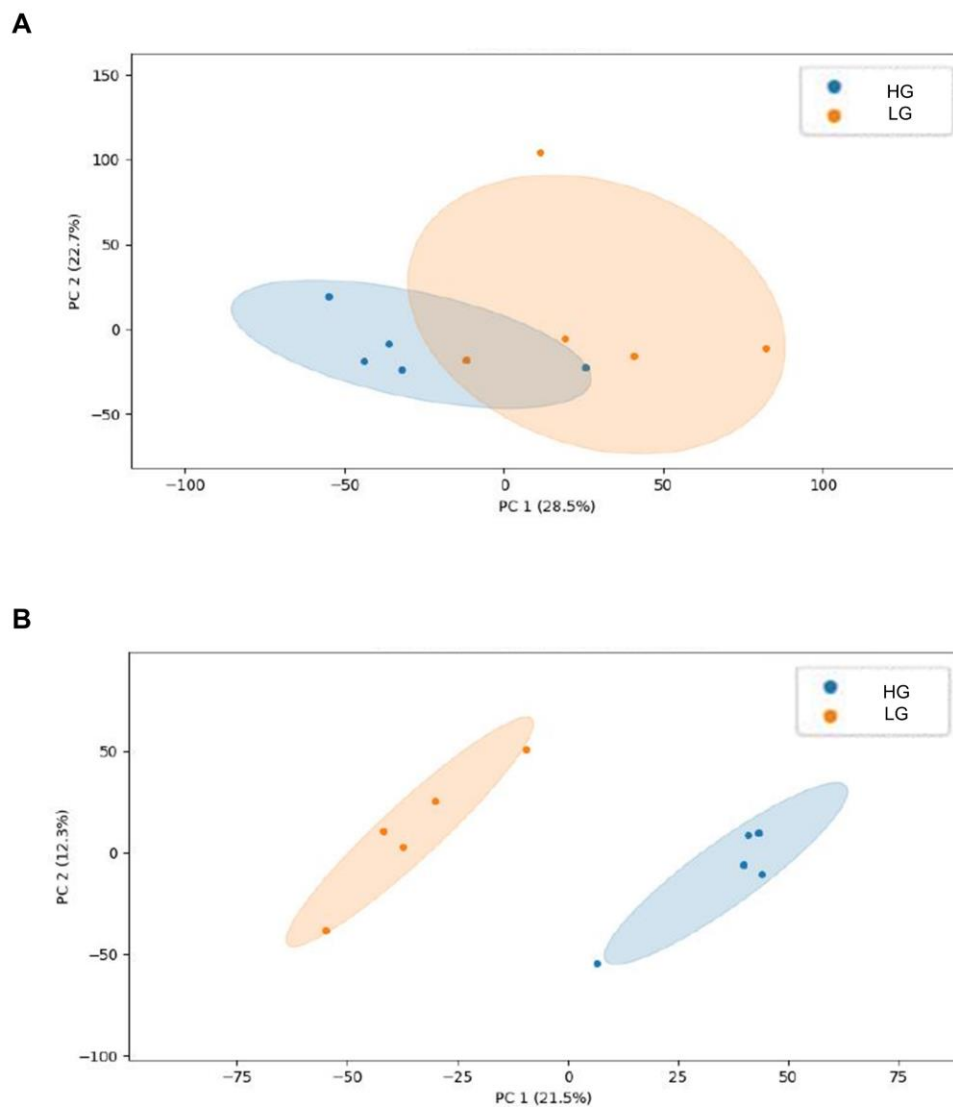


Figure 3-12 Visualization of the degree of separation between metabolite profiles in HG and LG cultured BeWo CT cells.

(A) Unsupervised principal component analysis (PCA) and (B) supervised partial least squares discriminant analysis (PLS-DA) plots were constructed to visualize the separation in metabolite concentrations between LG (orange dots) and HG-cultured (blue dots) BeWo CT cells.

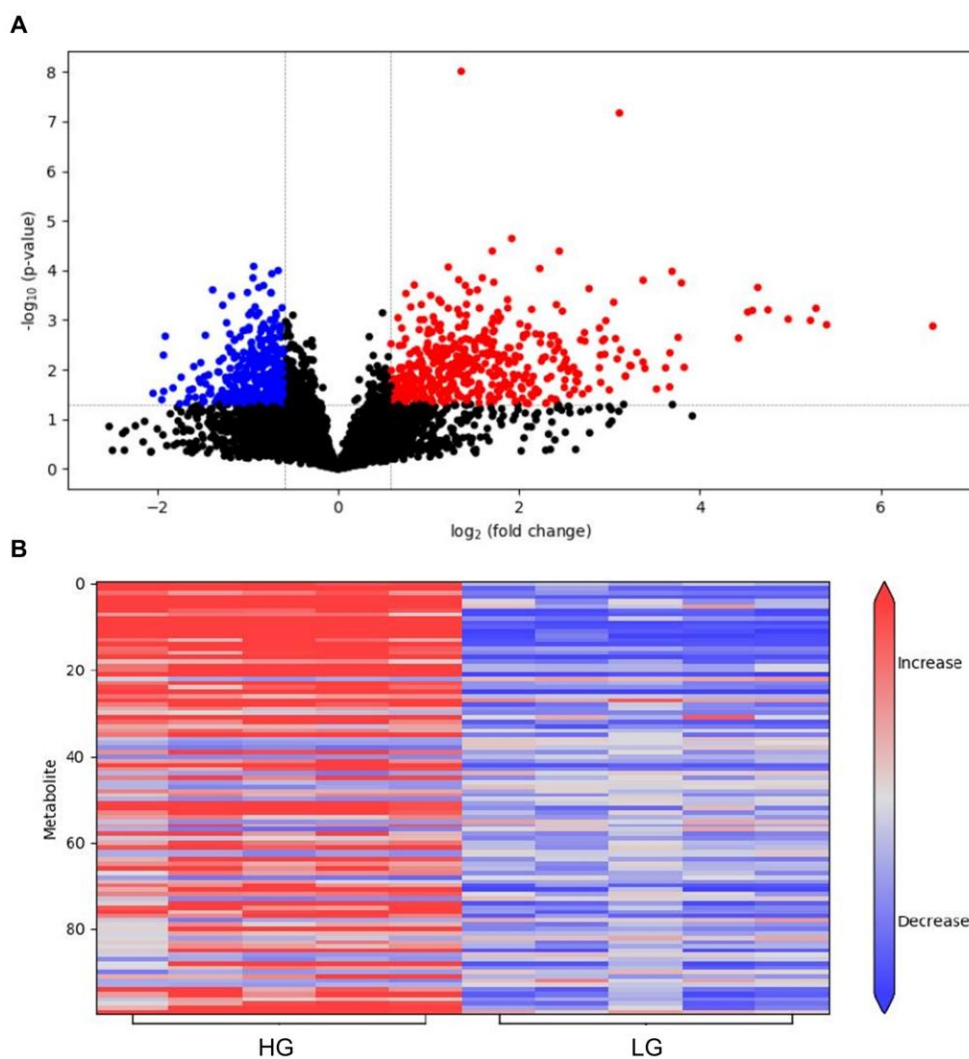


Figure 3-13 Visualization of differentially abundant metabolites in HG-cultured BeWo CT cells.

(A) Volcano plot visualizing differentially abundant metabolites in HG-cultured BeWo CT cells ($\geq \pm 1.5$ fold-change, raw- $p < 0.05$, $n = 5/\text{group}$). The x-axis indicated $\log_2(\text{fold-change})$ vs LG BeWo CTs, and the y-axis indicates the p-value ($-\log_{10}$). The red dots represent significantly increased metabolites, and the blue dots represent significantly decreased metabolites in HG-cultured BeWo CT cells. (B) heat map visualizing the top-100 (by p-value) differentially abundant metabolites in HG-cultured BeWo CT cells. Each column represents a different sample, and each row represents an individual differentially abundant metabolite. Metabolite abundance was color coded with red representing increased metabolite abundance and blue representing decreased metabolite abundance.

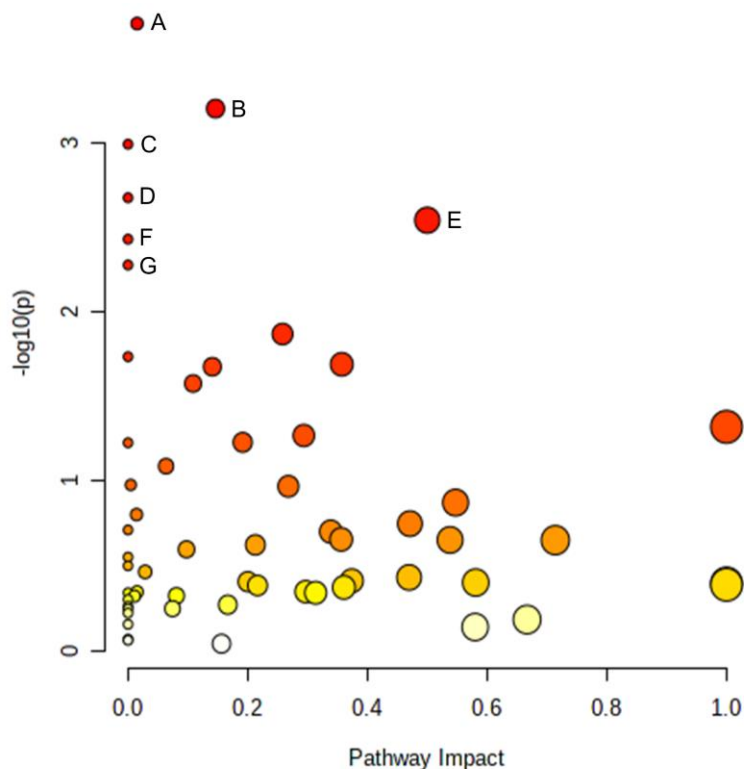


Figure 3-14 Pathway analysis of metabolites identified in tiers 1 and 2.

Identified peak pairs from tiers 1 and 2 were imported into MetaboAnalyst v5.0 for analysis of enriched KEGG pathways. A scatterplot was created to visualize identified pathways with pathway impact (ratio of identified metabolites to total metabolites in the pathway) on the x-axis and p-value ($-\log_{10}$) on the y-axis. Pathways with a false discovery rate $p < 0.05$ were determined to be significant and were labelled with uppercase letters. The (A) Glycolysis/Gluconeogenesis, (B) Pyruvate Metabolism, (C) Drug Metabolism – Cytochrome P450, (D) Ascorbate and Aldarate Metabolism, (E) Riboflavin Metabolism, (F) Fatty Acid Biosynthesis, and (G) Synthesis and Degradation of Ketone Bodies pathways were significantly enriched in HG-cultured BeWo CT cells.

3.3.10 Impacts of HG culture conditions of the lipidome profiles of BeWo CT cells.

On average 9406 ± 77 (mean \pm SD) lipid species peak pairs were identified in the LG and HG-treated BeWo CT cells. Of these features, 950 were positively identified in Tier 1, and 161 were identified with high confidence in Tier 2. An additional 6808 features were putatively identified in Tier 3. A summary of the lipid class types identified in the lipidome readouts, and their abbreviations is available in **Supplementary Table 4** (doi.org/10.5683/SP3/XMPKOK). A summary of the identified lipid species in tiers 1, 2 and 3 and the peak-pair data for LG and HG-cultured BeWo CT cells is available in **Supplementary Table 5** (doi.org/10.5683/SP3/XMPKOK).

Overall, 131 lipid species were identified as significantly increased and 49 as significantly decreased in HG-cultured BeWo CT cells ($\geq \pm 1.5$ FC vs LG; raw p-value < 0.05 , n=5/group). An unsupervised Principal Component Analysis (PCA) 2D scores plot as well as a supervised partial-least squares discriminant analysis (PLS-DA) 2D plot were constructed to visual the degree of separation in lipidome profiles between LG and HG-culture BeWo CT cells (**Figure 3-15**). Additionally, a volcano plot was constructed to visualize the differentially abundant lipid species in the hyperglycemia exposed BeWo CT cells (**Figure 3-16**). A summary of the differentially abundant lipid species in HG-cultured BeWo CT cells is available in **Supplementary Table 6** (doi.org/10.5683/SP3/XMPKOK).

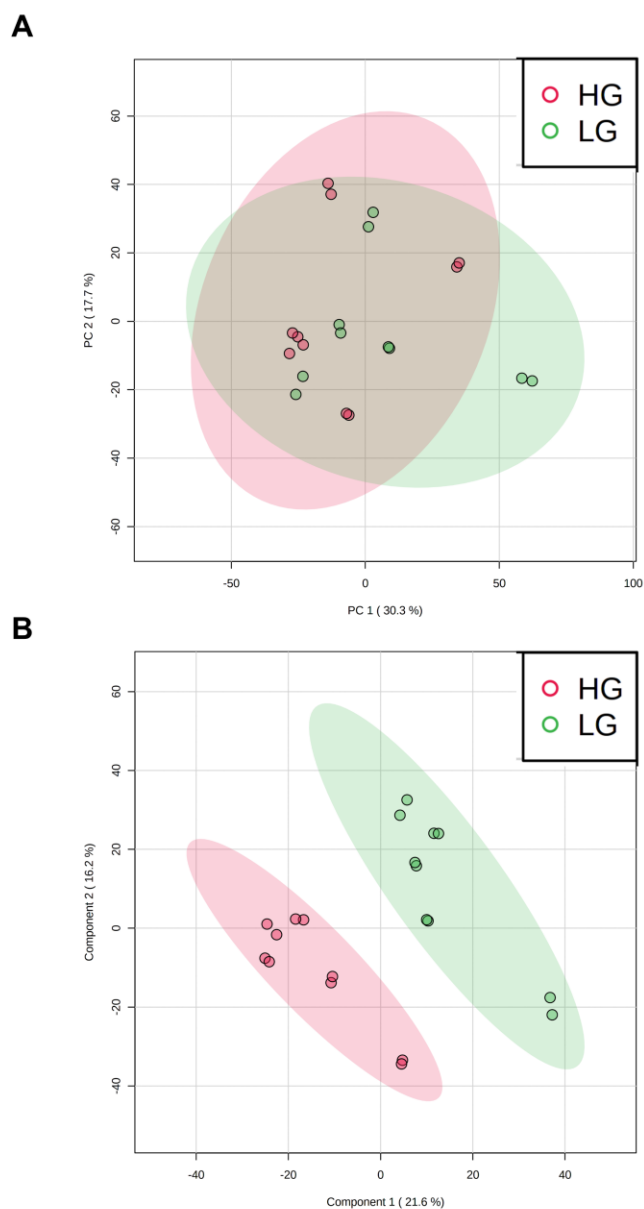


Figure 3-15 Multivariate visualization of the degree of separation in lipidome profiles between LG and HG-cultured BeWo CT cells.

(A) Unsupervised principal component analysis (PCA), and (B) supervised partial least squares-discriminant analysis (PLS-DA) plots were constructed to visualize the difference in lipidome profiles between LG (green dots) and HG (red dots) cultured BeWo CT cells.



Figure 3-16 Volcano plot visualization of differentially abundant lipid species in HG-cultured BeWo CT cells.

A volcano plot was constructed to visualize the differentially abundant lipid species in HG-cultured BeWo CT cells ($\geq \pm 1.5$ fold-change, raw- $p < 0.05$, $n = 5/\text{group}$). The x-axis indicated $\log_2(\text{fold-change})$ vs LG BeWo CT, and the y-axis indicates the p-value ($-\log_{10}$). The red dots represent significantly increased lipid species, and the blue dots represent significantly decreased lipid species in HG-cultured BeWo CT cells.

3.4 Discussion

The current study aimed to expand upon current published literature [22,30,31,34] and explore the independent impacts of hyperglycemia on placental trophoblasts in more depth by characterizing nutrient storage and mitochondrial respiratory activity in BeWo trophoblasts following a relatively prolonged 72-hour HG-exposure (25 mM glucose). While previous studies utilizing BeWo trophoblasts have specifically highlighted the impacts of high glucose exposure on progenitor CT cells [30,31,34] the current study is strengthened through the combined examination of both CT cells and differentiated SCT cells as well as by the use of functional readouts of metabolic and mitochondrial activity. The more chronic 72-hour culture protocol as utilized in this study allowed for exposure of villous trophoblast cell populations to hyperglycemia prior to and during differentiation, analogous to *in vivo* villous trophoblast layer development whereby progenitor CT cells are exposed to dietary nutrients prior to and during syncytialization. Subsequently, the current study utilized a multi-omics research approach and described altered transcriptomic, metabolomic, and lipidomic signatures in HG-exposed BeWo CT cells, that further described the glucose-mediated alterations to placental metabolic function. Overall, the data presented in this study demonstrated that a 72-hour exposure to hyperglycemia, while sufficient to modulate transcriptomic and metabolomic signatures as well as increase triglyceride and glycogen nutrient stores in BeWo trophoblast cells, is not associated with direct impairments in mitochondrial respiratory activity.

3.4.1 Hyperglycemia and nutrient stores in BeWo trophoblasts

As previously highlighted, DM during pregnancy is associated with aberrant nutrient storage in the villous trophoblast layer of the placenta [18–23]. Our results demonstrated that HG-culture conditions directly facilitate increased glycogen content in both BeWo CT and SCT cells, and additionally that CT cells have a greater glycogen storage potential than SCT cells. It is important to note that these differentiation state-dependent trends in glycogen content are consistent with previous reports from primary human placental tissue which described that glycogen storage predominately occurs within the CT cells of the placenta [24,48,49]. Increased glycogen abundance in diabetic

placentae has been thought to be a mechanism by which the placenta limits materno-fetal glucose transfer in times of nutrient overabundance to limit fetal overgrowth [24,25]. However, we speculate that the increased glycogen stores observed in the BeWo trophoblast cells also functions to limit the pool of glucose available for glycolysis and subsequent mitochondrial oxidation and in turn acts to protect trophoblast mitochondria from glucose-mediated oxidative damage.

High-glucose exposure in both BeWo CT and SCT cells was also associated with reduced relative protein abundance of glycogen synthase as well as with increased inhibitory Ser⁶⁴¹ phosphorylation [50] of glycogen synthase. As there were no glucose-mediated differences in the protein abundance of GSK3 β or the inhibitory Ser⁹ phosphorylation [51] of GSK3 β , the increased inhibitory phosphorylation of glycogen synthase in HG-cultured BeWo trophoblasts likely occurs via a GSK3 β -independent mechanism. These data could suggest that increased glycogen levels in placental trophoblasts act via a negative feedback mechanism to prevent excessive glycogen accumulation by altering glycogen synthase protein abundance and post-translational modifications, as has previously been described [52]. Overall, these data suggested that following 72-hours of hyperglycemia BeWo trophoblast cells have a diminished capacity to store excess glucose as glycogen. Thus, we speculate that HG-cultured BeWo trophoblast cells are at risk of developing glucose-toxicity if the exposure is continued beyond our 72-hour timepoint.

In addition to increased glycogen stores, our study also demonstrated increased triglyceride content in BeWo CT in response to excess glucose exposure. These data were consistent with previous reports that have highlighted an increased accumulation of triglyceride species in placental explants from healthy pregnancies under high glucose conditions [22]. The current study further identified that there were no differentiation state-dependent differences in triglyceride abundance in BeWo trophoblast cells, similar to reports from freshly isolated villous trophoblast samples [53]. Readouts from primary placenta samples have highlighted that lipid esterification processes occur primarily within villous CT cells, and that lipid droplets present in primary SCT cells are likely remnants from esterification process that occurred prior to syncytialization [53]. We

speculate that a similar reduction in esterification activity also occurs in BeWo SCT cells and may explain the absence of a HG-mediated difference in triglyceride content in our BeWo SCT cells. Future studies utilizing functional readouts of lipid esterification activity may be needed to better elucidate the mechanisms underlying differences in TG abundance between BeWo CT cells and differentiated BeWo SCT cells.

Overall, these data suggest that hyperglycemia is an independent modulator of nutrient storage in trophoblast cells and highlights that increased glucose availability may be a direct mechanism underlying aberrant placental nutrient storage in diabetic pregnancies.

3.4.2 Hyperglycemia and metabolic function in BeWo trophoblasts

The current study demonstrated that cellular mitochondrial respiratory activity (measured by the Seahorse XF Mito Stress Test) as well as that the activities of ETC complex I and II are not impacted in BeWo trophoblasts cultured under hyperglycemia at 72H. Additional analysis of metabolic function via the Seahorse Glycolysis Stress Test and activity assays for LDH and CS enzymes further indicated that isolated hyperglycemia does not impact functional aspects of metabolism in BeWo trophoblasts. Overall, our data suggests that hyperglycemia alone may not directly facilitate the impairments in mitochondrial respiratory activity that have previously been observed in DM-exposed primary placental samples [27–29].

Previous studies in other cell preparations, however, have demonstrated that the impacts of HG-culture conditions on mitochondrial respiratory function are dependent on the length of high-glucose exposure. For example, human kidney tubule (HK-2) cells displayed reduced basal and maximal mitochondrial respiratory activity only when cultured under HG-conditions (25 mM) for at least 4 days [54]. In contrast, mitochondrial respiratory activity in kidney glomerular (HMC) cells was not impacted prior to 8 days of high glucose exposure [54]. Likewise, mitochondrial activity of human umbilical cord endothelial (EA.hy926) cells was not impaired after 3 days of high glucose (25 mM) treatment, but was reduced after 6 days of HG-culture conditions, and this impairment in mitochondrial function was sustained through 9 days of high glucose exposure [55].

Overall, these studies suggest that there are time-course dependent factors that influence whether hyperglycemia impacts cellular mitochondrial respiratory activity. Thus, the conclusions of the current study may be limited due to the single timepoint utilized for all analyses of metabolic function. It is possible that prolonging HG-culture conditions in BeWo trophoblasts could ultimately lead to impaired mitochondrial function, as was observed in EA.hy926 and HMC cells, and the impacts of a longer duration of high glucose treatment in BeWo cells may need to be explored in future investigations.

In addition to impairing mitochondrial respiratory activity in trophoblast cells, hyperglycemia negatively regulates mitochondrial function in some cell types through altering mitochondrial fusion (regulated by OPA1) and fission (regulated by DRP1) dynamics leading increased mitochondrial fractionation [56–59]. Increased mitochondrial fission is associated with increased cellular oxidative stress, and impaired insulin sensitivity, and ultimately mitochondrial respiratory dysfunction [60,61]. We observed a trend towards increased (mean 19% increase) pSER⁶¹⁶ phosphorylation of DRP1 (a post-translational modification associated with increased mitochondrial translocation of DRP1 and subsequently increased mitochondrial fission) in HG-cultured BeWo trophoblasts [62]. These post-translational modifications of DRP1, although non-significant, may indicate that important underlying aspects of trophoblast mitochondrial function are negatively regulated by hyperglycemia, even though global readouts of BeWo mitochondrial respiratory activity were not impacted. We speculate that this could indicate that the HG-cultured BeWo trophoblasts are at an early timepoint in a transition towards mitochondrial dysfunction.

3.4.3 Transcriptomic analysis of HG-cultured BeWo CT cells

While functional readouts of BeWo trophoblast mitochondrial function were sustained in response to hyperglycemia, we did observe impaired mitochondrial respiratory activity in differentiated BeWo SCT cells. Syncytialization of BeWo trophoblasts was associated with reduced mitochondrial spare respiratory capacity, reduced coupling efficiency, concomitant with reduced activity of ETC complex II, and reduced protein expression of ETC complex IV. Furthermore, BeWo SCT cells displayed increased DRP1 protein abundance and decreased OPA1 protein abundance suggestive of

increased mitochondrial fractionation. These data may indicate that alterations in mitochondrial dynamics underlies the observed functional differences in mitochondrial respiration between BeWo CT and SCT cells. Previous work by our research group has likewise highlighted that BeWo CT cells are overall more metabolically active than BeWo SCT cells [37], and similar trends have been reported in cultured PHT cells [28,63]. As progenitor BeWo CT cells display greater metabolic activity and greater alterations to nutrient stores in response to hyperglycemia than in differentiated SCT cells, we speculated that alterations in omic profiles in response to high glucose culture conditions would be more prevalent in these progenitor cells. Thus, this current study sought to examine global gene expression as well as global metabolite and lipid species abundance solely in HG-cultured BeWo CT cells to further elucidate mechanisms underlying altered placental metabolic function in response to hyperglycemia.

The current study identified 197 differentially expressed genes ($\geq \pm 1.3$ FC) in BeWo CT cells cultured under hyperglycemia for 72H. However, previous reports in BeWo CT cells demonstrated more substantial variations in gene expression between BeWo trophoblasts cultured under similar high and low glucose conditions [30]. The differences between the current study and previous reports may be due in part to differences in study design (pooling samples for arrays vs independent arrays for each sample), cell media formulation (DMEM-F12 vs F12K) as well as length of hyperglycemic exposure (48H vs 72H). Despite these differences in the number of differentially expressed genes, our study did align with this previous transcriptomic report, and demonstrated that elevated glucose levels impact the expression of genes involved in metabolic processes [30]. Notably, HG-culture conditions in the current study were associated with increased mRNA expression of *ACSL1* in BeWo CT cells. Additionally, we observed a simultaneous trend towards increased protein abundance of *ACSL1*, although these trends did not reach statistical significance. Previous studies have highlighted that *ACSL1* is involved in lipid synthesis in various tissues and that knockdown of *ACSL1* is associated with reduced triglyceride and lipid droplet abundance [64–67]. More importantly, cells transfected to overexpress *ACSL1* have been found to have increased triglyceride accumulation [67–69]. Thus, we speculate that *ACSL1* may be

involved in the trafficking of lipid species to lipid droplets and may underlie the glucose-induced accumulation of triglyceride species that was observed in our BeWo CT cultures.

Our data additionally highlighted that isolated hyperglycemia in BeWo CT cells was associated with an increased expression of *HSD11B2*, an enzyme involved in the metabolism and inactivation of the glucocorticoid cortisol. In normal pregnancies, cortisol is thought to be involved in mediating the physiological increase in maternal insulin resistance that is necessary to support fetal growth [70,71], however, circulating cortisol levels may be pathologically elevated in some GDM pregnancies [72]. Interestingly, placentae from GDM pregnancies have been found to have increased expression of *HSD11B2* leading to increased cortisol inactivation [73]. Since elevated cortisol levels in fetal circulation have been associated with impaired brain development processes [74], increased placental *HSD11B2* expression in GDM pregnancies may act in a protective manner to limit fetal glucocorticoid exposures. However, as cortisol also activates the glucocorticoid receptor leading to modulated gene transcription [75,76]. Thus, alterations in placental cortisol metabolism may have downstream consequences on placental function through altering gene expression. Overall, the results from the current study demonstrated that hyperglycemia is an important regulator of placental *HSD11B2* expression. However, it remains poorly understood whether these glucose-mediated impacts to placental cortisol metabolism act in a protective or detrimental manner.

3.4.4 Metabolomic and lipidomic analysis of HG-cultured BeWo CT cells

Multivariate analysis PCA analysis of BeWo trophoblast metabolome profiles highlighted a divergence in metabolite signatures between HG and LG-cultured BeWo CT cells suggesting that high glucose levels impact polar metabolite levels in the placenta. In contrast, limited separation was observed between the lipidome profiles of LG and HG-cultured BeWo CT in the unsupervised PCA analysis.

Subsequent pathway analysis of the metabolome data highlighted specific intracellular accumulations of lactate (involved in the glycolysis/gluconeogenesis and pyruvate metabolism pathways), malonate (involved in the fatty acid biosynthesis

pathway), as well as riboflavin (involved in the riboflavin metabolism pathway) in the HG-cultured BeWo CT cells.

The observed lactate accumulation likely suggests that glycolytic flux is in fact increased in HG-cultured BeWo CT cells [77]. It is interesting to note that this study did not observe increased basal or maximal glycolytic activity when assessed via the Seahorse XF Glycolysis Stress Test. As the Glycolysis Stress Test utilizes extracellular media acidification (resulting from the co-export of lactate and H⁺ from the cell) as a proxy measurement of glycolytic activity, this functional assay may underestimate glycolytic activity in the event of reduced lactate export as could potentially occur in a “Cytosol-to-Mitochondrial Lactate Shuttle” metabolic pathway [77].

The observed increase in malonate levels may reflect an increase in *de novo* lipogenesis via FASN in HG-cultured BeWo CT and may be another mechanism underlying the increased TG levels observed in HG-cultured BeWo CT cells [78,79]. Interestingly, we also observed an increased accumulation of 16:0 carnitine levels in the HG-cultured BeWo CT cells (+ 1.63 FC vs LG cultures) in our lipidomic analyses. As FA species must be conjugated to carnitine to be transported into the mitochondrial matrix for oxidation, the increased 16:0 carnitine levels may be reflective of increased FA oxidation in HG-cultured BeWo CT cells [80]. However, as malonate has been demonstrated to decrease FA oxidation rates, the increased accumulation of 16:0 carnitine could also indicate malonate-facilitated inhibition of β -oxidation in HG-cultured BeWo CT cells [78]. Future studies and the use of radio-labelled metabolites may be required to further characterize glycolytic activity, *de novo* lipogenesis, and β -oxidation in high-glucose exposed BeWo trophoblasts.

The observed accumulation of riboflavin (the essential vitamin B₂) in HG-cultured BeWo CT cells either reflects an increased cellular uptake of riboflavin or an inhibition of riboflavin metabolism into the cofactors flavin adenine dinucleotide (FAD) and flavin mononucleotide (FMN) [81]. Reduced metabolism of riboflavin to its cofactor intermediaries has previously been implicated in the development of mitochondrial dysfunction [82]. However, riboflavin has also previously been suggested to act as an

antioxidant [83] and has been demonstrated to be beneficial in reducing oxidative stress in rodent models of DM [84,85]. Future investigations may be needed to assess the impacts of riboflavin accumulation in HG-cultured trophoblasts and elucidate whether accumulation of this vitamin is beneficial or harmful to the placenta.

3.4.5 Conclusion

The results of the current study highlighted that a 72-hour hyperglycemia exposure independently impacts metabolic function and nutrient storage in BeWo trophoblasts but does not mediate any global changes in functional readouts of mitochondrial respiratory activity. Interestingly, HG-cultured BeWo trophoblasts displayed markers of reduced glycogen storage capacity that potentially increases the supply of free glucose for oxidation, as well as markers suggestive of a transition towards altered mitochondrial dynamics, that overall may be indicative of early metabolic adaptations, or of more concern, a transition towards mitochondrial failure. It is important to note that while the 72-hour hyperglycemic exposure utilized in the current study is relatively prolonged in the setting of *in vitro* cell culture experiments, this timeline is acute in comparison to the 40-week duration of human pregnancy *in vivo*. Thus, preventing even short periods of hyperglycemia may be important in the clinical management of diabetic pregnancies to ensure appropriate placental function is sustained throughout gestation, and in turn that the risk of the offspring developing later life non-communicable metabolic diseases is limited.

3.5 References

- [1] D.S. Feig, J. Hwee, B.R. Shah, G.L. Booth, A.S. Bierman, L.L. Lipscombe, Trends in Incidence of Diabetes in Pregnancy and Serious Perinatal Outcomes: A Large, Population-Based Study in Ontario, Canada, 1996–2010, *Diabetes Care*. 37 (2014) 1590–1596. doi:10.2337/dc13-2717.
- [2] S. Behboudi-Gandevani, M. Amiri, R. Bidhendi Yarandi, F. Ramezani Tehrani, The impact of diagnostic criteria for gestational diabetes on its prevalence: a systematic review and meta-analysis, *Diabetol. Metab. Syndr.* 11 (2019) 11. doi:10.1186/s13098-019-0406-1.
- [3] R.L. Lawrence, C.R. Wall, F.H. Bloomfield, Prevalence of gestational diabetes according to commonly used data sources: an observational study, *BMC Pregnancy Childbirth*. 19 (2019) 349. doi:10.1186/s12884-019-2521-2.
- [4] B. Voaklander, S. Rowe, O. Sanni, S. Campbell, D. Eurich, M.B. Ospina, Prevalence of diabetes in pregnancy among Indigenous women in Australia, Canada, New Zealand, and the USA: a systematic review and meta-analysis, *Lancet Glob. Heal.* 8 (2020) e681–e698. doi:10.1016/S2214-109X(20)30046-2.
- [5] T.D. Clausen, E.R. Mathiesen, T. Hansen, O. Pedersen, D.M. Jensen, J. Lauenborg, P. Damm, High Prevalence of Type 2 Diabetes and Pre-Diabetes in Adult Offspring of Women With Gestational Diabetes Mellitus or Type 1 Diabetes: The role of intrauterine hyperglycemia, *Diabetes Care*. 31 (2008) 340–346. doi:10.2337/dc07-1596.
- [6] T. Farrell, L. Neale, T. Cundy, Congenital anomalies in the offspring of women with Type 1, Type 2 and gestational diabetes, *Diabet. Med.* 19 (2002) 322–326. doi:10.1046/j.1464-5491.2002.00700.x.
- [7] M.C. Aisa, B. Cappuccini, A. Barbati, G. Clerici, E. Torlone, S. Gerli, G.C. Di Renzo, Renal Consequences of Gestational Diabetes Mellitus in Term Neonates: A Multidisciplinary Approach to the DOHaD Perspective in the Prevention and Early Recognition of Neonates of GDM Mothers at Risk of Hypertension and Chronic Renal Diseases in Later Life, *J. Clin. Med.* 8 (2019) 429. doi:10.3390/jcm8040429.
- [8] T.J. Pereira, B.L. Moyce, S.M. Kereliuk, V.W. Dolinsky, Influence of maternal overnutrition and gestational diabetes on the programming of metabolic health outcomes in the offspring: experimental evidence, *Biochem. Cell Biol.* 93 (2015) 438–451. doi:10.1139/bcb-2014-0141.
- [9] R.S. Lindsay, S.M. Nelson, J.D. Walker, S.A. Greene, G. Milne, N. Sattar, D.W. Pearson, Programming of Adiposity in Offspring of Mothers With Type 1 Diabetes at Age 7 Years, *Diabetes Care*. 33 (2010) 1080–1085. doi:10.2337/dc09-1766.
- [10] P. Damm, A. Houshmand-Oeregaard, L. Kelstrup, J. Lauenborg, E.R. Mathiesen,

- T.D. Clausen, Gestational diabetes mellitus and long-term consequences for mother and offspring: a view from Denmark, *Diabetologia*. 59 (2016) 1396–1399. doi:10.1007/s00125-016-3985-5.
- [11] D. Dabelea, The Predisposition to Obesity and Diabetes in Offspring of Diabetic Mothers, *Diabetes Care*. 30 (2007) S169–S174. doi:10.2337/dc07-s211.
- [12] M.M. Pathirana, Z.S. Lassi, A. Ali, M.A. Arstall, C.T. Roberts, P.H. Andraweera, Association between metabolic syndrome and gestational diabetes mellitus in women and their children: a systematic review and meta-analysis, *Endocrine*. 71 (2021) 310–320. doi:10.1007/s12020-020-02492-1.
- [13] J. Huynh, D. Dawson, D. Roberts, R. Bentley-Lewis, A systematic review of placental pathology in maternal diabetes mellitus, *Placenta*. 36 (2015) 101–114. doi:10.1016/j.placenta.2014.11.021.
- [14] I. Carrasco-Wong, A. Moller, F.R. Giachini, V. V. Lima, F. Toledo, J. Stojanova, L. Sobrevia, S. San Martín, Placental structure in gestational diabetes mellitus, *Biochim. Biophys. Acta - Mol. Basis Dis.* 1866 (2020) 165535. doi:10.1016/j.bbadis.2019.165535.
- [15] E.M. Strøm-Roum, C. Haavaldsen, T.G. Tanbo, A. Eskild, Placental weight relative to birthweight in pregnancies with maternal diabetes mellitus, *Acta Obstet. Gynecol. Scand.* 92 (2013) 783–789. doi:10.1111/aogs.12104.
- [16] E. Taricco, T. Radaelli, M. Nobile de Santis, I. Cetin, Foetal and Placental Weights in Relation to Maternal Characteristics in Gestational Diabetes, *Placenta*. 24 (2003) 343–347. doi:10.1053/plac.2002.0913.
- [17] T.T. Lao, C.-P. Lee, W.-M. Wong, Placental weight to birthweight ratio is increased in mild gestational glucose intolerance, *Placenta*. 18 (1997) 227–230. doi:10.1016/S0143-4004(97)90097-7.
- [18] V. Gheorman, L. Gheorman, C. Ivănuş, R.C. Pană, A.M. Gogăna, A. Pătraşcu, Comparative study of placenta acute fetal distress and diabetes associated with pregnancy., *Rom. J. Morphol. Embryol.* 54 (2013) 505–11. doi:24068397.
- [19] G. Desoye, H.H. Hofmann, P.A.M. Weiss, Insulin binding to trophoblast plasma membranes and placental glycogen content in well-controlled gestational diabetic women treated with diet or insulin, in well-controlled overt diabetic patients and in healthy control subjects, *Diabetologia*. 35 (1992) 45–55. doi:10.1007/BF00400851.
- [20] L.K. Akison, M.D. Nitert, V.L. Clifton, K.M. Moritz, D.G. Simmons, Review: Alterations in placental glycogen deposition in complicated pregnancies: Current preclinical and clinical evidence, *Placenta*. 54 (2017) 52–58. doi:10.1016/j.placenta.2017.01.114.

- [21] E. Shafir, V. Barash, Placental glycogen metabolism in diabetic pregnancy., *Isr. J. Med. Sci.* 27 (n.d.) 449–61. doi:1835720.
- [22] C.H. Hulme, A. Nicolaou, S.A. Murphy, A.E.P. Heazell, J.E. Myers, M. Westwood, The effect of high glucose on lipid metabolism in the human placenta, *Sci. Rep.* 9 (2019) 14114. doi:10.1038/s41598-019-50626-x.
- [23] M.L.S. Lindegaard, P. Damm, E.R. Mathiesen, L.B. Nielsen, Placental triglyceride accumulation in maternal type 1 diabetes is associated with increased lipase gene expression, *J. Lipid Res.* 47 (2006) 2581–2588. doi:10.1194/jlr.M600236-JLR200.
- [24] S.J. Tunster, E.D. Watson, A.L. Fowden, G.J. Burton, Placental glycogen stores and fetal growth: insights from genetic mouse models, *Reproduction.* 159 (2020) R213–R235. doi:10.1530/REP-20-0007.
- [25] G. Desoye, E.T. Korgun, N. Ghaffari-Tabrizi, T. Hahn, Is fetal macrosomia in adequately controlled diabetic women the result of a placental defect? – a hypothesis, *J. Matern. Neonatal Med.* 11 (2002) 258–261. doi:10.1080/jmf.11.4.258.261.
- [26] L. Sobrevia, P. Valero, A. Grismaldo, R. Villalobos-Labra, F. Pardo, M. Subiabre, G. Armstrong, F. Toledo, S. Vega, M. Cornejo, G. Fuentes, R. Marín, Mitochondrial dysfunction in the fetoplacental unit in gestational diabetes mellitus, *Biochim. Biophys. Acta - Mol. Basis Dis.* 1866 (2020) 165948. doi:10.1016/j.bbadis.2020.165948.
- [27] S. Muralimanoharan, A. Maloyan, L. Myatt, Mitochondrial function and glucose metabolism in the placenta with gestational diabetes mellitus: role of miR-143., *Clin. Sci. (Lond).* 130 (2016) 931–41. doi:10.1042/CS20160076.
- [28] A.M. Valent, H. Choi, K.S. Kolahi, K.L. Thornburg, Hyperglycemia and gestational diabetes suppress placental glycolysis and mitochondrial function and alter lipid processing, *FASEB J.* 35 (2021). doi:10.1096/fj.202000326RR.
- [29] R. Hastie, M. Lappas, The effect of pre-existing maternal obesity and diabetes on placental mitochondrial content and electron transport chain activity., *Placenta.* 35 (2014) 673–83. doi:10.1016/j.placenta.2014.06.368.
- [30] C.H. Hulme, A. Stevens, W. Dunn, A.E.P. Heazell, K. Hollywood, P. Begley, M. Westwood, J.E. Myers, Identification of the functional pathways altered by placental cell exposure to high glucose: lessons from the transcript and metabolite interactome, *Sci. Rep.* 8 (2018) 5270. doi:10.1038/s41598-018-22535-y.
- [31] M. He, G. Wang, S. Han, Y. Jin, H. Li, X. Wu, Z. Ma, X. Cheng, X. Tang, X. Yang, G. Liu, Nrf2 signalling and autophagy are involved in diabetes mellitus-induced defects in the development of mouse placenta, *Open Biol.* 6 (2016) 160064. doi:10.1098/rsob.160064.

- [32] C. Guo, L. Sun, X. Chen, D. Zhang, Oxidative stress, mitochondrial damage and neurodegenerative diseases., *Neural Regen. Res.* 8 (2013) 2003–14. doi:10.3969/j.issn.1673-5374.2013.21.009.
- [33] A.J. Kowaltowski, A.E. Vercesi, Mitochondrial damage induced by conditions of oxidative stress, *Free Radic. Biol. Med.* 26 (1999) 463–471. doi:10.1016/S0891-5849(98)00216-0.
- [34] U. Weiss, M. Cervar, P. Puerstner, O. Schmut, J. Haas, R. Mauschwitz, G. Aarikan, G. Desoye, Hyperglycaemia in vitro alters the proliferation and mitochondrial activity of the choriocarcinoma cell lines BeWo, JAR and JEG-3 as models for human first-trimester trophoblast, *Diabetologia.* 44 (2001) 209–219. doi:10.1007/s001250051601.
- [35] S. Joseph, J.M. Walejko, S. Zhang, A.S. Edison, M. Keller-Wood, Maternal hypercortisolemia alters placental metabolism: a multiomics view, *Am. J. Physiol. Metab.* 319 (2020) E950–E960. doi:10.1152/ajpendo.00190.2020.
- [36] T.J. Stuart, K. O'Neill, D. Condon, I. Sasson, P. Sen, Y. Xia, R.A. Simmons, Diet-induced obesity alters the maternal metabolome and early placenta transcriptome and decreases placenta vascularity in the mouse†, *Biol. Reprod.* 98 (2018) 795–809. doi:10.1093/biolre/i0y010.
- [37] Z.J.W. Easton, F. Delhaes, K. Mathers, L. Zhao, C.M.G. Vanderboor, T.R.H. Regnault, Syncytialization and prolonged exposure to palmitate impacts BeWo respiration, *Reproduction.* 161 (2021) 73–88. doi:10.1530/REP-19-0433.
- [38] K. Kusama, R. Bai, K. Imakawa, Regulation of human trophoblast cell syncytialization by transcription factors STAT5B and NR4A3, *J. Cell. Biochem.* 119 (2018) 4918–4927. doi:10.1002/jcb.26721.
- [39] S.S. Malhotra, P. Suman, S. Kumar Gupta, Alpha or beta human chorionic gonadotropin knockdown decrease BeWo cell fusion by down-regulating PKA and CREB activation, *Sci. Rep.* 5 (2015) 11210. doi:10.1038/srep11210.
- [40] E.R. Price, J.T. McFarlan, C.G. Guglielmo, Preparing for Migration? The Effects of Photoperiod and Exercise on Muscle Oxidative Enzymes, Lipid Transporters, and Phospholipids in White-Crowned Sparrows, *Physiol. Biochem. Zool.* 83 (2010) 252–262. doi:10.1086/605394.
- [41] K. Guo, L. Li, Differential ¹²C-/¹³C-Isotope Dansylation Labeling and Fast Liquid Chromatography/Mass Spectrometry for Absolute and Relative Quantification of the Metabolome, *Anal. Chem.* 81 (2009) 3919–3932. doi:10.1021/ac900166a.
- [42] S. Zhao, L. Li, Chemical derivatization in LC-MS-based metabolomics study, *TrAC Trends Anal. Chem.* 131 (2020) 115988. doi:10.1016/j.trac.2020.115988.

- [43] S. Zhao, H. Li, W. Han, W. Chan, L. Li, Metabolomic Coverage of Chemical-Group-Submetabolome Analysis: Group Classification and Four-Channel Chemical Isotope Labeling LC-MS, *Anal. Chem.* 91 (2019) 12108–12115. doi:10.1021/acs.analchem.9b03431.
- [44] A. Zardini Buzatto, M. Abdel Jabar, I. Nizami, M. Dasouki, L. Li, A.M. Abdel Rahman, Lipidome Alterations Induced by Cystic Fibrosis, CFTR Mutation, and Lung Function, *J. Proteome Res.* 20 (2021) 549–564. doi:10.1021/acs.jproteome.0c00556.
- [45] M. Sud, E. Fahy, D. Cotter, A. Brown, E.A. Dennis, C.K. Glass, A.H. Merrill, R.C. Murphy, C.R.H. Raetz, D.W. Russell, S. Subramaniam, LMSD: LIPID MAPS structure database, *Nucleic Acids Res.* 35 (2007) D527–D532. doi:10.1093/nar/gkl838.
- [46] M. Lew, Good statistical practice in pharmacology Problem 2, *Br. J. Pharmacol.* 152 (2009) 299–303. doi:10.1038/sj.bjp.0707372.
- [47] T. Hahn, D. Hahn, A. Blaschitz, E.T. Korgun, G. Desoye, G. Dohr, Hyperglycaemia-induced subcellular redistribution of GLUT1 glucose transporters in cultured human term placental trophoblast cells, *Diabetologia.* 43 (2000) 173–180. doi:10.1007/s001250050026.
- [48] P. Georgiades, A.C. Ferguson-Smith, G.J. Burton, Comparative Developmental Anatomy of the Murine and Human Definitive Placentae, *Placenta.* 23 (2002) 3–19. doi:10.1053/plac.2001.0738.
- [49] G.B. Wislocki, H.S. Bennett, The histology and cytology of the human and monkey placenta, with special reference to the trophoblast, *Am. J. Anat.* 73 (1943) 335–449. doi:10.1002/aja.1000730303.
- [50] M. Bouskila, R.W. Hunter, A.F.M. Ibrahim, L. Delattre, M. Peggie, J.A. van Diepen, P.J. Voshol, J. Jensen, K. Sakamoto, Allosteric Regulation of Glycogen Synthase Controls Glycogen Synthesis in Muscle, *Cell Metab.* 12 (2010) 456–466. doi:10.1016/j.cmet.2010.10.006.
- [51] A. Krishnankutty, T. Kimura, T. Saito, K. Aoyagi, A. Asada, S.-I. Takahashi, K. Ando, M. Ohara-Imaizumi, K. Ishiguro, S. Hisanaga, In vivo regulation of glycogen synthase kinase 3 β activity in neurons and brains, *Sci. Rep.* 7 (2017) 8602. doi:10.1038/s41598-017-09239-5.
- [52] Y.-C. Lai, J.T. Stuenæs, C.-H. Kuo, J. Jensen, Glycogen content and contraction regulate glycogen synthase phosphorylation and affinity for UDP-glucose in rat skeletal muscles, *Am. J. Physiol. Metab.* 293 (2007) E1622–E1629. doi:10.1152/ajpendo.00113.2007.
- [53] K. Kolahi, S. Louey, O. Varlamov, K. Thornburg, Real-time tracking of BODIPY-C12 long-chain fatty acid in human term placenta reveals unique lipid dynamics in

cytotrophoblast cells, *PLoS One*. 11 (2016) 1–23.
doi:10.1371/journal.pone.0153522.

- [54] A. Czajka, A.N. Malik, Hyperglycemia induced damage to mitochondrial respiration in renal mesangial and tubular cells: Implications for diabetic nephropathy, *Redox Biol.* 10 (2016) 100–107. doi:10.1016/j.redox.2016.09.007.
- [55] A. Koziel, A. Woyda-Ploszczyca, A. Kicinska, W. Jarmuszkiewicz, The influence of high glucose on the aerobic metabolism of endothelial EA.hy926 cells, *Pflügers Arch. - Eur. J. Physiol.* 464 (2012) 657–669. doi:10.1007/s00424-012-1156-1.
- [56] S. Kumari, L. Anderson, S. Farmer, S.L. Mehta, P.A. Li, Hyperglycemia Alters Mitochondrial Fission and Fusion Proteins in Mice Subjected to Cerebral Ischemia and Reperfusion, *Transl. Stroke Res.* 3 (2012) 296–304. doi:10.1007/s12975-012-0158-9.
- [57] S. Kobayashi, F. Zhao, Z. Zhang, T. Kobayashi, Y. Huang, B. Shi, W. Wu, Q. Liang, Mitochondrial Fission and Mitophagy Coordinately Restrict High Glucose Toxicity in Cardiomyocytes, *Front. Physiol.* 11 (2020). doi:10.3389/fphys.2020.604069.
- [58] W. Wang, Y. Wang, J. Long, J. Wang, S.B. Haudek, P. Overbeek, B.H.J. Chang, P.T. Schumacker, F.R. Danesh, Mitochondrial Fission Triggered by Hyperglycemia Is Mediated by ROCK1 Activation in Podocytes and Endothelial Cells, *Cell Metab.* 15 (2012) 186–200. doi:10.1016/j.cmet.2012.01.009.
- [59] S.A. Detmer, D.C. Chan, Functions and dysfunctions of mitochondrial dynamics, *Nat. Rev. Mol. Cell Biol.* 8 (2007) 870–879. doi:10.1038/nrm2275.
- [60] H.-F. Jheng, P.-J. Tsai, S.-M. Guo, L.-H. Kuo, C.-S. Chang, I.-J. Su, C.-R. Chang, Y.-S. Tsai, Mitochondrial Fission Contributes to Mitochondrial Dysfunction and Insulin Resistance in Skeletal Muscle, *Mol. Cell. Biol.* 32 (2012) 309–319. doi:10.1128/MCB.05603-11.
- [61] S. Wu, F. Zhou, Z. Zhang, D. Xing, Mitochondrial oxidative stress causes mitochondrial fragmentation via differential modulation of mitochondrial fission-fusion proteins, *FEBS J.* 278 (2011) 941–954. doi:10.1111/j.1742-4658.2011.08010.x.
- [62] J.A. Kashatus, A. Nascimento, L.J. Myers, A. Sher, F.L. Byrne, K.L. Hoehn, C.M. Counter, D.F. Kashatus, Erk2 Phosphorylation of Drp1 Promotes Mitochondrial Fission and MAPK-Driven Tumor Growth, *Mol. Cell.* 57 (2015) 537–551. doi:10.1016/j.molcel.2015.01.002.
- [63] K. Kolahi, A. Valent, K.L. Thornburg, Cytotrophoblast, Not Syncytiotrophoblast, Dominates Glycolysis and Oxidative Phosphorylation in Human Term Placenta., *Sci. Rep.* (2017) 1–12. doi:10.1038/srep42941.

- [64] R. Joseph, J. Poschmann, R. Sukarieh, P.G. Too, S.G. Julien, F. Xu, A.L. Teh, J.D. Holbrook, K.L. Ng, Y.S. Chong, P.D. Gluckman, S. Prabhakar, W. Stümel, ACSL1 Is Associated With Fetal Programming of Insulin Sensitivity and Cellular Lipid Content, *Mol. Endocrinol.* 29 (2015) 909–920. doi:10.1210/me.2015-1020.
- [65] L.O. Li, J.M. Ellis, H.A. Paich, S. Wang, N. Gong, G. Altshuler, R.J. Thresher, T.R. Koves, S.M. Watkins, D.M. Muoio, G.W. Cline, G.I. Shulman, R.A. Coleman, Liver-specific Loss of Long Chain Acyl-CoA Synthetase-1 Decreases Triacylglycerol Synthesis and β -Oxidation and Alters Phospholipid Fatty Acid Composition, *J. Biol. Chem.* 284 (2009) 27816–27826. doi:10.1074/jbc.M109.022467.
- [66] E. Soupene, F.A. Kuypers, Mammalian Long-Chain Acyl-CoA Synthetases, *Exp. Biol. Med.* 233 (2008) 507–521. doi:10.3181/0710-MR-287.
- [67] T. Li, X. Li, H. Meng, L. Chen, F. Meng, ACSL1 affects Triglyceride Levels through the PPAR γ Pathway, *Int. J. Med. Sci.* 17 (2020) 720–727. doi:10.7150/ijms.42248.
- [68] H.A. Parkes, E. Preston, D. Wilks, M. Ballesteros, L. Carpenter, L. Wood, E.W. Kraegen, S.M. Furler, G.J. Cooney, Overexpression of acyl-CoA synthetase-1 increases lipid deposition in hepatic (HepG2) cells and rodent liver in vivo, *Am. J. Physiol. Metab.* 291 (2006) E737–E744. doi:10.1152/ajpendo.00112.2006.
- [69] Z. Zhao, S.H. Abbas Raza, H. Tian, B. Shi, Y. Luo, J. Wang, X. Liu, S. Li, Y. Bai, J. Hu, Effects of overexpression of ACSL1 gene on the synthesis of unsaturated fatty acids in adipocytes of bovine, *Arch. Biochem. Biophys.* 695 (2020) 108648. doi:10.1016/j.abb.2020.108648.
- [70] M. Keller-Wood, X. Feng, C.E. Wood, E. Richards, R. V. Anthony, G.E. Dahl, S. Tao, Elevated maternal cortisol leads to relative maternal hyperglycemia and increased stillbirth in ovine pregnancy, *Am. J. Physiol. Integr. Comp. Physiol.* 307 (2014) R405–R413. doi:10.1152/ajpregu.00530.2013.
- [71] P.J. Hornnes, C. Kühl, Gastrointestinal hormones and cortisol in normal pregnant women and women with gestational diabetes., *Acta Endocrinol. Suppl. (Copenh)*. 277 (1986) 24–6. <http://www.ncbi.nlm.nih.gov/pubmed/3464150>.
- [72] S.A. Ahmed, M.H. Shalayel, Role of cortisol in the deterioration of glucose tolerance in Sudanese pregnant women., *East Afr. Med. J.* 76 (1999) 465–7. doi:10520355.
- [73] R. Ma, J. Liu, L. Wu, J. Sun, Z. Yang, C. Yu, P. Yuan, X. Xiao, Differential expression of placental 11 β -hydroxysteroid dehydrogenases in pregnant women with diet-treated gestational diabetes mellitus, *Steroids*. 77 (2012) 798–805. doi:10.1016/j.steroids.2012.03.007.
- [74] A. Nath, G.V.S. Murthy, G.R. Babu, G.C. Di Renzo, Effect of prenatal exposure to

maternal cortisol and psychological distress on infant development in Bengaluru, southern India: a prospective cohort study, *BMC Psychiatry*. 17 (2017) 255. doi:10.1186/s12888-017-1424-x.

- [75] Z. Saif, N.A. Hodyl, E. Hobbs, A.R. Tuck, M.S. Butler, A. Osei-Kumah, V.L. Clifton, The human placenta expresses multiple glucocorticoid receptor isoforms that are altered by fetal sex, growth restriction and maternal asthma, *Placenta*. 35 (2014) 260–268. doi:10.1016/j.placenta.2014.01.012.
- [76] V.L. Clifton, J. Cuffe, K.M. Moritz, T.J. Cole, P.J. Fuller, N.Z. Lu, S. Kumar, S. Chong, Z. Saif, Review: The role of multiple placental glucocorticoid receptor isoforms in adapting to the maternal environment and regulating fetal growth, *Placenta*. 54 (2017) 24–29. doi:10.1016/j.placenta.2016.12.017.
- [77] M.J. Rogatzki, B.S. Ferguson, M.L. Goodwin, L.B. Gladden, Lactate is always the end product of glycolysis, *Front. Neurosci*. 9 (2015). doi:10.3389/fnins.2015.00022.
- [78] A. Honda, K. Yamashita, T. Ikegami, T. Hara, T. Miyazaki, T. Hirayama, M. Numazawa, Y. Matsuzaki, Highly sensitive quantification of serum malonate, a possible marker for de novo lipogenesis, by LC-ESI-MS/MS, *J. Lipid Res*. 50 (2009) 2124–2130. doi:10.1194/jlr.D800054-JLR200.
- [79] J. Kerner, P.E. Minkler, E.J. Lesnefsky, C.L. Hoppel, Fatty Acid Chain Elongation in Palmitate-perfused Working Rat Heart, *J. Biol. Chem*. 289 (2014) 10223–10234. doi:10.1074/jbc.M113.524314.
- [80] N. Longo, M. Frigeni, M. Pasquali, Carnitine transport and fatty acid oxidation, *Biochim. Biophys. Acta - Mol. Cell Res*. 1863 (2016) 2422–2435. doi:10.1016/j.bbamcr.2016.01.023.
- [81] S. Balasubramaniam, J. Christodoulou, S. Rahman, Disorders of riboflavin metabolism, *J. Inherit. Metab. Dis*. 42 (2019) 608–619. doi:10.1002/jimd.12058.
- [82] S. Balasubramaniam, J. Yaplito-Lee, Riboflavin metabolism: role in mitochondrial function, *J. Transl. Genet. Genomics*. (2020). doi:10.20517/jtgg.2020.34.
- [83] M. Ashoori, A. Saedisomeolia, Riboflavin (vitamin B 2) and oxidative stress: a review, *Br. J. Nutr*. 111 (2014) 1985–1991. doi:10.1017/S0007114514000178.
- [84] G. Wang, W. Li, X. Lu, X. Zhao, Riboflavin Alleviates Cardiac Failure in Type I Diabetic Cardiomyopathy, *Heart Int*. 6 (2011) hi.2011.e21. doi:10.4081/hi.2011.e21.
- [85] M.M. Alam, S. Iqbal, I. Naseem, Ameliorative effect of riboflavin on hyperglycemia, oxidative stress and DNA damage in type-2 diabetic mice: Mechanistic and therapeutic strategies, *Arch. Biochem. Biophys*. 584 (2015) 10–19. doi:10.1016/j.abb.2015.08.013.

Chapter 4

4 Elevated Dietary Non-Esterified Fatty Acid Levels Impact BeWo Trophoblast Metabolism and Lipid Processing: A Multi-OMICS Outlook

This chapter is a version of a manuscript under preparation for submission entitled “Elevated Dietary Non-Esterified Fatty Acid Levels Impact BeWo Trophoblast Metabolism and Lipid Processing: A Multi-OMICS Outlook”

4.1 Introduction

Adverse intrauterine environments that arise in conditions of maternal obesity and gestational diabetes mellitus (GDM) have been linked with an increased risk of pregnancy complications [1–3]. Further, offspring from these at risk pregnancies have an increased risk of developing non-communicable metabolic health disorders including metabolic syndrome, obesity, and type 2 diabetes [4–8]. Alarming, these children have been found to be impacted by these largely “adult-associated” metabolic diseases during adolescence, highlighting the profound influence of the aberrant *in utero* programming resulting from maternal obesity and GDM [9–11]. Investigating these poor health outcomes is of great importance as the rates of obesity and gestational diabetes mellitus (GDM) development during pregnancy have been increasing globally over the past several decades [12,13]. It is currently estimated that one-third of pregnancies are impacted by maternal obesity, and one-sixth of pregnancies are impacted by GDM, however these rates may be greater in certain at-risk demographics [14–16]. These drastic increase in the prevalence of maternal obesity and GDM and subsequent increased rates of metabolic disease development in affected offspring will create further strains on health care systems.

Aberrant placental metabolic function in diabetic and obese pregnancies may be an important factor underlying the *in-utero* programming of metabolic diseases [17–19]. Specifically, impairments in mitochondrial respiratory (oxidative) function have been identified in term villous trophoblast cells from obese and GDM pregnancies that impair placental energy production and reduce ATP content [20–24]. Furthermore, maternal obesity alters placental lipid processing at term highlighted by increased fatty acid desaturation, lipid esterification, and ultimately increased placental triglyceride abundance and steatosis [25–27]. Placental lysates from obese pregnancies have also been found to have decreased abundance of short-chain acylcarnitine species (β -oxidation intermediary metabolites) and reduced CPT1b expression that is indicative of reduced placental β -oxidative activity and suggests placental steatosis in obese pregnancies may be facilitated by reduced placental lipid oxidation [25,28,29]. Maternal GDM has also been associated with increased placental steatosis at term that has likewise been attributed

to reduced placental β -oxidative activity, further highlighting adverse maternal environmental conditions negatively regulate important aspects of placental lipid processing [24,30–32].

Recently, studies have highlighted the utility of “omics” based research approaches to help further identify and understand the underlying biological mechanisms that facilitate the development of placental disorders in at-risk pregnancies [33,34]. For example, metabolomic and lipidomic analyses have expanded our understanding of possible mechanisms underlying impaired placental lipid processing in obese and GDM pregnancies. These readouts have described altered neutral and polar lipid profiles highlighted by altered fatty acid (FA) compositions in placentae from obese and diabetic pregnancies [35–39]. Pre-clinical mouse models of diet induced maternal pre-gestational obesity have likewise described metabolomic and transcriptomic markers indicative of altered placental lipid composition and metabolism, further highlighting the prevalence of abnormal lipid processing in the obese placenta [40,41]. These alterations in placental metabolic function and lipid handling likely leads to suboptimal transplacental nutrient transport that impairs fetal growth, and development and ultimately resulting in *in utero* programming of metabolic diseases [36,42].

Underlying the development of this aberrant placental function in obese and GDM pregnancies is an increased fat supply to the placenta as a result of maternal dyslipidemia [43,44]. Analysis of the fasting serum of women during the third trimester of pregnancy has revealed that conditions of GDM and obesity elevate circulating levels of non-esterified fatty acids (NEFA) species [45]. These analyses also demonstrated that palmitate (C16:0; PA) and oleate (C18:1n9c; OA) are the most abundant NEFA species in serum during pregnancy [45,47]. Since PA and OA are the most abundantly consumed FA in the diets of Westernized populations, these fats themselves may be a link between poor maternal diet and impaired placental function in obese and GDM pregnancies [48–51]. Notably, maternal fat consumption has previously been demonstrated to be an important regulator of placental lipid handling [26,46]. Thus, it is likely the increased circulating NEFA levels in obese and GDM pregnancies directly impacts placental metabolism. However, the extent to which PA and OA directly impact important

placental lipid metabolic functions such as lipid esterification, FA desaturation, and beta-oxidation remains poorly understood.

The purpose of the current project, therefore, was to examine the impacts of a prolonged (72 hour) isolated dietary-FA exposure using an *in vitro* cell culture-based system and BeWo trophoblast cells to elucidate the underlying mechanisms that regulate placental nutrient processing and metabolism in response to elevated dietary fat supply. Our first objective was to utilize targeted lipidomic readouts to examine FA and neutral lipid profiles of BeWo cytotrophoblast (CT) and syncytiotrophoblast (SCT) cells, to gain an initial understanding of how NEFA exposures impact placental lipid processing. These analyses were additionally used to elucidate the impacts of NEFA exposures on placental FA desaturation and elongation processing. It was postulated that exposure to elevated levels of dietary NEFA would alter BeWo trophoblast lipid profiles, highlighted by increased TG abundance, and increased FA elongation and desaturation.

The second objective of this project was to utilize transcriptomics, in conjunction with untargeted metabolomics and lipidomics to characterize the underlying mechanisms that regulate BeWo CT metabolism in response to elevated dietary NEFA supply. As progenitor CT cells have previously been demonstrated to be the most metabolically active cells of the placenta villous trophoblast layer as well as the primary site of nutrient localization and storage in the placenta [24,52–54], the current study sought to examine “omic” profiles only in the more metabolically active CT cells. We postulated that dietary-FA treated BeWo CT cells would display altered transcriptomic, metabolomic and lipidomic profiles indicative of altered lipid processing.

4.2 Materials and methods:

4.2.1 Materials

All materials were purchased from Millipore Sigma (Oakville, Canada) unless otherwise indicated.

4.2.2 Cell culture protocol

BeWo trophoblast cells (CCL-98) were purchased from the American Type Culture Collection (ATCC; Cedarlane Labs, Burlington, Canada) and cultured in F12K media (Gibco, ThermoFisher Scientific, Mississauga, Canada) as per ATCC guidelines. Cell culture media was supplemented with 10% Fetal Bovine Serum (Gibco) and 1% Penicillin-Streptomycin (Invitrogen, ThermoFisher Scientific, Mississauga, Canada) for all experiments (complete F12K media). Cultures between passages 5-15 were utilized, and all cells were maintained at 5% CO₂/95% atmospheric air for all collections.

Cells were then cultured with exogenous NEFA species as previously reported in Chapter 2 [52]. In brief, BeWo trophoblast cells were plated onto cell culture dishes at the specific densities stated for each experiment and allowed to adhere to cell culture plates overnight prior to NEFA treatments. At T0H, cells were treated with complete F12K media further supplemented with either 100 µM PA, 100 µM OA, or 50 µM each PA and OA (P/O). All FAs were conjugated 2:1 (molar ratio) to Bovine Serum Albumin (BSA) for solubility in cell culture media. Complete F12K media supplemented with BSA-alone (0.3%) was utilized as a control. Cell media was replenished every 24 hours, and subsets of cells were additionally treated with 250 µM 8-Br-cAMP at T24H and T48H to induce CT-to-SCT differentiation. All cultures were collected for analysis after 72H of NEFA exposure.

This duration of NEFA exposure was specifically utilized as it represented the longest treatment period possible without being required to sub-culture the cells due to increasing confluency. Additionally, the 100 µM concentrations of NEFAs utilized were reflective of physiological fasting levels of PA and OA during the third trimester of gestation [45], and more importantly in Chapter 2 were found to not impact BeWo

trophoblast viability or differentiation capacity at 72-hours [52]. Thus, the data presented in the current study highlight alterations in placental metabolic function independent from lipotoxic effects.

4.2.3 Fatty acid and neutral lipid profile analysis

BeWo CT and SCT cells were plated at a density of 2×10^6 cells in 150 mm cell culture dishes and cultured with exogenous NEFA species as described. At T72H cells were collected via scraping and washed twice with PBS, and the resulting cell pellet was flash frozen in liquid nitrogen and stored at -80°C until analyzed.

Total cellular lipids were then collected from cell pellets via chloroform/methanol extraction (Folch extraction method) as has previously been reported and adapted for use with cell pellets [55–57]. In brief, cells were lysed in 2:1 chloroform:methanol with 0.01% butylated hydroxytoluene (BHT). Subsequently, 0.25% KCl was added, and samples were heated at 70°C for 5 mins to separate lipid and aqueous layers. Collected lipids were then dried under a gentle stream of N_2 gas, and resuspended in 2:1 chloroform:methanol (0.01% BHT) at 1 mg/mL concentrations and stored at -20°C until analysis.

To examine FA profiles, 100 μg of lipids were methylated to create FA methyl esters (FAMES), and subsequently separated and analyzed using gas chromatography coupled flame ionization detection (GC-FID), as previously reported [56,57]. A 6890 N gas chromatograph (Hewlett Packard, Palo Alto, CA, USA) with flame ionization detector (Agilent Technologies, Santa Clara, CA, USA) and a J&W Scientific High-Resolution Gas Chromatography Column (DB-23, Agilent Technologies; $30 \text{ m} \times 250 \mu\text{m}$ ID \times $0.25 \mu\text{m}$ film thickness) was utilized for the GC-FID. Helium was used as the carrier gas. Separated FA species were then identified via comparison of retention times with known standards (Supelco 37 Component FAME Mix). The peak area of each FA was then quantified and expressed as a percent of total FAs detected.

Calculated FA profiles were then utilized to quantify the activities of FA desaturase enzymes by calculating desaturation indices which reflect the ratio of enzyme

product to substrate. Stearoyl-CoA Desaturase 1 (*SCD1*) activity was calculated as the ratio of 16:1n7/16:0 as well as 18:1n9/18:0; Fatty Acid Desaturase 1 (*FADS1*) activity was calculated as the ratio of 20:4n6/20:3n6; and Fatty Acid Desaturase 2 (*FADS2*) activity was calculated as the ratio of 18:3n6/18:2n6 as previously reported [58–61]. Additionally, FA elongation indices of 20:1n9/18:1n9; 18:0/16:0 and 22:5n3/20:5n3 were quantified to calculate the activity of FA elongase enzymes (reflective of enzyme product to substrate ratio) as has previously been reported in placental lysates [62].

Finally, the profiles of neutral lipid species of NEFA treated BeWo trophoblasts were analyzed via Thin Liquid Chromatography coupled Flame Ionization Detection (TLC-FID) as previously described [63]. In brief, collected lipid samples were dried under a gentle stream of N₂ gas and resuspended in 100% chloroform. 1–4 µL of lipids were then spotted onto TLC rods (Chromarod Type S5; Shell-USA, Spotsylvania, VA, USA) and developed in a TLC chamber with benzene:chloroform:formic acid (70:30:0.5 v/v/v). Chromatography rods were then dried and analyzed using the Iatroscan MK-6 TLC-FID system (Shell-USA). Peaks were identified via comparison with known standards, and neutral lipid peak area was quantified and expressed as a percentage of all neutral lipid species identified.

Percent FA composition, percent neutral lipid composition and desaturation index data was analyzed via Randomized Block Two-Way ANOVA (2WA) and Tukey's Multiple Comparisons Test. All statistical analysis was performed with GraphPad Prism v9.2.0 software (GraphPad Software, San Diego, CA, USA).

4.2.4 Transcriptomic analysis of gene expression changes

BeWo CT cells were plated at a density of 3.5×10^5 cells/well in 60 mm cell culture dishes and cultured with exogenous NEFAs as described above. At T72H the CT cells were washed once with PBS and collected in 0.9 mL TRIzol reagent (Invitrogen) and stored at -80°C. Samples were then sent to the Genome Québec Innovation Centre for transcriptomic analysis using the Clariom S mRNA microarray (ThermoFisher Scientific, Mississauga, Canada) as detailed in Chapter 3.

Microarray data was subsequently analyzed using Transcriptome Analysis Console v4.0 (ThermoFisher Scientific). Raw data was normalized using the Robust Multiple-Array Averaging (RMA) method. Each NEFA treatment condition was then compared to the BSA control group in binary, and samples collected from the same passage were paired for analysis. Transcripts with $\geq \pm 1.3$ fold-change (FC) vs BSA control, and raw p-value < 0.05 were determined to be differentially expressed. Each set of differentially expressed genes was then imported into the WEB-based Gene Set AnaLysis Toolkit (WebGestalt) for enrichment analysis of functional pathways using the KEGG database. Functional pathways with FDR-corrected p-value < 0.05 were considered to be significantly enriched.

4.2.5 RT-qPCR validation of differentially expressed genes identified by mRNA microarray

Differentially expressed genes involved in lipid metabolic processes were subsequently individually identified and selected for validation by RT-qPCR. RNA extracted by Genome Québec for mRNA microarray analysis, as well as the RNA extracted for analysis of BeWo syncytialization in Chapter 2 was utilized for RT-qPCR validation. In brief, 2 μg of RNA was reverse transcribed using the High-Capacity cDNA Reverse Transcription Kit (Applied Biosystems; ThermoFisher Scientific). RT-qPCR was subsequently performed using sample cDNA and the CFX384 Real Time System (Bio-Rad, Mississauga, Canada). Relative expression of genes of interest was then determined using the $\Delta\Delta\text{Ct}$ method, with the geometric mean of *PSMB6* and *GAPDH* utilized as a reference. The expression of genes of interest were analyzed in each NEFA treatment in binary versus BSA control samples via paired two-tailed T-test. The sequences of RT-qPCR primers utilized for microarray validation are available in **Table 4-1**.

Table 4-1 Primer sequences used for quantitative Real-Time PCR validation of NEFA treatment microarrays, and their efficiencies.

Gene	Accession No.	Annealing Temperature (°C)	Primer Sequences	Efficiency
<i>GAPDH</i>	NM_001357943.2	60	F – ATGGCATCAAGAAGGTGGTG R – CATACCAGGAAAATGAGCTTG	102.0%
<i>PSMB6</i>	NM_002798	60	F – CGGGAAGACCTGATGGCGGGA R – TCCCGGAGCCTCCAATGGCAA	92.8%
<i>ACACA</i>	NM_198838.2	60	F – GGAGGTGCAGATCTTAGCGG R – CACAGTCCCAGCACTCACAT	95.2%
<i>ACACB</i>	NM_001093.4	60	F – ATTGCCAACAACGGGATTGC R – GGGACGTAATGATCCGCCAT	105.5%
<i>ACADVL</i>	NM_000018.4	60	F – CAGGTGTTCCCATACCCGTC R – GGGATCGTTCACCTCCTCGAA	98.5%
<i>ACSL5</i>	NM_203379.2	60	F – CACCCAAAAGGCATTGGTG R – AGGTCTTCTGGGCTAGGAGG	95.3%
<i>AQP3</i>	NM_004925.5	60	F – CATCTACACCCTGGCACAGA R – ATTGGGGCCCAGAAACAAAAG	98.3%
<i>CREB3L3</i>	NM_032607.3	60	F – TTTGGCCCAACAAAACCG R – GCAGCATCGTTGTGCAAAGT	102.4%
<i>PLIN2</i>	NM_001122.4	60	F – ACCTTCATGGGTAGAGTGGAA R – CACCTTGGATGTTGGACAGG	100.9%
<i>SCD1</i>	NM_005063.5	60	F – TTCGTTGCCACTTTCTTGCG R – AAGTTGATGTGCCAGCGGTA	97.6%

4.2.6 Cell collections for untargeted metabolomic and lipidomic profiling of BeWo CT cells.

BeWo trophoblasts were plated at a density of 2×10^6 cells/plate in 150 mm cell culture dishes and cultured with exogenous NEFAs as described above. AT T72H cell media was aspirated and cells were washed three times with cold PBS. Cellular metabolism was quenched with methanol, and cells were dried under a gentle stream of nitrogen and subsequently by lyophilization. Samples were then shipped to the Metabolomics Innovation Centre (Edmonton, Canada) for untargeted metabolomic and lipidomic profiling of NEFA treated BeWo CT cells as detailed in Chapter 3.

4.2.7 Untargeted metabolomic profiling

The collected metabolomic peak-pair data was then imported into IsoMS pro v1.2.7 for data processing and statistical analysis. Metabolites with $\geq \pm 1.2$ FC and raw p-value < 0.05 in each NEFA treatment versus BSA control were determined to be differentially abundant. Peak pairs of metabolites identified in tiers 1 and 2 that have an

associated KEGG pathway ID number were then imported into MetaboAnalyst v5.0 software for pathway enrichment analysis (using the homo sapiens KEGG Library) to determine biological impacts of differentially abundant metabolites. KEGG pathways with raw p-value < 0.05 were determined to be significantly enriched.

4.2.8 Integration of BeWo cytotrophoblast transcriptomic and metabolomic profiles

Peak Pair data of metabolites in tiers 1 and 2 that have an associated KEGG ID number were imported into MetaboAnalyst v5.0, and metabolites with a $\geq \pm 1.2$ FC and raw p-value < 0.05 in each NEFA treatment were identified. These differentially abundant metabolites associated with a KEGG ID number were subsequently integrated with the list of Differentially Expressed Genes (DEGs) identified in the Clariom S mRNA microarray using the Joint Pathway Analysis Tool in MetaboAnalyst v5.0 to determine enriched pathways containing both DEGs and differentially abundant metabolites. KEGG pathways with raw p-value < 0.05 were determined to be significantly enriched.

4.2.9 Untargeted lipidomic profiling

Lipidomic profiling of NEFA-treated BeWo CT cells was performed as detailed in Chapter 3. Identified and normalized lipid feature intensities were then imported in MetaboAnalyst v5.0 for statistical analysis. Lipid species in each NEFA treatment condition with $\geq \pm 1.5$ FC and raw p-value < 0.05 versus BSA control samples were considered to be differentially abundant. The peak intensities of lipid species from each lipid class from tiers 1 and 2 were subsequently summed to determine the total abundance of each lipid class in the NEFA treatments. These summed data were imported into MetaboAnalyst v5.0 and the total lipid class intensities of each NEFA condition were compared in to the BSA control in binary using a Wilcoxon rank-sum test to determine differentially abundant lipid classes in each NEFA treatment. Significance was determined with a Bonferroni-correct p-value of $p < 0.0167$.

4.2.10 Supplementary data and materials

Microarray data are available on the National Center for Biotechnology Information (NCBI) Gene Expression Omnibus (GEO) database (GSE197385). Supplementary tables were uploaded to a publicly available data repository (doi.org/10.5683/SP3/XMPKOK) and can be accessed via the Digital Object Identifier (DOI) webpage address. Metabolomic and lipidomic peak-pair data are available in Supplementary Tables 9 and 14, respectively.

4.3 Results

4.3.1 NEFA-treatments impact FA profiles of BeWo trophoblasts

A total of 10 saturated FAs (SFA) species, 6 monounsaturated FA (MUFA) species, and 9 polyunsaturated FA (PUFA) species were detected in all BeWo trophoblast samples from at least 4 out of 5 experimental replicates. Palmitic acid (16:0), stearic acid (18:0), Oleic acid (18:1n9c) and arachidonic acid (20:4n6) were highlighted as the most abundant FA species in BeWo trophoblast cultures (**Table 4-2**, n=4-5/group).

PA-treated BeWo cultures displayed increased relative abundances of total SFA species, 16:0, 16:1n7, 22:2, and 20:5n3 as well as decreased relative abundances of total MUFA species, 18:0, and 18:1n9c in both CT and SCT cultures compared to respective differentiation state BSA-control (**Table 4-2**; p<0.05, n=4-5/group). PA-treated BeWo CT cells further displayed increased relative abundance of 22:5n3, while PA-treated BeWo SCT cells displayed reduced relative abundances of 18:1n7 and 18:2n6 versus respective BSA-control cultures (**Table 4-2**; p<0.05, n=4-5/group).

Further, OA-treatment in BeWo CT and SCT trophoblasts was associated with an increased relative abundance of total MUFA species, 18:1n9c, and 20:1n9 as well as a reduced relative abundance of total SFA and PUFA species, 18:0, 24:0, 16:1n7, 18:1n7, 16:3n4, 18:2n6, 20:3n6, 20:4n6, and 22:5n3 versus respective differentiation state BSA-control cultures (**Table 4-2**; p<0.05, n=4-5/group). Additionally, OA-treated BeWo CT cells displayed a significantly decreased relative abundance of 14:0, and 16:0 while OA-

treated BeWo SCT cells displayed a significantly reduced relative abundance of 18:3n6 versus respective differentiation state BSA-control (**Table 4-2**; $p < 0.05$, $n = 4-5/\text{group}$).

P/O-treated BeWo CT and SCT cells were found to have an increased relative abundance of total MUFA species, 20:1n9, and 20:2 as well as decreased relative abundances of 18:0, 24:0, 18:1n7, 18:2n6, and 20:3n6 compared to BSA-control cultures (**Table 4-2**; $p < 0.05$). P/O-cultured BeWo CT cells further demonstrated an increased relative abundance of 18:1n9c as well as decreased relative abundance of total SFA species, 14:0, 16:1n7, and 16:3n4 versus BSA-control CT cultures (**Table 4-2**; $p < 0.05$, $n = 4-5/\text{group}$). Additionally, P/O-treated BeWo SCT cells displayed a decreased relative abundance of 18:3n6 compared to BSA-control SCT cultures (**Table 4-2**; $p < 0.05$, $n = 4-5/\text{group}$).

Syncytialization of BeWo cultures was associated with reduced relative abundances of 20:1n9 and 20:2, as well as increased relative abundances of 18:2n6 and 20:4n6 compared to BeWo CT cells (**Table 4-2**; $p < 0.05$, $n = 4-5/\text{group}$).

Table 4-2 FA profiles (% mol) of NEFA-treated BeWo trophoblast cells.

FA Species	CT				SCT				CT vs SCT
	BSA Ctrl	PA	OA	P/O	BSA Ctrl	PA	OA	P/O	
ΣSFA	39.64 ± 1.1 <i>a</i>	44.91 ± 1.63 <i>b</i>	20.73 ± 1.04 <i>c</i>	33.28 ± 2.99 <i>d</i>	37.20 ± 0.92 <i>a</i>	44.67 ± 0.85 <i>b</i>	24.32 ± 3.18 <i>c</i>	34.25 ± 3.29 <i>a</i>	NS
8:0	0.63 ± 0.23	0.32 ± 0.11	0.40 ± 0.16	0.54 ± 0.10	0.49 ± 0.14	0.34 ± 0.12	0.45 ± 0.11	0.45 ± 0.06	NS
10:0	0.40 ± 0.14	0.31 ± 0.09	0.37 ± 0.11	0.37 ± 0.11	0.21 ± 0.07	0.24 ± 0.05	0.30 ± 0.07	0.21 ± 0.05	NS
14:0	1.43 ± 0.35 <i>a</i>	0.85 ± 0.31 <i>ab</i>	0.52 ± 0.12 <i>b</i>	0.74 ± 0.25 <i>b</i>	1.03 ± 0.33	0.68 ± 0.24	0.40 ± 0.08	0.58 ± 0.18	NS
15:0	0.54 ± 0.16	0.51 ± 0.19	0.19 ± 0.03	0.34 ± 0.14	0.45 ± 0.10	0.59 ± 0.19	0.28 ± 0.02	0.48 ± 0.14	NS
16:0	19.73 ± 0.81 <i>a</i>	27.84 ± 2.12 <i>b</i>	8.27 ± 0.81 <i>c</i>	17.52 ± 2.87 <i>a</i>	16.32 ± 0.78 <i>ab</i>	28.07 ± 1.37 <i>c</i>	12.17 ± 3.01 <i>a</i>	19.74 ± 2.80 <i>b</i>	NS
18:0	14.98 ± 0.48 <i>a</i>	12.79 ± 0.76 <i>b</i>	9.23 ± 0.41 <i>c</i>	12.04 ± 0.79 <i>b</i>	16.20 ± 0.36 <i>a</i>	12.46 ± 0.89 <i>b</i>	9.26 ± 0.41 <i>c</i>	10.98 ± 0.43 <i>bc</i>	NS
20:0	0.78 ± 0.06	0.94 ± 0.09	0.79 ± 0.16	0.74 ± 0.07	1.21 ± 0.17	1.10 ± 0.24	0.73 ± 0.10	0.92 ± 0.14	NS
22:0	0.68 ± 0.11	0.80 ± 0.16	0.47 ± 0.10	0.53 ± 0.06	0.76 ± 0.11 <i>ab</i>	0.91 ± 0.08 <i>a</i>	0.47 ± 0.07 <i>b</i>	0.74 ± 0.08 <i>ab</i>	NS
23:0	0.49 ± 0.14	0.58 ± 0.11	0.52 ± 0.02	0.64 ± 0.05	0.23 ± 0.03	0.44 ± 0.12	0.27 ± 0.03	0.41 ± 0.09	NS
24:0	1.02 ± 0.05 <i>a</i>	1.08 ± 0.07 <i>a</i>	0.70 ± 0.06 <i>b</i>	0.79 ± 0.07 <i>b</i>	0.98 ± 0.05 <i>a</i>	0.89 ± 0.05 <i>a</i>	0.54 ± 0.02 <i>b</i>	0.63 ± 0.05 <i>b</i>	NS
ΣMUFA	42.82 ± 1.14 <i>a</i>	36.29 ± 1.21 <i>b</i>	68.11 ± 1.26 <i>c</i>	49.99 ± 4.19 <i>d</i>	42.91 ± 1.15 <i>a</i>	34.91 ± 0.43 <i>b</i>	63.40 ± 4.28 <i>c</i>	49.35 ± 4.35 <i>d</i>	NS
16:1n7	3.12 ± 0.18 <i>a</i>	5.23 ± 0.67 <i>b</i>	0.80 ± 0.12 <i>c</i>	1.87 ± 0.42 <i>c</i>	2.86 ± 0.33 <i>a</i>	6.20 ± 0.46 <i>b</i>	1.43 ± 0.41 <i>c</i>	2.42 ± 0.39 <i>ab</i>	NS
18:1n9c	33.09 ± 1.32 <i>a</i>	24.76 ± 1.59 <i>b</i>	63.73 ± 1.47 <i>c</i>	43.84 ± 4.64 <i>d</i>	32.65 ± 1.29 <i>a</i>	23.08 ± 0.54 <i>b</i>	62.64 ± 0.68 <i>c</i>	38.52 ± 0.83 <i>ab</i>	NS
18:1n9t	0.23 ± 0.02	0.34 ± 0.08	0.38 ± 0.07	0.23 ± 0.04	0.28 ± 0.03	0.46 ± 0.23	0.33 ± 0.07	0.41 ± 0.19	NS
18:1n7	5.99 ± 0.26 <i>a</i>	5.69 ± 0.23 <i>a</i>	2.91 ± 0.17 <i>b</i>	3.78 ± 0.31 <i>c</i>	6.86 ± 0.23 <i>a</i>	4.89 ± 0.20 <i>b</i>	3.03 ± 0.16 <i>c</i>	3.39 ± 0.18 <i>c</i>	NS
20:1n9	0.49 ± 0.02 <i>a</i>	0.45 ± 0.02 <i>a</i>	1.46 ± 0.08 <i>b</i>	0.92 ± 0.14 <i>c</i>	0.48 ± 0.04 <i>a</i>	0.37 ± 0.02 <i>a</i>	0.99 ± 0.10 <i>b</i>	0.77 ± 0.17 <i>c</i>	*
22:1n9	0.29 ± 0.13	0.21 ± 0.08	0.19 ± 0.01	0.20 ± 0.03	0.16 ± 0.03	0.24 ± 0.09	0.18 ± 0.02	0.20 ± 0.06	NS
ΣPUFA	16.30 ± 0.94 <i>ab</i>	17.47 ± 0.82 <i>a</i>	9.18 ± 0.44 <i>c</i>	15.02 ± 1.79 <i>b</i>	18.89 ± 0.78 <i>a</i>	18.96 ± 0.42 <i>a</i>	10.68 ± 1.24 <i>b</i>	14.84 ± 1.27 <i>b</i>	NS
16:3n4	0.34 ± 0.04 <i>ab</i>	0.23 ± 0.02 <i>ab</i>	0.16 ± 0.02 <i>b</i>	0.22 ± 0.03 <i>b</i>	0.37 ± 0.04 <i>a</i>	0.30 ± 0.05 <i>a</i>	0.19 ± 0.02 <i>b</i>	0.28 ± 0.03 <i>ab</i>	NS
18:2n6	2.52 ± 1.21 <i>ab</i>	1.36 ± 0.24 <i>a</i>	0.61 ± 0.04 <i>b</i>	0.82 ± 0.08 <i>b</i>	3.24 ± 0.98 <i>a</i>	1.45 ± 0.04 <i>b</i>	0.94 ± 0.04 <i>c</i>	1.11 ± 0.07 <i>c</i>	*
18:3n6	0.230 ± 0.005	0.234 ± 0.029	0.194 ± 0.006	0.226 ± 0.022	0.324 ± 0.016 <i>a</i>	0.265 ± 0.024 <i>ab</i>	0.201 ± 0.009 <i>c</i>	0.235 ± 0.011 <i>bc</i>	NS
20:2	1.48 ± 0.12 <i>ab</i>	3.03 ± 0.24 <i>b</i>	1.69 ± 0.11 <i>a</i>	3.23 ± 0.48 <i>b</i>	0.97 ± 0.15 <i>a</i>	2.00 ± 0.18 <i>b</i>	1.23 ± 0.27 <i>a</i>	1.83 ± 0.23 <i>b</i>	*
20:3n6	1.45 ± 0.07 <i>ab</i>	1.43 ± 0.08 <i>a</i>	0.72 ± 0.05 <i>b</i>	1.09 ± 0.12 <i>c</i>	1.66 ± 0.06 <i>a</i>	1.46 ± 0.05 <i>a</i>	0.76 ± 0.08 <i>b</i>	1.03 ± 0.08 <i>c</i>	NS
20:4n6	8.68 ± 0.39 <i>ab</i>	9.18 ± 0.50 <i>a</i>	5.08 ± 0.25 <i>b</i>	8.07 ± 0.94 <i>a</i>	11.12 ± 0.28 <i>a</i>	11.34 ± 0.38 <i>a</i>	6.52 ± 0.78 <i>b</i>	8.82 ± 0.85 <i>c</i>	*
20:4n3	0.15 ± 0.06	0.19 ± 0.10	0.07 ± 0.01	0.15 ± 0.04	0.14 ± 0.03	0.28 ± 0.11	0.08 ± 0.02	0.21 ± 0.09	NS
20:5n3	0.54 ± 0.14 <i>ac</i>	0.95 ± 0.14 <i>b</i>	0.16 ± 0.02 <i>a</i>	0.64 ± 0.15 <i>bc</i>	0.39 ± 0.05 <i>a</i>	0.92 ± 0.13 <i>b</i>	0.27 ± 0.06 <i>a</i>	0.63 ± 0.11 <i>ab</i>	NS
22:5n3	0.43 ± 0.05 <i>a</i>	0.52 ± 0.03 <i>b</i>	0.31 ± 0.01 <i>c</i>	0.39 ± 0.04 <i>ac</i>	0.53 ± 0.01 <i>a</i>	0.61 ± 0.02 <i>a</i>	0.33 ± 0.02 <i>b</i>	0.41 ± 0.04 <i>b</i>	NS

Data are mean ± SEM (n=4-5/group). Different lower-case letters denote statistical difference in FA abundance between NEFA treatments within a differentiation state. * denotes a differentiation state dependent difference in FA abundance between BeWo CT and SCT cells; NS indicates no statistical significance between differentiation states.

4.3.2 The impact of NEFA treatments on desaturation and elongation indices in BeWo trophoblasts

FA profile data was utilized to quantify the activity of FA desaturase and elongase enzymes via calculation of the ratios of enzyme products to substrates (desaturation/elongation index). OA and P/O-treated BeWo SCT and SCT cells displayed a reduced SCD1 index compared to respective BSA-control cultures when assessed by the 16:1n7/16:0 index (**Figure 4-1 A**; $p < 0.05$, $n = 5/\text{group}$). However, when the SCD1 index was assessed by the ratio of 18:1n9c/18:0, OA and P/O-treated BeWo CT and SCT cells were found to have increased SCD1 activity compared to respective BSA-control cultures (**Figure 4-1 B**; $p < 0.05$, $n = 5/\text{group}$). Furthermore, OA-treated BeWo CT cells displayed an increased FADS2 index (**Figure 4-1 C**; $p < 0.05$, $n = 5/\text{group}$) while OA-treated SCT cells displayed increased FADS2 and FADS1 indices compared to BSA-control cultures (**Figure 4-1 C,D**; $p < 0.05$, $n = 5/\text{group}$). P/O-treated BeWo CT and SCT also displayed increased FADS1 and FADS2 indices compared to BSA-controls (**Figure 4-1 C,D**; $p < 0.05$, $n = 5/\text{group}$). Finally, PA-treated BeWo SCT cells displayed an increased FADS2 index compared to BSA-control SCT cells (**Figure 4-1 C**; $p < 0.05$, $n = 5/\text{group}$). BeWo syncytialization was additionally linked with an increased SCD1 (when assessed as 16:1n7/16:0), and FADS1 index as well as with a decreased FADS2 index (**Figure 4-1 A,C,D**; $p < 0.05$, $n = 5/\text{group}$).

OA-treatment was additionally increased elongation of 18:1n9, 16:0, and 20:5n3 in BeWo CT cells, while P/O-treated BeWo CT were only observed to have increased 18:1n9 elongation (**Figure 4-2 A-C**). PA-treatment in BeWo SCT cells, however, was linked with reduced 16:0, and 20:5n3 elongation (**Figure 4-2 B,C**). BeWo SCT also displayed an overall reduced elongation of 18:1n9 compared to BeWo CT cells (**Figure 4-2 A**).

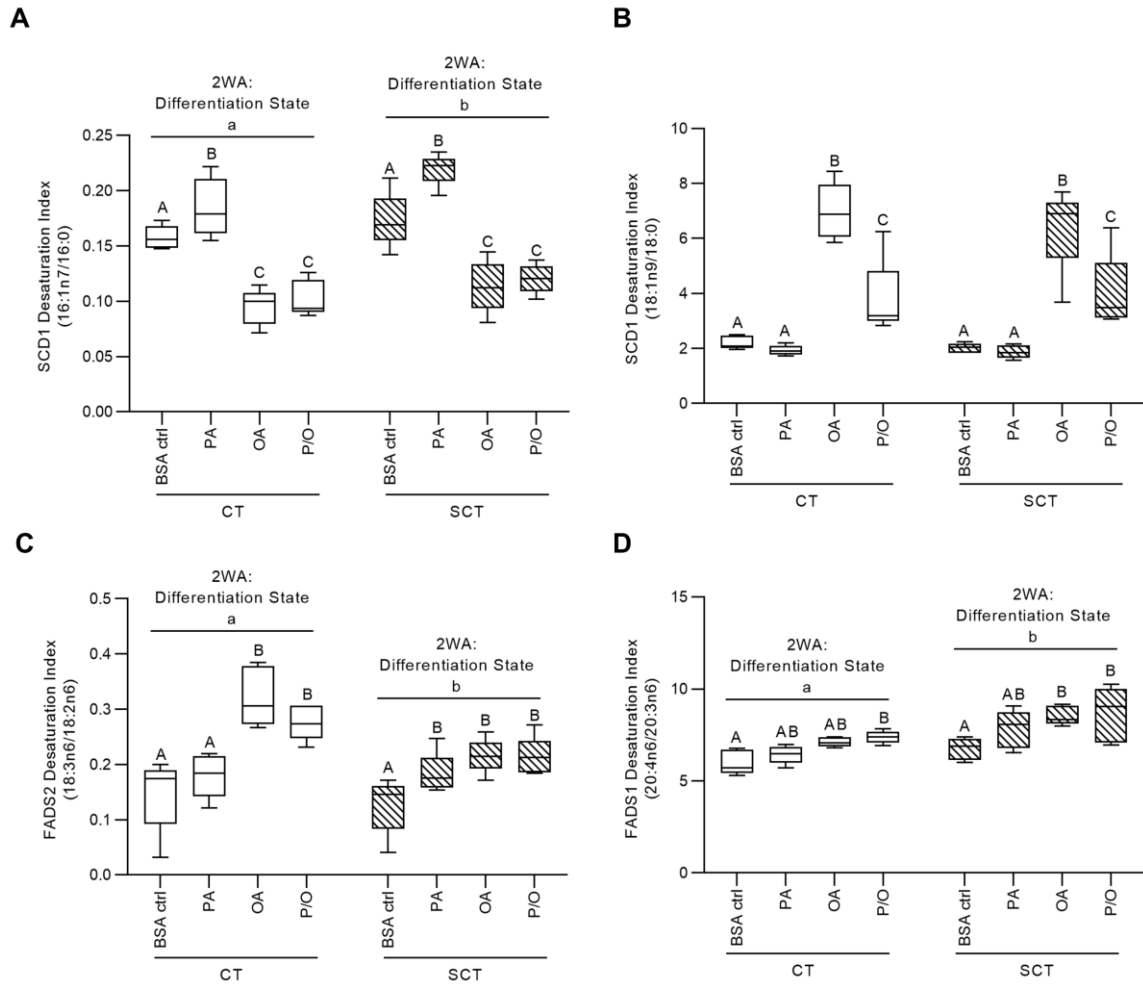


Figure 4-1 FA desaturase enzyme activity indices in NEFA-treated BeWo CT and SCT cells.

The abundance of desaturase enzyme substrate and product FAs were quantified via Gas Chromatography-coupled Flame Ionization Detection, and the activity of each desaturase enzyme was quantified via desaturation index, reflecting the ratio of enzyme product to substrate. The Stearoyl-CoA Desaturase-1 (SCD1) index was quantified via the ratios **(A)** 16:1n7/16:0 ratio and **(B)** 18:1n9/18:0; **(C)** the Fatty Acid Desaturase 1 index was quantified via the ratio of 18:3n6/18:2n6; and **(D)** the Fatty Acid Desaturase 2 index was quantified via the ratio of 20:4n6/20:3n6 (N=5/group; different upper-case letters denote statistical significance between NEFA treatments within each BeWo differentiation state, and different lower-case represents statistical significance between differentiation states; Two-Way Randomized Block ANOVA, Tukey's multiple comparisons Test).

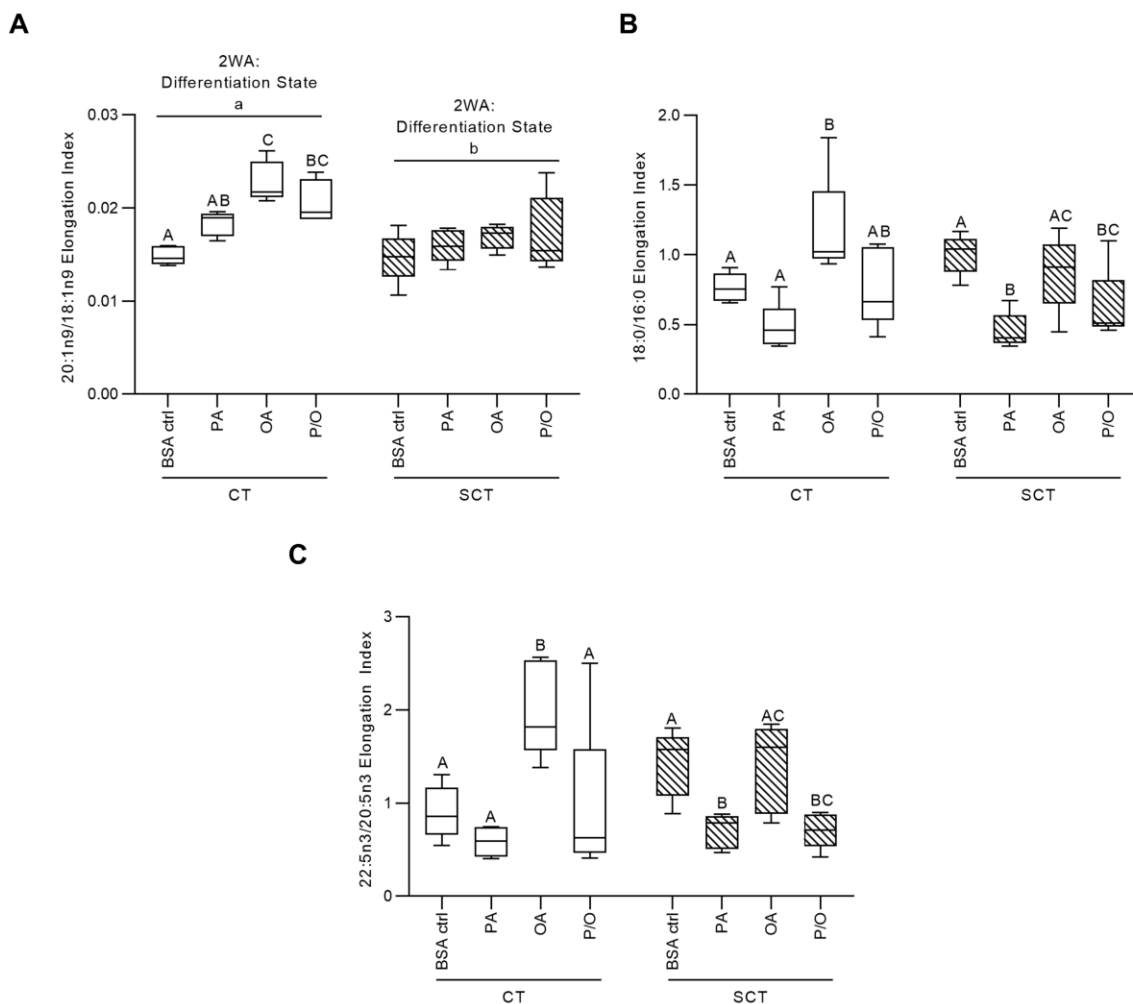


Figure 4-2 FA elongase enzyme activity Indices in NEFA-treated BeWo CT and SCT cells.

The abundance of products and substrates of FA elongase enzymes were quantified via gas chromatography coupled flame ionization detection. Subsequently the ratios of (A) 20:1n9/18:1n9, (B) 18:0/16:0, and (C) 22:5n3/20:5n3 (elongation indices) were quantified to determine elongase enzyme activities (N=5/group; different upper-case letters denote statistical significance between NEFA treatments within each BeWo differentiation state, and different lower-case represents statistical significance between differentiation states; Two-Way Randomized Block ANOVA, Tukey's multiple comparisons Test).

4.3.3 OA-treatment alters neutral lipid profiles of BeWo trophoblasts

TLC-FID analysis of extracted lipids from BeWo cultures identified five neutral lipid species in all samples. Specifically, these analyses identified cholesterol ester, free FAs, triglycerides, free cholesterol, and diacylglycerols in the neutral lipid fractions of BeWo trophoblast cells. OA-treated BeWo CT and SCT displayed increased relative triglyceride abundances as well as decreased relative free cholesterol abundances relative to respective differentiation state BSA-control cultures (**Table 4-3**; 2WA: NEFA treatment $p < 0.05$, $n=5/\text{group}$).

Table 4-3 Neutral lipid profiles of NEFA-treated BeWo trophoblast cells.

Neutral Lipid Species	CT				SCT			
	BSA Ctrl	PA	OA	P/O	BSA Ctrl	PA	OA	P/O
Cholesterol Esters	10.07 ± 2.66	25.46 ± 9.52	11.29 ± 2.28	15.44 ± 4.39	9.03 ± 1.69	17.56 ± 6.19	12.19 ± 4.33	19.18 ± 7.54
Free FAs	10.46 ± 3.67	11.91 ± 5.12	8.90 ± 3.36	10.05 ± 4.04	11.33 ± 3.69	9.93 ± 2.81	7.81 ± 2.89	8.72 ± 2.55
Triglycerides	15.99 ± 5.14 <i>a</i>	17.12 ± 2.63 <i>a</i>	39.47 ± 2.59 <i>b</i>	18.35 ± 2.88 <i>a</i>	14.34 ± 1.97 <i>a</i>	14.74 ± 1.51 <i>a</i>	30.86 ± 4.95 <i>b</i>	17.96 ± 1.19 <i>a</i>
Free Cholesterol	61.80 ± 6.21 <i>a</i>	43.6 ± 5.91 <i>bc</i>	37.84 ± 1.32 <i>b</i>	53.79 ± 3.88 <i>ac</i>	62.88 ± 3.19 <i>a</i>	56.39 ± 5.57 <i>ab</i>	46.40 ± 4.62 <i>b</i>	52.24 ± 6.66 <i>ab</i>
Diacylglycerols	1.68 ± 0.32	1.91 ± 0.77	2.51 ± 0.35	2.37 ± 0.42	2.43 ± 0.89	1.38 ± 0.24	2.75 ± 0.07	1.90 ± 0.26

Data are percent of neutral lipid fraction (mean ± SEM; n=5/group). Different lower-case letters denote statistical differences between NEFA-treatments within each differentiation state.

4.3.4 Transcriptomic profiles of BeWo cytotrophoblasts are impacted by NEFA treatment.

PA-treated BeWo CT cultures displayed 340 differentially expressed genes (DEGs) (140 up-regulated, and 200 down-regulated); OA-treated CT cultures displayed 208 DEGs (88 up-regulated, and 120 down-regulated); and P/O-treated BeWo CT cultures displayed 221 DEGs (96 up-regulated, and 125 down-regulated) when compared to BSA-control CT cultures ($\geq \pm 1.3$ FC vs BSA control CT cultures; raw- $p < 0.05$, $n=5$ /group). A 3D Principal Component Analysis (PCA) plot was constructed to visualize the degree of separation in transcriptome profiles between the NEFA-treated BeWo CT cells (**Figure 4-3**). Volcano plots were additionally constructed to visualize differentially expressed transcripts in each NEFA-treatment versus the BSA control samples (**Figure 4-4 A-C**). A summary of the DEGs identified in each NEFA-treatment condition is available in **Supplementary Table 7** (doi.org/10.5683/SP3/XMPKOK).

The DEG sets from each NEFA condition were then imported into WebGestalt to examine enrichment of functional pathways in the Wikipathways database. No significantly enriched functional pathways were highlighted in the DEG sets for PA and OA-treated BeWo CT cells (**Figure 4-5 A,B**; FDR-corrected $p > 0.05$). The Fatty Acid Biosynthesis Pathway (DEG involved were *ACACB* (+1.32 FC), *ACSL5* (+1.77 FC), *ACSL6* (-1.34 FC), and *SCD* (-1.24 FC)) was found to be significantly enriched in the P/O-cultured cells (**Figure 4-5 C**; FDR-corrected $p < 0.05$).

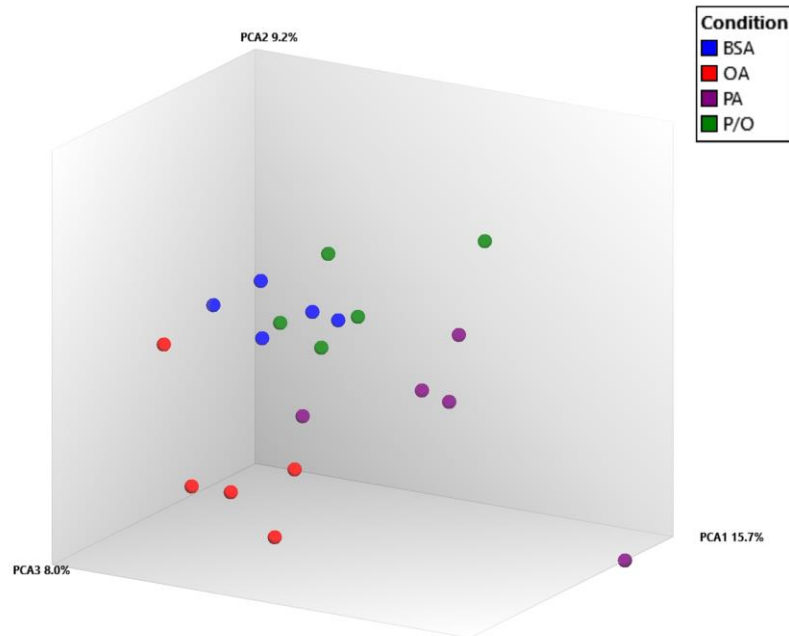


Figure 4-3 Principal Component Analysis (PCA) plot highlighting separation in transcriptome profiles between NEFA-treated BeWo CT cells.

An unsupervised PCA plot was constructed to visualize the degree of separation in transcriptomic profiles between PA-treated (purple dots), OA-treated (red dots), P/O-treated (green dots), and BSA-control (blue dots) BeWo CT cells.

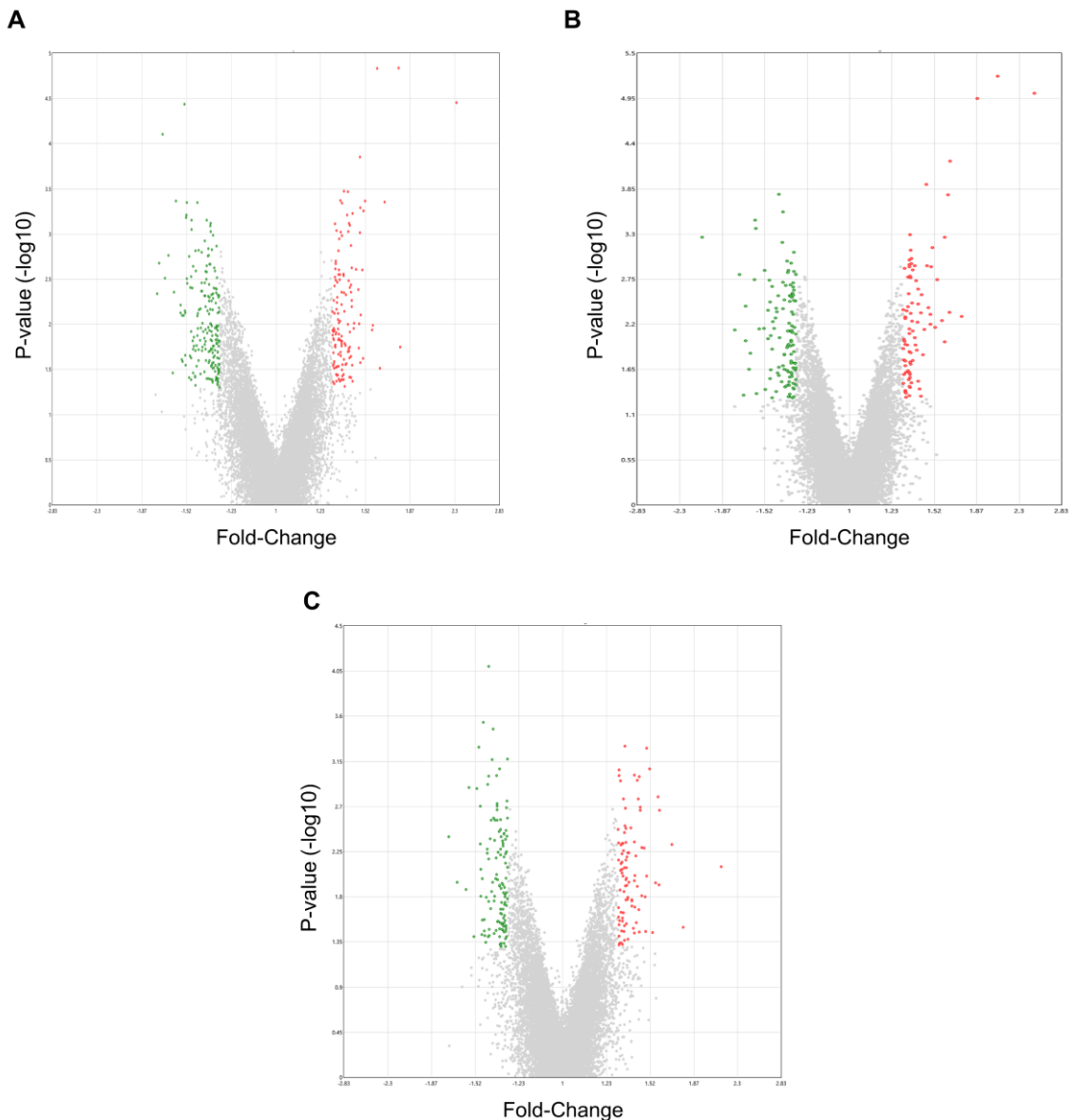


Figure 4-4 Volcano plot visualization of differentially expressed genes in BeWo CT cells cultured with 100 μ M NEFAs for 72 hours.

The transcriptome profiles of NEFA-treated BeWo cytotrophoblast cells was determined via Clariom S mRNA microarray, and differentially expressed genes were determined with ± 1.3 fold-change and raw $p < 0.05$ cut-offs. Volcano plots were constructed to visualize differentially expressed genes in (A) PA-treated cells; (B) OA-treated cells; and (C) P/O-treated cells compared to BSA-alone treated cells ($n=5$ /group). The x-axis indicates fold-change vs BSA control, and the y-axis indicates p-value ($-\log_{10}$). Red dots represent up-regulated genes, green dots represent down-regulated genes while the black dots represent non-statistically significant transcripts.

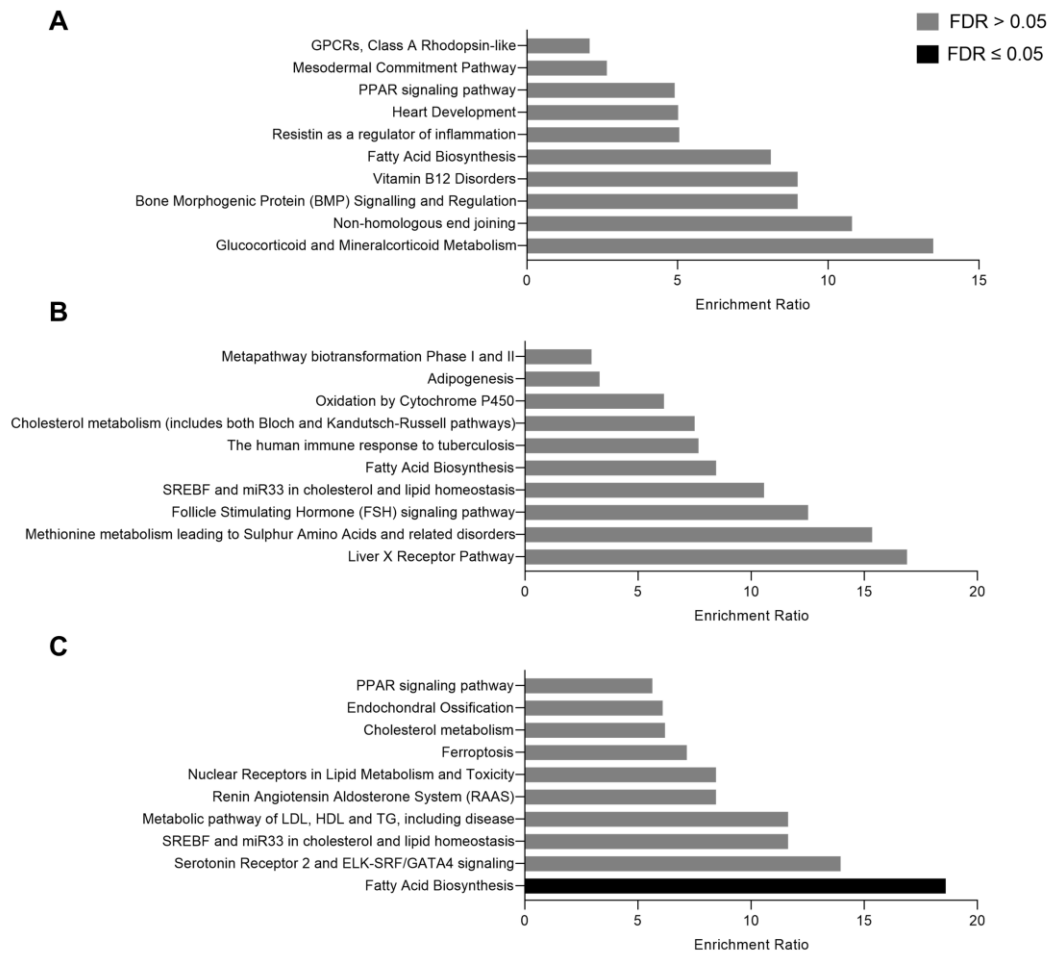


Figure 4-5 Functional pathways enriched by NEFA-treatments in BeWo CT cells.

The WEB-based Gene SeT AnaLysis Toolkit (Webgestalt) was utilized to examine functional pathway enrichment in **(A)** PA-treated; **(B)** OA-treated; and **(C)** P/O-treated BeWo CT cultures. Each plot highlights the top 10 (by FDR-corrected p-value) functional pathways enriched in the differentially expressed gene sets. Black bars represent significantly enriched functional pathways (FDR-corrected $p < 0.05$), and grey bars highlight non-significantly enriched functional pathways. The Fatty Acid Biosynthesis pathway was identified as significantly enriched in P/O-treated BeWo CT cells.

4.3.5 RT-qPCR Validation of Differentially Expressed Genes

A Venn-diagram was additionally then constructed to visualize the DEGs that were unique to each NEFA-treatment, as well as those common in two or all of the NEFA-treatment conditions (**Figure 4-6A**). Twenty-three differentially expressed transcripts were found to be common between PA and OA-treated CT cells; 32 DEGs were common between PA and P/O treatments; and 9 genes were found to be differentially expressed in both OA and PO-treated cells (**Figure 4-6A**). A further 9 genes were found to be differentially expressed in all NEFA-treated BeWo CT cells (**Figure 4-6 A**). A summary list of unique and common DEGs is available in **Supplementary Table 8** (doi.org/10.5683/SP3/XMPKOK).

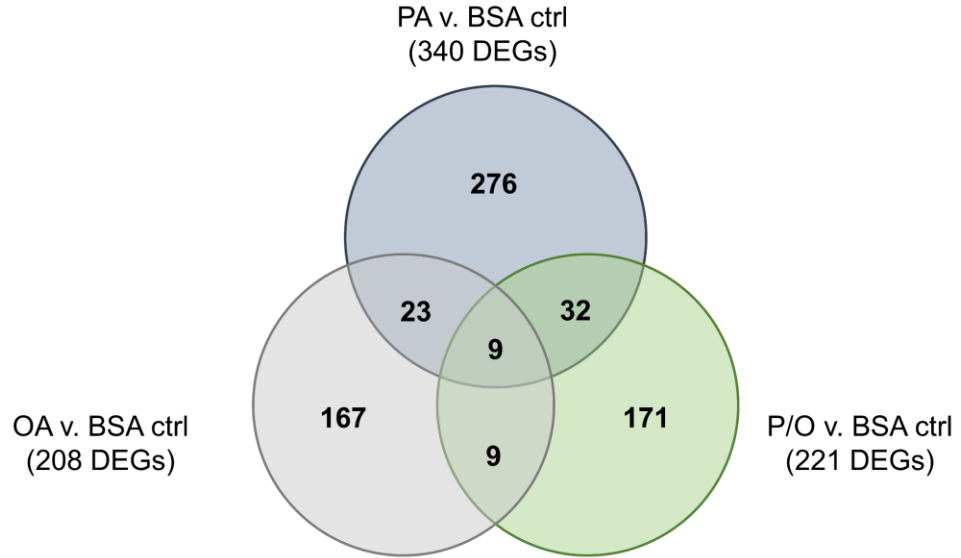
In PA-treated BeWo CT cells, RT-qPCR analysis confirmed differential expression of *ACACB* (+1.57 FC microarray; +1.34 FC RT-qPCR); *ACADVL* (+1.32 FC microarray; +1.47 FC RT-qPCR); *ACSL5* (+1.77 FC microarray; +2.57 FC RT-qPCR); *CREB3L3* (+2.31 FC microarray; +5.29 FC RT-qPCR); *PLIN2* (+1.35 FC microarray; +1.83 FC RT-qPCR) (**Figure 4-6 B**, $p < 0.05$, $n=9$). It is important to note that *SCD* mRNA abundance although statistically significant ($p < 0.05$) in the microarray panel did not meet the ± 1.3 FC cut-off to be considered differentially expressed in PA-treated CT cells (-1.16 FC). However, subsequent RT-qPCR analysis highlighted a significant decrease in *SCD* mRNA abundance in PA-treated BeWo CT cells (-1.24 FC; **Figure 4-6 B**, $p < 0.05$, $n=9$). The microarray panel also highlighted a significant downregulation in a transcript best identified as *ACACA*, however RT-qPCR analysis demonstrated no significant alterations in *ACACA* mRNA abundance (**Figure 4-6 B**, $p=0.057$, $n=9$). Finally, *AQP3* was highlighted as differentially expressed in the microarray panel, however there was no significant difference in *AQP3* mRNA abundance when assessed by RT-qPCR (**Figure 4-6 B**, $p=0.4287$, $n=9$).

In OA-treated BeWo CT cells, RT-qPCR analysis confirmed the differential expression of: *ACSL5* (+1.87 FC microarray; +2.60 FC RT-qPCR); *CREB3L3* (+2.48 FC microarray; +7.38 FC RT-qPCR); *PLIN2* (+1.46 FC microarray; +1.90 FC RT-qPCR); and *SCD* (-1.41 FC microarray; -1.98 FC RT-qPCR) (**Figure 4-6 C**, $p < 0.05$, $n=9$). The microarray panel also highlighted a significant increase in *ACADVL* mRNA abundance

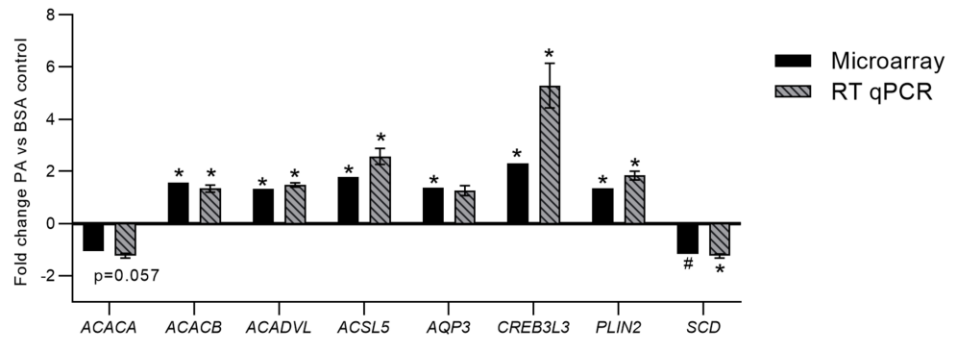
although this transcript did not meet the ± 1.3 FC cut-off to be considered differentially expressed. However, the RT-qPCR analysis highlighted a significant increase in *ACADVL* mRNA abundance in OA-treated BeWo CT cells (+1.43 FC; **Figure 4-6 C**, $p < 0.05$, $n = 9$).

In P/O-treated BeWo CT cells, RT-qPCR analysis confirmed the differential expression of *ACACB* (+1.32 FC microarray; +1.12 FC RT-qPCR); *ACSL5* (+1.77 FC microarray; +2.50 FC RT-qPCR); *CREB3L3* (+2.13 FC microarray; +6.23 FC RT-qPCR); *PLIN2* (+1.30 FC microarray; +1.79 FC RT-qPCR); and *SCD* (-1.34 FC microarray; -1.52 FC RT-qPCR) (**Figure 4-6 D**; $p < 0.05$, $n = 9/\text{group}$). The RT-qPCR analysis additionally highlighted a significant increase in the expression of *ACADVL* (+1.48 FC) and a decrease in the expression of *ACACA* (-1.32 FC) (**Figure 4-6 D**, $p < 0.05$, $n = 9/\text{group}$). Interestingly, the expression of both *ACADVL* (+1.22 FC, $p = 0.0609$) and *ACACA* (-1.11 FC, $p = 0.0862$) were trending towards significance in the microarray panel.

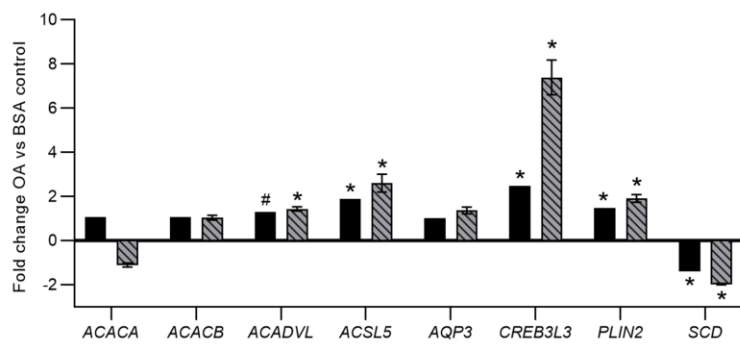
A



B



C



D

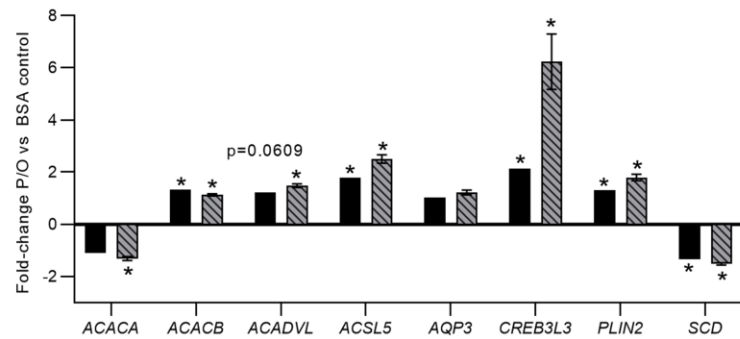


Figure 4-6 Venn-diagram representation of differentially expressed genes between NEFA-treated BeWo CT cells and RT-qPCR validation of differentially expressed genes.

(A) A Venn-diagram was constructed to visualize the number of differentially expressed transcripts that are unique to each NEFA-treatment or common to multiple NEFA-treatments. Differential expression of genes involved in lipid metabolic processes were validated in (B) PA, (C) OA, and (D) P/O-treated BeWo CT cells via RT-qPCR. RT-qPCR data were analyzed via paired two-tailed t-test (n=9/group), and the data expressed as fold-change vs BSA-control cultures (mean±SEM). *indicates $\geq \pm 1.3$ FC vs BSA-control, $p < 0.05$ for microarray data; and $p < 0.05$ for RT-qPCR data. #indicates < 1.3 FC vs BSA-control, $p < 0.05$ for microarray data.

4.3.6 Metabolomic profiles of BeWo Cytotrophoblast in response to NEFA treatment

On average, 6569 ± 50 (\pm SD) metabolite features were identified in each NEFA-treated BeWo CT samples. A summary of the identified metabolite features and peak-pair data in NEFA-treated BeWo CT cells is available in **Supplementary Table 9** (doi.org/10.5683/SP3/XMPKOK). Of these features, 179 metabolites were identified with high confidence in tier 1 and a further 602 metabolites were identified with high confidence in tier 2. In PA-treated cultures, 2 metabolites in tier 1, 7 metabolites in tier 2, and 97 metabolites in tier 3 were found to be differentially abundant when compared to BSA-control samples ($\geq \pm 1.2$ FC vs BSA control CT cultures, raw- $p < 0.05$, $n = 5$ /group). Furthermore, 5 metabolites identified in tier 1, 12 metabolites from tier 2, and 78 metabolites in tier 3 were found to be differentially abundant in OA-treated CT cells when compared to BSA-control samples ($\geq \pm 1.2$ FC vs BSA control CT cultures, raw- $p < 0.05$, $n = 5$ /group). Finally, 7 metabolites identified in tier 1; 7 metabolites identified in tier 2; and 92 metabolites identified in tier 3 were found to be differentially abundant in P/O-treated BeWo CT cultures when compared to BSA-control samples ($\geq \pm 1.2$ FC vs BSA control CT cultures, raw- $p < 0.05$, $n = 5$ /group). A summary of the differentially abundant metabolites (from all tiers) in each NEFA treatment versus the BSA control is available in **Supplementary Tables 10–12** (doi.org/10.5683/SP3/XMPKOK).

An unsupervised principal component analysis (PCA) 2D plot as well as supervised partial-least squares discriminant analysis (PLS-DA) 2D plot was constructed to visualize the degree of difference between metabolite profiles in all NEFA-treatment groups (**Figure 4-7**). Volcano plots were constructed to visualize the differentially abundant metabolite species in each NEFA-treatment group versus BSA-control samples (**Figure 4-8 A-C**). Additionally, a Venn-diagram was constructed to highlight the number of unique and shared differentially abundant metabolites in the NEFA treatments which highlighted that most differentially abundant metabolites were unique to one NEFA treatment (**Figure 4-9**). Only 3 high confidence identified metabolites from tiers 1 and 2 were found to be differentially abundant in at least 2 of the NEFA treatments. Specifically, the abundance of Kahweol was found to be significantly increased (+1.69

FC in OA; +1.64 FC in P/O), and the abundance of N-acetyethanolamine was found to be significantly decreased in both the OA and P/O treatments (-1.66 FC in OA; -1.46 FC in P/O), while the abundance of 3-hydroxymethylglutaric acid was found to be significantly decreased in both the PA and P/O treatments (-2.89 FC in PA; -2.00 FC in P/O). A summary of the unique and shared differentially abundant metabolites in the NEFA-treated BeWo CT cells is available in **Supplementary Table 13** (doi.org/10.5683/SP3/XMPKOK).

Analysis of KEGG pathway enrichment of the metabolite sets from tiers 1 and 2 was subsequently performed using MetaboAnalyst software. Scatterplots were created to visualize the KEGG pathway nodes highlighted by each metabolite (**Figure 4-10**). No significantly KEGG pathways were identified as significantly enriched in the metabolite sets from PA and P/O-treated BeWo CT cells (**Figure 4-10 A,C**). The KEGG pathways for **i**) Ether lipid metabolism (highlighted by increased sn-glycerol-3-phosphoethanolamine (+3.44 FC) levels), **ii**) Amino sugar and nucleotide sugar metabolism (highlighted by reduced 6-deoxy-L-galactose (-1.17 FC) levels); **iii**) Fructose and mannose metabolism (highlighted by reduced 6-deoxy-L-galactose (-1.17 FC) levels); and **iv**) Taurine and hypotaurine metabolism (highlighted by a trend towards reduced abundance of 5-L-Glutamyl taurine (-1.82 FC; $p=0.062$) and 3-sulfino-L-alanine (-1.47 FC; $p=0.054$)) were determined to be significantly enriched in the OA-treated CT metabolite set (**Figure 4-10 B**).

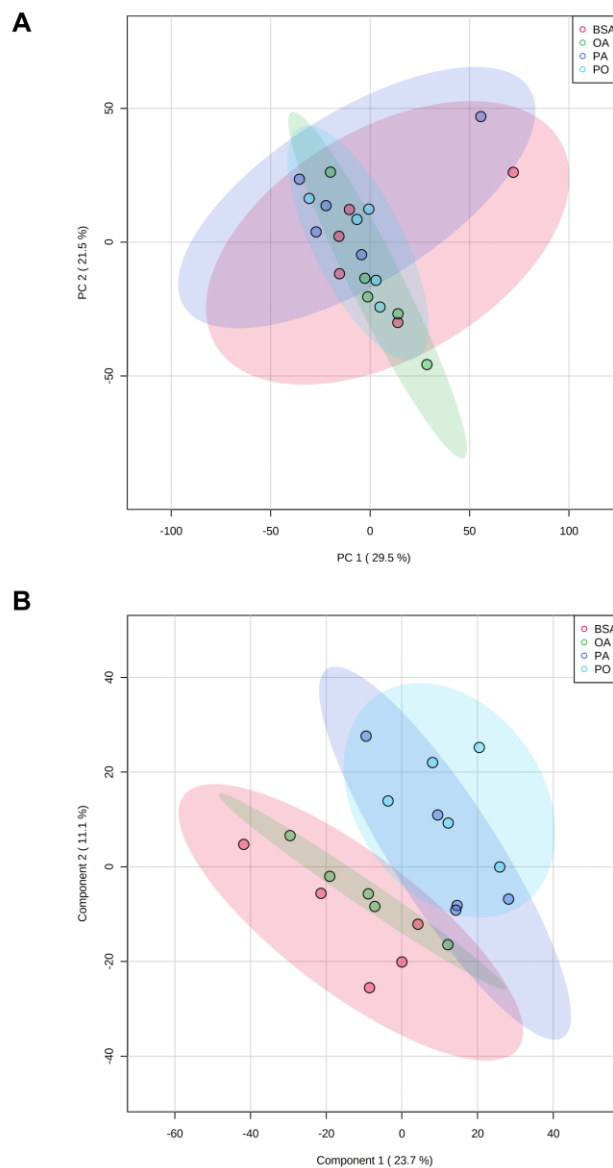


Figure 4-7 Multivariate visualization of the degree of separation between metabolite profiles in NEFA-treated BeWo CT cells.

(A) Unsupervised principal component analysis (PCA) and (B) supervised partial least squares discriminant analysis (PLS-DA) plots were utilized to visualize the degree of difference in metabolite profiles between PA, OA, P/O and BSA-control cultures.

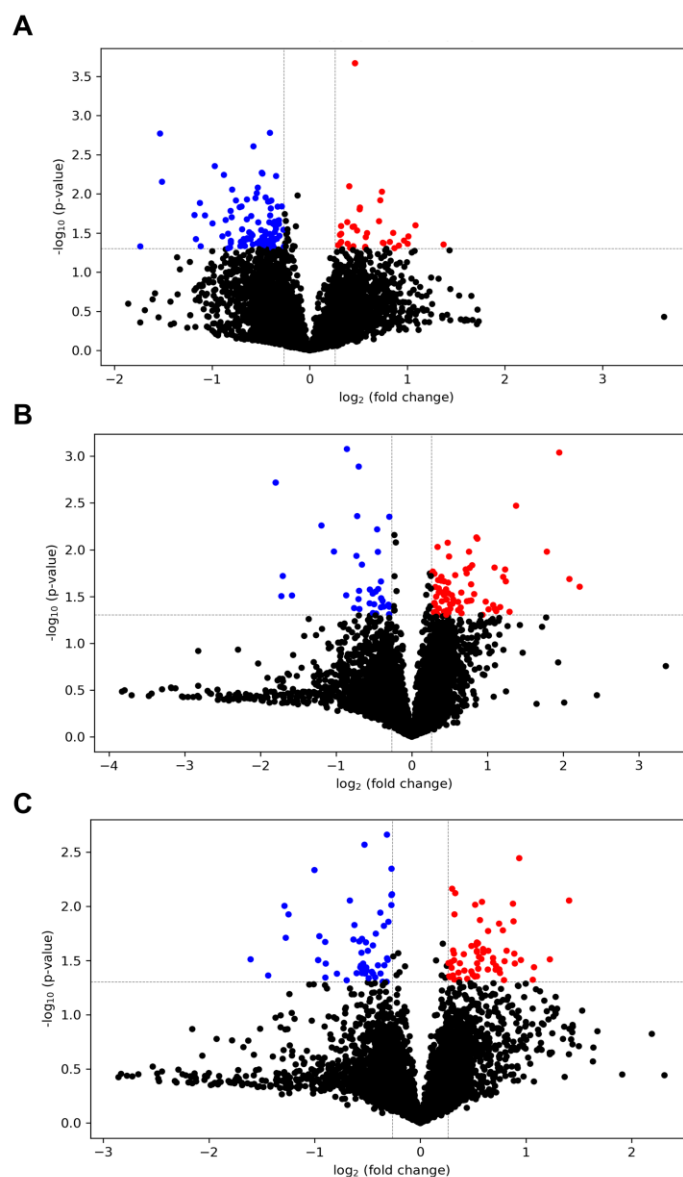


Figure 4-8 Volcano plot visualization of the differentially abundant metabolites in NEFA-treated BeWo CT cultures.

Volcano plots were constructed to visualize differentially abundant metabolites in (A) PA-treated; (B) OA-treated; and (C) P/O-treated BeWo CT cultures vs BSA-control cultures. Statistically significant differentially expressed metabolites were determined as $\geq \pm 1.2$ fold-change vs BSA-control and raw $p < 0.05$ ($n=5/\text{group}$). The x-axis represents $\log_2(\text{fold-change})$ vs BSA-control and the y-axis represents p-value ($-\log_{10}$). Red dots represent individual metabolites with significantly increased abundance while the blue dots represent metabolites with significantly reduced abundance.

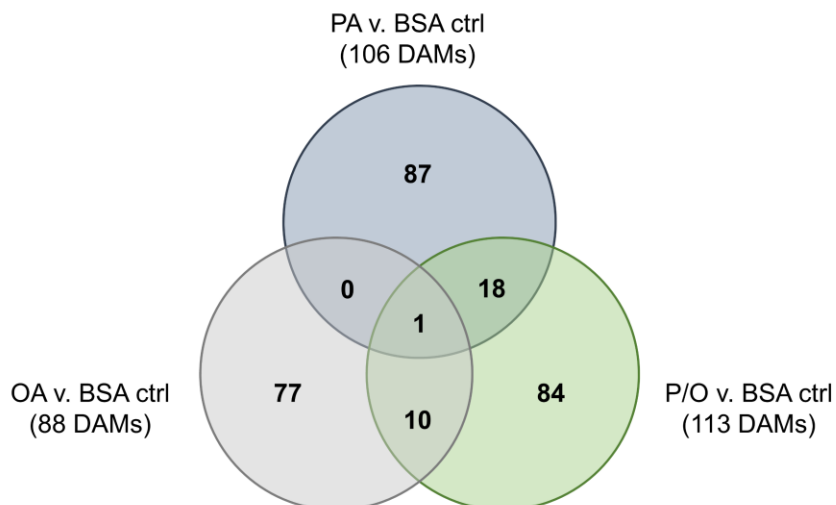


Figure 4-9 Venn Diagram highlighting the number of shared and unique differentially abundant metabolites in NEFA treated BeWo CT cells.

A Venn-diagram was constructed to visualize the number of differentially abundant metabolites species that were unique to each NEFA-treatment or common to multiple NEFA-treatments.

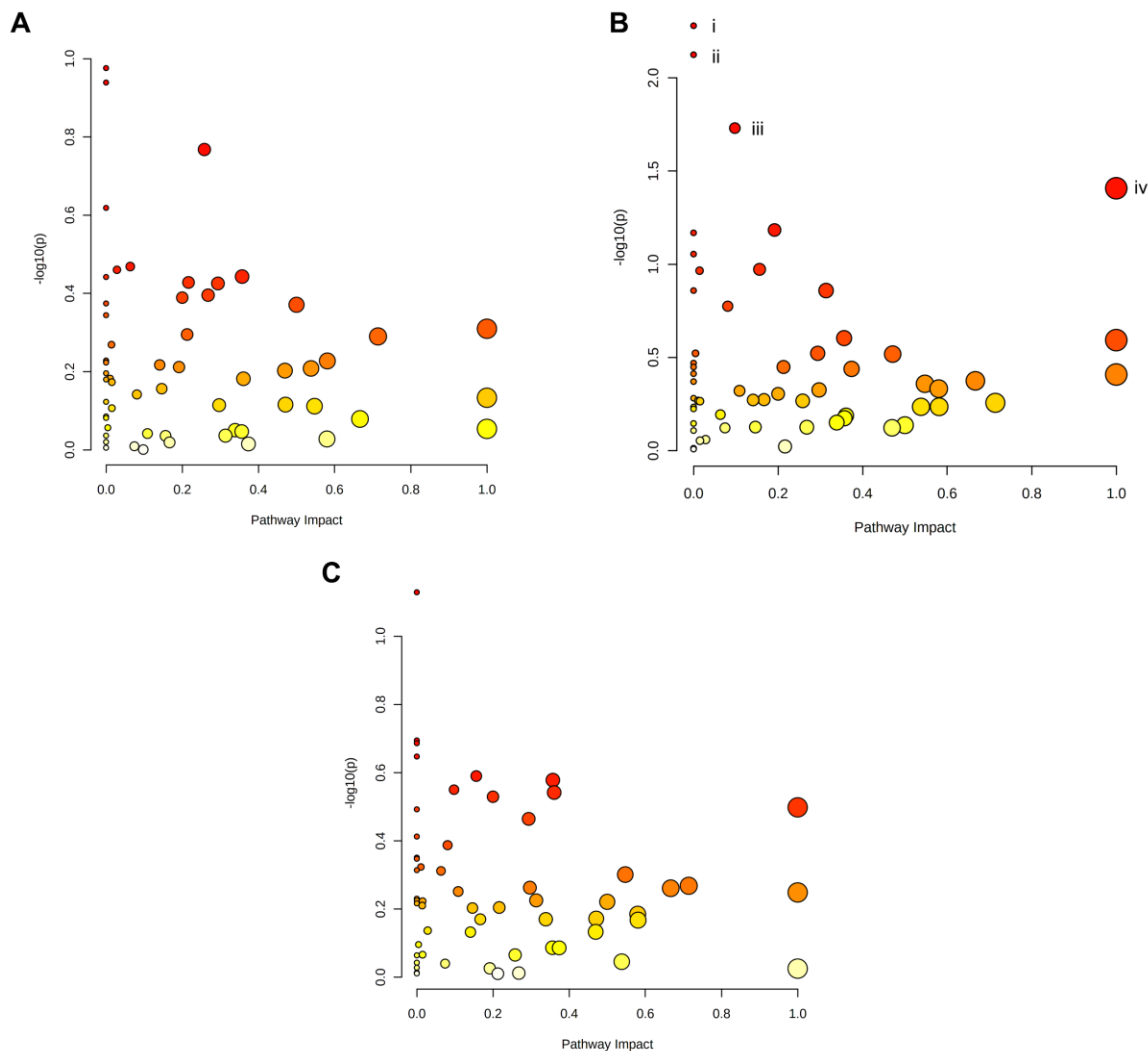


Figure 4-10 Pathway analysis of metabolite profiles of NEFA-treated BeWo CT cells.

Metabolite peak pairs identified in tier 1 and tier 2 were imported into MetaboAnalyst v5.0 for analysis of enriched KEGG pathways. Pathways with raw- $p < 0.05$ were considered significantly enriched and scatterplots were created for (A) PA-treated; (B) OA-treated; and (C) P/O-treated cultures to visualize identified KEGG pathways. The x-axis represents pathway impact and y-axis represents pathway enrichment p-value ($-\log_{10}$). The KEGG pathways for i) Ether lipid metabolism; ii) Amino sugar and nucleotide sugar metabolism; iii) Fructose and mannose metabolism; and iv) Taurine and hypotaurine metabolism were highlighted to be significantly enriched in the OA-treated BeWo CT cultures.

4.3.7 BeWo Cytotrophoblast transcriptome and metabolome integration

Integration of the transcriptomic and metabolomic datasets revealed no significantly enriched pathways in the KEGG database containing both differential genes and differential metabolites in the PA and P/O-treated BeWo CT cells. However, the integration analysis highlighted significantly enriched pathways only containing differentially expressed genes in the PA and P/O treatments. Specifically, there was a significant enrichment in the **i) Inositol Phosphate Metabolism** and **ii) Phosphatidylinositol Signaling System** KEGG pathways (both highlighted by downregulation of *IMPA1* (-1.34 FC) and *PIP5K1B* (-1.37 FC) as well as upregulation of *PLCE1* (+1.50 FC) and *INPP5D* (+1.447 FC)) in the PA-treated BeWo CT cells, as well as a significant enrichment in the **i) Fatty Acid Biosynthesis** KEGG Pathway (highlighted by upregulation of *ACACB* (+1.32 FC) and *ACSL5* (+1.77 FC) and downregulation of *ACSL6* (-1.34 FC)) in the P/O-treated BeWo CT cells (**Figure 4-11 A,C**; raw- $p < 0.05$).

Integration analysis of the OA-treated BeWo CT cell transcriptome and metabolome profiles highlight significantly enriched pathways containing both differential genes and metabolites. Specifically, the **i) Ether Lipid Metabolism** pathway (highlighted by increased accumulation of sn-glycero-3-phosphoethanolamine (+3.44 FC) in conjunction with upregulation of *GDPDI* (+1.34 FC) and downregulation of *PLA2G1A* (-1.35 FC) and **ii) Purine Metabolism** pathway (highlighted by increased levels of adenosine (+3.30 FC), inosine (+2.45 FC), and guanosine (+1.69 FC), in conjunction with upregulation of *PRPS1* (+1.31 FC), and *ADK* (+1.31 FC), as well as downregulation of *GMPR* (-1.76 FC) were found to be significantly enriched in OA-treated BeWo CT cells (**Figure 4-11 B**).

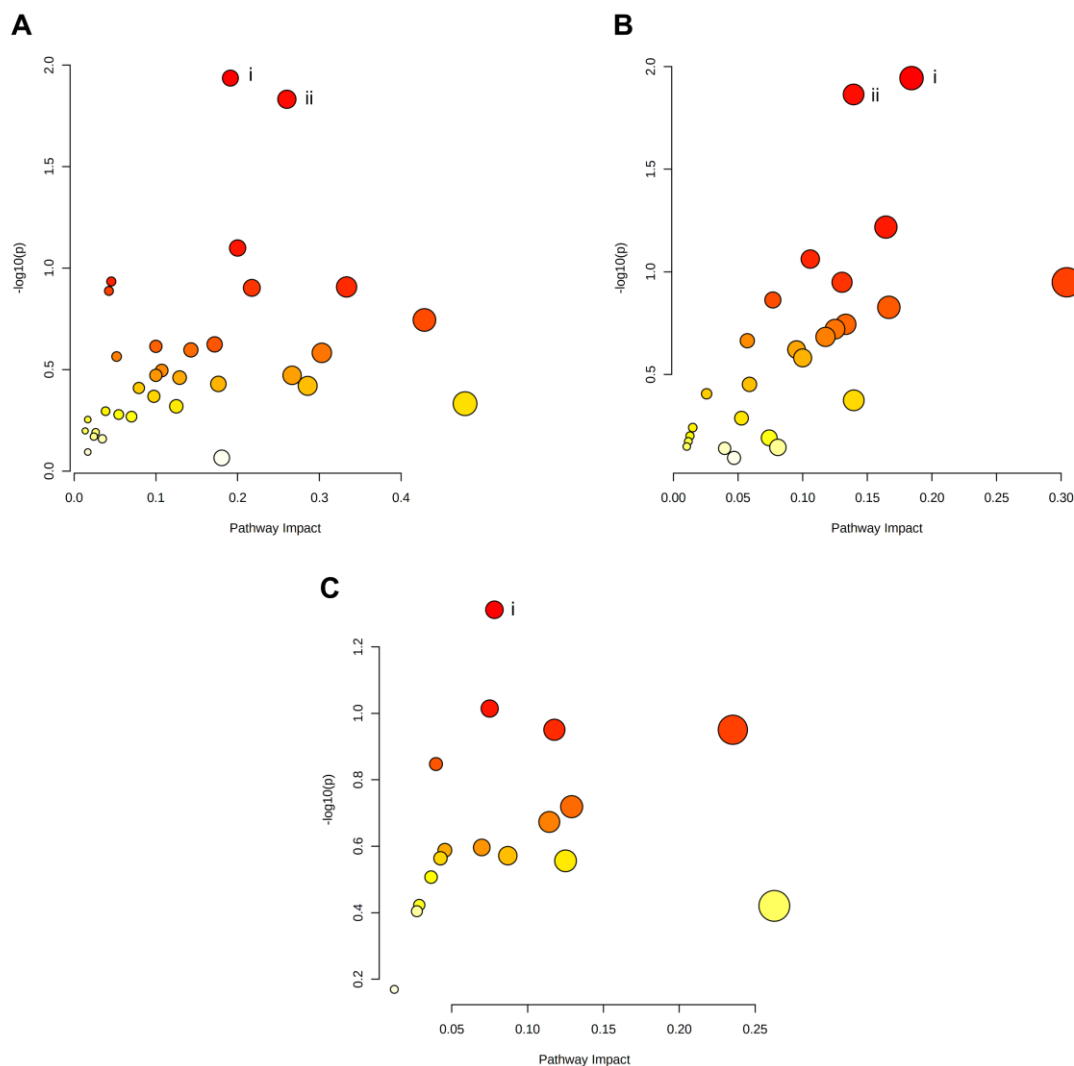


Figure 4-11 Joint Pathway Analysis of Transcriptome and Metabolome Profiles of NEFA-treated BeWo CT cells.

Differentially expressed gene and differentially abundant metabolites (from identification tiers 1 and 2) datasets were analyzed via the Joint Pathway Analysis module in MetaboAnalyst Software. Pathways with raw- $p < 0.05$ were considered significantly enriched, and scatterplots were constructed to visualize identified pathways. The x-axis represents pathway impact and y-axis represents pathway enrichment p-value ($-\log_{10}$). **(A)** The i) inositol phosphate metabolism and ii) phosphatidylinositol signaling system KEGG pathways were highlighted as significantly enriched in PA-treated BeWo CT cells. **(B)** The i) ether lipid metabolism and ii) purine metabolism KEGG pathways were highlighted as significantly enriched in the OA-treated BeWo CT cells. **(C)** The i) fatty acid biosynthesis KEGG pathway was highlighted as significantly enriched in P/O-treated BeWo CT cells.

4.3.8 The impact of NEFA-treatment of BeWo cytotrophoblast lipidome profiles

An average of 9199 ± 295 (\pm SD) lipid species were identified in each sample. Of these features, 950 were positively identified in tier 1, 161 were positively identified in tier 2, and a further 6808 features were putatively identified in tier 3. A summary of the identified features and peak-pair data for NEFA-treated BeWo CT cells and quality control (QC) samples is available in **Supplementary Table 14** (doi.org/10.5683/SP3/XMPKOK). An unsupervised principal component analysis (PCA) 2D plot as well as supervised partial-least squares discriminant analysis (PLS-DA) 2D plot was constructed to visualize the degree of difference between lipidome profiles in all NEFA-treatment groups and highlighted a separation in lipid profiles between the different NEF treatments (**Figure 4-12 A,B**).

Non-parametric volcano plots were then constructed to visualize differentially abundant lipid species in each NEFA-treatment compared to BSA-control samples (**Figure 4-13**; $\geq \pm 1.5$ FC vs BSA control; raw- $p < 0.05$, $n=5$ /group). In PA-treated samples, 679 lipid species were found to have significantly reduced abundance, while 676 lipid species were found to have significantly increased abundance (**Figure 4-13 A**). In OA-treated samples, 834 lipid species were found to have significantly reduced abundance, while 799 lipid species were found to have significantly increased abundance (**Figure 4-13 B**). In P/O-treated samples, 640 lipid species were found to have significantly reduced abundance, while 639 lipid species were found to have significantly increased abundance (**Figure 4-13 C**). A summary of the differentially abundant lipid species is available in **Supplementary Table 15** (doi.org/10.5683/SP3/XMPKOK).

Analysis of the totaled peak intensities of lipids from each independent class revealed 8 differentially abundant lipid classes in PA-treated BeWo CT cells; 6 differentially abundant lipid classes in OA-treated BeWo CT cell; and 7 differentially abundant lipid classes in P/O-treated BeWo CT cells (**Figure 4-14 A-C**; raw- $p < 0.0167$, $n=5$ /group). A Venn-diagram was subsequently constructed to visualize the number of shared and unique differentially abundant lipid classes in each NEFA treatment (**Figure 4-15**). Specifically, the abundance of lipids in the CER, PE, and PI classes were only

significantly increased in PA-treated BeWo CT cells. The lipids in the BMP class were only significantly decreased in OA-treated BeWo CT cells. No significantly altered lipid classes were unique to the P/O treatment group. The Car, LPG and TG lipid classes were found to be significantly elevated in all NEFA treatment groups relative to BSA control. The DG class was significantly increased, and ST lipid class was significantly decreased in both the PA and P/O treatments. Finally, the HexCer and SM lipid classes were found to be significantly elevated in both the OA and P/O treated BeWo CT cells.

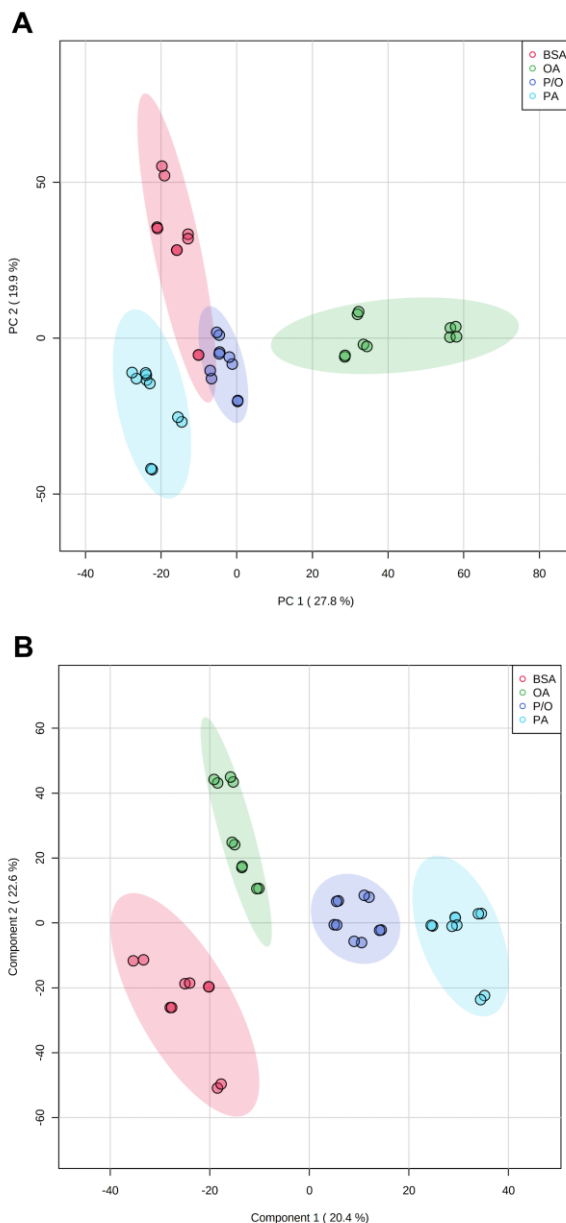


Figure 4-12 Visualization of the degree of separation between lipidome profiles in NEFA-treated BeWo CT cells.

(A) Unsupervised principal component analysis (PCA) and (B) supervised partial least squares discriminant analysis (PLS-DA) plots were utilized to visualize the degree of difference in lipidome profiles between PA, OA, P/O and BSA-control cultures.

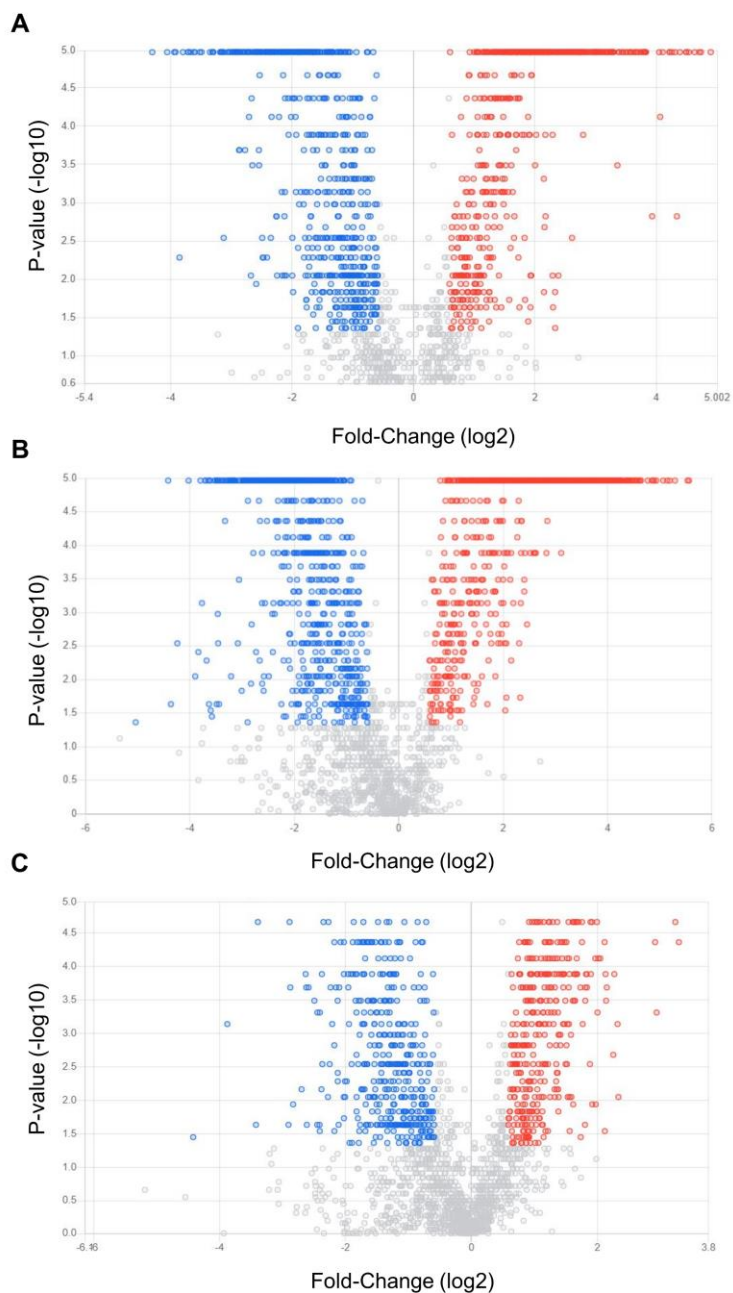


Figure 4-13 Volcano Plot visualization of differentially abundant lipid species in NEFA-treated BeWo CT cells.

Differentially abundant metabolites in (A) PA-treated; (B) OA-treated; and (C) P/O-treated BeWo CT cells were determined with $\geq \pm 1.5$ fold-change vs LG, raw p-value < 0.05 cut-offs and visualized via non-parametric volcano plot ($n=5/\text{group}$). The x-axis represents $\log_2(\text{fold-change})$, and the y-axis represents p-value ($-\log_{10}$). Lipid species with significantly increased abundance vs BSA-control cultures are represented by red dots and lipid species with significantly decreased abundance are represented by blue dots.

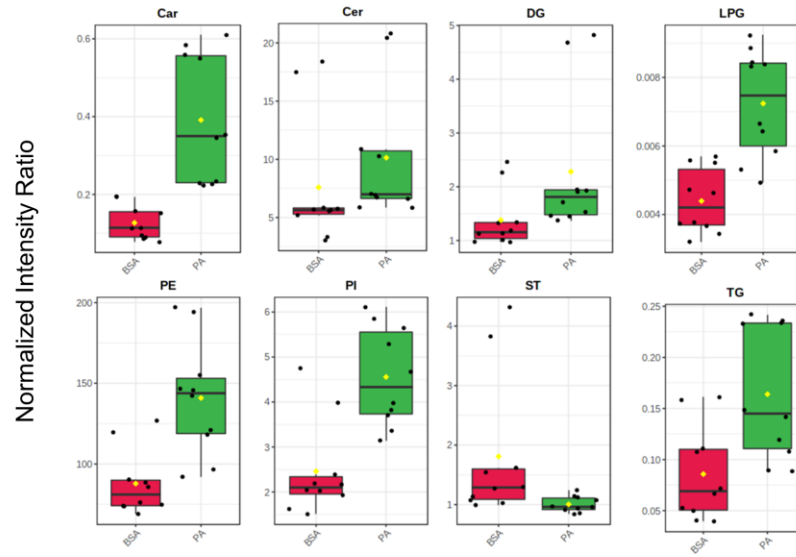
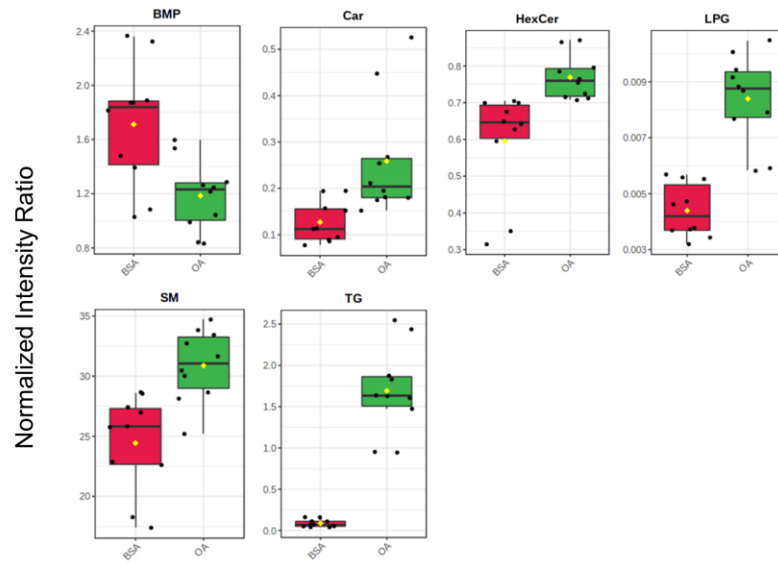
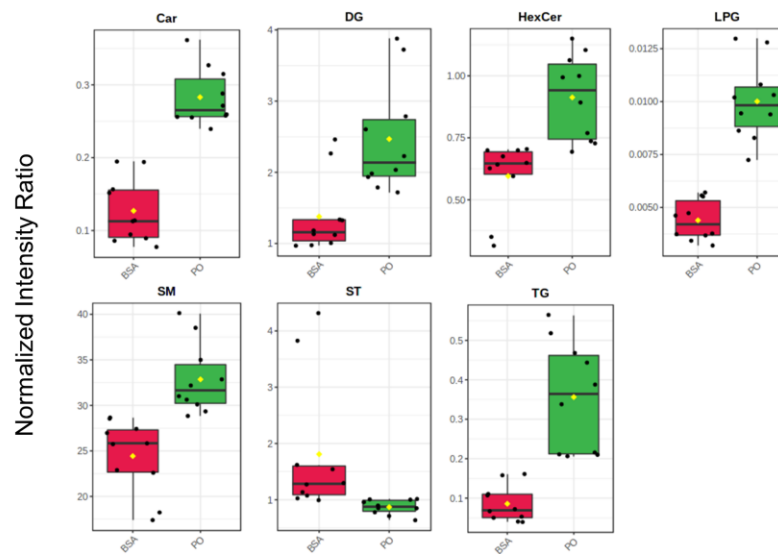
A**B****C**

Figure 4-14 Differentially Abundant Lipid Classes in NEFA-treated BeWo CT cells.

Differentially abundant lipid species identified in tiers 1 and 2 were sorted by lipid subclass and total peak intensity of lipid class was determined. The abundances of lipid class in each NEFA treatment were compared to the BSA-control samples in binary via Wilcoxon-rank sum test. Boxplot were constructed to highlight lipid classes with differential abundance versus BSA-control in (A) PA-treated, (B) OA-treated, and (C) P/O-treated BeWo CT cells (raw-p<0.0167, n=5/group). Lipid class abbreviations: **BMP** (Bis[monoacylglycero]phosphates); **Car** (Fatty acyl carnitines); **Cer** (Ceramides); **DG** (Diacylglycerols); **HexCer** (Glucosylceramides); **LPG** (Lysophosphatidylglycerol); **PE** (Diacylglycerophosphoethanolamines); **PI** (Phosphatidylinositols); **SM** (Ceramide-1-phosphates); **ST** (Cholesterol and Derivatives); **TG** (Triacylglycerols).

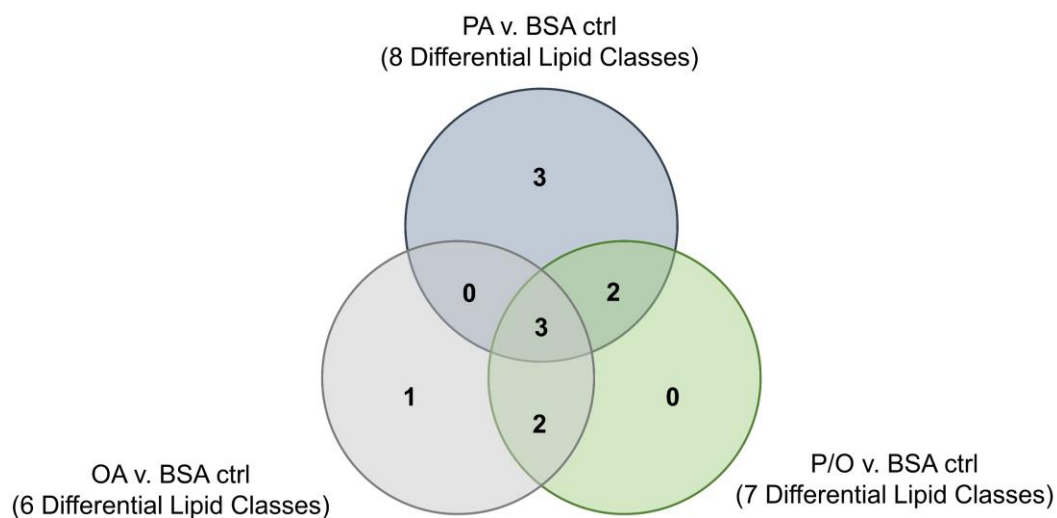


Figure 4-15 Venn Diagram highlighting the number of shared and unique differentially abundant lipid classes in NEFA treated BeWo CT cells.

A Venn-diagram was constructed to provide visualization of the differentially abundant lipid classes that were unique to each NEFA-treatment or common to multiple NEFA-treatments in the box-plot analyses in **Figure 4-14**.

4.4 Discussion:

PA and OA are the most abundant circulating NEFA species in the serum of pregnant women, and the concentrations of these NEFA are increased under conditions of maternal GDM and obesity [45]. As maternal diet has been demonstrated to be an important regulator of placental metabolic function [26,46], and dietary fat consumption data has highlighted that PA and OA are the most abundantly consumed dietary fats [48–51], these fats themselves may be important in regulating placental function in obese and GDM pregnancies. The current study is the first, to our knowledge, to utilize a multi-omics research approach to characterize the independent and combined impacts of the dietary NEFA species PA and OA on the lipid metabolic processing of BeWo villous trophoblast cells.

The first objective of the current study was to utilize targeted lipidomic analyses via GC-FID and TLC-FID to characterize cellular FA and neutral profiles, as well as FA desaturation and elongation indices to better understand lipid processing in BeWo CT and SCT cells cultured with dietary NEFA species. The current study subsequently aimed to utilize a multi-omics research approach (combining transcriptomic data, with untargeted metabolomic and lipidomic data) to elucidate the underlying biochemical impacts of increased NEFA supply on the metabolic function of BeWo CT cells, given that previous studies have highlighted the dominant metabolic profile of these progenitor placental trophoblast cells [24,52–54]. Overall, our results highlighted that the dietary NEFAs PA and OA have different metabolic fates in placental trophoblast cells, as well as demonstrated that these FAs are processed differentially when exposed to trophoblasts independently (PA and OA treatments) and in combination (P/O treatments). Our multi-omic analyses demonstrated that PA exposure (either alone or in combination with oleate) is associated with an oxidative fuel switch indicative of increased β -oxidation. Further, these analyses highlighted underlying metabolic changes that suggested OA exposure exerts anti-inflammatory and anti-oxidant effects in placental trophoblasts.

4.4.1 Impacts of dietary NEFA on BeWo FA and Neutral Lipid Profiles

The current study utilized GC-FID as a preliminary readout of the impacts of increased dietary NEFA supply on BeWo trophoblasts via analysis of cellular FA profiles. It is important to note that altered FA compositions have been described in placentae from obese and GDM pregnancies [35–37], as well as in the development of placental dysfunctions including preeclampsia [64]. Thus, specific dietary NEFA-induced alterations to FA profiles may be reflective of a transition towards aberrant placental function. The current study highlighted that a 72-hour PA exposure was associated with increased SFA levels in both CT and SCT cultures, with specific elevations in the C16:0 content in these cells. OA exposure however, resulted in a profound increase in cellular MUFA species, and strikingly C18:1n9 accounted for almost two-thirds of all FA content in both OA-treated CT and SCT cells. In contrast, the P/O treatments only moderately impacted BeWo SFA and PUFA compositions, and no specific alterations in C16:0 composition were observed in both the P/O-treated CT and SCT cells. However, the P/O-treated cells displayed altered MUFA and profiles and increased C18:1n9 levels similar to the trends in the OA- treatments although with lower magnitude of change. Interestingly, previous data from rodent models have highlighted that placental MUFA but not SFA content correlates with maternal plasma FA levels [65], similar to the findings in P/O-treated BeWo cells reported here. Overall, these data highlighted that altering the supply of dietary NEFA to placental trophoblasts independently impacts trophoblast cell FA composition and suggests that increased circulating NEFA levels contribute to alterations to placental lipid compositions.

The collected FA profile data also allowed for investigation into elongation and desaturation metabolic processing of dietary FA through the calculation of FA elongase and desaturase indices, as has previously been demonstrated [58–62]. Of particular interest to the current study was FA desaturation mediated by Stearoyl-CoA Desaturase 1 (*SCD1*), which is responsible for the production of palmitoleate (C16:1n7) and OA (C18:1n9) from PA (C16:0) and stearate (C18:0), respectively. Previously, obesity has been found to impact placental FA desaturation via *SCD1*, although current reports have

been somewhat inconsistent. Specifically, obese placentae have been found to display increased placental abundance of SCD1 mRNA suggesting increased FA desaturation [25]. However, a subsequent report described an overall decrease in SCD1 activity in obese placentae and highlighted no alterations in SCD protein abundance, suggesting that FA desaturation may be regulated by post-translational modifications [66]. In the current study, we observed decreased SCD1 activity (assessed as POA/PA ratio) in OA and P/O-treated BeWo CT and SCT cells, that suggested previously observed reductions in SCD1 activity in term obese placentae may be facilitated in part by increased placental OA or MUFA supply [66]. Interestingly, all NEFA-treated BeWo CT cells displayed reduced expression of SCD1, that could indicate elevated NEFA levels modulate SCD1-mediated FA desaturation in placental trophoblasts by altering enzyme transcription. Despite an overall reduction in SCD1 mRNA expression, we observed increased SCD1 activity in PA-treated BeWo CT and SCT cells. As palmitoleate has previously been linked with increased oxygen consumption and β -oxidation activity in adipocytes [67,68], we speculate that increased PA desaturation to POA in PA-treated BeWo CT cells may underlie the increased mitochondrial respiratory activity that we have previously observed in these cells [52].

Further, our results demonstrated that OA-exposure whether alone or in combination with PA resulted in increased Fatty Acid Desaturase 2 (FADS2) production of γ -Linoleic Acid (GLA; C18:2n6), as well as increased elongation of OA to Gondoic Acid (C20:1n9). Increased levels of these specific FA species have previously been associated with anti-inflammatory outcomes [69,70]. As OA has been demonstrated to attenuate the lipotoxic effects of increased PA levels in trophoblast cells [71,72], we speculate that OA partially exert its protective effects on trophoblast cells via the increased production of anti-inflammatory lipid intermediaries. Overall, our data demonstrated that modulating dietary FA composition impacts placental FA elongation and desaturation, and in turn leads to altered production of various FA species which themselves may be able to directly impact placental metabolic processes.

Using TLC-FID, the current study also demonstrated that the proportion of TG in the neutral lipid fractions of BeWo CT and SCT cells was elevated only in cells exposed

to with OA independently, likely reflecting that OA is highly lipogenic in trophoblasts. These results were consistent with previous reports in cultured placental explants and isolated trophoblasts [71,73] and NEFA-treated BeWo [74,75] cells that have demonstrated that imported OA is highly localized to TG lipid fractions. This may indicate that increased supply of OA to the placenta is an important regulator of the increased TG synthesis that has previously been reported in obese and GDM placentae [24,25,27,30]. Interestingly, the combination P/O-treated BeWo CT and SCT cells were not observed to have altered neutral lipid and TG compositions when assessed by TLC-FID. These data aligned with reports from isolated primary human trophoblasts, demonstrating reduced lipid droplet formation with a combined OA and PA exposure versus OA-alone exposures [71]. Subsequent analysis of lipid class abundance using untargeted LC-MS/MS also highlighted increased levels of PI, and PE lipid species in PA-treated BeWo CT cells. These results were also consistent with readouts in primary placental samples that have highlighted PA is highly localized to trophoblast phospholipid fractions [66]. Overall, this suggests that saturated and monounsaturated dietary NEFA have different metabolic fates in placental trophoblasts as well as that the metabolic fates of these FA species are altered when present in combination with other dietary FAs.

The FA and neutral lipid profile data, however, highlighted limited alterations in trophoblast lipid composition following syncytialization and, specifically, only four differentially abundant FA species were found in BeWo SCT cells. In contrast, previous work in cultured PHT cells demonstrated profound reductions in the levels of many FA species in placental villous trophoblast cells following syncytialization [76]. The differences between the current study and previous reports are likely due to differences in the reporting of FA profile data and may highlight a limitation in the current study. While previous reports highlighted protein normalized FA quantity, the current study highlighted FA profiles as a percentage of total FA abundance. Thus, the current study was not able to report whether BeWo trophoblast cells demonstrate similar reductions in the absolute quantities of different FA species as was highlighted with PHT cultures. Future works using quantitative readouts of FA abundances are therefore needed to

establish if BeWo trophoblasts exhibit similar differences in lipid metabolism between differentiated and progenitor states.

4.4.2 A multi-omics analysis of NEFA-treated BeWo CT metabolic function

Overall, the multi-omic analyses in the current study revealed that exposure to different dietary NEFA species extensively altered BeWo CT cellular transcriptome and lipidome profiles but led to limited alterations in cellular metabolome profiles. The mRNA microarray transcriptomic analyses highlighted 340 DEG in PA-treated BeWo CT cells; 308 DEGs in OA-treated BeWo CT cells; as well as 221 DEGs in P/O-treated BeWo CT cells. Gene-set over-representation analysis, however, only found one significantly enriched functional pathway in the transcriptomic datasets with the Fatty Acid Biosynthesis Pathway enriched in P/O-treated BeWo CT cells. Despite limited enrichment in functional pathways, the transcriptomic analysis demonstrated differential expression of key genes involved in lipid metabolic pathways in all NEFA treatment groups, suggesting that placental trophoblasts modulate lipid processing functions in direct response to an increased supply of PA and OA.

Specifically, we highlighted an increase in the mRNA abundance of cAMP responsive element-binding protein 3-like 3 (CREB3L3) in all NEFA treatment groups. CREB3L3 is a transcription factor that has previously been demonstrated to regulate lipid metabolism via modulating the expression of genes involved in FA oxidation [77–79]. Interestingly, CREB3L3 has also been implicated in the pathophysiology of inflammation and Endoplasmic Reticulum (ER) stress [78–80]. This could indicate that CREB3L3 controls lipid processing functions in trophoblasts, as well as underlies the development of inflammation and ER stress that has previously been observed in some PA-treated placental trophoblasts [71,72,81]. The microarray analysis in the current study revealed that BeWo CT cells exposed to elevate PA levels for 72 hours do not have elevated expression of genes related to inflammation (such as TNF α , IL6, and IL-32), and ER stress (such as BCL2, DDIT3, and XBP1) that have previously been highlighted in PA-treated primary trophoblasts [71,81]. These differential responses may arise from variations in PA dose utilized (100 μ M in the current study compared to 200-500 μ M in

primary trophoblasts [71,81]). We speculate that the increased CREB3L3 expression highlighted in the current study may reflect an early timepoint in transition towards ER stress and inflammation in PA-exposed BeWo trophoblasts.

The microarray readouts also highlighted an upregulation of Acyl-CoA Synthetase Long Chain Family Member 5 (ACSL5) in NEFA-treated BeWo CT cells. Acyl-CoA synthetase (ACSL) enzymes have been highlighted to be directly involved in FA uptake and are responsible for conjugating FA species to Coenzyme A, an important first step in lipid metabolism that helps prevent FA efflux [66,82,83]. Interestingly, ACSL5 expression has also been found to be induced in PUFA-exposed BeWo trophoblasts, leading to an overall increase in FA uptake [84]. The data from the current study therefore suggests that ACSL5 is also involved in the processing of PA and OA in BeWo trophoblasts, and its increased expression likely facilitates increased cellular uptake of FA species.

Additionally, our microarray data also described an upregulation of perilipin 2 (PLIN2) expression in BeWo trophoblasts exposed to dietary NEFAs. Previously, PLIN2 has been shown to be required for lipid droplet synthesis in trophoblasts [85]. More importantly, placental expression of PLIN2 has been demonstrated to be elevated in GDM pregnancies [86], and its expression has been found to be correlated with maternal pre-pregnancy Body-Mass-Index (BMI) [27]. Thus, the current study suggests that increased supply of dietary NEFAs to the placenta in obese and GDM pregnancies directly facilitates an increased expression of PLIN2. In turn, this dietary NEFA-mediated modulation of PLIN2 expression may promote TG accumulation in lipid droplets, and subsequently placental steatosis in obese and GDM pregnancies.

Subsequently, the current study utilized an integrative approach with the multi-omic readouts to further describe the impacts of dietary NEFA exposure on BeWo CT metabolic function. Specifically, the transcriptome and metabolome datasets were integrated via the Joint Pathway Analysis module of MetaboAnalyst. This analysis highlighted a significant enrichment in the Purine Metabolism pathway in OA-treated BeWo CT cells that was associated with increased cellular accumulations of adenosine

(+3.30 FC), inosine (+2.45 FC), and guanosine (+1.69 FC) that may be suggestive of reduced purine breakdown. As increased degradation of purines is involved in placental responses to increased inflammation [87], the increased purine accumulation in OA-treated trophoblasts in the current study may further highlight anti-inflammatory processes in dietary OA-treated trophoblasts. Alternatively, the increased purine abundances, in conjunction with the upregulation of phosphoribosyl pyrophosphate synthetase 1 (*PRPS1*) observed in the microarray panel, could reflect increased purine synthesis via the Pentose Phosphate Pathway (PPP) [88]. As the PPP increases generation of NADPH, a metabolite with antioxidant effects [89,90], these data may highlight that OA also acts to reduce oxidative stress in placental trophoblasts.

Combining readouts from the transcriptomic, metabolomic and lipidomic datasets also highlighted a potential shift in oxidative substrate selection in BeWo trophoblasts cultured with PA (both alone and in conjunction with OA) towards increased FA oxidation (β -oxidation). Examination of differentially abundant metabolites in PA and P/O-treated BeWo CT revealed a significant reduction in intracellular levels of 3-hydroxymethylglutaric acid (-2.89 FC in PA-treated CT cells; -2.00 FC in P/O-treated CT cells), a byproduct of leucine degradation [91]. We speculate that this may indicate a reduced breakdown of branched-chain amino acid species into byproducts that can enter into The Tricarboxylic Acid Cycle (TCA Cycle) in BeWo trophoblasts cultured under increased PA levels. Additionally, we observed increased C16:0 carnitine (+13.92 FC in PA-treated CT cells; +3.79 FC in P/O-treated CT cells) levels in BeWo trophoblasts treated with PA. As FA species must first be conjugated to carnitine before being translocated to the mitochondrial matrix for oxidation [92], the increased acylcarnitine levels in the cells may reflect a metabolic shift towards using PA as an oxidative fuel.

Moreover, PA and P/O-treated BeWo CT cells were found to have elevated expression of genes involved in β -oxidative metabolism. Specifically, we observed increased expression of Very-Long Chain Acyl-CoA Dehydrogenase (*ACADVL*), the enzyme responsible for the catalyzing the preliminary step in β -oxidation metabolism, and an increased expression of Acetyl-CoA Carboxylase Beta (*ACACB*), an enzyme thought to control β -oxidative activity by catalyzing the carboxylation of acetyl-CoA to

malonyl-CoA. Notably, elevated beta-oxidative activity has previously been linked with increased generation of Reactive Oxygen Species (ROS) [93,94], that ultimately promotes oxidative mitochondrial damage [95,96]. Therefore, the PA-mediated increase in β -oxidative activity in BeWo trophoblasts could be indicative of an early transition towards placental mitochondrial dysfunction.

Interestingly, malonic acid, an end-point metabolic byproduct of beta-oxidation that is synthesized by *ACACB*, was only found to be increased in P/O-cultured BeWo CT cells (+1.85 FC), but not PA-cultured cells. As malonate has been found to limit β -oxidation activity by inhibiting acylcarnitine transport into the mitochondrial matrix [97], these data may highlight that BeWo trophoblasts exposed to PA in combination with OA, but not PA-alone, are able to prevent excessive β -oxidation activity. Malonate-mediated inhibition of β -oxidation in the P/O-cultured BeWo CT cells may act to suppress excessive mitochondrial ROS production and could therefore protect against mitochondrial damage. We additionally speculate that these data may highlight a shift towards incomplete beta-oxidation in BeWo trophoblasts cultured with PA alone, as these cells (but not P/O-treated CT cells) also displayed increased intracellular levels of the shortened-chain C14:0 carnitine (+3.99 FC). Increased production of short-chain acylcarnitine species has previously been linked with pro-inflammatory processes [98], and thus these data may further highlight a transition towards inflammation in PA-exposed trophoblasts. However, the insights of the current study into incomplete beta-oxidation are minimized due to the limited identifications of short chain acylcarnitine species in our untargeted lipidomic readouts. Future studies may need to utilize targeted metabolomic approaches or utilize radio-labelled FA species to better identify the production of short-chain acylcarnitine species and incomplete β -oxidation in PA-treated BeWo trophoblasts.

4.4.3 Conclusion

Overall, the results of the current study highlighted the continued utility of the BeWo preparation as a pre-clinical placental model, and that the dietary FAs PA and OA are important regulators of placental trophoblast lipid metabolism. Moreover, it is shown that excessive availability of these fats is associated with changes in FA desaturation,

elongation, esterification, and oxidation processes in placental trophoblast cells. These results further support the concept that increased levels of certain dietary fats in maternal circulation are involved in facilitating the aberrant placental function that underlies the development of metabolic health complications in offspring exposed to obesity and GDM. In turn these data suggest that monitoring circulating FA levels in obese and GDM pregnancies, and subsequently implementing dietary interventions through modulating dietary fat content and composition continues to be needed in the clinical management of these at-risk pregnancies. Implementation of healthy diet and lifestyle choices in these “at-risk” pregnancies could act to preserve appropriate placental metabolic function throughout gestation and in turn reduce risk of future metabolic health complication in the offspring.

4.5 References

- [1] W. Zhuang, J. Lv, Q. Liang, W. Chen, S. Zhang, X. Sun, Adverse effects of gestational diabetes-related risk factors on pregnancy outcomes and intervention measures, *Exp. Ther. Med.* (2020). doi:10.3892/etm.2020.9050.
- [2] Z. Yang, H. Phung, L. Freebairn, R. Sexton, A. Raulli, P. Kelly, Contribution of maternal overweight and obesity to the occurrence of adverse pregnancy outcomes, *Aust. New Zeal. J. Obstet. Gynaecol.* 59 (2019) 367–374. doi:10.1111/ajo.12866.
- [3] Y. Yogev, G.H.A. Visser, Obesity, gestational diabetes and pregnancy outcome, *Semin. Fetal Neonatal Med.* 14 (2009) 77–84. doi:10.1016/j.siny.2008.09.002.
- [4] J.A. Armitage, L. Poston, P.D. Taylor, Developmental origins of obesity and the metabolic syndrome: the role of maternal obesity., *Front. Horm. Res.* 36 (2008) 73–84. doi:10.1159/000115355.
- [5] J. Manderson, B. Mullan, C. Patterson, D. Hadden, A. Traub, D. McCance, Cardiovascular and metabolic abnormalities in the offspring of diabetic pregnancy, *Diabetologia.* 45 (2002) 991–996. doi:10.1007/s00125-002-0865-y.
- [6] P. Agarwal, T.S. Morriseau, S.M. Kereliuk, C.A. Doucette, B.A. Wicklow, V.W. Dolinsky, Maternal obesity, diabetes during pregnancy and epigenetic mechanisms that influence the developmental origins of cardiometabolic disease in the offspring, *Crit. Rev. Clin. Lab. Sci.* 55 (2018) 71–101. doi:10.1080/10408363.2017.1422109.
- [7] P.M. Catalano, The impact of gestational diabetes and maternal obesity on the mother and her offspring, *J. Dev. Orig. Health Dis.* 1 (2010) 208–215. doi:10.1017/S2040174410000115.
- [8] N. Shrestha, H.C. Ezechukwu, O.J. Holland, D.H. Hryciw, Developmental programming of peripheral diseases in offspring exposed to maternal obesity during pregnancy, *Am. J. Physiol. Integr. Comp. Physiol.* 319 (2020) R507–R516. doi:10.1152/ajpregu.00214.2020.
- [9] R.C. Whitaker, Predicting Preschooler Obesity at Birth: The Role of Maternal Obesity in Early Pregnancy, *Pediatrics.* 114 (2004) e29–e36. doi:10.1542/peds.114.1.e29.
- [10] C.M. Boney, A. Verma, R. Tucker, B.R. Vohr, Metabolic syndrome in childhood: association with birth weight, maternal obesity, and gestational diabetes mellitus., *Pediatrics.* 115 (2005) e290-6. doi:10.1542/peds.2004-1808.
- [11] M. Väärasmäki, A. Pouta, P. Elliot, P. Tapanainen, U. Sovio, A. Ruokonen, A.-L. Hartikainen, M. McCarthy, M.-R. Järvelin, Adolescent Manifestations of Metabolic Syndrome Among Children Born to Women With Gestational Diabetes in a General-Population Birth Cohort, *Am. J. Epidemiol.* 169 (2009) 1209–1215. doi:10.1093/aje/kwp020.
- [12] A. Ferrara, Increasing Prevalence of Gestational Diabetes Mellitus: A public health perspective, *Diabetes Care.* 30 (2007) S141–S146. doi:10.2337/dc07-s206.

- [13] S.Y. Kim, P.M. Dietz, L. England, B. Morrow, W.M. Callaghan, Trends in Pre-pregnancy Obesity in Nine States, 1993–2003*, *Obesity*. 15 (2007) 986–993. doi:10.1038/oby.2007.621.
- [14] G. Li, T. Wei, W. Ni, A. Zhang, J. Zhang, Y. Xing, Q. Xing, Incidence and Risk Factors of Gestational Diabetes Mellitus: A Prospective Cohort Study in Qingdao, China, *Front. Endocrinol. (Lausanne)*. 11 (2020). doi:10.3389/fendo.2020.00636.
- [15] M. Hod, A. Kapur, D.A. Sacks, E. Hadar, M. Agarwal, G.C. Di Renzo, L.C. Roura, H.D. McIntyre, J.L. Morris, H. Divakar, The International Federation of Gynecology and Obstetrics (FIGO) Initiative on gestational diabetes mellitus: A pragmatic guide for diagnosis, management, and care #, *Int. J. Gynecol. Obstet.* 131 (2015) S173–S211. doi:10.1016/S0020-7292(15)30033-3.
- [16] A.K. Driscoll, E.C.W. Gregory, Increases in Prepregnancy Obesity: United States, 2016-2019., *NCHS Data Brief*. (2020) 1–8. <http://www.ncbi.nlm.nih.gov/pubmed/33270551>.
- [17] K.R. Howell, T.L. Powell, Effects of maternal obesity on placental function and fetal development, *Reproduction*. 153 (2017) R97–R108. doi:10.1530/REP-16-0495.
- [18] J.F. Hebert, L. Myatt, Placental mitochondrial dysfunction with metabolic diseases: Therapeutic approaches, *Biochim. Biophys. Acta - Mol. Basis Dis.* 1867 (2021) 165967. doi:10.1016/j.bbadis.2020.165967.
- [19] A.C. Kelly, T.L. Powell, T. Jansson, Placental function in maternal obesity, *Clin. Sci.* 134 (2020) 961–984. doi:10.1042/CS20190266.
- [20] R. Hastie, M. Lappas, The effect of pre-existing maternal obesity and diabetes on placental mitochondrial content and electron transport chain activity., *Placenta*. 35 (2014) 673–83. doi:10.1016/j.placenta.2014.06.368.
- [21] C. Mandò, G.M. Anelli, C. Novielli, P. Panina-Bordignon, M. Massari, M.I. Mazzocco, I. Cetin, Impact of Obesity and Hyperglycemia on Placental Mitochondria, *Oxid. Med. Cell. Longev.* 2018 (2018) 1–10. doi:10.1155/2018/2378189.
- [22] A. Maloyan, J. Mele, S. Muralimanoharan, L. Myatt, Placental metabolic flexibility is affected by maternal obesity, *Placenta*. 45 (2016) 69. doi:10.1016/j.placenta.2016.06.031.
- [23] J. Mele, S. Muralimanoharan, A. Maloyan, L. Myatt, Impaired mitochondrial function in human placenta with increased maternal adiposity., *Am. J. Physiol. Endocrinol. Metab.* 307 (2014) E419-25. doi:10.1152/ajpendo.00025.2014.
- [24] A.M. Valent, H. Choi, K.S. Kolahi, K.L. Thornburg, Hyperglycemia and gestational diabetes suppress placental glycolysis and mitochondrial function and alter lipid processing, *FASEB J.* 35 (2021). doi:10.1096/fj.202000326RR.
- [25] V. Calabuig-Navarro, M. Hagiaci, J. Minium, P. Glazebrook, G.C. Ranasinghe, C. Hoppel, S. Hauguel de-Mouzon, P. Catalano, P. O'Tierney-Ginn, Effect of Maternal Obesity on Placental Lipid Metabolism, *Endocrinology*. 158 (2017)

2543–2555. doi:10.1210/en.2017-00152.

- [26] V. Calabuig-Navarro, M. Puchowicz, P. Glazebrook, M. Haghiac, J. Minium, P. Catalano, S. Hauguel deMouzon, P. O’Tierney-Ginn, Effect of ω -3 supplementation on placental lipid metabolism in overweight and obese women., *Am. J. Clin. Nutr.* 103 (2016) 1064–72. doi:10.3945/ajcn.115.124651.
- [27] B. Hirschmugl, G. Desoye, P. Catalano, I. Klymiuk, H. Scharnagl, S. Payr, E. Kitzinger, C. Schliefersteiner, U. Lang, C. Wadsack, S. Hauguel-de Mouzon, Maternal obesity modulates intracellular lipid turnover in the human term placenta, *Int. J. Obes.* 41 (2017) 317–323. doi:10.1038/ijo.2016.188.
- [28] M. Bucher, K.R.C. Montaniel, L. Myatt, S. Weintraub, H. Tavori, A. Maloyan, Dyslipidemia, insulin resistance, and impairment of placental metabolism in the offspring of obese mothers, *J. Dev. Orig. Health Dis.* 12 (2021) 738–747. doi:10.1017/S2040174420001026.
- [29] T.L. Powell, K. Barner, L. Madi, M. Armstrong, J. Manke, C. Uhlson, T. Jansson, V. Ferchaud-Roucher, Sex-specific responses in placental fatty acid oxidation, esterification and transfer capacity to maternal obesity, *Biochim. Biophys. Acta - Mol. Cell Biol. Lipids.* 1866 (2021) 158861. doi:10.1016/j.bbalip.2020.158861.
- [30] C.H. Hulme, A. Nicolaou, S.A. Murphy, A.E.P. Heazell, J.E. Myers, M. Westwood, The effect of high glucose on lipid metabolism in the human placenta, *Sci. Rep.* 9 (2019) 14114. doi:10.1038/s41598-019-50626-x.
- [31] F. Visiedo, F. Bugatto, R. Quintero-Prado, I. Cózar-Castellano, J.L. Bartha, G. Perdomo, Glucose and Fatty Acid Metabolism in Placental Explants From Pregnancies Complicated With Gestational Diabetes Mellitus, *Reprod. Sci.* 22 (2015) 798–801. doi:10.1177/1933719114561558.
- [32] F. Visiedo, F. Bugatto, V. Sánchez, I. Cózar-Castellano, J.L. Bartha, G. Perdomo, High glucose levels reduce fatty acid oxidation and increase triglyceride accumulation in human placenta, *Am. J. Physiol. Metab.* 305 (2013) E205–E212. doi:10.1152/ajpendo.00032.2013.
- [33] M.A. Ortega, M.A. Saez, F. Sainz, O. Fraile-Martínez, S. García-Gallego, L. Pekarek, C. Bravo, S. Coca, M.Á.- Mon, J. Buján, N. García-Honduvilla, Á. Asúnsolo, Lipidomic profiling of chorionic villi in the placentas of women with chronic venous disease, *Int. J. Med. Sci.* 17 (2020) 2790–2798. doi:10.7150/ijms.49236.
- [34] S. Mohammad, J. Bhattacharjee, T. Vasanthan, C.S. Harris, S.A. Bainbridge, K.B. Adamo, Metabolomics to understand placental biology: Where are we now?, *Tissue Cell.* 73 (2021) 101663. doi:10.1016/j.tice.2021.101663.
- [35] C. Fattuoni, C. Mandò, F. Palmas, G.M. Anelli, C. Novielli, E. Parejo Laudicina, V.M. Savasi, L. Barberini, A. Dessì, R. Pintus, V. Fanos, A. Noto, I. Cetin, Preliminary metabolomics analysis of placenta in maternal obesity, *Placenta.* 61 (2018) 89–95. doi:10.1016/j.placenta.2017.11.014.
- [36] M.T. Segura, H. Demmelmair, S. Krauss-Etschmann, P. Nathan, S. Dehmel, M.C. Padilla, R. Rueda, B. Koletzko, C. Campoy, Maternal BMI and gestational

- diabetes alter placental lipid transporters and fatty acid composition, *Placenta*. 57 (2017) 144–151. doi:10.1016/j.placenta.2017.07.001.
- [37] Y. Yang, Z. Pan, F. Guo, H. Wang, W. Long, H. Wang, B. Yu, Placental metabolic profiling in gestational diabetes mellitus: An important role of fatty acids, *J. Clin. Lab. Anal.* (2021). doi:10.1002/jcla.24096.
- [38] S. Furse, D.S. Fernandez-Twinn, B. Jenkins, C.L. Meek, H.E.L. Williams, G.C.S. Smith, D.S. Charnock-Jones, S.E. Ozanne, A. Koulman, A high-throughput platform for detailed lipidomic analysis of a range of mouse and human tissues, *Anal. Bioanal. Chem.* 412 (2020) 2851–2862. doi:10.1007/s00216-020-02511-0.
- [39] O. Uhl, H. Demmelmair, M.T. Segura, J. Florido, R. Rueda, C. Campoy, B. Koletzko, Effects of obesity and gestational diabetes mellitus on placental phospholipids, *Diabetes Res. Clin. Pract.* 109 (2015) 364–371. doi:10.1016/j.diabres.2015.05.032.
- [40] K.L. Bidne, A.L. Rister, A.R. McCain, B.D. Hitt, E.D. Dodds, J.R. Wood, Maternal obesity alters placental lysophosphatidylcholines, lipid storage, and the expression of genes associated with lipid metabolism, *Biol. Reprod.* 104 (2021) 197–210. doi:10.1093/biolre/ioaa191.
- [41] T.J. Stuart, K. O’Neill, D. Condon, I. Sasson, P. Sen, Y. Xia, R.A. Simmons, Diet-induced obesity alters the maternal metabolome and early placenta transcriptome and decreases placenta vascularity in the mouse†, *Biol. Reprod.* 98 (2018) 795–809. doi:10.1093/biolre/ioy010.
- [42] F. Delhaes, S.A. Giza, T. Koreman, G. Eastabrook, C.A. McKenzie, S. Bedell, T.R.H. Regnault, B. de Vrijer, Altered maternal and placental lipid metabolism and fetal fat development in obesity: Current knowledge and advances in non-invasive assessment, *Placenta*. 69 (2018) 118–124. doi:10.1016/j.placenta.2018.05.011.
- [43] A. Herrera Martínez, Hyperlipidemia during gestational diabetes and its relation with maternal and offspring complications, *Nutr. Hosp.* (2018). doi:10.20960/nh.1539.
- [44] C.M. Scifres, J.M. Catov, H.N. Simhan, The impact of maternal obesity and gestational weight gain on early and mid-pregnancy lipid profiles, *Obesity*. 22 (2014) 932–938. doi:10.1002/oby.20576.
- [45] X. Chen, T.O. Scholl, M. Leskiw, J. Savaille, T.P. Stein, Differences in maternal circulating fatty acid composition and dietary fat intake in women with gestational diabetes mellitus or mild gestational hyperglycemia, *Diabetes Care*. 33 (2010) 2049–2054. doi:10.2337/dc10-0693.
- [46] F.L. Alvarado, V. Calabuig-Navarro, M. Haghiac, M. Puchowicz, P.-J.S. Tsai, P. O’Tierney-Ginn, Maternal obesity is not associated with placental lipid accumulation in women with high omega-3 fatty acid levels, *Placenta*. 69 (2018) 96–101. doi:10.1016/j.placenta.2018.07.016.
- [47] P.M. Villa, H. Laivuori, E. Kajantie, R. Kaaja, Free fatty acid profiles in preeclampsia, *Prostaglandins, Leukot. Essent. Fat. Acids*. 81 (2009) 17–21.

doi:10.1016/j.plefa.2009.05.002.

- [48] J. Denomme, K.D. Stark, B.J. Holub, Directly quantitated dietary (n-3) fatty acid intakes of pregnant Canadian women are lower than current dietary recommendations., *J. Nutr.* 135 (2005) 206–11. doi:135/2/206 [pii].
- [49] C. Savard, S. Lemieux, S. Weisnagel, B. Fontaine-Bisson, C. Gagnon, J. Robitaille, A.-S. Morisset, Trimester-Specific Dietary Intakes in a Sample of French-Canadian Pregnant Women in Comparison with National Nutritional Guidelines, *Nutrients*. 10 (2018) 768. doi:10.3390/nu10060768.
- [50] D. Iggman, U. Risérus, Role of different dietary saturated fatty acids for cardiometabolic risk, *Clin. Lipidol.* 6 (2011) 209–223. doi:10.2217/clp.11.7.
- [51] C.L. Kien, J.Y. Bunn, R. Stevens, J. Bain, O. Ikayeva, K. Crain, T.R. Koves, D.M. Muoio, Dietary intake of palmitate and oleate has broad impact on systemic and tissue lipid profiles in humans, *Am. J. Clin. Nutr.* 99 (2014) 436–445. doi:10.3945/ajcn.113.070557.
- [52] Z.J.W. Easton, F. Delhaes, K. Mathers, L. Zhao, C.M.G. Vanderboor, T.R.H. Regnault, Syncytialization and prolonged exposure to palmitate impacts BeWo respiration, *Reproduction*. 161 (2021) 73–88. doi:10.1530/REP-19-0433.
- [53] K. Kolahi, A. Valent, K.L. Thornburg, Cytotrophoblast, Not Syncytiotrophoblast, Dominates Glycolysis and Oxidative Phosphorylation in Human Term Placenta., *Sci. Rep.* (2017) 1–12. doi:10.1038/srep42941.
- [54] K. Kolahi, S. Louey, O. Varlamov, K. Thornburg, Real-time tracking of BODIPY-C12 long-chain fatty acid in human term placenta reveals unique lipid dynamics in cytotrophoblast cells, *PLoS One*. 11 (2016) 1–23. doi:10.1371/journal.pone.0153522.
- [55] J. Folch, M. Lees, G.H.S. Stanley, A SIMPLE METHOD FOR THE ISOLATION AND PURIFICATION OF TOTAL LIPIDES FROM ANIMAL TISSUES, *J. Biol. Chem.* 226 (1957) 497–509. doi:10.1016/S0021-9258(18)64849-5.
- [56] J.M. Klaiman, E.R. Price, C.G. Guglielmo, Fatty acid composition of pectoralis muscle membrane, intramuscular fat stores and adipose tissue of migrant and wintering white-throated sparrows (*Zonotrichia albicollis*), *J. Exp. Biol.* 212 (2009) 3865–3872. doi:10.1242/jeb.034967.
- [57] O. Sarr, K.E. Mathers, L. Zhao, K. Dunlop, J. Chiu, C.G. Guglielmo, Y. Bureau, A. Cheung, S. Raha, T.-Y. Lee, T.R.H. Regnault, Western diet consumption through early life induces microvesicular hepatic steatosis in association with an altered metabolome in low birth weight Guinea pigs, *J. Nutr. Biochem.* 67 (2019) 219–233. doi:10.1016/j.jnutbio.2019.02.009.
- [58] D.M. Merino, H. Johnston, S. Clarke, K. Roke, D. Nielsen, A. Badawi, A. El-Sohemy, D.W.L. Ma, D.M. Mutch, Polymorphisms in FADS1 and FADS2 alter desaturase activity in young Caucasian and Asian adults, *Mol. Genet. Metab.* 103 (2011) 171–178. doi:10.1016/j.ymgme.2011.02.012.
- [59] V. Chajès, V. Joulin, F. Clavel-Chapelon, The fatty acid desaturation index of

- blood lipids, as a biomarker of hepatic stearyl-CoA desaturase expression, is a predictive factor of breast cancer risk, *Curr. Opin. Lipidol.* 22 (2011) 6–10. doi:10.1097/MOL.0b013e3283404552.
- [60] S.M. Jeyakumar, P. Lopamudra, S. Padmini, N. Balakrishna, N. V Giridharan, A. Vajreswari, Fatty acid desaturation index correlates with body mass and adiposity indices of obesity in Wistar NIN obese mutant rat strains WNIN/Ob and WNIN/GR-Ob, *Nutr. Metab. (Lond)*. 6 (2009) 27. doi:10.1186/1743-7075-6-27.
- [61] Y.N. Massih, A.G. Hall, J. Suh, J.C. King, Zinc Supplements Taken with Food Increase Essential Fatty Acid Desaturation Indices in Adult Men Compared with Zinc Taken in the Fasted State, *J. Nutr.* 151 (2021) 2583–2589. doi:10.1093/jn/nxab149.
- [62] A. Gómez-Vilarrubla, B. Mas-Parés, M. Díaz, S. Xargay-Torrent, G. Carreras-Badosa, M. Jové, M. Martin-Gari, A. Bonmatí-Santané, F. de Zegher, L. Ibañez, A. López-Bermejo, J. Bassols, Fatty acids in the placenta of appropriate- versus small-for-gestational-age infants at term birth, *Placenta*. 109 (2021) 4–10. doi:10.1016/j.placenta.2021.04.009.
- [63] K.P. Dunlop, Skeletal Muscle Lipid Metabolism and Markers of Insulin Resistance in Young Male Low Birth Weight Offspring in Combination With a Postnatal Western Diet, *Electron. Thesis Diss. Respository*. 2946 (2015).
- [64] S.H.J. Brown, S.R. Eather, D.J. Freeman, B.J. Meyer, T.W. Mitchell, A Lipidomic Analysis of Placenta in Preeclampsia: Evidence for Lipid Storage, *PLoS One*. 11 (2016) e0163972. doi:10.1371/journal.pone.0163972.
- [65] E. Amusquivar, E. Herrera, Influence of Changes in Dietary Fatty Acids during Pregnancy on Placental and Fetal Fatty Acid Profile in the Rat, *Neonatology*. 83 (2003) 136–145. doi:10.1159/000067963.
- [66] V. Ferchaud-Roucher, K. Barner, T. Jansson, T.L. Powell, Maternal obesity results in decreased syncytiotrophoblast synthesis of palmitoleic acid, a fatty acid with anti-inflammatory and insulin-sensitizing properties, *FASEB J.* 33 (2019) 6643–6654. doi:10.1096/fj.201802444R.
- [67] M.M. Cruz, J.J. Simão, R.D.C.C. de Sá, T.S.M. Farias, V.S. da Silva, F. Abdala, V.J. Antraco, L. Armelin-Correa, M.I.C. Alonso-Vale, Palmitoleic Acid Decreases Non-alcoholic Hepatic Steatosis and Increases Lipogenesis and Fatty Acid Oxidation in Adipose Tissue From Obese Mice, *Front. Endocrinol. (Lausanne)*. 11 (2020). doi:10.3389/fendo.2020.537061.
- [68] M.M. Cruz, A.B. Lopes, A.R. Crisma, R.C.C. de Sá, W.M.T. Kuwabara, R. Curi, P.B.M. de Andrade, M.I.C. Alonso-Vale, Palmitoleic acid (16:1n7) increases oxygen consumption, fatty acid oxidation and ATP content in white adipocytes, *Lipids Health Dis.* 17 (2018) 55. doi:10.1186/s12944-018-0710-z.
- [69] J. Muralidharan, C. Papandreou, A. Sala-Vila, N. Rosique-Esteban, M. Fitó, R. Estruch, M. Angel Martínez-González, D. Corella, E. Ros, C. Razquín, O. Castañer, J. Salas-Salvadó, M. Bulló, Fatty Acids Composition of Blood Cell Membranes and Peripheral Inflammation in the PREDIMED Study: A Cross-

- Sectional Analysis, *Nutrients*. 11 (2019) 576. doi:10.3390/nu11030576.
- [70] R. Kapoor, Y.-S. Huang, Gamma Linolenic Acid: An Antiinflammatory Omega-6 Fatty Acid, *Curr. Pharm. Biotechnol.* 7 (2006) 531–534. doi:10.2174/138920106779116874.
- [71] B.N. Colvin, M.S. Longtine, B. Chen, M.L. Costa, D.M. Nelson, Oleate attenuates palmitate-induced endoplasmic reticulum stress and apoptosis in placental trophoblasts, *Reproduction*. 153 (2017) 369–380. doi:10.1530/REP-16-0576.
- [72] S.K. Natarajan, T. Bruett, P.G. Muthuraj, P.K. Sahoo, J. Power, J.L. Mott, C. Hanson, A. Anderson-Berry, Saturated free fatty acids induce placental trophoblast lipoapoptosis, *PLoS One*. 16 (2021) e0249907. doi:10.1371/journal.pone.0249907.
- [73] O.C. Watkins, M.O. Islam, P. Selvam, R.A. Pillai, A. Cazenave-Gassiot, A.K. Bendt, N. Karnani, K.M. Godfrey, R.M. Lewis, M.R. Wenk, S.-Y. Chan, Metabolism of ¹³C-Labeled Fatty Acids in Term Human Placental Explants by Liquid Chromatography–Mass Spectrometry, *Endocrinology*. 160 (2019) 1394–1408. doi:10.1210/en.2018-01020.
- [74] F.M. Campbell, A.M. Clohessy, M.J. Gordon, K.R. Page, A.K. Dutta-Roy, Uptake of long chain fatty acids by human placental choriocarcinoma (BeWo) cells: role of plasma membrane fatty acid-binding protein., *J. Lipid Res.* 38 (1997) 2558–68. <http://www.ncbi.nlm.nih.gov/pubmed/9458279>.
- [75] K.A.R. Tobin, G.M. Johnsen, A.C. Staff, A.K. Duttaroy, Long-chain Polyunsaturated Fatty Acid Transport across Human Placental Choriocarcinoma (BeWo) Cells, *Placenta*. 30 (2009) 41–47. doi:10.1016/j.placenta.2008.10.007.
- [76] V. Ferchaud-Roucher, M.C. Rudolph, T. Jansson, T.L. Powell, Fatty acid and lipid profiles in primary human trophoblast over 90 h in culture, *Prostaglandins, Leukot. Essent. Fat. Acids*. 121 (2017) 14–20. doi:10.1016/j.plefa.2017.06.001.
- [77] Y. Nakagawa, A. Satoh, H. Tezuka, S. Han, K. Takei, H. Iwasaki, S. Yatoh, N. Yahagi, H. Suzuki, Y. Iwasaki, H. Sone, T. Matsuzaka, N. Yamada, H. Shimano, CREB3L3 controls fatty acid oxidation and ketogenesis in synergy with PPAR α , *Sci. Rep.* 6 (2016) 39182. doi:10.1038/srep39182.
- [78] H. Wade, K. Pan, Q. Su, CREBH: A Complex Array of Regulatory Mechanisms in Nutritional Signaling, Metabolic Inflammation, and Metabolic Disease, *Mol. Nutr. Food Res.* 65 (2021) 2000771. doi:10.1002/mnfr.202000771.
- [79] L. Sampieri, P. Di Giusto, C. Alvarez, CREB3 Transcription Factors: ER-Golgi Stress Transducers as Hubs for Cellular Homeostasis, *Front. Cell Dev. Biol.* 7 (2019). doi:10.3389/fcell.2019.00123.
- [80] K. Zhang, X. Shen, J. Wu, K. Sakaki, T. Saunders, D.T. Rutkowski, S.H. Back, R.J. Kaufman, Endoplasmic Reticulum Stress Activates Cleavage of CREBH to Induce a Systemic Inflammatory Response, *Cell*. 124 (2006) 587–599. doi:10.1016/j.cell.2005.11.040.
- [81] J. Saben, Y. Zhong, H. Gomez-Acevedo, K.M. Thakali, S.J. Borengasser, A. Andres, K. Shankar, Early growth response protein-1 mediates lipotoxicity-

- associated placental inflammation: role in maternal obesity, *Am. J. Physiol. Metab.* 305 (2013) E1–E14. doi:10.1152/ajpendo.00076.2013.
- [82] D.G. Mashek, M.A. McKenzie, C.G. Van Horn, R.A. Coleman, Rat Long Chain Acyl-CoA Synthetase 5 Increases Fatty Acid Uptake and Partitioning to Cellular Triacylglycerol in McArdle-RH7777 Cells, *J. Biol. Chem.* 281 (2006) 945–950. doi:10.1074/jbc.M507646200.
- [83] A.K. Dutta-Roy, Cellular uptake of long-chain fatty acids: role of membrane-associated fatty-acid-binding/transport proteins, *Cell. Mol. Life Sci.* 57 (2000) 1360–1372. doi:10.1007/PL00000621.
- [84] G.M. Johnsen, M.S. Weedon-Fekjær, K.A.R. Tobin, A.C. Staff, A.K. Duttaroy, Long-chain Polyunsaturated Fatty Acids Stimulate Cellular Fatty Acid Uptake in Human Placental Choriocarcinoma (BeWo) Cells, *Placenta.* 30 (2009) 1037–1044. doi:10.1016/j.placenta.2009.10.004.
- [85] I. Bildirici, W.T. Schaiff, B. Chen, M. Morizane, S.-Y. Oh, M. O'Brien, C. Sonnenberg-Hirche, T. Chu, Y. Barak, D.M. Nelson, Y. Sadovsky, PLIN2 Is Essential for Trophoblastic Lipid Droplet Accumulation and Cell Survival During Hypoxia, *Endocrinology.* 159 (2018) 3937–3949. doi:10.1210/en.2018-00752.
- [86] L. Stirm, M. Kovářová, S. Perschbacher, R. Michlmaier, L. Fritsche, D. Siegel-Axel, E. Schleicher, A. Peter, J. Pauluschke-Fröhlich, S. Brucker, H. Abele, D. Wallwiener, H. Preissl, C. Wadsack, H.-U. Häring, A. Fritsche, R. Ensenauer, G. Desoye, H. Staiger, BMI-Independent Effects of Gestational Diabetes on Human Placenta, *J. Clin. Endocrinol. Metab.* 103 (2018) 3299–3309. doi:10.1210/jc.2018-00397.
- [87] Y.-C. Lien, Z. Zhang, G. Barila, A. Green-Brown, M.A. Elovitz, R.A. Simmons, Intrauterine Inflammation Alters the Transcriptome and Metabolome in Placenta, *Front. Physiol.* 11 (2020). doi:10.3389/fphys.2020.592689.
- [88] A. Stincone, A. Prigione, T. Cramer, M.M.C. Wamelink, K. Campbell, E. Cheung, V. Olin-Sandoval, N. Grüning, A. Krüger, M. Tauqeer Alam, M.A. Keller, M. Breitenbach, K.M. Brindle, J.D. Rabinowitz, M. Ralser, The return of metabolism: biochemistry and physiology of the pentose phosphate pathway, *Biol. Rev.* 90 (2015) 927–963. doi:10.1111/brv.12140.
- [89] C. Riganti, E. Gazzano, M. Polimeni, E. Aldieri, D. Ghigo, The pentose phosphate pathway: An antioxidant defense and a crossroad in tumor cell fate, *Free Radic. Biol. Med.* 53 (2012) 421–436. doi:10.1016/j.freeradbiomed.2012.05.006.
- [90] C.M. Grant, Metabolic reconfiguration is a regulated response to oxidative stress, *J. Biol.* 7 (2008) 1. doi:10.1186/jbiol63.
- [91] Y. Duan, F. Li, Y. Li, Y. Tang, X. Kong, Z. Feng, T.G. Anthony, M. Watford, Y. Hou, G. Wu, Y. Yin, The role of leucine and its metabolites in protein and energy metabolism, *Amino Acids.* 48 (2016) 41–51. doi:10.1007/s00726-015-2067-1.
- [92] N. Longo, M. Frigeni, M. Pasquali, Carnitine transport and fatty acid oxidation, *Biochim. Biophys. Acta - Mol. Cell Res.* 1863 (2016) 2422–2435. doi:10.1016/j.bbamcr.2016.01.023.

- [93] R.H. Lambertucci, S.M. Hirabara, L. dos R. Silveira, A.C. Levada-Pires, R. Curi, T.C. Pithon-Curi, Palmitate increases superoxide production through mitochondrial electron transport chain and NADPH oxidase activity in skeletal muscle cells, *J. Cell. Physiol.* 216 (2008) 796–804. doi:10.1002/jcp.21463.
- [94] M.G. Rosca, E.J. Vazquez, Q. Chen, J. Kerner, T.S. Kern, C.L. Hoppel, Oxidation of Fatty Acids Is the Source of Increased Mitochondrial Reactive Oxygen Species Production in Kidney Cortical Tubules in Early Diabetes, *Diabetes*. 61 (2012) 2074–2083. doi:10.2337/db11-1437.
- [95] M. Zhao, Y. Wang, L. Li, S. Liu, C. Wang, Y. Yuan, G. Yang, Y. Chen, J. Cheng, Y. Lu, J. Liu, Mitochondrial ROS promote mitochondrial dysfunction and inflammation in ischemic acute kidney injury by disrupting TFAM-mediated mtDNA maintenance, *Theranostics*. 11 (2021) 1845–1863. doi:10.7150/thno.50905.
- [96] H. Rizwan, S. Pal, S. Sabnam, A. Pal, High glucose augments ROS generation regulates mitochondrial dysfunction and apoptosis via stress signalling cascades in keratinocytes, *Life Sci.* 241 (2020) 117148. doi:10.1016/j.lfs.2019.117148.
- [97] A. Honda, K. Yamashita, T. Ikegami, T. Hara, T. Miyazaki, T. Hirayama, M. Numazawa, Y. Matsuzaki, Highly sensitive quantification of serum malonate, a possible marker for de novo lipogenesis, by LC-ESI-MS/MS, *J. Lipid Res.* 50 (2009) 2124–2130. doi:10.1194/jlr.D800054-JLR200.
- [98] J.M. Rutkowski, T.A. Knotts, K.D. Ono-Moore, C.S. McCain, S. Huang, D. Schneider, S. Singh, S.H. Adams, D.H. Hwang, Acylcarnitines activate proinflammatory signaling pathways., *Am. J. Physiol. Endocrinol. Metab.* 306 (2014) E1378-87. doi:10.1152/ajpendo.00656.2013.

Chapter 5

5 General Discussion and Conclusions

5.1 Overview of thesis and major findings

Recent advances in the Developmental Origins of Health and Disease (DOHaD) field have highlighted that obese and diabetic pregnancies are associated with abnormal maternal intrauterine environments high in circulating nutrients that lead to pathological *in utero* programming of fetal development [1–3]. Aberrant maternal environments such as these increase the risk of offspring developing non-communicable cardiometabolic health complications early in their lives [1–3]. Impairments in placental metabolic and mitochondrial function, induced by overabundant circulating nutrient levels, are thought to specifically underlie the development of non-communicable diseases in the offspring of these “at-risk” pregnancies [4–6]. However, the direct impacts of increased nutrient levels on placental metabolic functions are poorly understood, and the underlying mechanisms that regulate placental metabolic function in response to nutrient overabundance have not yet been characterized. Thus, through the work in this thesis, we sought to further elucidate the direct impacts of nutrient overabundance on placental metabolic function, mitochondrial respiration, and nutrient processing using an *in vitro* cell culture model.

The governing hypothesis of this thesis was: *increased nutrient abundance will impact placental metabolic function specifically highlighted by altered nutrient storage, impaired mitochondrial respiratory activity, as well as an altered transcriptomic, metabolomic, and lipidomic profile representative of dysfunctional metabolism.*

This hypothesis was explored using BeWo cytotrophoblast (CT) and syncytiotrophoblast (SCT) cells to model the two primary cell types of the placental chorionic villi that are involved in materno-fetal nutrient exchange. BeWo CT and SCT cells were exposed to increased levels of the dietary non-esterified fatty acids (NEFA) palmitate (PA) and oleate (OA) to model hyperlipidemia in obese and gestational diabetic (GDM) pregnancies caused by a poor maternal diet. Further, BeWo trophoblast cells were exposed to increased levels of glucose to model hyperglycemia in diabetic pregnancies. The main findings that support this hypothesis are:

- (1) Increased levels of saturated NEFAs and glucose were associated with altered metabolic function that was suggestive of a transition towards mitochondrial dysfunction in BeWo trophoblast cells.
- (2) Independent exposure to elevated levels of monounsaturated NEFAs and glucose was linked to increased nutrient storage in BeWo placental trophoblasts
- (3) Increased nutrient abundance modulated transcriptomic, metabolomic, and lipidomic profiles in BeWo trophoblast cells that were indicative of altered placental nutrient processing and metabolic function

5.2 Summary of Findings

5.2.1 Chapter 2: Syncytialization and prolonged exposure to palmitate impacts BeWo respiration

In chapter 2, we investigated BeWo trophoblast cell metabolic function following a prolonged exposure to PA, a saturated dietary NEFA; OA, a monounsaturated dietary NEFA; as well as a combination of PA and OA (P/O). As these NEFA are the most abundant in maternal circulation, and are elevated with obesity, we postulated that they may be directly involved in facilitating impaired placental metabolic function in pregnancies complicated by maternal pre-pregnancy obesity [7–9]. Additionally, as these NEFA are the most abundantly consumed in westernized diets, their elevated levels in obese pregnancies have been considered reflective of increased maternal consumption of these fats and highlight a link between poor maternal diet and impaired placental function [10–12]. The overall hypothesis of this specific investigation was that *a prolonged exposure to the dietary NEFAs PA and OA both independently and in combination would impair mitochondrial function in BeWo CT and SCT cells.*

In these experiments, we established a 72-hour cell culture protocol in which the impacts of these NEFA could be observed in both progenitor BeWo cytotrophoblast (CT) cells and differentiated BeWo syncytiotrophoblast (SCT) cells. Under normal culture conditions BeWo trophoblasts display low spontaneous cell fusion and a CT phenotype, however treating BeWo cells with 8-Br-cAMP (250 μ M) enables fusion and

differentiation to a SCT phenotype. Following a 24-hour pre-treatment with the NEFA species, subsets of BeWo trophoblasts were cultured with 8-Br-cAMP to facilitate CT-to-SCT differentiation over the final 48 hours of the culture period. This specific differentiation protocol was utilized as it is analogous to human placenta syncytialization whereby underlying progenitor CT cells divide and propagate under exposure to maternal nutrients, before undergoing terminal differentiation under those same nutrient conditions. Prior to our investigations of metabolic and mitochondrial function in NEFA-treated BeWo trophoblast cells, we first examined cell viability and differentiation capacity of these cells to ensure differences in metabolic activity were not the result of lipotoxicity. We determined that 100 μ M doses of NEFA were the most appropriate for these investigations as they did not impact BeWo viability or differentiation capacity. It is important to note that the 100 μ M doses of PA and OA utilized in this study aligned with fasting serum levels of these dietary fats during the third trimester [7], demonstrating a physiological relevance of these NEFA treatments.

We next utilized functional readouts of mitochondrial activity using the Seahorse Extracellular Flux Analyzer and the Mito Stress Test to examine BeWo mitochondrial function following NEFA exposure in live cells. Through the use of this functional activity assay, we demonstrated that BeWo CT cells exposed to PA, either alone or in combination with OA (P/O-treatment) have increased basal and maximal mitochondrial respiratory activity. Our subsequent functional analysis of individual metabolic enzymes and electron transport chain (ETC) complexes, however, highlighted no impacts to the underlying metabolic machinery in BeWo CT cells cultured with PA. Previously, increased mitochondrial respiratory activity has been associated with increased generation of Reactive Oxygen Species (ROS) that induce oxidative damage in mitochondria leading to an overall mitochondrial dysfunction [13,14]. In these investigations, we did not observe evidence of increased oxidative stress in NEFA-exposed BeWo trophoblasts at 72-hours of NEFA exposure when examined by endpoint immunoblots for 4-Hydroxynonenol (4-HNE, a marker of lipid peroxidation) and total nitrotyrosine residues (a marker of nitrative stress). Thus, we speculated that the observed increase in mitochondrial activity without a simultaneous increase in cellular oxidative

stress indicated that the PA-exposed BeWo CT cells were in an early stage of a progression towards mitochondrial dysfunction.

The investigations in Chapter 2 also highlighted a suppressed metabolic activity in differentiated BeWo SCT cultures, independent of NEFA exposure. Specifically, our Seahorse Mito Stress Test analyses revealed reduced basal and maximal mitochondrial respiratory activity, as well as a reduced spare respiratory capacity in BeWo SCT cells. Reductions in mitochondrial respiratory activity have previously been described in syncytialized primary human trophoblast (PHT) cultures, demonstrating that BeWo trophoblast mitochondrial function is similar to that of primary placental cells following differentiation [15–17]. Subsequent investigations into underlying metabolic enzyme activities demonstrated that reduced ETC complex 2 activity and reduced total Pyruvate Dehydrogenase (PDH) activity (concomitant with reduced total PDH protein abundance) underlies the observed reduction in mitochondrial respiration in differentiated BeWo SCT cultures. Overall, these data provided novel insight into the mechanisms that may underlie the reduced mitochondrial function that has been observed in differentiated placental syncytiotrophoblasts. However, future studies are still needed to confirm if the specific mechanisms associated with reduced mitochondrial function of syncytialized BeWo trophoblasts also regulated mitochondrial respiratory activity in differentiated PHT cultures.

5.2.2 Chapter 3: The impact of hyperglycemia upon BeWo trophoblast cell metabolic function: A multi-omics and functional metabolic analysis

In Chapter 3 we shifted our focus from dietary NEFAs to glucose to evaluate the impacts of diabetic hyperglycemia on placental metabolic and mitochondrial function. In addition to examining functional readouts of mitochondrial function and metabolic enzyme activity as was done in Chapter 2, this study also utilized a multi-omics research approach combining transcriptome, metabolome, and lipidome readouts to characterize the underlying impacts of hyperglycemic (HG) culture conditions on BeWo trophoblast metabolism. Overall, it was postulated that *HG-culture conditions would be associated with increased nutrient storage and impaired mitochondrial respiratory function in BeWo*

CT and SCT cells, in association with altered transcriptome, metabolome, and lipidome signatures in BeWo CT cells indicative of altered metabolic function.

To examine the impacts of high glucose culture conditions on BeWo trophoblast metabolism, we employed the prolonged 72-hour cell culture protocol that was developed in Chapter 2. In these analyses, F12K growth media supplemented to 25 mM total glucose was utilized for the HG treatments. It is important to note that this dose has previously been used with BeWo trophoblast cells and *ex vivo* placental explants and has been demonstrated to alter BeWo transcriptomic and metabolomic profiles in a manner suggestive of altered metabolic function after 48 hours in culture [18,19]. Our preliminary validation experiments revealed that BeWo trophoblasts were over 90% viable following 72-hours of hyperglycemia exposure, which aligned with previous reports of BeWo trophoblast and PHT viability after 48-hours of high glucose exposure [18,20]. Furthermore, our analysis of syncytialization capacity highlighted that increased glucose levels did not impact the syncytialization ability of BeWo trophoblasts. Overall, these validation experiments demonstrated that BeWo trophoblasts are highly stable following a 72-hour exposure to 25 mM of glucose.

The Seahorse Extracellular Flux Analyzer assays and individual metabolic enzyme activity assays used in this study were the first experiments, to our knowledge, to examine functional readouts of metabolic and mitochondrial activity of BeWo placental trophoblasts cultured under independent hyperglycemia. Additionally, while previous studies investigating the impacts of high glucose on BeWo trophoblasts have focused on progenitor CT cells [18,21,22], our analyses also discussed metabolic activity of differentiated BeWo SCT cells. Thus, the results in this chapter increased our general understanding of how hyperglycemia impacts different placental villous trophoblast cell lineages. Overall, we highlighted that HG-exposure was not associated with alterations in global functional readouts of mitochondrial and metabolic enzyme activity in BeWo CT and SCT cells. Subsequent investigation into underlying mitochondrial fission/fusion dynamics in these cells suggested that key aspects of placental mitochondrial physiology could be impacted by HG exposures. Future studies utilizing high-resolution microscopy imaging techniques that better characterize mitochondrial morphology and cristae

structure, could allow for the impacts of hyperglycemia on mitochondrial fission/fusion dynamics to be explored in more detail.

In this chapter we also investigated the impacts of high glucose conditions on placental nutrient storage and its regulation. Overall, we highlighted that HG-cultured BeWo CT cells displayed increased glycogen and triglyceride (TG) content, and that HG-cultured BeWo SCT cells displayed increased glycogen abundance compared to respective LG controls. These data also highlighted that progenitor BeWo CT cells have a greater capacity for generating new nutrient stores than differentiated SCT cells. As a similar differentiation-state suppression in nutrient storage capacity has been highlighted in primary trophoblast cells [23–26], these data further highlighted similarities between BeWo cells and primary placental material following syncytialization. Surprisingly, our investigations into the underlying regulation of nutrient storage found a reduced total glycogen synthase abundance and increased inhibitory pSer⁶⁴¹ phosphorylation of glycogen synthase in HG-cultured BeWo trophoblast cells. These data suggested that following 72 hours of high glucose exposure, BeWo trophoblasts have a diminished capacity to continue to store excess glucose as glycogen. This may reflect the presence of a negative feedback loop mediated by the increased cellular glycogen content itself [27], that acts to limit excessive glycogen accumulation in BeWo trophoblasts. We speculated that if hyperglycemic conditions were continued beyond our 72-hour timepoint, this reduced glycogen storage capacity will increase free glucose available for oxidation and in turn lead to increased ROS generation and oxidative mitochondrial damage. This speculation is supported by previous cell culture systems utilizing kidney glomerular cells and human umbilical cord endothelial cells which have demonstrated that prolonging glucose exposure is associated with an eventual development of impaired mitochondrial respiratory function [28,29].

We therefore suspect that we have established a cell culture system that captures an early timepoint in a progression of BeWo trophoblasts towards ultimate mitochondrial failure in response to high glucose. As previously stated, we speculated the 72-hour exposure to excess PA in Chapter 2 also likely reflected an early timepoint in a progression towards ultimate mitochondrial dysfunction. Therefore, the data from

Chapter 2 and Chapter 3 together suggest that increased nutrient supply primes placental trophoblasts for mitochondrial dysfunction, and that saturated NEFAs and glucose overabundance both negatively regulate placental metabolism.

Notably, the functional investigations of mitochondrial and metabolic activity completed in this chapter were found to align with the readouts in Chapter 2 in that syncytialized BeWo trophoblast cells display suppressed mitochondrial activity. In this study, differentiated BeWo SCT cells specifically displayed reduced mitochondrial respiratory spare capacity, and reduced mitochondrial coupling efficiency, concomitant with reduced activity of ETC complex II, and reduced protein abundance of ETC complex IV. Readouts of mitochondrial fission/fusion dynamics in this chapter provided further insight into the mechanisms underlying reduced mitochondrial function in SCT cells. Specifically, we observed reduced total protein abundance of optic atrophy type 1 (OPA1, a marker of mitochondrial fusion) in conjunction with increased total protein abundance of DRP1 in BeWo SCT cells indicative of increased mitochondrial fission. As increased mitochondrial fission has also been described in differentiating PHTs [15,30], these data provided further evidence of similarities between BeWo trophoblasts and primary placental cells following differentiation. A schematic illustrating the syncytialization-induced changes in BeWo trophoblast nutrient processing and metabolic function is available in **Figure 5-1**.

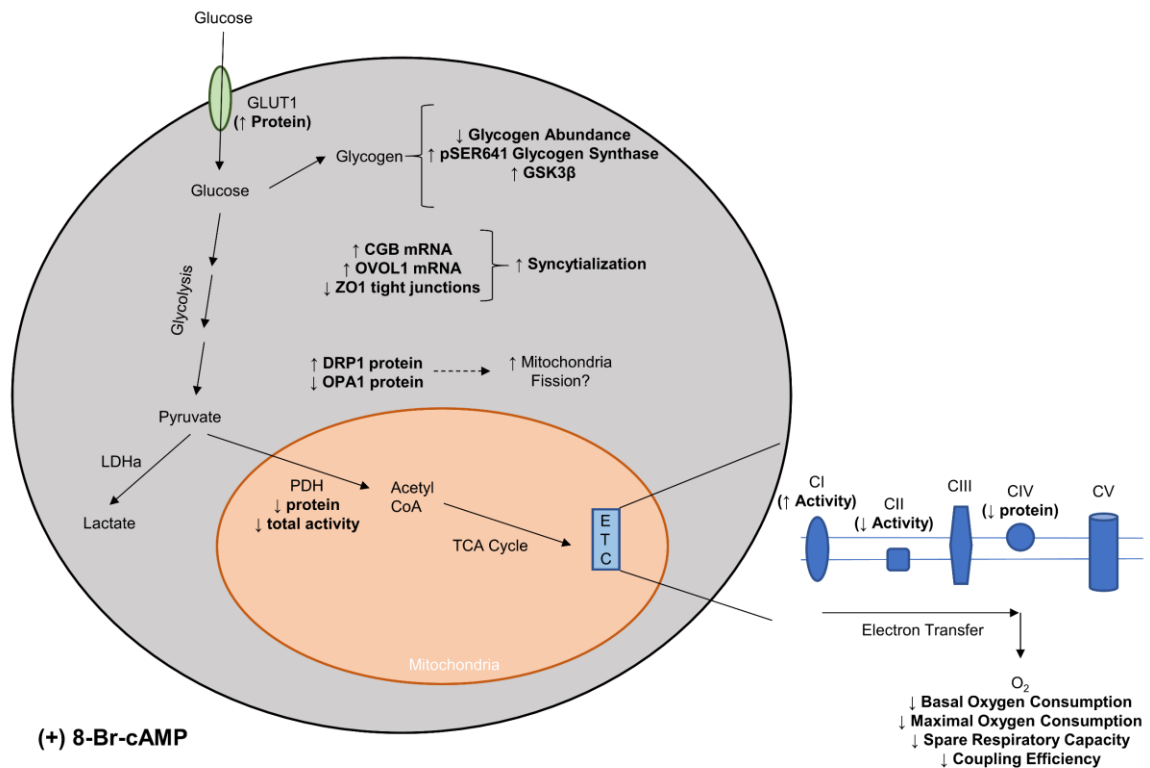


Figure 5-1 Summary illustration of the impacts of 8-Br-cAMP exposure on BeWo trophoblast cells.

Treating BeWo trophoblast cells with 8-Br-cAMP (250 μ M) increased mRNA expression of *CGB* and *OVOLI* concomitant with reduced abundance of ZO1 tight junctions; these changes are indicative of placental trophoblast syncytialization. These BeWo SCT cells were found to have decreased nutrient store (glycogen) abundance, which was linked to increased inhibitory phosphorylation (pSer⁶⁴¹) of glycogen synthase. BeWo SCT cells were additionally found to have decreased basal and maximal mitochondrial respiratory activity that was associated with reduced PDH activity, decreased ETC complex II activity and reduced ETC complex IV protein abundance. Further underlying these alterations in functional aspects of mitochondrial respiration was an increased protein abundance of DRP1 in conjunction with decreased protein abundance of OPA1 that may lead to mitochondrial fission in these cells.

Recently, studies utilizing placental villous trophoblast models have highlighted that “omics” based investigations are useful to gain an in-depth understanding of the underlying mechanisms governing placental development and function [31–33]. Therefore, to further characterize the impacts of hyperglycemia on BeWo trophoblast metabolism in this study, we utilized a multi-omic research approach combining transcriptomics, metabolomics and lipidomics. In these analyses, we specifically examined progenitor BeWo CT cells due to the higher basal metabolic activity that we, and others [15,16], have observed in this cell type. With multivariate principal component analyses (PCA) we highlighted divergences in transcriptomic and metabolomic profiles between HG and low glucose (LG)-cultured BeWo CT cells, but a limited separation in lipidome profiles between LG and HG-cultured BeWo CT cells. Our subsequent investigations into the “omic” profiles of HG-culture BeWo CT cells revealed biomarkers that provided insight into the underlying regulation of mitochondrial function and nutrient storage in hyperglycemia exposed BeWo trophoblasts.

First, we demonstrated increased mRNA expression of *ACSL1* (+1.36 fold-change (FC)) in HG-cultured BeWo CT cells. The protein encoded by this gene is involved in lipid trafficking and may facilitate the increased TG synthesis in these cells [34–36]. Additional readouts from the metabolomic analyses showed increased accumulation of malonate (+3.74 FC) in HG-cultured BeWo CT cells. These data may highlight that *de novo* lipogenesis is also involved in the production of TG species in HG-exposed BeWo trophoblasts. However, malonate has also been demonstrated to inhibit β -oxidative activity [37]. As HG-cultured BeWo also displayed increased (+1.63 FC) 16:0 acylcarnitine levels (a β -oxidation intermediary), these data could also indicate that FA oxidation is reduced in placental trophoblasts in response to high glucose, and this change may further enhance placental steatosis.

Interestingly, we also observed an increased accumulation of lactate (+2.72 FC) in HG-cultured BeWo CT cells that was suggestive of increased glycolytic activity in these cells. These findings are notable as our analyses using the Seahorse XF Glycolysis Stress Test did not detect differences in glycolysis function between LG and HG-cultured BeWo trophoblasts. These data could indicate that the Seahorse XF Glycolysis Stress Test

readouts are less sensitive than the metabolomic readouts and that the Seahorse functional assay does not accurately quantify BeWo trophoblast glycolytic activity. Any future study examining more prolonged glucose exposures in BeWo trophoblasts will need to consider these experimental limitations, especially considering BeWo cells appear to downregulate glycogen storage in hyperglycemic conditions and these changes could lead to initially increased rates of glycolysis.

Finally, our metabolomic analysis highlighted increased accumulation of riboflavin (+3.68 FC) in HG-cultured BeWo trophoblasts that may either be reflective of increased riboflavin uptake, or reduced riboflavin metabolism. As riboflavin metabolites (flavin mononucleotide (FMN) and flavin adenine dinucleotide (FAD)) are important co-factors needed for appropriate mitochondrial respiratory activity, the observed riboflavin accumulation may indicate that BeWo trophoblast mitochondria are not functioning appropriately following exposure to high glucose conditions [38,39].

Overall, the multi-omic research approach utilized in Chapter 3 provided greater insight into the underlying mechanisms that regulate placental trophoblast metabolism in response to high glucose exposures, and further highlighted nutrient (TG) storage, and mitochondrial function are important areas of trophoblast metabolism that are impacted by glucose. A schematic summarizing the changes we observed in BeWo trophoblast cells exposed to hyperglycemia for 72 hours is available in **Figure 5-2**.

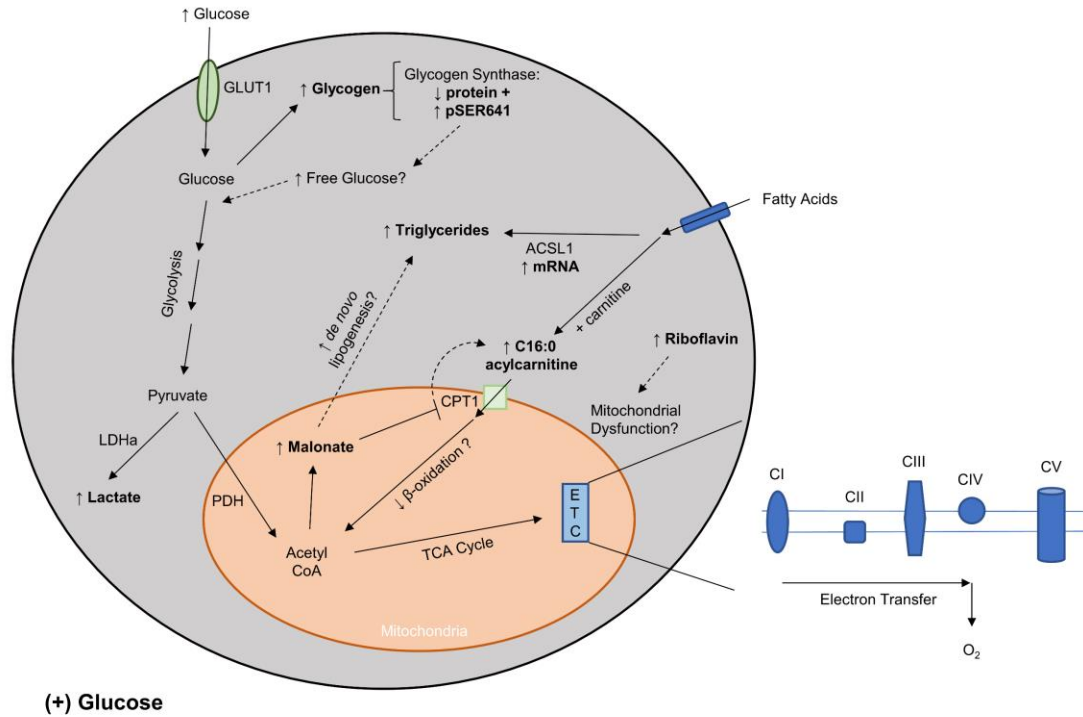


Figure 5-2 Summary illustration of the impacts of hyperglycemia (25 mM) on BeWo trophoblast cells.

BeWo trophoblasts cultured under hyperglycemic (HG) conditions for 72 hours were found to have increased nutrient stores. Specifically, HG-cultured BeWo CT (but not SCT) cells were found to have increased triglyceride abundance that may be related to increased fatty acid trafficking to lipid droplets by *ACSL1* and/or increased *de novo* lipogenesis. Further, both BeWo CT and SCT cells displayed increased glycogen content. Investigations into underlying regulation of glycogen synthesis revealed reduced protein abundance of glycogen synthase and increased inhibitory phosphorylation (pSer⁶⁴¹) of glycogen synthase in the HG-cultured BeWo trophoblasts. These changes could increase free glucose available for glycolysis and subsequent mitochondrial oxidation and may ultimately result in increased ROS generation and mitochondrial oxidative damage. HG-cultured BeWo CT cells were also found to have increased accumulation of riboflavin which may further indicate the development of mitochondrial dysfunction. The increased malonate and C16:0 acylcarnitine levels observed in HG-cultured BeWo CT cells suggested reduced fatty acid β -oxidation and may be reflective of an oxidative fuel switch induced by increased glucose levels.

Ultimately the alterations in placental nutrient storage (particularly the diminished glycogen storage capacity potentially leading to increased free glucose) and transition towards mitochondrial dysfunction that we observed in high glucose treated BeWo trophoblasts may impact transplacental nutrient transport. Our data could highlight that the increased prevalence of macrosomia in diabetic pregnancies [40] is in part facilitated by hyperglycemia-mediated modifications in placental nutrient processing that promotes an increased transfer of glucose from mother to the developing fetus [41]. Therefore, ensuring proper and consistent glycemic control that limits periods of maternal hyperglycemia is likely of paramount importance in the clinical management of diabetic pregnancies. As we have demonstrated that even a short-term (72-hour) high glucose exposure can negatively impact placental nutrient processing, preventing any placental hyperglycemic exposures may be necessary to limit fetal overgrowth and in turn limit the prevalence of DOHaD-related metabolic health complications in the exposed offspring.

5.2.3 Chapter 4: Elevated Dietary Non-Esterified Fatty Acid Levels Impact BeWo Trophoblast Metabolism and Lipid Processing: A Multi-OMICS Outlook

In Chapter 3 we highlighted that utilizing a multi-omics research approach provided in-depth insight into the underlying mechanisms that regulate BeWo trophoblast metabolic function in response to elevated glucose. In Chapter 4, we turned our attention back to the dietary NEFA species PA and OA and sought to utilize these integrative “omics” approaches to better characterize the impacts of dietary NEFA species on placental metabolic function. In these analyses we utilized transcriptomic, metabolomic, and lipidomic readouts as were performed with hyperglycemia exposed BeWo CT cells in Chapter 3. In this chapter, we additionally utilized targeted Gas Chromatography (GC) and targeted Thin Layer Chromatograph (TLC) to specifically characterize cellular fatty acid (FA) and neutral lipid profiles in both BeWo CT cells and SCT cells. We postulated that *exposure to elevated levels of dietary NEFA would alter BeWo trophoblast lipid profiles, highlighted by increased TG abundance, and increased FA elongation and desaturation*. It was additionally postulated that that *dietary-FA treated BeWo CT cells*

would display altered transcriptomic, metabolomic and lipidomic profiles indicative of altered lipid processing.

Our targeted analyses of FA and neutral lipid profiles highlighted that PA and OA are differentially processed by BeWo trophoblast cells. Of particular interest, our TLC analyses demonstrated that BeWo CT and SCT cells have increased TG content when cultured with OA alone. These data suggested that OA is highly lipogenic in BeWo trophoblasts, and interestingly, similar trends have been reported in OA-cultured PHT cells [42]. However, co-culture of BeWo trophoblasts with both PA and OA (P/O treatment) was not associated with elevated TG abundance. Overall, these data demonstrated that both NEFA concentration and composition are important in regulating placental trophoblast lipid processing.

The utilization of targeted FA analyses in this chapter also allowed for investigations into FA desaturation and elongation processing in NEFA-exposed BeWo trophoblasts. These FA metabolic pathways were specifically examined by calculating elongase and desaturase indices (enzyme product to substrate ratios) that are reflective of enzyme activity. These analyses specifically revealed that OA-treated BeWo CT displayed increased production of gondoic acid (20:1n9; via OA elongation) and γ -linolenic acid (18:3n6; via desaturation of linoleic acid). As these FA species have been associated with anti-inflammatory outcomes [43,44], the data could suggest that OA reduces inflammatory signaling in placental trophoblasts.

Integrating the transcriptomic and metabolomic datasets in this chapter provided further evidence that OA exposure is associated with anti-inflammatory outcomes in BeWo trophoblast cells. Specifically, we observed a significant enrichment in the Purine metabolism KEGG pathway in OA-treated BeWo CT cells that was associated with accumulations of the purine metabolites adenosine (+3.30 FC), inosine (+2.45 FC), and guanosine (+1.69 FC) compared to BSA-control cultures. As purine breakdown has been previously observed in placental responses to inflammation [45], these data may highlight that OA-exposure exerts anti-inflammatory benefits by preventing purine degradation. However, an alternate explanation may be that BeWo trophoblasts have increased purine

synthesis via the Pentose Phosphate Pathway (PPP) when exposed to elevated OA levels. As the PPP generates NADPH, a molecule with antioxidant effects, these data could also indicate that OA exerts antioxidant effects in BeWo trophoblasts [46,47]. Overall, these data alluded that altered FA elongation and desaturation, as well as altered purine metabolism may specifically underlie the previously observed anti-apoptotic effects of OA on placental trophoblasts [42,48]. A schematic summarizing the alterations observed in OA-cultured BeWo trophoblasts in chapters 2 and 4 is available in **Figure 5-3**.

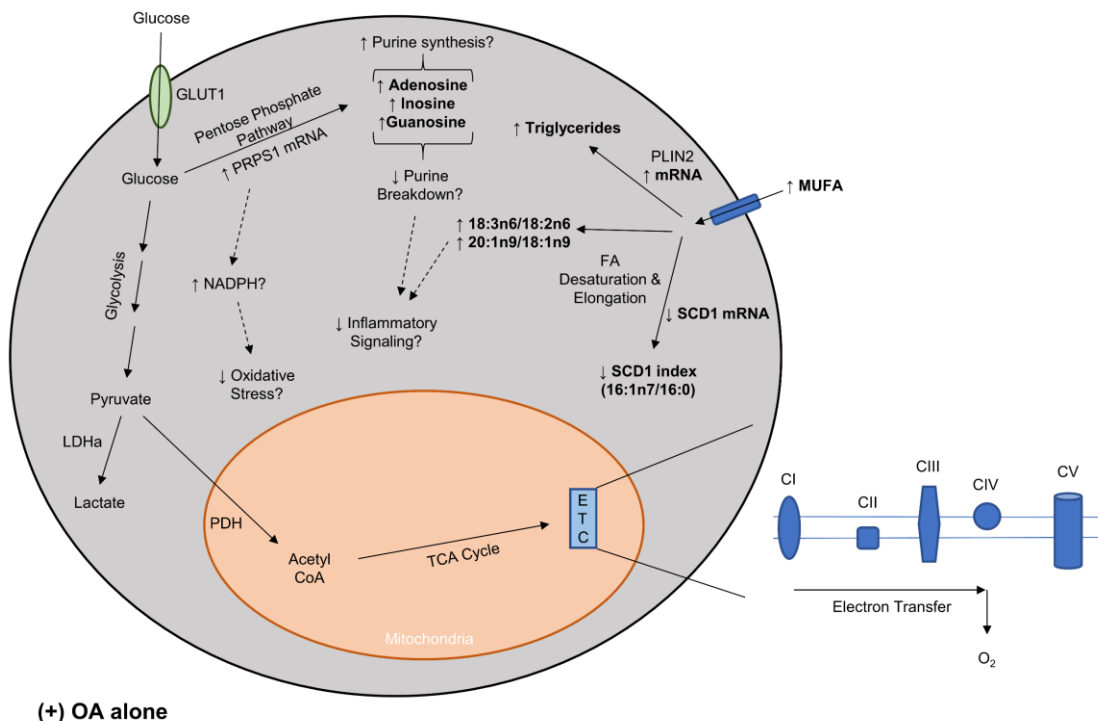


Figure 5-3 Summary illustration of the impact of OA-exposure (100 μ M) on BeWo trophoblast cells.

BeWo trophoblasts cultured with OA for 72 hours were found to have altered lipid processing highlighted by increased triglyceride abundance and altered fatty acid metabolism via desaturase and elongase enzymes. This altered desaturation and elongation processing was highlighted by increased production of gondoic acid (C20:1n9) and γ -linolenic acid (C18:3n6), that may be associated with anti-inflammatory outcomes. Additionally, OA-cultured BeWo CT cell displayed increased purine (adenosine, inosine, and guanosine) accumulations that may be reflective of decreased purine breakdown or increased purine synthesis via the Pentose Phosphate Pathway. As purine breakdown has been implicated in placental responses to inflammatory stimuli, the observed purine accumulation may further highlight anti-inflammatory signaling in OA-cultured BeWo trophoblasts. Further, as the Pentose Phosphate Pathway generates NADPH, a molecule with antioxidant properties, purine accumulation could indicate that OA acts as an antioxidant in BeWo trophoblasts leading to decreased oxidative stress.

Combining the transcriptome, metabolome, and lipidome readouts in Chapter 4 additionally suggested that PA treatments, both independently and in combination with OA (P/O treatments) increased β -oxidative activity in BeWo CT cells. Specifically, we observed upregulated expression of the β -oxidation genes *ACADVL* and *ACACB* in PA and P/O-treated BeWo CT cells. Additionally, PA and P/O-cultured BeWo CT cells displayed elevated levels of C16:0 acylcarnitine, a β -oxidation intermediary that facilitates the transport of PA into the mitochondrial matrix for oxidation. Notably, BeWo CT cells cultured with PA-alone (But not the P/O mixture) also displayed increased C14:0 acylcarnitine levels that may be reflective of incomplete β -oxidation processes. In contrast, P/O-cultured BeWo CT cells displayed elevated malonate levels that may be reflective of complete β -oxidation.

Further, these data may indicate that the increased basal and maximal mitochondrial respiratory activities observed in PA and P/O-treated BeWo CT cells in Chapter 2 were the result of increased β -oxidation activity. Additionally, as increased β -oxidation has in itself been linked with increased ROS generation, mitochondrial oxidative stress, and mitochondrial dysfunction [49–51], the data in Chapter 4 further suggests that our 72-hour PA exposure (both alone and in combination with OA) represents an early timepoint in a progression towards mitochondrial impairments. However, as the data in Chapter 4 also highlighted that OA may exert anti-inflammatory effects and act as an antioxidant in BeWo trophoblasts, future investigations may need to better elucidate if the combination P/O-exposure ultimately results in mitochondrial dysfunction, or if the additional OA exposure in this treatment group helps preserve appropriate mitochondrial function. Schematics summarizing the impacts of PA and P/O exposure on BeWo trophoblasts are available in **Figure 5-4**, and **Figure 5-5**.

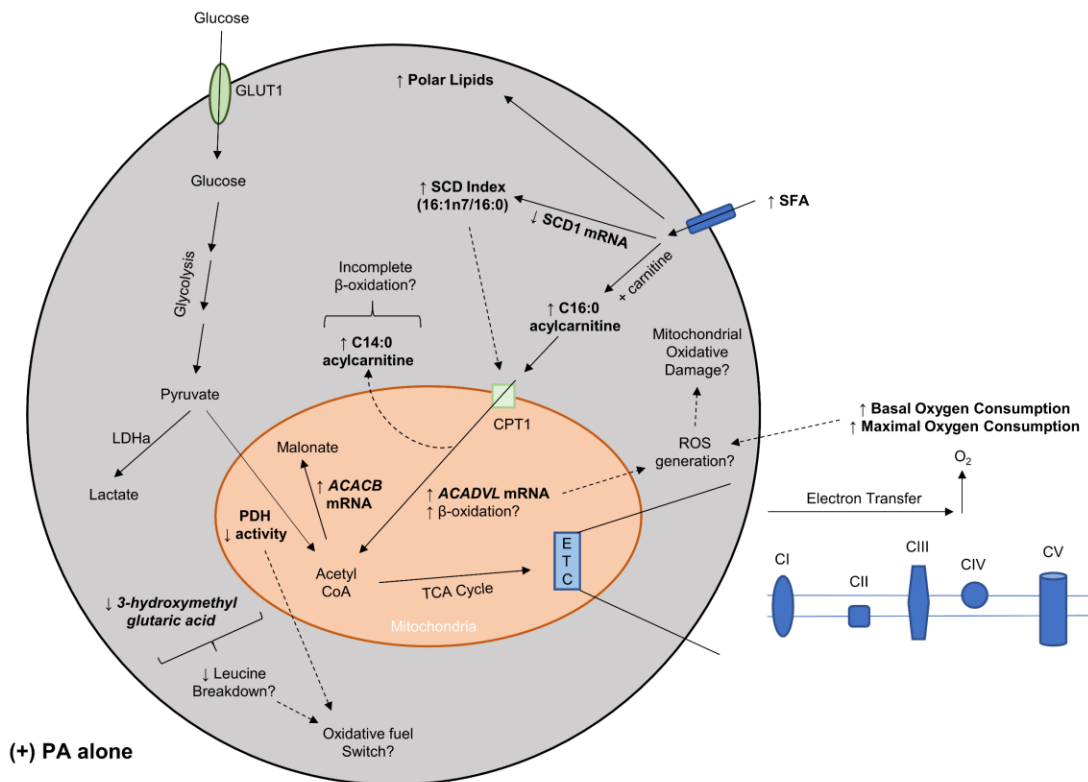


Figure 5-4 Summary illustration of the impacts of PA-exposure (100 μ M) on BeWo trophoblast cells.

BeWo CT cells cultured with PA for 72 hours were found to have increased basal and maximal mitochondrial respiratory activity. These changes in mitochondrial function were associated with markers suggestive of an oxidative fuel switch that favoured increased β -oxidation. Specifically, reduced 3-hydroxymethylglutaric acid levels and reduced PDH activity in PA-cultured BeWo CT cells suggested reduced oxidation of amino acid fuels and carbohydrate fuels. Further, the observed accumulation of C16:0 acylcarnitine in conjunction with increased mRNA expression of β -oxidation enzymes (*ACADVL* and *ACACB*) was indicative of increased fatty acid oxidation for ATP production. Interestingly, PA-cultured BeWo CT cells also displayed an increased accumulation of C14:0 acylcarnitine, that could be indicative of incomplete β -oxidation, a marker of a dysfunctional mitochondria. Overall, we speculated that the increased mitochondrial respiratory activity and β -oxidation in PA-culture BeWo CT cells would lead to increased ROS generation, and ultimately oxidative mitochondrial damage.

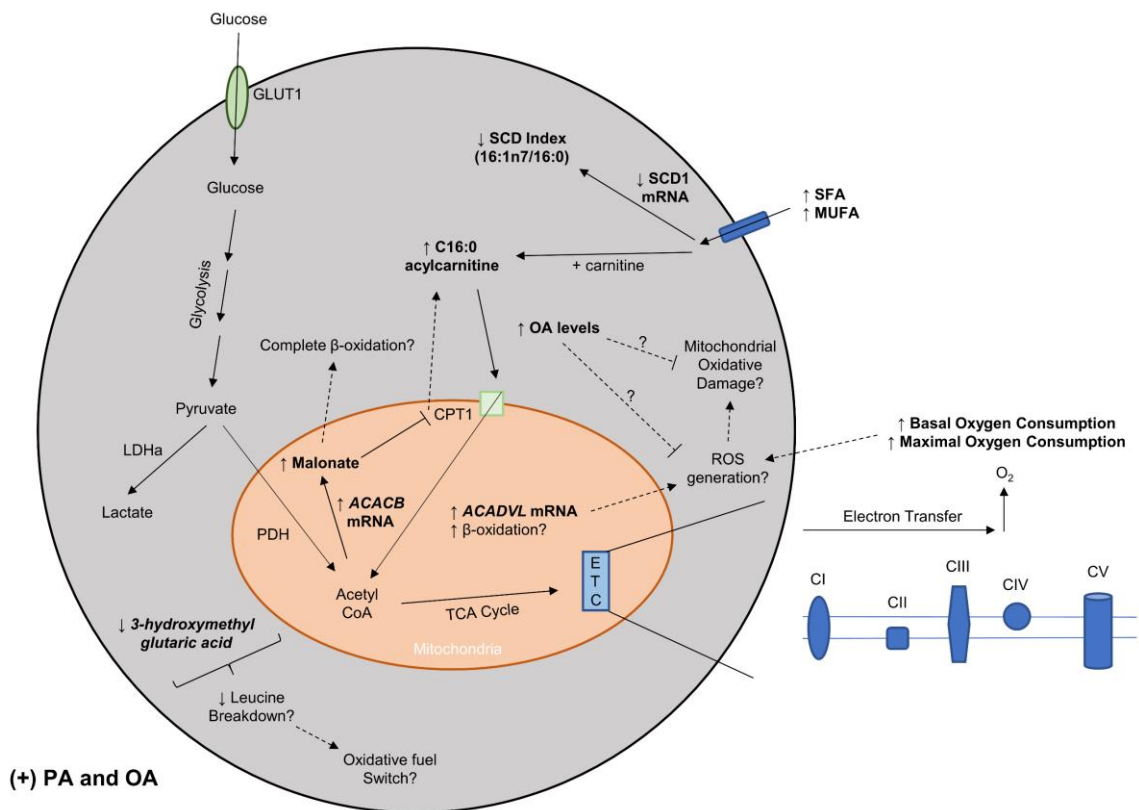


Figure 5-5 Summary illustration of the impacts of P/O-exposure (50 μ M each PA and OA) on BeWo trophoblast cells.

BeWo CT cells cultured with a combination of PA and OA were, like PA-alone cultured BeWo CT cells, found to have increased basal and maximal mitochondrial respiratory activity. Increased C16:0 acylcarnitine levels, and increased expression of β -oxidation enzymes (*ACADVL* and *ACACB*) in these cells suggested that the observed increased mitochondrial respiration was resultant from increased fatty acid oxidation. We speculated that these increases in mitochondrial respiration and β -oxidation would ultimately lead to increased ROS generation and oxidative mitochondrial damage. However, P/O-cultured BeWo CT cells also displayed increased malonate levels that may indicate complete β -oxidation, as well as a functional negative feedback system that acts to reduce excessive fatty acid oxidation. These changes in conjunction with increased OA levels may act to reduce excessive ROS generation in P/O combination cultured BeWo CT cells and may help to preserve appropriate mitochondrial function despite exposure to lipid overabundance.

We speculate that mitochondrial impairments in placental trophoblasts that develop in response to elevated levels of dietary saturated FA could lead to subsequent increases in transplacental transport of lipid species [52], as well as placental lipid storage. Therefore, the data in Chapter 2 and Chapter 4 could indicate that the increased prevalence of placental steatosis [19,53] and fetal macrosomia [40,54,55] that has been observed in obese and GDM pregnancies is directly facilitated by increased saturated FA delivery to the placenta. Reducing placental saturated NEFA exposure, perhaps through maternal dietary interventions (e.g. adherence to a Mediterranean-style [56] or pacific-style [57] style high in omega-3 FA species), may be of increasing importance in the clinical management of obese and GDM pregnancies to help preserve appropriate placental nutrient processing and in turn facilitate healthy fetal development.

5.3 Considerations for clinical diagnosis of placental dysfunction

The data presented in this thesis overall suggested that a 72-hour exposure to elevated levels of both dietary NEFAs and glucose was associated with a transition towards mitochondrial dysfunction in placental villous trophoblast cells. These mitochondrial impairments are specifically important as in both conditions of nutrient overabundance they could impact placental nutrient processing leading to increased nutrient delivery to the fetus. Increased transplacental nutrient transport would promote increased fetal growth and macrosomia, and in turn, *in utero* programming associated with later-life development of DOHaD-related non-communicable cardio-metabolic health complications [58,59]. However, in order to properly implement and personalize clinical interventions that prevent, or potentially reverse these placental mitochondrial impairments, clinical diagnostic tests must be developed in order to accurately assess in real time during gestation if the placenta is on a trajectory towards failure. Ideally, these diagnostic tests would assess biomarker abundance in easily accessible biofluids (i.e. urine and blood samples) that can be collected during routine prenatal care appointments.

Interestingly, the data in this thesis highlighted that while increased saturated NEFAs and glucose supply were both associated with altered BeWo metabolic function suggestive of a transition towards ultimate mitochondrial failure, these nutrients have

vastly different underlying impacts to placental metabolism. In our multi-omic analyses, we utilized multivariate PCA analyses to examine the degree of separation in metabolome, lipidome and transcriptome profiles in BeWo CT cells cultured with different NEFA species and hyperglycemia. Specifically, the glucose treatments in Chapter 3 were associated with divergent transcriptome and metabolome profiles, but limited differences in cellular lipidome profiles. In contrast, the omic analyses in Chapter 4 revealed that BeWo CT transcriptome and lipidome profiles, but not polar metabolome profiles were divergent following exposure to elevated dietary NEFA levels. Thus, the biomarkers that are associated with an early phenotype of mitochondrial dysfunction in placenta trophoblasts are likely different in cells exposed to high NEFA levels and hyperglycemia. Future studies that seek to utilize the biomarkers reported in our studies in preliminary clinical tests to diagnose failing placenta mitochondria in cases of maternal obesity, GDM and pre-existing type 1 diabetes will need to consider these differences to enable an accurate point of care assessment of placental function.

The altered abundances of acylcarnitine species (e.g. C16:0 and C14:0 acylcarnitines) in PA and P/O-cultured BeWo trophoblast cells could indicate that acylcarnitine analysis can be utilized to diagnose aberrant placental mitochondrial function in response to excessive saturated fats. Interestingly, diagnostic tests measuring circulating acylcarnitine species (reflective of abnormal placental lipid oxidation) in maternal serum and plasma have already been utilized in the early detection of placenta disorders such as pre-eclampsia, although they are not yet suitable for implementation in reproductive clinical settings [60,61]. Therefore, it may be possible to adapt these previously established protocols to integrate new biomarkers and better develop diagnostic tests that assess placental mitochondrial function and the transition towards mitochondrial failure in high fat environments such as obesity. Acylcarnitine analysis has been utilized to detect the metabolic perturbations associated with cardiovascular disease [62,63], further highlighting the future potential clinical utility of these readouts.

In contrast, utilizing different metabolomic strategies that emphasize the detection of small, polar metabolites will likely need to be developed to detect early onset placental mitochondrial dysfunction in response to a hyperglycemic environment. Notably, such

metabolomic analyses have previously been utilized to detect placental dysfunctions in pregnancies complicated with intrauterine growth restriction [64], and pre-eclampsia [65], although these tests have, like acylcarnitine analysis, not been approved for use in clinical settings.

5.4 Limitations and Future Considerations

The current thesis demonstrated that both dietary NEFAs and glucose are important independent regulators of BeWo trophoblast cell metabolic function. However, as some pregnancies complicated with GDM are associated with concurrent elevations in both dietary fat and glucose levels [66,67], the combined impacts of these nutrient exposures still need to be explored. A logical extension of the work in the current thesis would be to combine the NEFA and glucose exposures, potentially by supplementing the P/O NEFA media with 25 mM glucose. These specific investigations will allow greater insight into whether the combined nutrient exposures result in a synergistic “double-hit” that ultimately worsens or accelerates the development of metabolic and mitochondrial impairments in placental trophoblast cells.

A major limitation of the work presented in the current thesis is that a single timepoint (72 hours) was utilized for all assessments of BeWo trophoblast metabolic function. As we speculated our glucose and PA-treated BeWo trophoblasts are progressing towards mitochondrial dysfunction after 72-hours of nutrient exposure, more chronic exposures may better highlight the development of nutrient-induced placental mitochondrial impairments. However, BeWo trophoblast cells quickly grow to form a confluent monolayer, and interestingly do not display contact inhibition, ultimately leading to the creation of a confluent multi-layer of cells [68–70]. The 72-hour protocol was specifically utilized in these investigations as it represented the longest possible cell culture exposure prior to the cells becoming confluent and forming a multi-layered culture system. The avoidance of a multi-layered cell culture system was important in the investigations in this thesis to ensure accurate measurements of metabolic activity in the Seahorse XF assays performed in chapters 2 and 3 [71]. One possible method of extending the nutrient exposures while avoiding the production of confluent multi-layers would be through sub-culturing the cells prior to confluence and redistributing them onto

new cell culture dishes. However, this would require additional manipulation of the cell culture system that could lead to increased cellular stress, and potentially lead to the unwanted selection of nutrient-resistant cell populations. Future studies may look to prolong these treatment durations to characterize markers associated with endpoint mitochondrial failure in BeWo trophoblasts, although care must be taken to avoid selecting NEFA and glucose resistant cell populations during sub-culturing procedures.

Further, the data in this thesis are limited as all cell culture experiments were performed in 5% CO₂/95% atmospheric air, corresponding to a growth environment with approximately 20% oxygen. Additional analysis of BeWo trophoblast mitochondrial and metabolic activity may need to be performed at physiological placental oxygenation levels (approximately 8% during the third trimester) [72,73] to better model *in vivo* placental conditions, and further characterize placental responses to nutrient overabundance.

Additionally, these studies are limited as only a single placental cell line model was utilized to assess metabolic function in response to nutrient overabundance. In addition to BeWo trophoblast cells, previous studies have highlighted that the JAR, and JEG-3 placental cell lines are useful in *in vitro* analyses of placental villous trophoblast function [74–77]. Future investigations using these other placental cell systems may be needed to elucidate if the underlying mechanisms governing trophoblast responses to nutrient overabundance are common to all human trophoblast cell line lineages, or if the responses discussed in the current thesis are unique to BeWo trophoblast cells. However, as JEG-3 cells have previously been found to have lower glucose transport capabilities than BeWo cells, JAR cells and PHTs [76], this particular cell line may not be useful in examining placental responses to hyperglycemia. Further, as only BeWo trophoblast cells, and not JAR or JEG-3 trophoblast cells, have been found to form large multi-nucleated syncytia [75], these other placental cell line systems may be limited in their evaluation of differentiation-state dependent differences in metabolic function between placental CT and SCT cells.

While these placental cell line models are useful to investigate the independent impacts of nutrient overabundance on trophoblast metabolic function, the cancerous origins of these cells may ultimately impact their underlying physiology [78]. Thus, future investigations may be needed to elucidate if elevated nutrient supply also directly regulates metabolic and mitochondrial function in *ex vivo* primary placental cells to strengthen the data obtained in this thesis. Additionally, the JEG-3, JAR and BeWo placental cell lines are all genetically male [79,80]. As recent studies have highlighted placental responses to an adverse intrauterine environment are sex-dependent [81–84], these placental cell line studies are limited in that they cannot discuss how fetal sex influences placental metabolic function in a nutrient-rich environment. Interestingly, male placentae have also been found to display fewer adaptations in response to the nutrient stresses of obese and diabetic pregnancies [82,83]. This sex-dependent influence and the male sex of BeWo trophoblasts may highlight a high stability of the BeWo transcriptome and could be an underlying explanation of why only 3 transcripts (SGK1, CREB3L3, and MAMDC2) displayed a $> \pm 2$ -fold change in NEFA-treated BeWo cells, and also why no transcripts displayed > 2 -fold-change in HG-cultured BeWo CT cells. Future investigations utilizing primary placental material may be needed to better understand how fetal sex influences the regulation of placental metabolism and gene expression following a nutrient overload challenge.

One method of examining these responses in primary placental material is through the isolation and culture of term CT cells (PHTs) from healthy control pregnancies using well validated methodologies [85,86]. However, PHT cultures have been demonstrated to display spontaneous fusion and display a SCT phenotype as soon as 48 hours in culture [87,88]. Thus, these studies may themselves be limited in examining differentiation-state dependent differences in the responses of CT and SCT cells to elevated nutrient content. Additionally, this spontaneous fusion capacity also highlights that more prolonged and chronic NEFA, and glucose exposures cannot be examined in primary human CT cultures, and thus these models may not have the capability to examine endpoint CT mitochondrial failure.

An additional method of examining responses to elevated nutrient levels in primary placental material is through the use of *ex vivo* explants, as has previously been described [89,90]. Explant-based analysis may have increased physiological relevance compared to other *in vitro* and *ex vivo* placental models due to the co-culture of many different placental cell types including trophoblast cells, fetal mesenchymal cells, and placental immune cells in their proper three-dimensional physiological orientations [89]. These explant-based studies may help elucidate how “cross-talk” between different placental cells impacts overall placental metabolic function. Additionally, as placental explants have the ability to be cultured for up to 12 days, these systems may be beneficial in elucidating the impacts of more chronic nutrient exposures on placental trophoblasts [89,91]. A potential shortfall of these explant studies, however, is that it may be difficult to determine how the different placental cell types individually contribute to the overall observed metabolic phenotypes. However, the use of single cell “omics” techniques, such as single cell RNA sequencing (scRNAseq), in these studies may allow for the identification and characterization of unique placental cell types, as has been performed in other tissue models [92,93].

Finally, while the results in the current study have demonstrated that nutrient overabundance modulates placental trophoblast metabolism and nutrient processing functions, the ultimate impact that these changes have on transplacental nutrient transport remains poorly understood. The work in this thesis could additionally be extended to elucidate these outcomes by utilizing BeWo transwell culture systems that better model placental barrier functions, as has previously been described [94–96]. In these systems, BeWo trophoblasts can be cultured on semi-permeable membranes on an inner cell culture chamber. Subsequently, the transport of nutrients through the BeWo cell layer and into an outer cell culture chamber can be examined, most likely via metabolomic analyses of the conditioned media in the outer chamber. Additionally, some previously established transwell systems have utilized co-culture of BeWo trophoblasts and human umbilical vein endothelial cells (HUVEC cells) on opposite sides of the semi-permeable transwell membranes [96]. These co-culture systems have the ability to examine how different placental cell types work together to modulate transplacental nutrient transport. More recently, “placenta-on-a-chip” systems have also been developed to better model *in vivo*

placental barrier functions [97,98]. In these systems, much like transwell systems, BeWo cells can be cultured on semi-permeable membrane in co-culture with other placental cells like HUVECs, and nutrient transfer across the cellular barrier can be quantified. However, unlike transwell cultures, placenta-on-a-chip system utilize a dynamic flow of cell culture media that also models *in vivo* blood flow, and trophoblast responses to fluid shear stresses [99,100]. Overall, the use of these placental barrier cell culture systems in future investigations could provide better insight into how nutrient overabundance impacts transplacental nutrient transport.

5.5 Conclusion

The work in this thesis evaluated the impacts of independent dietary NEFA and glucose exposure on BeWo placental trophoblast nutrient processing and mitochondrial function. These investigations have expanded our understanding of how dietary nutrients regulate placental metabolism. We highlighted that a 72-hour exposure to elevated dietary nutrient levels impacted nutrient storage and was associated with altered transcriptome, metabolome and lipidome profiles in BeWo trophoblast cells. Additionally, we observed markers indicative of a transition towards overall oxidative mitochondrial failure in BeWo trophoblast cells exposed to both elevated saturated NEFA and glucose levels. Furthermore, we demonstrated a differentiation-state dependent suppression of mitochondrial activity and nutrient storage in BeWo SCT cells. Overall, the data in this thesis suggests that an increased delivery of nutrients to the placenta in pregnancies complicated by nutrient overabundance (often clinically displayed in obese and diabetic pregnancies) may facilitate the development of placental impairments that increase the risk of non-communicable metabolic diseases development in the exposed offspring. These data continue to support the idea that modulating maternal nutrient levels through healthy lifestyle choice, dietary interventions, and glycemic management strategies is important in the clinical management of these “high-risk” pregnancies to ensure appropriate placental function is maintained throughout gestation.

5.6 References

- [1] J.A. Armitage, L. Poston, P.D. Taylor, Developmental Origins of Obesity and the Metabolic Syndrome: The Role of Maternal Obesity, in: *Obe. Metab.*, KARGER, Basel, 2008: pp. 73–84. doi:10.1159/000115355.
- [2] L.J. Monteiro, J.E. Norman, G.E. Rice, S.E. Illanes, Fetal programming and gestational diabetes mellitus, *Placenta*. 48 (2016) S54–S60. doi:10.1016/j.placenta.2015.11.015.
- [3] P.M. Catalano, The impact of gestational diabetes and maternal obesity on the mother and her offspring, *J. Dev. Orig. Health Dis.* 1 (2010) 208–215. doi:10.1017/S2040174410000115.
- [4] B. Brenseke, M.R. Prater, J. Bahamonde, J.C. Gutierrez, Current Thoughts on Maternal Nutrition and Fetal Programming of the Metabolic Syndrome, *J. Pregnancy*. 2013 (2013) 1–13. doi:10.1155/2013/368461.
- [5] T. Jansson, T.L. Powell, Role of the placenta in fetal programming: underlying mechanisms and potential interventional approaches, *Clin. Sci.* 113 (2007) 1–13. doi:10.1042/CS20060339.
- [6] A. Tarrade, P. Panchenko, C. Junien, A. Gabory, Placental contribution to nutritional programming of health and diseases: epigenetics and sexual dimorphism, *J. Exp. Biol.* 218 (2015) 50–58. doi:10.1242/jeb.110320.
- [7] X. Chen, T.O. Scholl, M. Leskiw, J. Savaille, T.P. Stein, Differences in maternal circulating fatty acid composition and dietary fat intake in women with gestational diabetes mellitus or mild gestational hyperglycemia, *Diabetes Care*. 33 (2010) 2049–2054. doi:10.2337/dc10-0693.
- [8] T. Zhang, W.-R. Jiang, Y.-Y. Xia, T. Mansell, R. Saffery, R.D. Cannon, J. De Seymour, Z. Zou, G. Xu, T.-L. Han, H. Zhang, P.N. Baker, Complex patterns of circulating fatty acid levels in gestational diabetes mellitus subclasses across pregnancy, *Clin. Nutr.* 40 (2021) 4140–4148. doi:10.1016/j.clnu.2021.01.046.
- [9] P.M. Villa, H. Laivuori, E. Kajantie, R. Kaaja, Free fatty acid profiles in preeclampsia, *Prostaglandins, Leukot. Essent. Fat. Acids*. 81 (2009) 17–21. doi:10.1016/j.plefa.2009.05.002.
- [10] D. Iggman, U. Risérus, Role of different dietary saturated fatty acids for cardiometabolic risk, *Clin. Lipidol.* 6 (2011) 209–223. doi:10.2217/clp.11.7.
- [11] C.L. Kien, J.Y. Bunn, R. Stevens, J. Bain, O. Ikayeva, K. Crain, T.R. Koves, D.M. Muoio, Dietary intake of palmitate and oleate has broad impact on systemic and tissue lipid profiles in humans, *Am. J. Clin. Nutr.* 99 (2014) 436–445. doi:10.3945/ajcn.113.070557.

- [12] J. Denomme, K.D. Stark, B.J. Holub, Directly quantitated dietary (n-3) fatty acid intakes of pregnant Canadian women are lower than current dietary recommendations., *J. Nutr.* 135 (2005) 206–11. doi:135/2/206 [pii].
- [13] C.M. Palmeira, F.M.L. Ferreira, D.L. Santos, R. Ceiça, K. Suzuki, M.S. Santos, Higher efficiency of the liver phosphorylative system in diabetic Goto-Kakizaki (GK) rats, *FEBS Lett.* 458 (1999) 103–106. doi:10.1016/S0014-5793(99)01144-8.
- [14] N.E. Sunny, E.J. Parks, J.D. Browning, S.C. Burgess, Excessive Hepatic Mitochondrial TCA Cycle and Gluconeogenesis in Humans with Nonalcoholic Fatty Liver Disease, *Cell Metab.* 14 (2011) 804–810. doi:10.1016/j.cmet.2011.11.004.
- [15] K. Kolahi, A. Valent, K.L. Thornburg, Cytotrophoblast, Not Syncytiotrophoblast, Dominates Glycolysis and Oxidative Phosphorylation in Human Term Placenta., *Sci. Rep.* (2017) 1–12. doi:10.1038/srep42941.
- [16] A.M. Valent, H. Choi, K.S. Kolahi, K.L. Thornburg, Hyperglycemia and gestational diabetes suppress placental glycolysis and mitochondrial function and alter lipid processing, *FASEB J.* 35 (2021). doi:10.1096/fj.202000326RR.
- [17] J. Fisher, D. McKeating, E. Pennell, J. Cuffe, O. Holland, A. Perkins, Mitochondrial isolation, cryopreservation and preliminary biochemical characterisation from placental cytotrophoblast and syncytiotrophoblast, *Placenta.* 82 (2019) 1–4. doi:10.1016/j.placenta.2019.05.004.
- [18] C.H. Hulme, A. Stevens, W. Dunn, A.E.P. Heazell, K. Hollywood, P. Begley, M. Westwood, J.E. Myers, Identification of the functional pathways altered by placental cell exposure to high glucose: lessons from the transcript and metabolite interactome, *Sci. Rep.* 8 (2018) 5270. doi:10.1038/s41598-018-22535-y.
- [19] C.H. Hulme, A. Nicolaou, S.A. Murphy, A.E.P. Heazell, J.E. Myers, M. Westwood, The effect of high glucose on lipid metabolism in the human placenta, *Sci. Rep.* 9 (2019) 14114. doi:10.1038/s41598-019-50626-x.
- [20] T. Hahn, D. Hahn, A. Blaschitz, E.T. Korgun, G. Desoye, G. Dohr, Hyperglycaemia-induced subcellular redistribution of GLUT1 glucose transporters in cultured human term placental trophoblast cells, *Diabetologia.* 43 (2000) 173–180. doi:10.1007/s001250050026.
- [21] U. Weiss, M. Cervar, P. Puerstner, O. Schmut, J. Haas, R. Mauschitz, G. Arikan, G. Desoye, Hyperglycaemia in vitro alters the proliferation and mitochondrial activity of the choriocarcinoma cell lines BeWo, JAR and JEG-3 as models for human first-trimester trophoblast, *Diabetologia.* 44 (2001) 209–219. doi:10.1007/s001250051601.
- [22] M. He, G. Wang, S. Han, Y. Jin, H. Li, X. Wu, Z. Ma, X. Cheng, X. Tang, X. Yang, G. Liu, Nrf2 signalling and autophagy are involved in diabetes mellitus-

- induced defects in the development of mouse placenta, *Open Biol.* 6 (2016) 160064. doi:10.1098/rsob.160064.
- [23] S.J. Tunster, E.D. Watson, A.L. Fowden, G.J. Burton, Placental glycogen stores and fetal growth: insights from genetic mouse models, *Reproduction.* 159 (2020) R213–R235. doi:10.1530/REP-20-0007.
- [24] P. Georgiades, A.C. Ferguson-Smith, G.J. Burton, Comparative Developmental Anatomy of the Murine and Human Definitive Placentae, *Placenta.* 23 (2002) 3–19. doi:10.1053/plac.2001.0738.
- [25] G.B. Wislocki, H.S. Bennett, The histology and cytology of the human and monkey placenta, with special reference to the trophoblast, *Am. J. Anat.* 73 (1943) 335–449. doi:10.1002/aja.1000730303.
- [26] K. Kolahi, S. Louey, O. Varlamov, K. Thornburg, Real-time tracking of BODIPY-C12 long-chain fatty acid in human term placenta reveals unique lipid dynamics in cytotrophoblast cells, *PLoS One.* 11 (2016) 1–23. doi:10.1371/journal.pone.0153522.
- [27] Y.-C. Lai, J.T. Stuenæs, C.-H. Kuo, J. Jensen, Glycogen content and contraction regulate glycogen synthase phosphorylation and affinity for UDP-glucose in rat skeletal muscles, *Am. J. Physiol. Metab.* 293 (2007) E1622–E1629. doi:10.1152/ajpendo.00113.2007.
- [28] A. Czajka, A.N. Malik, Hyperglycemia induced damage to mitochondrial respiration in renal mesangial and tubular cells: Implications for diabetic nephropathy, *Redox Biol.* 10 (2016) 100–107. doi:10.1016/j.redox.2016.09.007.
- [29] A. Koziel, A. Woyda-Ploszczyca, A. Kicinska, W. Jarmuszkiewicz, The influence of high glucose on the aerobic metabolism of endothelial EA.hy926 cells, *Pflügers Arch. - Eur. J. Physiol.* 464 (2012) 657–669. doi:10.1007/s00424-012-1156-1.
- [30] F. Martínez, M. Kiriakidou, J.F. Strauss, Structural and Functional Changes in Mitochondria Associated with Trophoblast Differentiation: Methods to Isolate Enriched Preparations of Syncytiotrophoblast Mitochondria 1, *Endocrinology.* 138 (1997) 2172–2183. doi:10.1210/endo.138.5.5133.
- [31] S. Hauguel-de Mouzon, G. Desoye, The Placenta in Diabetic Pregnancy: New Methodological Approaches, in: 2020: pp. 145–154. doi:10.1159/000480171.
- [32] Y. Yang, F. Guo, Y. Peng, R. Chen, W. Zhou, H. Wang, J. OuYang, B. Yu, Z. Xu, Transcriptomic Profiling of Human Placenta in Gestational Diabetes Mellitus at the Single-Cell Level, *Front. Endocrinol. (Lausanne).* 12 (2021) 145–154. doi:10.3389/fendo.2021.679582.
- [33] S. Mohammad, J. Bhattacharjee, T. Vasanthan, C.S. Harris, S.A. Bainbridge, K.B. Adamo, Metabolomics to understand placental biology: Where are we now?,

- Tissue Cell. 73 (2021) 101663. doi:10.1016/j.tice.2021.101663.
- [34] T. Li, X. Li, H. Meng, L. Chen, F. Meng, ACSL1 affects Triglyceride Levels through the PPAR γ Pathway, *Int. J. Med. Sci.* 17 (2020) 720–727. doi:10.7150/ijms.42248.
- [35] H.A. Parkes, E. Preston, D. Wilks, M. Ballesteros, L. Carpenter, L. Wood, E.W. Kraegen, S.M. Furler, G.J. Cooney, Overexpression of acyl-CoA synthetase-1 increases lipid deposition in hepatic (HepG2) cells and rodent liver in vivo, *Am. J. Physiol. Metab.* 291 (2006) E737–E744. doi:10.1152/ajpendo.00112.2006.
- [36] Z. Zhao, S.H. Abbas Raza, H. Tian, B. Shi, Y. Luo, J. Wang, X. Liu, S. Li, Y. Bai, J. Hu, Effects of overexpression of ACSL1 gene on the synthesis of unsaturated fatty acids in adipocytes of bovine, *Arch. Biochem. Biophys.* 695 (2020) 108648. doi:10.1016/j.abb.2020.108648.
- [37] A. Honda, K. Yamashita, T. Ikegami, T. Hara, T. Miyazaki, T. Hirayama, M. Numazawa, Y. Matsuzaki, Highly sensitive quantification of serum malonate, a possible marker for de novo lipogenesis, by LC-ESI-MS/MS, *J. Lipid Res.* 50 (2009) 2124–2130. doi:10.1194/jlr.D800054-JLR200.
- [38] S. Balasubramaniam, J. Yaplito-Lee, Riboflavin metabolism: role in mitochondrial function, *J. Transl. Genet. Genomics.* (2020). doi:10.20517/jtgg.2020.34.
- [39] S. Balasubramaniam, J. Christodoulou, S. Rahman, Disorders of riboflavin metabolism, *J. Inherit. Metab. Dis.* 42 (2019) 608–619. doi:10.1002/jimd.12058.
- [40] K. KC, S. Shakya, H. Zhang, Gestational Diabetes Mellitus and Macrosomia: A Literature Review, *Ann. Nutr. Metab.* 66 (2015) 14–20. doi:10.1159/000371628.
- [41] G. Desoye, E.T. Korgun, N. Ghaffari-Tabrizi, T. Hahn, Is fetal macrosomia in adequately controlled diabetic women the result of a placental defect? – a hypothesis, *J. Matern. Neonatal Med.* 11 (2002) 258–261. doi:10.1080/jmf.11.4.258.261.
- [42] B.N. Colvin, M.S. Longtine, B. Chen, M.L. Costa, D.M. Nelson, Oleate attenuates palmitate-induced endoplasmic reticulum stress and apoptosis in placental trophoblasts, *Reproduction.* 153 (2017) 369–380. doi:10.1530/REP-16-0576.
- [43] J. Muralidharan, C. Papandreou, A. Sala-Vila, N. Rosique-Esteban, M. Fitó, R. Estruch, M. Angel Martínez-González, D. Corella, E. Ros, C. Razquín, O. Castañer, J. Salas-Salvadó, M. Bulló, Fatty Acids Composition of Blood Cell Membranes and Peripheral Inflammation in the PREDIMED Study: A Cross-Sectional Analysis, *Nutrients.* 11 (2019) 576. doi:10.3390/nu11030576.
- [44] R. Kapoor, Y.-S. Huang, Gamma Linolenic Acid: An Antiinflammatory Omega-6 Fatty Acid, *Curr. Pharm. Biotechnol.* 7 (2006) 531–534. doi:10.2174/138920106779116874.

- [45] Y.-C. Lien, Z. Zhang, G. Barila, A. Green-Brown, M.A. Elovitz, R.A. Simmons, Intrauterine Inflammation Alters the Transcriptome and Metabolome in Placenta, *Front. Physiol.* 11 (2020). doi:10.3389/fphys.2020.592689.
- [46] C. Riganti, E. Gazzano, M. Polimeni, E. Aldieri, D. Ghigo, The pentose phosphate pathway: An antioxidant defense and a crossroad in tumor cell fate, *Free Radic. Biol. Med.* 53 (2012) 421–436. doi:10.1016/j.freeradbiomed.2012.05.006.
- [47] C.M. Grant, Metabolic reconfiguration is a regulated response to oxidative stress, *J. Biol.* 7 (2008) 1. doi:10.1186/jbiol63.
- [48] S.K. Natarajan, T. Bruett, P.G. Muthuraj, P.K. Sahoo, J. Power, J.L. Mott, C. Hanson, A. Anderson-Berry, Saturated free fatty acids induce placental trophoblast lipoapoptosis, *PLoS One.* 16 (2021) e0249907. doi:10.1371/journal.pone.0249907.
- [49] R.H. Lambertucci, S.M. Hirabara, L. dos R. Silveira, A.C. Levada-Pires, R. Curi, T.C. Pithon-Curi, Palmitate increases superoxide production through mitochondrial electron transport chain and NADPH oxidase activity in skeletal muscle cells, *J. Cell. Physiol.* 216 (2008) 796–804. doi:10.1002/jcp.21463.
- [50] M.G. Rosca, E.J. Vazquez, Q. Chen, J. Kerner, T.S. Kern, C.L. Hoppel, Oxidation of Fatty Acids Is the Source of Increased Mitochondrial Reactive Oxygen Species Production in Kidney Cortical Tubules in Early Diabetes, *Diabetes.* 61 (2012) 2074–2083. doi:10.2337/db11-1437.
- [51] M. Zhao, Y. Wang, L. Li, S. Liu, C. Wang, Y. Yuan, G. Yang, Y. Chen, J. Cheng, Y. Lu, J. Liu, Mitochondrial ROS promote mitochondrial dysfunction and inflammation in ischemic acute kidney injury by disrupting TFAM-mediated mtDNA maintenance, *Theranostics.* 11 (2021) 1845–1863. doi:10.7150/thno.50905.
- [52] J.F. Hebert, L. Myatt, Placental mitochondrial dysfunction with metabolic diseases: Therapeutic approaches, *Biochim. Biophys. Acta - Mol. Basis Dis.* 1867 (2021) 165967. doi:10.1016/j.bbadis.2020.165967.
- [53] V. Calabuig-Navarro, M. Haghiac, J. Minium, P. Glazebrook, G.C. Ranasinghe, C. Hoppel, S. Hauguel de-Mouzon, P. Catalano, P. O'Tierney-Ginn, Effect of Maternal Obesity on Placental Lipid Metabolism, *Endocrinology.* 158 (2017) 2543–2555. doi:10.1210/en.2017-00152.
- [54] M. Jolly, The causes and effects of fetal macrosomia in mothers with type 1 diabetes, *J. Clin. Pathol.* 53 (2000) 889–889. doi:10.1136/jcp.53.12.889.
- [55] E.M. Alfadhli, Maternal obesity influences birth weight more than gestational diabetes, *BMC Pregnancy Childbirth.* 21 (2021) 111. doi:10.1186/s12884-021-03571-5.
- [56] F. Amati, S. Hassounah, A. Swaka, The Impact of Mediterranean Dietary Patterns

- During Pregnancy on Maternal and Offspring Health, *Nutrients*. 11 (2019) 1098. doi:10.3390/nu11051098.
- [57] F.L. Alvarado, V. Calabuig-Navarro, M. Haghiac, M. Puchowicz, P.-J.S. Tsai, P. O'Tierney-Ginn, Maternal obesity is not associated with placental lipid accumulation in women with high omega-3 fatty acid levels, *Placenta*. 69 (2018) 96–101. doi:10.1016/j.placenta.2018.07.016.
- [58] C.M. Boney, A. Verma, R. Tucker, B.R. Vohr, Metabolic syndrome in childhood: association with birth weight, maternal obesity, and gestational diabetes mellitus., *Pediatrics*. 115 (2005) e290-6. doi:10.1542/peds.2004-1808.
- [59] M. Palatianou, Y. Simos, S. Andronikou, D. Kiortsis, Long-Term Metabolic Effects of High Birth Weight: A Critical Review of the Literature, *Horm. Metab. Res.* 46 (2014) 911–920. doi:10.1055/s-0034-1395561.
- [60] I.G.I. Thiele, K.E. Niezen-Koning, A.H. van Gennip, J.G. Aarnoudse, Increased Plasma Carnitine Concentrations in Preeclampsia, *Obstet. Gynecol.* 103 (2004) 876–880. doi:10.1097/01.AOG.0000125699.60416.03.
- [61] M.P.H. Koster, R.J. Vreeken, A.C. Harms, A.D. Dane, S. Kuc, P.C.J.I. Schielen, T. Hankemeier, R. Berger, G.H.A. Visser, J.L.A. Pennings, First-Trimester Serum Acylcarnitine Levels to Predict Preeclampsia: A Metabolomics Approach, *Dis. Markers*. 2015 (2015) 1–8. doi:10.1155/2015/857108.
- [62] J.R. Ussher, S. Elmariah, R.E. Gerszten, J.R.B. Dyck, The Emerging Role of Metabolomics in the Diagnosis and Prognosis of Cardiovascular Disease, *J. Am. Coll. Cardiol.* 68 (2016) 2850–2870. doi:10.1016/j.jacc.2016.09.972.
- [63] M. Ruiz, F. Labarthe, A. Fortier, B. Bouchard, J. Thompson Legault, V. Bolduc, O. Rigal, J. Chen, A. Ducharme, P.A. Crawford, J.-C. Tardif, C. Des Rosiers, Circulating acylcarnitine profile in human heart failure: a surrogate of fatty acid metabolic dysregulation in mitochondria and beyond., *Am. J. Physiol. Heart Circ. Physiol.* 313 (2017) H768–H781. doi:10.1152/ajpheart.00820.2016.
- [64] A. Karaer, A. Mumcu, S. Arda Düz, G. Tuncay, B. Doğan, Metabolomics analysis of placental tissue obtained from patients with fetal growth restriction, *J. Obstet. Gynaecol. Res.* 48 (2022) 920–929. doi:10.1111/jog.15173.
- [65] B.F. Nobakht M. Gh, Application of metabolomics to preeclampsia diagnosis, *Syst. Biol. Reprod. Med.* 64 (2018) 324–339. doi:10.1080/19396368.2018.1482968.
- [66] E.G. O'Malley, C.M.E. Reynolds, A. Killalea, R. O'Kelly, S.R. Sheehan, M.J. Turner, Maternal obesity and dyslipidemia associated with gestational diabetes mellitus (GDM), *Eur. J. Obstet. Gynecol. Reprod. Biol.* 246 (2020) 67–71. doi:10.1016/j.ejogrb.2020.01.007.

- [67] M. Lenin, R. Ramesh, V.K. Velu, S. Ghose, Association of Dyslipidemia and Glycated Haemoglobin in Gestational Diabetes Mellitus, *J. Diabetes Mellit.* 07 (2017) 275–280. doi:10.4236/jdm.2017.74022.
- [68] F. Liu, M.J. Soares, K.L. Audus, Permeability properties of monolayers of the human trophoblast cell line BeWo, *Am. J. Physiol. Physiol.* 273 (1997) C1596–C1604. doi:10.1152/ajpcell.1997.273.5.C1596.
- [69] S.J. Heaton, J.J. Eady, M.L. Parker, K.L. Gotts, J.R. Dainty, S.J. Fairweather-Tait, H.J. McArdle, K.S. Srai, R.M. Elliott, The use of BeWo cells as an in vitro model for placental iron transport, *Am. J. Physiol. Physiol.* 295 (2008) C1445–C1453. doi:10.1152/ajpcell.00286.2008.
- [70] M. Liu, S. Hassana, J.K. Stiles, Heme-mediated apoptosis and fusion damage in BeWo trophoblast cells, *Sci. Rep.* 6 (2016) 36193. doi:10.1038/srep36193.
- [71] M. Lange, Y. Zeng, A. Knight, A. Windebank, E. Trushina, Comprehensive Method for Culturing Embryonic Dorsal Root Ganglion Neurons for Seahorse Extracellular Flux XF24 Analysis, *Front. Neurol.* 3 (2012). doi:10.3389/fneur.2012.00175.
- [72] G.J. Burton, T. Cindrova-Davies, H. wa Yung, E. Jauniaux, HYPOXIA AND REPRODUCTIVE HEALTH: Oxygen and development of the human placenta, *Reproduction.* 161 (2021) F53–F65. doi:10.1530/REP-20-0153.
- [73] H. Schneider, Oxygenation of the placental–fetal unit in humans, *Respir. Physiol. Neurobiol.* 178 (2011) 51–58. doi:10.1016/j.resp.2011.05.009.
- [74] N.J. Hannan, P. Paiva, E. Dimitriadis, L.A. Salamonsen, Models for Study of Human Embryo Implantation: Choice of Cell Lines?1, *Biol. Reprod.* 82 (2010) 235–245. doi:10.1095/biolreprod.109.077800.
- [75] M. Borges, P. Bose, H.-G. Frank, P. Kaufmann, A.J.G. Pötgens, A Two-Colour Fluorescence Assay for the Measurement of Syncytial Fusion between Trophoblast-Derived Cell Lines, *Placenta.* 24 (2003) 959–964. doi:10.1016/S0143-4004(03)00173-5.
- [76] M. Rothbauer, N. Patel, H. Gondola, M. Siwetz, B. Huppertz, P. Ertl, A comparative study of five physiological key parameters between four different human trophoblast-derived cell lines, *Sci. Rep.* 7 (2017) 5892. doi:10.1038/s41598-017-06364-z.
- [77] E. Drwal, A. Rak, E. Gregoraszczyk, Co-culture of JEG-3, BeWo and syncBeWo cell lines with adrenal H295R cell line: an alternative model for examining endocrine and metabolic properties of the fetoplacental unit, *Cytotechnology.* 70 (2018) 285–297. doi:10.1007/s10616-017-0142-z.
- [78] B. Novakovic, L. Gordon, N.C. Wong, A. Moffett, U. Manuelpillai, J.M. Craig, A.

- Sharkey, R. Saffery, Wide-ranging DNA methylation differences of primary trophoblast cell populations and derived cell lines: implications and opportunities for understanding trophoblast function†, *MHR Basic Sci. Reprod. Med.* 17 (2011) 344–353. doi:10.1093/molehr/gar005.
- [79] D.M. Sheppard, R.A. Fisher, S.D. Lawler, Karyotypic analysis and chromosome polymorphisms in four choriocarcinoma cell lines, *Cancer Genet. Cytogenet.* 16 (1985) 251–258. doi:10.1016/0165-4608(85)90052-4.
- [80] H.-G. Frank, B. Gunawan, I. Ebeling-Stark, H.-J. Schulten, H. Funayama, U. Cremer, B. Huppertz, G. Gaus, P. Kaufmann, L. Füzesi, Cytogenetic and DNA-Fingerprint Characterization of Choriocarcinoma Cell Lines and a Trophoblast /Choriocarcinoma Cell Hybrid, *Cancer Genet. Cytogenet.* 116 (2000) 16–22. doi:10.1016/S0165-4608(99)00107-7.
- [81] S.M. Leon-Garcia, H.A. Roeder, K.K. Nelson, X. Liao, D.P. Pizzo, L.C. Laurent, M.M. Parast, D.Y. LaCoursiere, Maternal obesity and sex-specific differences in placental pathology, *Placenta.* 38 (2016) 33–40. doi:10.1016/j.placenta.2015.12.006.
- [82] S. Muralimanoharan, C. Guo, L. Myatt, A. Maloyan, Sexual dimorphism in miR-210 expression and mitochondrial dysfunction in the placenta with maternal obesity, *Int. J. Obes.* 39 (2015) 1274–1281. doi:10.1038/ijo.2015.45.
- [83] J. Strutz, S. Cvitic, H. Hackl, K. Kashofer, H.M. Appel, A. Thüringer, G. Desoye, P. Koolwijk, U. Hiden, Gestational diabetes alters microRNA signatures in human fetoplacental endothelial cells depending on fetal sex, *Clin. Sci.* 132 (2018) 2437–2449. doi:10.1042/CS20180825.
- [84] C.S. Rosenfeld, Sex-Specific Placental Responses in Fetal Development, *Endocrinology.* 156 (2015) 3422–3434. doi:10.1210/en.2015-1227.
- [85] M.G. Petroff, T.A. Phillips, H. Ka, J.L. Pace, J.S. Hunt, Isolation and Culture of Term Human Trophoblast Cells, in: *Placenta Trophobl.*, Humana Press, New Jersey, n.d.: pp. 201–216. doi:10.1385/1-59259-983-4:201.
- [86] L. Sagrillo-Fagundes, H. Clabault, L. Laurent, A.-A. Hudon-Thibeault, E.M.A. Salustiano, M. Fortier, J. Bienvenue-Pariseault, P. Wong Yen, T.J. Sanderson, C. Vaillancourt, Human Primary Trophoblast Cell Culture Model to Study the Protective Effects of Melatonin Against Hypoxia/reoxygenation-induced Disruption, *J. Vis. Exp.* (2016). doi:10.3791/54228.
- [87] R. Wang, Y.-L. Dang, R. Zheng, Y. Li, W. Li, X. Lu, L.-J. Wang, C. Zhu, H.-Y. Lin, H. Wang, Live Cell Imaging of In Vitro Human Trophoblast Syncytialization1, *Biol. Reprod.* 90 (2014). doi:10.1095/biolreprod.113.114892.
- [88] H.J. KLIMAN, J.E. NESTLER, E. SERMASI, J.M. SANGER, J.F. STRAUSS, Purification, Characterization, and in vitro Differentiation of Cytotrophoblasts

from Human Term Placentae*, *Endocrinology*. 118 (1986) 1567–1582.
doi:10.1210/endo-118-4-1567.

- [89] R.K. Miller, O. Genbacev, M.A. Turner, J.D. Aplin, I. Caniggia, B. Huppertz, Human placental explants in culture: Approaches and assessments, *Placenta*. 26 (2005) 439–448. doi:10.1016/j.placenta.2004.10.002.
- [90] S.R. Sooranna, E. Oteng-Ntim, R. Meah, T.A. Ryder, R. Bajoria, Characterization of human placental explants: morphological, biochemical and physiological studies using first and third trimester placenta, *Hum. Reprod.* 14 (1999) 536–541. doi:10.1093/humrep/14.2.536.
- [91] C.M. Simán, C.P. Sibley, C.J.P. Jones, M.A. Turner, S.L. Greenwood, The functional regeneration of syncytiotrophoblast in cultured explants of term placenta, *Am. J. Physiol. Integr. Comp. Physiol.* 280 (2001) R1116–R1122. doi:10.1152/ajpregu.2001.280.4.R1116.
- [92] P.A. Reyfman, J.M. Walter, N. Joshi, K.R. Anekalla, A.C. McQuattie-Pimentel, S. Chiu, R. Fernandez, M. Akbarpour, C.-I. Chen, Z. Ren, R. Verma, H. Abdala-Valencia, K. Nam, M. Chi, S. Han, F.J. Gonzalez-Gonzalez, S. Soberanes, S. Watanabe, K.J.N. Williams, A.S. Flozak, T.T. Nicholson, V.K. Morgan, D.R. Winter, M. Hinchcliff, C.L. Hrusch, R.D. Guzy, C.A. Bonham, A.I. Sperling, R. Bag, R.B. Hamanaka, G.M. Mutlu, A. V. Yeldandi, S.A. Marshall, A. Shilatifard, L.A.N. Amaral, H. Perlman, J.I. Sznajder, A.C. Argento, C.T. Gillespie, J. Dematte, M. Jain, B.D. Singer, K.M. Ridge, A.P. Lam, A. Bharat, S.M. Bhorade, C.J. Gottardi, G.R.S. Budinger, A. V. Misharin, Single-Cell Transcriptomic Analysis of Human Lung Provides Insights into the Pathobiology of Pulmonary Fibrosis, *Am. J. Respir. Crit. Care Med.* 199 (2019) 1517–1536. doi:10.1164/rccm.201712-2410OC.
- [93] J. Chen, B.T. Lau, N. Andor, S.M. Grimes, C. Handy, C. Wood-Bouwens, H.P. Ji, Single-cell transcriptome analysis identifies distinct cell types and niche signaling in a primary gastric organoid model, *Sci. Rep.* 9 (2019) 4536. doi:10.1038/s41598-019-40809-x.
- [94] C.J. Bode, H. Jin, E. Rytting, P.S. Silverstein, A.M. Young, K.L. Audus, In vitro models for studying trophoblast transcellular transport., *Methods Mol. Med.* 122 (2006) 225–39. doi:10.1385/1-59259-989-3:225.
- [95] L. Aengenheister, K. Keevend, C. Muoth, R. Schönenberger, L. Diener, P. Wick, T. Buerki-Thurnherr, An advanced human in vitro co-culture model for translocation studies across the placental barrier, *Sci. Rep.* 8 (2018) 5388. doi:10.1038/s41598-018-23410-6.
- [96] M.K. Wong, E.W. Li, M. Adam, P.R. Selvaganapathy, S. Raha, Establishment of an in vitro placental barrier model cultured under physiologically relevant oxygen levels, *Mol. Hum. Reprod.* 26 (2020) 353–365. doi:10.1093/molehr/gaaa018.

- [97] R.L. Pemathilaka, J.D. Caplin, S.S. Aykar, R. Montazami, N.N. Hashemi, Placenta-on-a-Chip: In Vitro Study of Caffeine Transport across Placental Barrier Using Liquid Chromatography Mass Spectrometry, *Glob. Challenges*. 3 (2019) 1800112. doi:10.1002/gch2.201800112.
- [98] J.S. Lee, R. Romero, Y.M. Han, H.C. Kim, C.J. Kim, J.-S. Hong, D. Huh, Placenta-on-a-chip: a novel platform to study the biology of the human placenta, *J. Matern. Neonatal Med.* 29 (2016) 1046–1054. doi:10.3109/14767058.2015.1038518.
- [99] L.C. Morley, D.J. Beech, J.J. Walker, N.A.B. Simpson, Emerging concepts of shear stress in placental development and function, *Mol. Hum. Reprod.* 25 (2019) 329–339. doi:10.1093/molehr/gaz018.
- [100] B.A. Brugger, J. Guettler, M. Gauster, Go with the Flow—Trophoblasts in Flow Culture, *Int. J. Mol. Sci.* 21 (2020) 4666. doi:10.3390/ijms21134666.

Appendices

Appendix A Copyright permissions for Chapter 1.

Dear Authors,

Congratulations that your paper "The Impact of Maternal Body Composition and Dietary Fat Consumption upon Placental Lipid Processing and Offspring Metabolic Health" has been published in *Nutrients* (ISSN 2072-6643, IF 4.546, CiteScore 5.2). We really enjoy cooperating with you.

Your paper is collected in *Nutrients*, Volume 12, Issue 10, which will be released on 12 October 2020. After that, any changes and updates will be unacceptable. Please carefully check your paper (Abstract:

<https://www.mdpi.com/2072-6643/12/10/3031>

PDF Version: <https://www.mdpi.com/2072-6643/12/10/3031/pdf>). If there are incorrect contents, please inform us within 24 hours. Please kindly understand in this stage we do not accept any changes in linguistic issues.

In the meanwhile, may we kindly emphasize again that *Nutrients* is a full Open Access journal, you and all the co-authors have the copyright of your paper. Please feel free to share this paper in your academic and social media accounts (Twitter, LinkedIn, Researchgate, Facebook, Mendeley, etc.). You may wish to tag us and follow the journal @Nutrients_MDPI on Twitter.

We look forward to our next collaboration.

Best regards,

Jessie

Appendix B Copyright permissions for Chapter 2



This is a License Agreement between Zachary Easton ("User") and Copyright Clearance Center, Inc. ("CCC") on behalf of the Rightsholder identified in the order details below. The license consists of the order details, the CCC Terms and Conditions below, and any Rightsholder Terms and Conditions which are included below. All payments must be made in full to CCC in accordance with the CCC Terms and Conditions below.

Order Date	18-Jan-2022	Type of Use	Republish in a thesis/dissertation
Order License ID	1179275-1	Publisher	SOCIETY FOR REPRODUCTION AND FERTILITY
ISSN	1741-7899	Portion	Chapter/article

LICENSED CONTENT

Publication Title	Reproduction : the official journal of the Society for the Study of Fertility	Country	United Kingdom of Great Britain and Northern Ireland
Author/Editor	Society for the Study of Fertility., Society for Reproduction and Fertility., Society for Reproduction and Fertility, Society for the Study of Fertility	Rightsholder	Bioscientifica Limited
Date	01/01/2001	Publication Type	e-Journal
Language	English	URL	http://www.jrf-journals.org.uk

REQUEST DETAILS

Portion Type	Chapter/article	Rights Requested	Main product and any product related to main product
Page range(s)	73-88	Distribution	Worldwide
Total number of pages	16	Translation	Original language of publication
Format (select all that apply)	Print, Electronic	Copies for the disabled?	No
Who will republish the content?	Academic institution	Minor editing privileges?	Yes
Duration of Use	Life of current and all future editions	Incidental promotional use?	No
Lifetime Unit Quantity	Up to 999	Currency	CAD

NEW WORK DETAILS

Title	The Impacts of Dietary Nutrients on Placental Trophoblast Metabolic Function	Institution name	Western University
Instructor name	Timothy Regnault	Expected presentation date	2022-04-29

ADDITIONAL DETAILS

Order reference number	N/A	The requesting person / organization to appear on the license	Zachary Easton
------------------------	-----	---	----------------

REUSE CONTENT DETAILS

Title, description or numeric reference of the portion(s)	Syncytialization and prolonged exposure to palmitate impacts BeWo respiration	Title of the article/chapter the portion is from	N/A
Editor of portion(s)	N/A	Author of portion(s)	Society for the Study of Fertility.; Society for Reproduction and Fertility.; Society for Reproduction and Fertility; Society for the Study of Fertility
Volume of serial or monograph	161	Issue, if republishing an article from a serial	1
Page or page range of portion	73-88	Publication date of portion	2021-01-01

Curriculum Vitae

EDUCATION

Western University, London ON 2016–2022

PhD in Physiology and Pharmacology, collaborative specialization in Developmental Biology

anticipated completion April 2022

Thesis title: The impacts of dietary nutrients on placental trophoblast metabolic function

Thesis Supervisor: Dr. Timothy RH Regnault

Western University, London, ON 2012–2016

Bachelor of Medical Science, Western Scholars: Honors Specialization Physiology and Pharmacology with distinction

Fourth year thesis project title: The influence of exercise on lipid metabolism in a rodent model of type 1 diabetes mellitus

Thesis Supervisor: Dr. Jamie Melling

TEACHING EXPERIENCE

Graduate Teaching Assistant Sept 2020–April 2021

Physiology and Pharmacology 4980E: Honors Thesis Project

Course Co-Coordinator and Graduate Teaching Assistant Sept 2018–Dec 2019

Physiology and Pharmacology 9550: Molecular Techniques

Graduate Teaching Assistant Jan 2019–April 2019

Physiology 4700: Fetal Physiology

Graduate Teaching Assistant Sept 2017–April 2018

Physiology and Pharmacology 3000E: The Physiology and Pharmacology Laboratory

Graduate Teaching Assistant Sept 2016–April 2017

Pharmacology 3580Z: The Pharmacology Laboratory

MENTORSHIP EXPERIENCE

Fourth Year Thesis Student In-lab Supervisor and Mentor Sept 2021–present

Project Title: Dietary fats and placental trophoblast epigenetic modifications: A time-course investigation

Fourth Year Thesis Student In-lab Supervisor & Mentor Sept 2020–April 2021

Project Title: Epigenetic modifications in response to prolonged hyperglycemia in placental trophoblasts

Fourth Year Thesis Student In-Lab Supervisor and Mentor Sept 2017–April 2018

Project Title: Acute hyperglycemia and placental trophoblast mitochondrial function and oxidative stress

PUBLICATIONS

Easton ZJW, Delhaes F, Mathers K, Zhao L, Vanderboor CMG, and Regnault TRH.

Syncytialization and prolonged exposure to palmitate impacts BeWo respiration.

Reproduction. 2021 Jan; 161(1):73-88. PMID: 33151905.

Easton ZJW, and Regnault TRH. The impact of maternal body composition and dietary fat consumption upon placental lipid processing and offspring metabolic health. *Nutrients*. 2020 Oct; 3; 12(10):3031. PMID: 33022934.

Lojpur T, **Easton ZJW**, Raez-Villanueva A, Laviolette S, Holloway AC, and Hardy DB. Δ^9 -Tetrahydrocannabinol leads to endoplasmic reticulum stress and mitochondrial dysfunction in human BeWo trophoblasts. *Reproductive Toxicology*. 2019 Aug; 87:21-31. PMID: 3105432

PUBLISHED CONFERENCE ABSTRACTS

Easton ZJW, Sarr O, and Regnault TRH. Prolonged exposure to dietary-fatty acids alters BeWo trophoblast mitochondrial function and fatty acid desaturation. SRI supplement to *Reproductive Sciences*. 2020 Mar; Vol 27, Supplement 1.

Easton ZJW, Mathers K, Delhaes F, and Regnault TRH. Differential metabolic responses of BeWo villous trophoblast cells to prolonged glucose or fatty acid exposure. SRI supplement to *Reproductive Sciences*. 2019 Mar; Vol 26, Supplement 1.

Easton ZJW, Vanderboor, CMG, and Regnault TRH. The response of human villous trophoblasts to prolonged fatty acid exposure. SRI supplement to *Reproductive Sciences*. 2018 Mar; Vol 25, Supplement 1.

Delhaes F, Vanderboor CMG, **Easton ZJW**, and Regnault TRH. Low-oxygen levels induce remodeling of cellular morphology and inhibit differentiation in trophoblastic cell culture. SRI supplement to *Reproductive Sciences*. 2018 Mar; Vol 25, Supplement 1.

PRESENTATIONS AND CONFERENCE ABSTRACTS

Luo X, **Easton ZJW**, Li L and Regnault TRH. In-depth Metabolomic Profiling of Fatty Acid or Glucose Treated Placental Cells Reveals Differential Metabolomic Signature. 69th ASMS Conference on Mass Spectrometry and Allied Topics. Philadelphia, PA, USA. October 31 - November 4th 2021.

Abstract author

Easton ZJW, Sarr O, Zhao L, and Regnault TRH. The Dietary Fatty Acids Palmitate and Oleate Differentially Impact BeWo Trophoblast Lipid Processing. 34th Annual Canadian Student Health Research Forum. Virtual Conference. June 15th 2021.

Virtual Poster Presenter

Easton ZJW, and Regnault TRH. Characterization of BeWo trophoblast metabolic function in response to hyperglycemia culture conditions. 5th Annual DOHaD Canada Research Meeting. Virtual Conference. May 31–June 2nd 2021.

Virtual Poster Presenter

Easton ZJW, and Regnault TRH. Transcriptomic and functional characterization of BeWo trophoblast metabolism in response to hyperglycemia. London Health Research Day. Virtual Conference. May 11th 2021.

Virtual Poster Presenter

Easton ZJW, and Regnault TRH. BeWo trophoblast metabolic function in response to prolonged hyperglycemia. 8th Annual Canadian National Perinatal Research Meeting. Virtual Conference. February 8–12th 2021.

Virtual Poster Presenter

Easton ZJW, Sarr O, and Regnault TRH. BeWo Trophoblast Mitochondrial Function and Fatty Acid Desaturase Enzyme Activities are Impacted with Prolonged Exposure to Dietary-Fatty Acids. 7th Annual Canadian National Perinatal Research Meeting. Banff, AB, Canada. February 12–15th 2020.

Poster Presenter

Easton ZJW, and Regnault TRH. Prolonged exposure to dietary fatty acids alters mitochondrial activity and lipid metabolism of BeWo trophoblast cells. Lawson Talks on Fridays (TOFs) Seminar Series. London, ON, Canada. January 31st 2020.

Oral Presenter

Easton ZJW, Mathers K, Delhaes F, Vanderboor CMG, and Regnault TRH. Mitochondrial activities of BeWo trophoblast cells following prolonged glucose and fatty acid treatment. Southern Ontario Reproductive Biology Research Day. Toronto, ON, Canada. June 7th 2019.
Poster Presenter

Easton ZJW, Mathers K, Delhaes F, and Regnault TRH. Mitochondrial activity of BeWo villous trophoblast cells following prolonged glucose or fatty acid exposure. London Health Research Day. London, ON, Canada. April 30th 2019.
Poster Presenter

Easton ZJW, Mathers K, Delhaes F, and Regnault TRH. Differential mitochondrial activity responses of BeWo villous trophoblast cells to prolonged glucose or fatty acid exposure. 6th Annual Canadian National Perinatal Research Meeting, Mont Tremblant, QC, Canada. February 12–15th 2019.
Poster Presenter

Easton ZJW, Delhaes F, Vanderboor CMG, and Regnault TRH. The response of BeWo trophoblast cells to a prolonged fatty acid exposure. Southern Ontario Reproductive Biology Meeting. Guelph, ON, Canada. May 18th 2018.
Poster Presenter

Easton ZJW, Delhaes F, Vanderboor CMG, and Regnault TRH. The metabolic response of human villous trophoblasts to prolonged fatty acid exposure. London Health Research Day. London, ON Canada. May 10th 2018.
Poster Presenter

Easton ZJW, and Regnault TRH. The response of BeWo trophoblast cells to a prolonged fatty acid exposure. Lawson Talks on Fridays (TOFs) Seminar Series. London, ON, Canada. April 20th 2018.
Oral Presenter

Easton ZJW, Vanderboor CMG, and Regnault TRH. The response of BeWo trophoblast cells to a prolonged fatty acid exposure. 16th Annual Paul Harding Research Awards Day. London ON, Canada. April 18th 2018.
Oral Presenter

Easton ZJW, Vanderboor CMG, and Regnault TRH. The metabolic response of human villous trophoblasts to prolonged fatty acid exposure. 5th Annual Canadian National Perinatal Research Meeting. Banff, AB, Canada. February 14–17th 2018.
Oral Presenter

Easton ZJW, Vanderboor CMG, and Regnault TRH. Altered human villous trophoblast metabolism in response to a maternal high fat and high sugar diet: Optimizing the use of the BeWo cell line. Southern Ontario Reproductive Biology Meeting, London, ON, Canada. May 12th 2017.
Poster Presenter

HONORS & AWARDS

Second Prize Oral Presentation

16th Annual Paul Harding Research Awards Day, April 18th 2018

Obstetrics and Gynaecology Graduate Research Scholarship (OGGS)

Awarded September 2016-August 2017

Faculty of Science Undergraduate Dean's Honor List

2012-2016 academic years

VOLUNTEER EXPERIENCE

StemCellTalks Western <i>Co-chair, symposium organizing committee</i>	2020–present
StemCellTalks Western <i>Volunteer, symposium organizing committee</i>	2018–2020
Physiology and Pharmacology Graduate Student’s Counsel <i>Departmental Representative to the Society of Graduate Students (SOGS)</i>	2016–2018
Western Foot Patrol, London, ON <i>Patroller</i>	2014–2017